

Members of the Jury

Prof. Dr. ir. Wim Soetaert (Chairman)

Department of Biotechnology

Faculty of Bioscience Engineering, Ghent University

Prof. Dr. Stefan Bräse

Institut für Organische Chemie

Karlsruher Institut für Technologie (KIT)

Dr. Marc Ongena

Gembloux Agro-Bio Tech - Bioindustries Unit

Université de Liège

Prof. Dr. ir. Inge Van Bogaert

Department of Biotechnology

Faculty of Bioscience Engineering, Ghent University

Prof. Dr. ir. Matthias D'hooghe

Department of Green Chemistry and Technology

Faculty of Bioscience Engineering, Ghent University

Promoters

Prof. Dr. ir. Sven Mangelinckx

Department of Green Chemistry and Technology

Faculty of Bioscience Engineering, Ghent University

Em. Prof. Dr. ir. Norbert De Kimpe

Department of Green Chemistry and Technology

Faculty of Bioscience Engineering, Ghent University

Prof. Dr. ir. Chris Stevens

Department of Green Chemistry and Technology

Faculty of Bioscience Engineering, Ghent University

Dean of the Faculty

Prof. Dr. ir. Marc Van Meirvenne

Rector of the University

Prof. Dr. ir. Rik Van de Walle



ir. Ewout Ruysbergh

**Reactivity of *N*-(3-hydroxyacyl)amino
acids and influence of their corresponding
homoserine lactones on cyclic lipopeptide
production**

Thesis submitted in fulfillment of the requirements for the degree of Doctor
(PhD) in Applied Biological Sciences: Chemistry and Bioprocess Technology

Dutch translation of the title: ‘Reactiviteit van *N*-(3-hydroxyacyl)aminozuren en de invloed van de overeenkomstige homoserine lactonen op de productie van cyclische lipopeptiden’

To be cited as: Ruysbergh, E. ‘Reactivity of *N*-(3-hydroxyacyl)amino acids and influence of their corresponding homoserine lactones on cyclic lipopeptide production’, PhD dissertation, Ghent University, 2018.

This research was funded by the Bijzonder onderzoeksfonds (BOF, UGent).

Cover illustration: swarming behavior displayed by a *Pseudomonas* sp. CMR12a mutant strain.

ISBN number: 978-94-6357-069-5

The author and the promoters give the authorisation to consult and to copy parts of this work for personal use only. Every other use is subject to the copyright laws. Permission to reproduce any material contained in this work should be obtained from the author.

The author:

The promoters:

ir. Ewout Ruysbergh

Prof. Dr. ir. S. Mangelinckx

Em. Prof. Dr. ir. N. De Kimpe

Prof. Dr. ir. C. Stevens

Woord vooraf

Eindelijk, ein-delijk, ein-de-lijk, ben ik aanbeland bij het laatste deeltje van dit doctoraat dat nog op papier gezet moet worden. Het laatste maar vermoedelijk ook het meest gelezen deel. Beginnen doe ik met een huizenhoog (en dus op waarheid berust) cliché: een doctoraat schrijf je niet alleen. Dat was ook bij mij niet het geval, daarom zou ik graag een aantal mensen willen bedanken.

In de eerste plaats wil ik mijn promotoren bedanken, om me te gidsen doorheen de wereld der organische chemie. Prof. Chris Stevens, bedankt om in de bres te springen toen ik op papier een promotorloos doctoraatsweesje was. Prof. Norbert De Kimpe, bedankt om mijn schrijfsels ook tijdens uw emeritaat snel en grondig te blijven nalezen. Ik hoop dat onze correspondentie uw filatelistische collectie mooi heeft uitgebreid. Prof. Sven Mangelinckx, als ik vastzat met een synthetisch probleem of geen goede invalshoek vond om bepaalde resultaten neer te schrijven kon ik steeds bij u terecht. Meermaals viel mijn mond open van verbazing wanneer u mijn antwoord op een opmerking van een reviewer toch nog net dat tikkeltje beter kon formuleren. Sven, bedankt om ook na mijn shortcut richting industrie me toch steeds te blijven steunen.

I also would like to thank the members of the examination committee: Prof. Dr. ir. Wim Soetaert, Prof. Dr. Stefan Bräse, Dr. Marc Ongena, Prof. Dr. ir. Inge Van Bogaert and Prof. Dr. ir. Matthias D'hooghe for the critical reading of this thesis and the interesting discussions we had, both about chemical and biological topics. Your remarks helped me to improve the quality of this work.

Daarnaast wil ik alle doctoraatsstudenten, postdocs, ATP-leden en thesisstudenten bedanken voor de bijzonder leuke sfeer die er heerst in het labo. Ook de congressen in Spa en Blankenberge waren steeds dik in orde, met de avatarverkleedpartij als absoluut hoogtepunt. Iedereen bij naam noemen zonder iemand te vergeten is bijna onmogelijk maar ik zou toch een aantal mensen specifiek willen bedanken.

Vooreerst mijn collega's van 'het vierde' waar ik het merendeel van mijn syntheseseloopbaan doorbracht. Gert, Nils, Pieter, Frederik, Sofie, Marine, Tamara, Koen, Elena & Iris, bedankt voor leuke atmosfeer en het delen van jullie chemische kennis. Gert en Koen, naast de vele miseries bij het kaarten tijdens de pauze om drie uur, mocht ik met jullie (en Bart) de vreugde delen de faculteitsquiz (meermaals) te winnen en alzo de SynBioC-eer hoog te houden. Iris, we vonden al snel een goed evenwicht over het verdelen van de roerplaten in de trekkast en

het glaswerk. Ook onze rotavapor Helmut werd goed verzorgd en gekuist. Zelfs toen ik besloot de binnenkant van onze trekkast te coaten met jouw product bleef je (relatief) kalm. Gelukkig ben je toen niet tegen mijn schuif gelopen. Ik had me alvast geen betere labobuurvrouw kunnen wensen!

Michail, *ευχαριστω*, thank you for being my guide during my first steps in the wonderful world of quorum sensing. I still have fond memories of our Sterre biotesting parties during my master thesis and often think with a smile about your different theories such as the bicycle theory (aren't they in fact hypotheses rather than theories, as I have only seen indications but no real proof so far?). ΠΟΑΚΑΡΑ!

Elena, my sovjet comrade, thank you for the nice lessons in Russian during the flashing of our precious compounds. When I'm stuck in Russia, I'm now able to tell people that I'm hungry, that I'm thirsty and that they are beautiful. I'm convinced that this will help me a lot! I hope that my lessons in Dutch helped you during your stay in Belgium. During our lunches in the kitchen, I really enjoyed our conversations about amino acid chemistry, mother Russia, global politics, hot yoga and traveling. I really hope I'll be able to visit Moscow someday with you as my guide.

Hang 'I DIE' Dao Thi, I still remember when you told me that you liked to work in the garden and I said 'what a nice coincidence, I have a garden'. I admire the precision and pace at which you were able to remove weeds from between the carrots and your special care for the onions. I hope the gardening was a nice alternation from the lab work. Lena & Marine, bedankt voor het advies op chemische maar vooral andere gebieden. De vele voetbal- en badmintonpartijtjes waren zeer ontspannend! Lena, bedankt voor het veelvuldig gebruik van je *N*-methylmorpholine en ook een speciale dank u wel om mijn laatste HRMS-stalen onder jouw hoede te nemen.

De Boedapestbende, Iris, Sigrid, Sofie, Nicola en Stijn, wil ik bedanken voor het zeer ontspannend reisje. Ik denk niet dat ik ooit nog een zoete, 'fruity' witte wijn zal kunnen drinken zonder aan deze trip terug te denken.

Ans, jou wil ik uit de grond van mijn hart bedanken voor de bijstand in praktische zaken, en zeker naar het einde toe, me zeer snel van antwoord te dienen als ik niet echt goed wist hoe iets geregeld moest worden. Els, bedankt voor de practicum- en printassistentie, en het doet me iedere keer plezier om te zien hoeveel het bananenscheutje dat ik je ooit gaf al gegroeid is dankzij jouw goede zorgen. Pieter, bedankt om met jouw technische kennis vele praktische laboproblemen van de baan te helpen, hoe druk je het ook had, een rotavapor was snel gefikst.

Naast synthese, voerde ik ook heel wat bioassays uit. Nam, thank you for teaching me how to perform swarming and plant assays. I really liked the moments we were making dilutions and plating several mutant strains side by side and our curiosity when we took the plates out of the incubator. Feyi, thank you for your kind advice and as well assistance during some of the final experiments. Prof. Höfte, bedankt voor de interessante discussies in verband met mijn resultaten. Je leerde me dat micro-organismen soms wel degelijk een eigen willetje hebben en een onverwacht resultaat niet noodzakelijk een slecht resultaat is. Je enthousiasme werkt aanstekelijk!

Mijn buromies, Stijn (Brabie), Matthias (Moenski) en Koen (... Koen) zou ik willen bedanken voor de met voorsprong tofste bureau van de B-blok (en omstreken). Omringd door boeiende literatuur en met een prachtuitzicht op de coupure hebben we vele chemische onderwerpen vol passie bediscussieerd. En misschien ook enkele niet zo chemische, heel af en toe dan. Koen ook bedankt om met je arendsoog nog enkele fouten uit mijn schrijfsels te halen. Dat we echt wel hetzelfde type humor hebben bleek meermaals uit je toevoegsels tijdens het corrigeren.

Ook mijn labo- en procescollega's en in het bijzonder mijn eilandgenoten van op Oleon wil ik bedanken voor de leuke sfeer, waardoor ik 's avonds altijd goedgezind thuiskwam om vervolgens aan de tweede (doctoraats)shift te beginnen.

Daarnaast wil ik ook de vaste cinecrew, Lino, Thibaut, Thomas en Nicolas, bedanken voor de ontspannende vrijdagavonden toen ik die nodig had. Recent heb ik wel enkele keren verstek moeten geven maar vanaf 2018 ben ik terug trouw van de partij! Amber, mijn petekindje, in 2017 kon ik je doctoraatsgewijs niet zoveel zien als ik wou, maar ik kijk er naar om de schade in te halen en het olifantendansje te leren. Ik wil ook mijn studiegenoten, de bioboyz, bedanken voor de vele ontspannende momenten tijdens onze studies buiten (maar ook tijdens) de lessen. Leen, Melissa, Jorik, Mike, Inge en de rest van the gang, iedere keer als we afspreken is het er weer boenk op, dat doet me altijd plezier. Jorik, amigo, haal je beste tennis maar boven want die (re)match moet er nu toch eens van komen. Of een komiek, dat kan ook natuurlijk, zolang er maar een burgerrestaurant in de buurt is.

Mijn ouders wil ik bedanken voor hun onvoorwaardelijke steun, al mijn hele leven lang. Bedankt om van kinds af aan mijn nieuwsgierigheid en honger naar (wetenschappelijke) kennis steeds te voeden en me te helpen de persoon te worden die ik nu ben. Ook een speciale dank aan mijn grootouders, om me te steunen in wat ik ook doe. De kaars die jullie hebben laten branden tijdens mijn interne verdediging gaf me een extra duwtje in de rug! Mijn broers, Ruben en Arne, wil ik bedanken voor alle ontspannende momenten en ook al had ik vorig jaar niet

bijster veel tijd, ik weet dat jullie er altijd voor mij zijn. Ook een welgemeende bedankt aan alle (schoon)familie en vrienden, die mij door dik en dun steunden.

En tot slot, Inge, tijd voor jouw paragraaf. We hebben al veel meegemaakt op onze reizen samen: met de tent door weer (regen regen regen) en wind (ook die was er zeker) over de Hardangervidda, bear proof koken in Canada en de VS (Wat! Kaas? Kaas, in onze tent?!), met de auto door (en tegen) kleine straatjes in Kroatië, vast met de jeep in de sneeuw in IJsland, in Namibië overdag omsingeld worden door olifanten en 's nachts dan de melkweg zien, zwemmen vlakbij watervallen en ara's in Costa Rica maar niet veel later dan stuijterend en slippend met de auto over een quadweg ('shortcut'), ... Maar ook dicht bij huis: de eerste oogst van ons tuintje, het wel en wee van onze kipjes, het trekken van de gasleiding, standvastige wespen, ... Kortom, we hadden al veel gekke beesten gezien, maar een doctoraat dat had ons pad nog niet gekruist. Je hebt me van start tot finish hierin gesteund. Ieder dipje werd moeiteloos uitgewist door je stralende glimlach. Bedankt om de draad op te nemen waar ik steken liet vallen en begrip te hebben voor mijn periode van social lockdown, zeker naar het einde toe (wat zeggen ze nu ook weer over die laatste loodjes?). Inge, je zorgt er iedere dag opnieuw voor dat ik de beste versie van mezelf ben. Ik wist al dat we een geweldig team waren maar dat is nog maar eens gebleken. 2017 Was het jaar van het doctoraat, maar de volgende jaren zijn voor ons. Honsie, ik zie je graag!

Ewout Ruysbergh

18 januari 2018

Table of contents

List of abbreviations	v
PhD abstract	1
1 Introduction and goals	3
2 Literature overview	9
2.1 Quorum sensing	9
2.1.1 <i>N</i> -Acyl-L-homoserine lactone (AHL) regulated quorum sensing	9
2.1.2 Quorum quenching	11
2.1.2.1 Abiotic degradation	12
2.1.2.2 Enzymatic degradation	13
2.1.3 Interkingdom signaling	15
2.1.3.1 Effect of AHLs on plants	16
2.1.3.2 Effect of plants on QS signaling	21
2.2 Cyclic lipopeptides	24
2.2.1 Introduction	24
2.2.2 Classification	24
2.2.2.1 <i>Pseudomonas</i> CLPs	24
2.2.2.2 <i>Bacillus</i> CLPs	30
2.2.2.3 Relevant CLPs produced by other microorganisms	33
2.2.3 Biosynthesis	33
2.2.3.1 Adenylation (A) domain	34
2.2.3.2 Thiolation (T) or peptidyl carrier protein (PCP) domain	35
2.2.3.3 Condensation (C) domain	36
2.2.3.4 Thioesterase (TE) domain	37
2.2.3.5 Editing domains	38
2.2.3.6 Fatty acid introduction	39
2.2.3.7 Comparison ribosomal - non-ribosomal peptide synthesis	40
2.2.4 Regulation of CLP production	40
2.2.4.1 Regulation of CLP production in <i>Pseudomonas</i>	41

2.2.4.2	Regulation of CLP production in other bacteria	43
2.2.5	Natural functions	44
2.2.6	Commercial applications of bacterial CLPs	46
2.3	Concluding remarks	49
3	Results and discussion	51
3.1	Synthesis and analysis of stable isotope-labelled <i>N</i> -acyl-L-homoserine lactones	51
3.1.1	Introduction	52
3.1.2	Synthesis of unlabelled AHLs	53
3.1.3	Synthesis of a monodeuterated HO-AHL	55
3.1.4	Synthesis of dideuterated AHLs	56
3.1.5	GC-MS analysis of deuterated AHLs	62
3.1.6	Synthesis of deuterated AHL-degradation products	66
3.1.7	Conclusion	67
3.2	Evaluation of the chemical reactivity of <i>N</i> -(3-hydroxyacyl)-L-homoserine lactones and derivatives	69
3.2.1	Introduction	70
3.2.2	Rearrangement of <i>N</i> -(3-hydroxyacyl)-L-homoserine lactones	71
3.2.3	Rearrangement of <i>N</i> -(3-hydroxynonanoyl)-L-serine	72
3.2.4	Cyclization of <i>N</i> -(3-hydroxyacyl)amino acids	75
3.2.5	Cyclization of <i>N</i> -(3-hydroxyacyl)amino acids with a deprotectable group at nitrogen	81
3.2.6	Application of photoremovable protecting groups (PPGs)	85
3.2.7	PPG-protected <i>N</i> -(3-hydroxyacyl)-L-homoserine lactones	92
3.2.8	Post-cyclization modification	94
3.2.9	Pseudo-prolines (Ψ Pro)	95
3.2.10	Conclusion	107
3.3	The influence of quorum sensing signal molecules on plants and fungi	109
3.3.1	Introduction	110
3.3.2	Evaluating the effect of AHLs on the growth of lettuce	112
3.3.3	Evaluating the effect of AHLs and TA on the growth of <i>Arabidopsis thaliana</i>	114
3.3.4	Evaluating the effect of AHLs and TA on the growth of fungi	116
3.3.5	Conclusions	117

3.4	The influence of the quorum sensing signal molecule <i>N</i> -(3-hydroxyoctanoyl)-L-homoserine lactone on the regulation of cyclic lipopeptide production by <i>Pseudomonas</i> sp. CMR12a	119
3.4.1	Introduction	120
3.4.2	Recycling of the fatty acid tail of HO-AHLs into CLPs	121
3.4.3	Effect of HO8 on the swarming phenotype of <i>Pseudomonas</i> sp. CMR12a and its QS mutants	125
3.4.4	Possible QS-regulated secretion of CLPs	127
3.4.5	Quantification of CLPs	128
3.4.6	Interaction orfamide-sessilin	135
3.4.7	Conclusions	137
4	Perspectives	139
5	Experimental part	147
5.1	General methods	147
5.2	Synthesis of deuterated AHLs	149
5.3	GC-MS conditions for the analysis of deuterated AHLs	161
5.4	Synthesis of 1,4-oxazepane-2,5-diones	162
5.5	Biotesting	181
6	Summary	185
7	Samenvatting	193
8	Appendix	201
	References	209
	Curriculum Vitae	227

List of abbreviations

A domain	adenylation domain
AA	amino acid
ACC	acetyl-CoA-carboxylase
ACP	acyl carrier protein
ADME	absorption, distribution, metabolism and excretion
AHL	<i>N</i> -acylated-L-homoserine lactone
AIBN	azobis(isobutyronitril)
AIP	autoinducing peptide
AI-2	autoinducer-2
aq.	aqueous
Asp(3-HO)	3-hydroxyaspartic acid
<i>a</i> Thr	<i>allo</i> -threonine
Bn	benzyl
BSTFA-TMCS	<i>N,O</i> -bis(trimethylsilyl)trifluoroacetamide-trimethylchlorosilane
C domain	condensation domain
CAN	ceric ammonium nitrate
Cbz	carboxybenzyl
CDA	calcium-dependent antibiotic
CFU	colony forming units
CLP	cyclic lipopeptide
CV	column volume
C _x	<i>N</i> -acyl-L-homoserine lactone with x the number of carbon atoms in the acyl chain
Dab	2,4-diaminobutyric acid
DCC	<i>N,N'</i> -dicyclohexylcarbodiimide
DDQ	2,3-dichloro-5,6-dicyano-1,4-benzoquinone
Dhb	2,3-dehydroaminobutyric acid

DMAP	4-(<i>N,N</i> -dimethylamino)pyridine
DMF	dimethylformamide
DMP	2,2-dimethoxypropane
DMSO	dimethyl sulfoxide
DSF	diffusible signal factor
EDC	1-ethyl-3-(3-dimethylaminopropyl)carbodiimide
EI	electron impact
equiv	equivalent
ESI-MS	electrospray ionization mass spectrometry
FA	fatty acid
FAAH	fatty acid amide hydrolase
FDA	food and drug administration
GC	gas chromatography
gfp	green fluorescent protein
GPCR	G-protein-coupled receptor
HIV-1 IN	human immunodeficiency virus type-1 integrase
HL	homoserine lactone
HOFA	β -hydroxy fatty acid
HO _x	<i>N</i> -(3-hydroxyacyl)- <i>L</i> -homoserine lactone with <i>x</i> the number of carbon atoms in the acyl chain
HPLC	high-performance liquid chromatography
HSe	homoserine
IDMS	isotope dilution mass spectrometry
IR	infrared
ISR	induced systemic resistance
LB medium	Luria Bertani medium
LC	liquid chromatography
LDA	lithium diisopropylamide
LPS	lipopolysaccharide
MIC	minimum inhibitory concentration
MPAK	mitogen-activated protein kinase

MRSA	methicillin-resistant <i>Staphylococcus aureus</i>
MS medium	Murashige and Skoog medium
MsCl	methanesulfonyl chloride
MTA	methylthioadenosine
NA	not applicable
NAE	<i>N</i> -acyl ethanolamines
NBS	<i>N</i> -bromosuccinimide
NIR	near infrared
NM	not mentioned
NMA	<i>N</i> -methylacetamide
NMM	<i>N</i> -methylnmorpholine
NMR	nuclear magnetic resonance
NOESY	nuclear Overhauser effect spectroscopy
NRPS	non-ribosomal peptide synthetase
OD	optical density
Orn	ornithine
oxox	<i>N</i> -(3-oxoacyl)- <i>L</i> -homoserine lactone with x the number of carbon atoms in the acyl chain
o.n.	overnight
PCN	phenazine-1-carboxamide
PCP	peptidyl carrier protein
PHA	poly- β -hydroxyalkanoates
PKS	polyketide synthase
PMB	<i>p</i> -methoxybenzyl
ppant	4'-phosphopantetheinyl
PPG	photoremovable protecting group
PPTase	phosphopantetheinyl transferase
PQS	<i>Pseudomonas</i> quinolone signal
PTSA	<i>p</i> -toluenesulfonic acid
QS	quorum sensing
r.t.	room temperature

SA	salicylic acid
SAM	<i>S</i> -adenosyl-L-methionine
SIM	selected ion monitoring
T domain	thiolation domain
TA	tetramic acid
TE domain	thioesterase domain
TEAF	triethylammonium formate
TES	<i>N</i> -[tris-(hydroxymethyl)methyl]-2-aminoethanesulfonic acid
TFA	trifluoroacetic acid
THF	tetrahydrofuran
Thr(4-Cl)	4-chlorothreonine
TIC	total ion chromatogram
TLC	thin layer chromatography
TMS	trimethylsilyl
TMSOTf	trimethylsilyl trifluoromethanesulfonate
UV	ultraviolet
VRE	vancomycin-resistant <i>Enterococci</i>
WLIP	white line-inducing principle
XIAP	X-linked inhibitor of apoptosis protein
ΨPro	pseudo-proline

PhD abstract

Quorum sensing, the phenomenon in which bacteria express their genes in a cell density-dependent manner, plays a pivotal role in the production of several secondary metabolites. Gram-negative bacteria rely mostly on *N*-acylated-L-homoserine lactones (AHLs) for this type of regulation. Besides communication between bacteria, AHLs are also involved in bacteria-plant interactions (the so-called interkingdom signaling). Cyclic lipopeptides are an example of a class of secondary metabolites with interesting activities, in which quorum sensing can play an important regulating role. The overall goal of this PhD research was to study the role of a certain class of AHLs, *N*-(3-hydroxyacyl)-L-homoserine lactones, in nature.

In a first part of this PhD thesis several isotope-labelled AHLs, belonging to all three major classes of AHLs, were synthesized. To further extend the possible applications of these compounds, two important AHL-degradation products, a tetramic acid and a *N*-acyl-L-homoserine were synthesized departing from these deuterated compounds. To aid their application as internal standards in isotope dilution mass spectrometry, the MS fragmentation pattern was studied extensively. The isotope-labelled AHLs can be used as well as a tool to study the metabolization of the fatty acid side chain of AHLs.

In a second part, the spontaneous rearrangement of *N*-(3-hydroxyacyl)-L-homoserine lactones, which proved to be very unlikely, was investigated. This investigation resulted however in the successful development of a synthetic entry toward 1,4-oxazepane-2,5-diones, which are extremely difficult to synthesize due to the presence of a lactam with a preference for the *trans*-conformation and a labile lactone moiety in one ring structure. However, some of the reported natural products with such a 1,4-oxazepane-2,5-dione core display interesting biological activities. By applying the disclosed methodology on the synthesis of the natural product serratin, the incorrect structural assignment of this compound was identified.

The following two research parts aimed to gain a better understanding of the biocontrol activity of *Pseudomonas* species CMR12a and more specific the role of quorum sensing. Therefore, the effect of one of its quorum sensing signal molecules, *N*-(3-hydroxydodecanoyl)-L-homoserine lactone, on plant growth was studied. However, no direct growth promoting effect could be observed. No growth promoting or inhibiting effects were observed either for a tetramic acid, which is formed via the rearrangement of an oxo-AHL. On the other hand, as

an antifungal effect was found for this compound, which has already known algicidal effects, the use in hydroculture could form an interesting application, although further research is required. Subsequently, the profound effect of another QS signal molecule of this *Pseudomonas* strain, *N*-(3-hydroxyoctanoyl)-L-homoserine lactone, on its cyclic lipopeptide production was demonstrated. It was hypothesized that quorum sensing plays a crucial role in determining the swarming behavior of this *Pseudomonas* sp. CMR12a. The influence of QS goes via an elegant fine-tuning of the ratio of the two produced CLPs, orfamide and sessilin, via the control of orfamide production.

Chapter 1

Introduction and goals

For many years, researchers thought of bacteria as individual cells, unable to interact with one another. However, this view changed dramatically with the discovery of population density-dependent light production by the marine bacterium *Vibrio fischeri* some decades ago.¹ Individual cells of *V. fischeri* do not produce light, but when accumulated in high cell densities such as in the light organ of the Hawaiian bobtail squid *Euprymna scolopes*, bioluminescence is observed (Figure 1.1, left). By providing a nutrient-rich environment, the squid can benefit from this bioluminescence to counter-illuminate itself and hide its silhouette from predators on clear nights.² The pineapplefish (*Cleidopus gloriamaris*) uses a similar light organ as a spot to search for prey at night and to communicate with its own kind (Figure 1.1, right).²

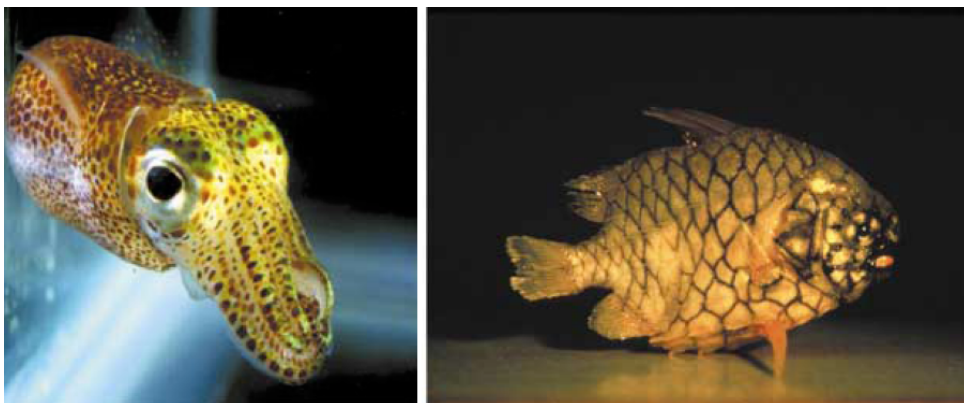


Figure 1.1. Bioluminescence in marine organisms. Left: *Euprymna scolopes*. Right: *Cleidopus gloriamaris*.²

Because this type of gene regulation is linked to the population density or quorum, the term ‘quorum sensing’ (QS) was used to describe this phenomenon. First thought to be restricted to a limited number of bacteria, QS was later on found to be present in many other bacteria. To communicate with each other, the bacteria rely on small, diffusible signal molecules, termed autoinducers. Once a certain threshold concentration of these autoinducers is reached, several phenotypes can be activated. A chemically diverse array of these autoinducers is known (Figure 1.2). One of the most studied types are *N*-acylated-L-homoserine lactones (AHLs), which are used by Gram-negative bacteria. The general structure of an AHL consists of a homoserine lactone ring coupled to a variable *N*-acyl chain. This acyl chain can contain four to eighteen car-

bon atoms and the third carbon atom can be unfunctionalized (C4-C18 **1**) or carry a hydroxy- (HO4-HO18 **2**) or oxo-group (oxo4-oxo18 **3**).^{2,3} Recently, an AHL **4** lacking the typical acyl chain but with a *p*-coumaryl group instead was discovered, expanding the range of possible AHLs.⁴ AHL-Mediated QS has been observed in more than 70 genera of Gram-negative proteobacteria. Several other QS signal molecules are known, for example *Streptomyces* species use γ -butyrolactones **5** as signal compounds. *Pseudomonas aeruginosa* uses 2-heptyl-3-hydroxy-4(1*H*)-quinolone, named *Pseudomonas* quinolone signal (**6**) (PQS), as an additional autoinducer beside AHLs. Some other QS signal molecules are derived solely from fatty acids such as the diffusible signal factor (**7**) (DSF) used by *Xanthomonas* or 3-hydroxypalmitate methyl ester **8** which is used by *Ralstonia*.⁵ Gram-positive bacteria rely on cyclic peptides such as autoinducing peptide III (**9**) (AIP-III) to coordinate their gene expression in a cell density-dependent manner. Furanosyl borate diester or autoinducer-2 (**10**) (AI-2) is used as a signal molecule in interspecies cell-to-cell communication, although there remains some controversy about its function.⁵ In this PhD thesis the focus will be on AHL-mediated QS.

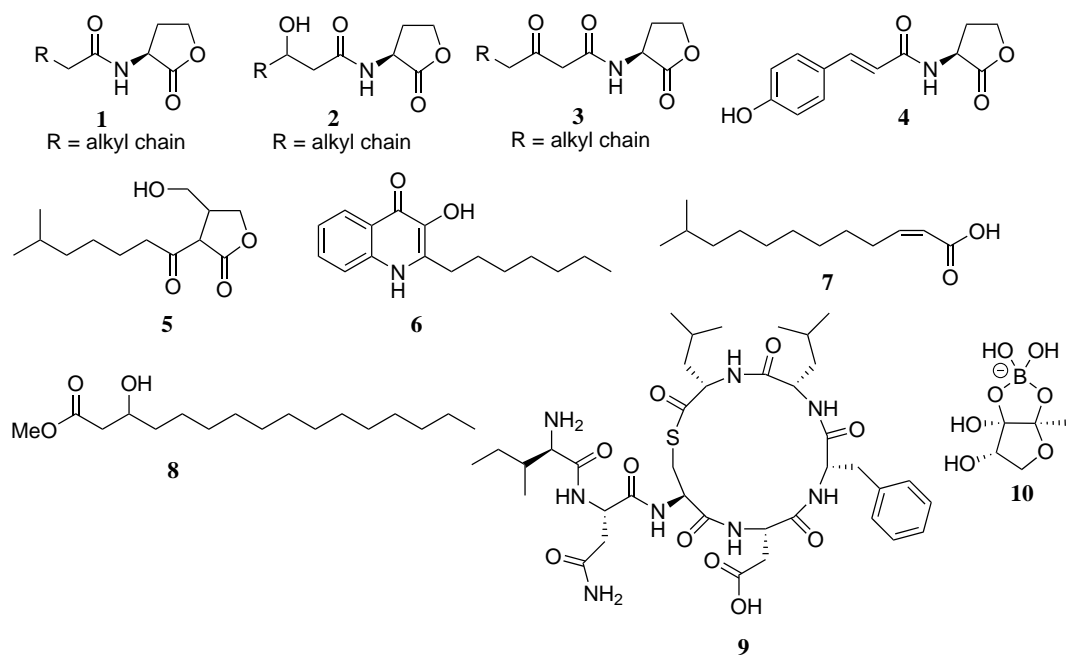
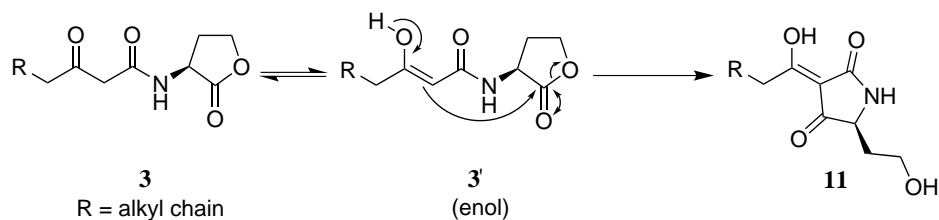


Figure 1.2. Some examples of QS signal molecules, demonstrating the diversity of compounds used as QS signals by bacteria.

QS enables bacteria to express certain genes under the right conditions, e.g. only inducing light production when a sufficient quorum is reached to generate a strong light signal or delay virulence until sufficient bacteria are present to overwhelm the host and mount a successful infection.² Instead of sensing the population density, it has been argued that autoinducers could be used to determine whether secreted compounds move rapidly away from the cell in a process

called diffusion sensing. As a high diffusion rate corresponds to a low concentration of signal molecules and *vice versa*, bacteria can determine whether it is advantageous to excrete certain enzymes or metal chelators.^{6,7} Both concepts are unified in the efficiency sensing theory, postulating that bacteria sense the combination of cell density, spatial distribution and mass transfer to fine-tune their actions.⁸ AHLs themselves can also have another function than solely signaling. *N*-(3-Oxoacyl)-L-homoserine lactones **3** for example can rearrange to tetramic acids **11** (Scheme 1.1) with interesting bioactivity such as iron chelation and antimicrobial activity.⁹



Scheme 1.1. Rearrangement of *N*-(3-oxoacyl)-L-homoserine lactones **3** to tetramic acids **11**.

QS Plays a pivotal role in both pathogenic and symbiotic bacteria-host interactions. Processes regulated by QS include bioluminescence, conjugation, pigment production, antibiotic production, virulence, root nodulation, motility, biofilm formation, etc.^{2,3} Several clinically relevant pathogens, e.g. *Pseudomonas aeruginosa*, rely on QS systems to regulate their virulence. Therefore, a great interest exists to use QS as a novel target to tackle bacterial infections.² As the emergence of resistant bacteria poses a rising threat to the effectiveness of antibiotics, QS could form an interesting target to combat several bacterial pathogens. Unlike traditional antibiotics, no harsh selective pressure for development of resistance is applied by QS inhibitors as QS is not essential for microbial survival.^{10,11} Several natural and synthetic compounds exist which are able to interfere with QS.^{5,12,13} Alternatively, several enzymes such as lactonases and acylases (also referred to as amidases) are able to degrade AHLs.⁵

When Alexander Fleming serendipitously discovered penicillin in 1928, by observing that a contaminating *Penicillium* fungus was able to kill the cultured bacteria, mankind had finally the powerful means to combat bacterial infections.¹⁴ After the penicillins (belonging to the β -lactam group), many other classes of antibiotics have been discovered between 1940 and 1970 (the golden age of antibiotics). After the 1970s the pipeline with new antibiotics started to run dry (Figure 1.3). However, already in 1960 the first resistant bacterial strains occurred and due to misuse and over-usage of antibiotics, the number of resistant human pathogens is increasing. This causes the urgent need to find new antibiotics, able to circumvent the resistance of these bacteria. Rather than derivatives of known compound classes, totally new scaffolds are preferred as they could have a totally new target for which bacteria have not yet acquired resistance. One

example of such a class with presumably a different mode of action are the lipopeptides. The use of these compounds as antibiotics was approved in 2003.^{15,16}

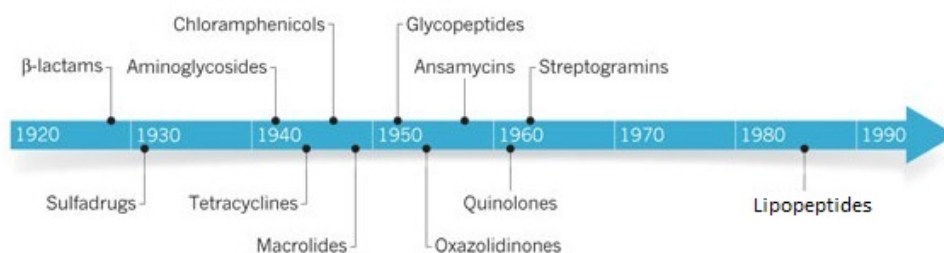


Figure 1.3. Antibiotic discovery time line. Reprinted from Lewis, 2012.¹⁵

Cyclic lipopeptides (CLPs) are a diverse class of compounds composed out of a fatty acid tail linked to an oligopeptide moiety. This oligopeptide contains 7-25 amino acids and 4-14 of these residues form a cyclic structure. As these compounds are synthesized non-ribosomally, unusual amino acids, such as D-amino acids, β -amino acids and *N*-methylated amino acids, can often be found in these compounds. As an example of a CLP, the structure of the commercial CLP-antibiotic daptomycin (**12**) is represented in figure 1.4.^{17,18}

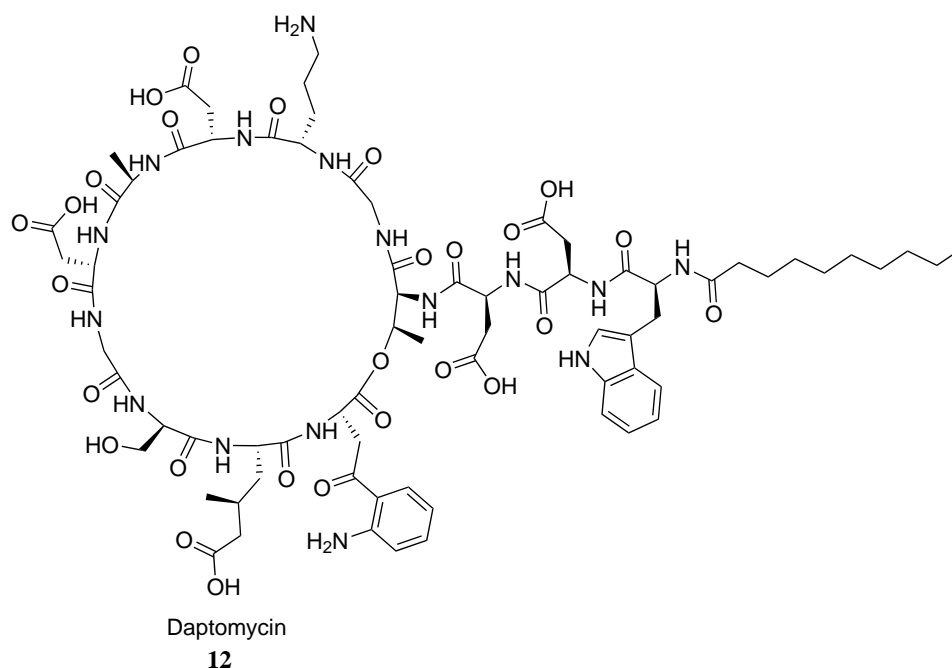


Figure 1.4. Chemical structure of the CLP-antibiotic daptomycin (**12**).

The *Pseudomonas* genus represents an interesting source for CLPs.^{18,19} These Gram-negative bacteria can be found in many different niches and some are plant- and human-pathogenic whereas other strains can promote plant growth and offer protection against pathogens. The CLPs produced by these bacteria can serve several purposes such as biofilm formation, virulence, motility, etc.²⁰ Although the production of some CLPs is AHL-controlled,²¹⁻²⁵ these are

the exception rather than the rule.

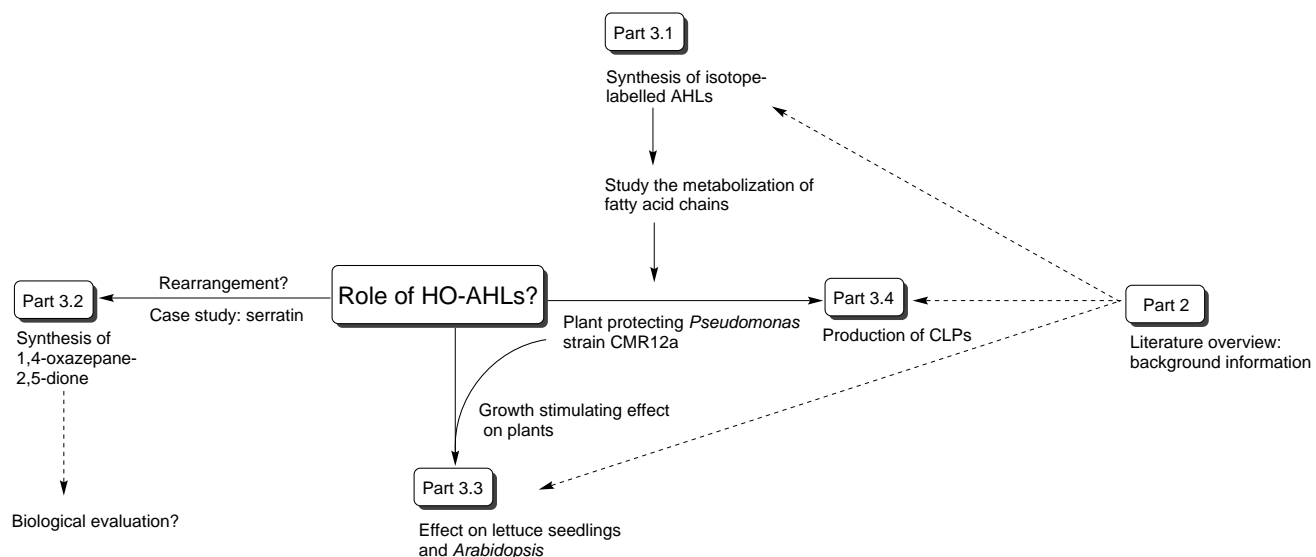
The overall structure of this PhD research is schematically presented in scheme 1.2 and the different goals are discussed hereafter. The main goal is to obtain a better understanding of the role of *N*-(3-hydroxyacyl)-L-homoserine lactones **2** in nature.

To be able to study the metabolization of these AHLs, a first goal is to develop a protocol to synthesize isotope-labelled AHLs. In order to use these labelled AHLs to study the metabolization of the fatty acid side chain, the isotope label will be included in the acyl chain of the AHL. To be able to synthesize a broad library of tailor-made deuterated AHLs, the goal is to construct a robust synthetic route toward different AHLs starting from one, easily accessible deuterated building block.

A second research interest is to study the reactivity of these QS signal molecules **2**. It is known that *N*-(3-oxoacyl)-L-homoserine lactones **3** can rearrange to tetramic acids **11** (Scheme 1.1) with fascinating biological properties. The goal of this part of the thesis is to evaluate if HO-AHLs **2** can participate in a similar rearrangement wherein the hydroxy group attacks the lactone to form a 1,4-oxazepane-2,5-dione. Several natural products, such as serratin, containing such a seven-membered core have been reported. The conditions required for such a rearrangement to occur will be scrutinized.

Subsequently the biological activity of *N*-(3-hydroxyacyl)-L-homoserine lactones **2** will be investigated. The promising biocontrol strain *Pseudomonas* sp. CMR12a possesses two QS systems using HO-AHLs **2**. In previous research, it was found that one of its QS molecules had growth stimulatory effects on lettuce plants. Therefore, to fully understand the biocontrol properties of this strain, these growth stimulatory effects of AHLs on plants will be studied in the third part of this PhD research. *Pseudomonas* sp. CMR12a produces two types of CLPs which play an important role in its biocontrol capacity. The regulation of this CLP-production will therefore be subject of a thorough investigation as well. The role of AHLs in this regulation will be evaluated. To test if the fatty acid moieties of certain AHLs get recycled into the CLPs, the isotope-labelled AHLs which were synthesized in the first part of this research work, will be used.

To give the reader a better insight in AHL-mediated QS, a short overview of this type of QS is presented in the literature overview. Also the interplay between plants and AHLs will be discussed. In the second part of the literature overview, the different types of CLPs are mentioned, followed by the biosynthesis of CLPs, with special attention for the (QS) regulation of CLP production.



Scheme 1.2. Schematic representation of the structure of this PhD research.

Chapter 2

Literature overview

2.1 Quorum sensing

2.1.1 *N*-Acyl-L-homoserine lactone (AHL) regulated quorum sensing

To coordinate their behavior in a cell density-dependent manner, Gram-negative bacteria mostly rely on *N*-acylated-L-homoserine lactones (AHLs). A general representation of a system regulated by AHL-mediated QS is depicted in figure 2.1.² This QS system typically consists of two components: a LuxI-homologue responsible for the synthesis of the AHL, and a LuxR-homologue which detects the AHL and stimulates the translation of genes preceded by a so-called *lux*-box. Some bacteria contain more than one QS system. *P. aeruginosa* for example possesses LasI/LasR and RhlI/RhlR which control biofilm formation and exoenzyme and virulence-factor synthesis in a hierarchical manner.³

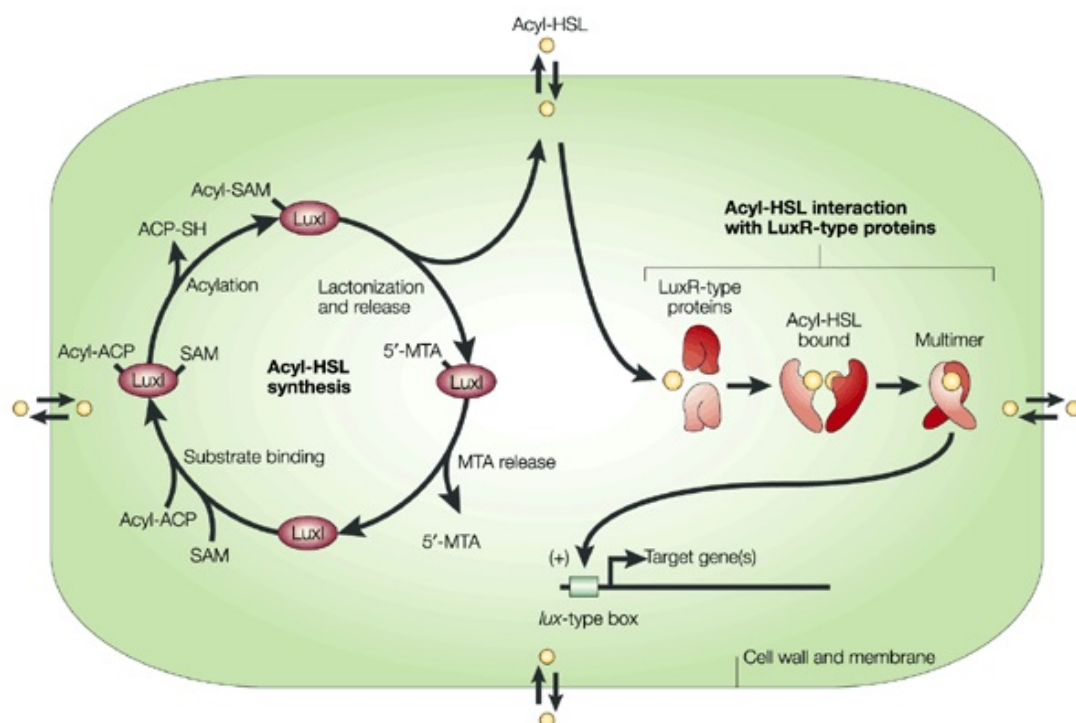


Figure 2.1. A representation of a typical LuxI/LuxR QS circuit. Small circles represent AHLs. 5'-MTA: 5'-methylthioadenosine, ACP: acyl carrier protein, SAM: S-adenosyl-L-methionine. Figure reprinted from Fuqua and Greenberg, 2002.²

AHLs are produced by a LuxI-type protein starting from *S*-adenosyl-L-methionine (SAM) and an acylated acyl carrier protein (acyl-ACP) as substrates.^{3,26} The acyl-ACP, 3-oxoacyl-ACP and 3-hydroxyacyl-ACP are intermediates of the fatty acid metabolism, explaining the fact that the majority of AHLs has an acyl chain with an even number of carbon atoms.^{26,27} However, some AHLs with an odd acyl chain are known.^{28,29} The link between fatty acid metabolism and AHL-synthesis in the case of *P. aeruginosa*, is represented in figure 2.2.²⁷

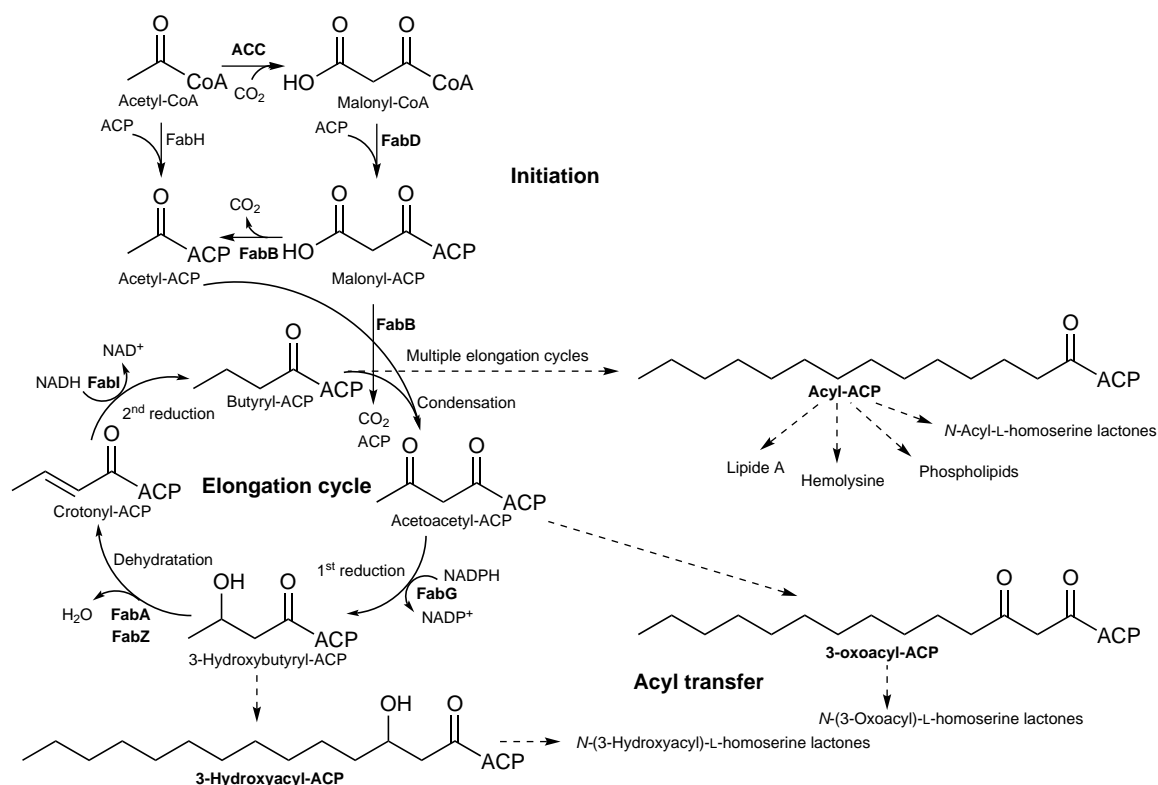


Figure 2.2. The link between the biosynthesis of fatty acids and AHLs in *P. aeruginosa*. ACC: acetyl-CoA-carboxylase, ACP: acyl carrier protein.²⁷

The LuxI-enzyme catalyzes the nucleophilic attack of the amino group of SAM **13** on the acyl chain loaded onto the ACP. Subsequently, a lactonization occurs and the AHL and 5'-methylthioadenosine (5'-MTA) **14** are released from the enzyme (Figure 2.3). The size of the hydrophobic pocket of the LuxI-enzyme determines the length of the acyl chain and consequently the AHL that is synthesized. Also the functionality of the acyl chain on the 3-position is determined by hydrogen bonding inside this hydrophobic pocket, allowing different LuxI-homologues to synthesize different AHLs from the same acyl-ACP pool.³⁰⁻³² Whereas short-chain AHLs can diffuse freely out of the cells, long-chain AHLs rely on active transport to be excreted.³³ In the supernatant of planktonic *P. aeruginosa* cultures, grown at 37 °C under shaking conditions, concentrations of 1 to 10 μM of oxo12 **3i** are observed.^{34,35} However, in *P. aeruginosa* biofilms, concentrations as high as 600 μM have been measured.³⁴

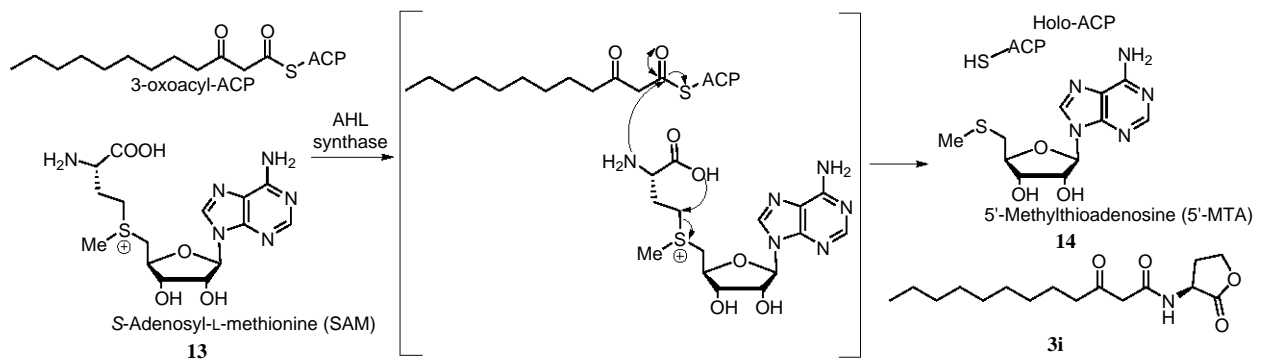
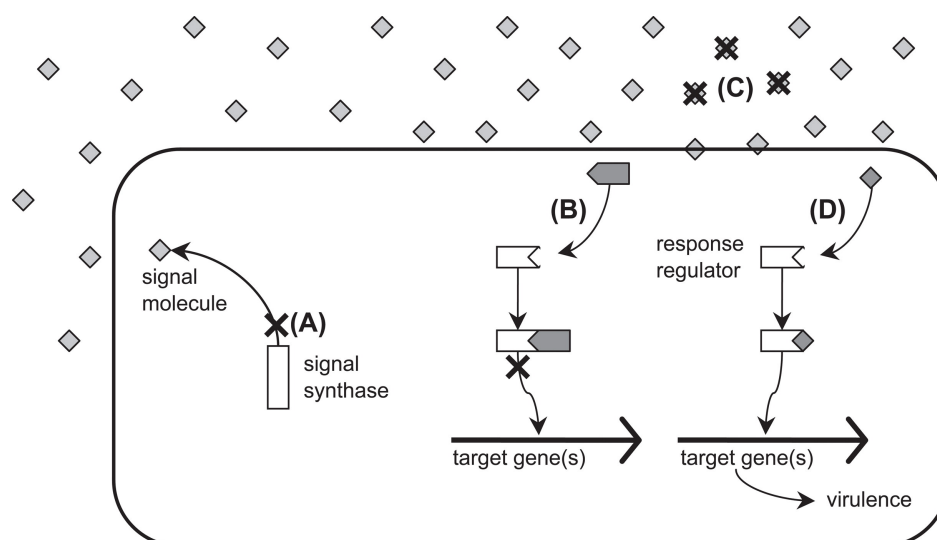


Figure 2.3. LuxI-directed biosynthesis of oxo12 **3i**.³¹

The LuxR-homologue contains two structurally different domains connected by a linker domain: a DNA-binding and an AHL-binding domain. When a certain threshold concentration is reached, the AHL binds to the LuxR-homologue. Without the AHL ligand, LuxR proteins are typically unstable and degrade rapidly. By binding to the AHL, a large conformational change occurs and the DNA-binding domain of the LuxR-protein is exposed, allowing interaction with the dyad symmetric *lux*-box. Typically LuxR-protein dimerization is also promoted upon binding an AHL and those multimers bind the promoter DNA sequences and cause transcription of certain target genes (Figure 2.1).^{3,12,32} Whereas many R-proteins act as transcriptional activator, some function rather as a repressor, blocking the transcriptional activation of certain genes by RNA polymerase in the absence of a sufficient amount of AHLs.¹² Also the expression of the LuxI-proteins is stimulated by AHL-bound LuxR-proteins, hence explaining the name autoinducer.¹³

2.1.2 Quorum quenching

There are several phenomena and mechanisms which are able to interfere with quorum sensing (Figure 2.1).¹⁰ To describe all these processes that are able to disrupt quorum sensing, the term quorum quenching is used.⁵ In this section, only abiotic and enzymatic degradation of the AHL signal molecules will be discussed.



Scheme 2.1. Different strategies to interfere with QS. The small squares represent QS signal molecules. (A) Inhibition of QS signal generation. (B) Application of QS antagonists to prevent signal transduction. (C) Inactivation of the QS signal molecules. (D) Premature activation of QS via the application of QS agonists. Figure reprinted from Defoirdt *et al.*¹⁰

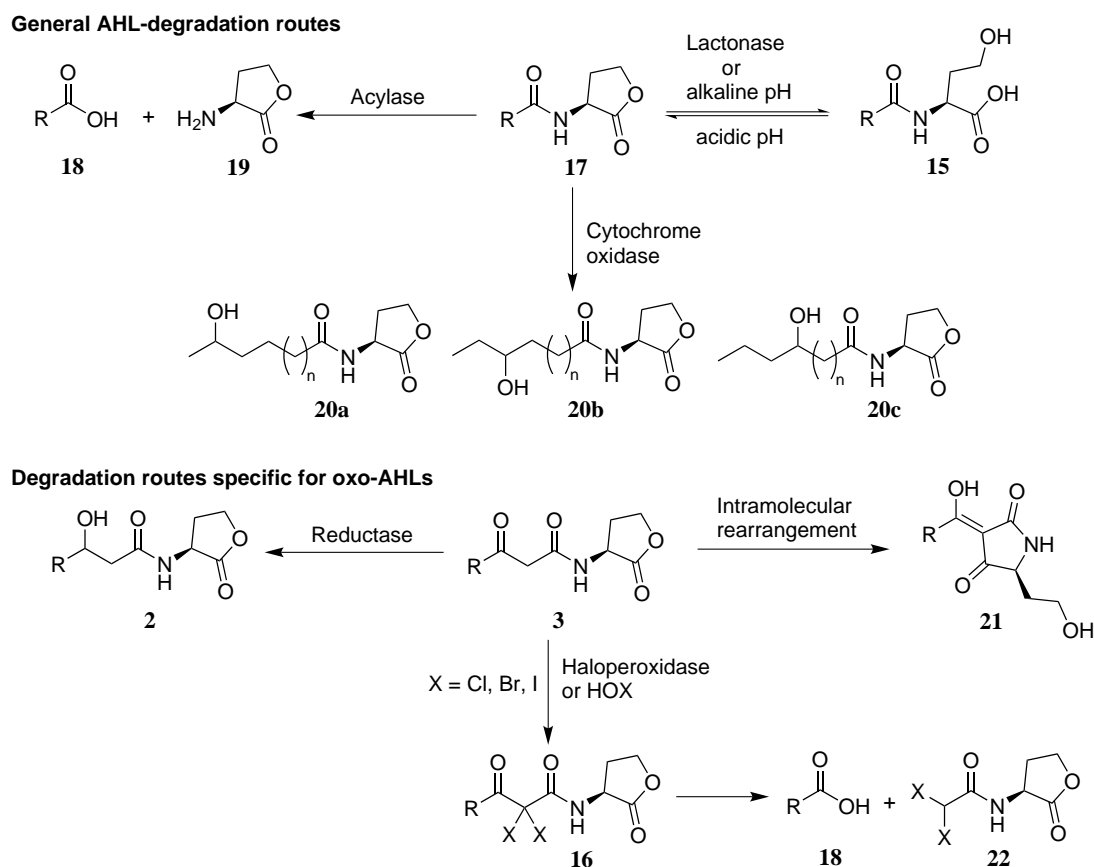
2.1.2.1 Abiotic degradation

The lactonolysis of AHL-molecules occurs spontaneously in aquatic solutions to produce the corresponding *N*-acyl-L-homoserines **15**.⁷ Short-chain AHLs degrade faster than long-chain AHLs and this degradation goes faster at higher temperature and higher pH.^{7,36} For example the half-life of C6 **1c** at pH 5.5 and 20 °C is over 8 d whereas at pH 8.5 and 20 °C, this is less than 6 h.³⁷ As the lactone ring is crucial for signal recognition, all QS activity is lost after this hydrolysis. However, at low pH these ring-opened AHLs **15** can cyclize again, albeit to a limited extent (Scheme 2.2).^{36,38}

A second type of abiotic degradation can occur upon reaction with oxidized halogen antimicrobials. These compounds are able to inactivate oxo-AHLs **3**, but are inactive toward unsubstituted ones (Scheme 2.2). This deactivation is caused by reaction of the oxo-AHL **3** with two hypobromous or hypochlorous acid molecules, followed by the cleavage of the resulting *N*-(2,2-dihalo-3-oxoacyl)-L-homoserine lactones **16**.^{39,40}

Oxo-AHLs **3** can be degraded via another route as well (Scheme 2.2). Instead of lactonolysis, an intramolecular Claisen-like rearrangement leads to tetramic acids **11**. These rearrangement products **11** exhibit antimicrobial activity against Gram-positive bacteria (EC₅₀: 8-55 μM), presumably by causing cell lysis after interaction with the cell membrane.^{9,41} Tetramic acids **11** can bind iron in a 3:1 complex and can function as primordial siderophores.⁹ Although at neutral pH in aqueous medium, the reaction rate to form the ring-opened degradation product **15** is three-

fold higher than the formation rate of tetramic acid, tetramic acids **11** are stable compounds and can accumulate in the environment.⁹ For example, in sputum samples of cystic fibrosis patients, oxo12 **3i** was detected in concentrations ranging from 20 nM to 7 μM, whereas the corresponding tetramic acid was found in concentrations of 13-900 nM.⁴²



Scheme 2.2. Different abiotic and enzymatic degradation routes of AHLs.

2.1.2.2 Enzymatic degradation

There are four classes of AHL-inactivating enzymes known (Scheme 2.2). They can be produced by organisms lacking an AHL-regulated QS system to gain a competitive advantage over AHL-producers. Alternatively, it has been suggested that some Gram-positive bacteria inactivate oxo-AHLs **3** to prevent the formation of the toxic tetramic acids **11**. Also utilization of AHLs as a carbon and nitrogen source is a possibility. Some AHL-producers are able to inactivate their own signals as well, either to recycle them as nutrients or to remove old signals (signal clearance).⁵ However, it must be kept in mind that AHL-degradation might not be the primary role of all these enzymes, as several other compounds can function as substrate for these enzymes.⁴³

Lactonases

Lactonases are enzymes that catalyze the opening of the homoserine lactone ring and typically display a broad substrate specificity (Scheme 2.2). The first lactonase that was reported, AiiA, can be found in several *Bacillus* strains.⁴⁴ Transgenic tobacco plants expressing this enzyme were more resistant toward the soft root rot disease caused by *Pectobacterium carotovora*, which uses oxo6 **3c** to regulate its virulence by the production of cell wall degrading enzymes.⁴⁵ *Agrobacterium tumefaciens* produces two lactonases, AiiB and AttM, which are able to degrade its own AHL oxo8 **3e**. Added AHLs cannot be used as the sole carbon or nitrogen source. A clearing function, to prevent premature activation of the QS operon, is therefore proposed to describe the biological role of these enzymes in *A. tumefaciens*.^{5,46}

Paraoxonases degrade AHLs in a similar manner and rely on a metal ion in the active site to make the carbonyl carbon atom more electrophilic. These enzymes can be found in serum and tracheal epithelial cells of mammals and efficiently inactivate long-chain AHLs.^{5,47}

During a screening of 16 fungal isolates, lactonase activity was discovered in two of these forest root-associated fungi.⁴⁸ The basidiomycetous yeast *Trichosporon loubieri*, isolated from tropical wetland waters, displayed a similar lactonase activity toward AHL with an acyl chain ranging from 4 to 10 carbon atoms.⁴⁹

Acylases or amidases

Acylases or amidases cleave the AHL irreversibly at the amide bond and release a homoserine lactone **19** and a fatty acid **18** (Scheme 2.2). Whereas lactonases target the common lactone core, acylases can be acyl chain length specific. *Variovax paradoxus* VAI-C cleaves AHLs via an acylase enzyme, and can use AHLs as the only carbon and nitrogen source.⁵⁰ A *Ralstonia* strain isolated from a mixed biofilm, contains the AiiD enzyme which has a similar AHL-inactivation mechanism.⁵¹ Both long and short-chain AHLs can be metabolized by these strains.^{50,51}

Also *P. aeruginosa* displays AHL-acylase activity but only for AHLs with an acyl chain composed of eight or more carbon atoms.⁵² This preference for long-chain AHLs might be linked with one of its own QS signal compounds, oxo12 **3i**. *Pseudomonas* strains expressing this type of enzyme are able to use AHLs as the sole carbon and energy source.^{5,53} Porcine kidney acylase I belongs to this class of AHL-degrading enzymes as well.⁵ Also plants contain enzymes, fatty acid amide hydrolases (FAAH), with similar activity (*vide infra*).^{54,55}

Haloperoxidases

This third class of enzymes is able to inactivate oxo-AHLs **3** via a similar mechanism as oxidized halogen antimicrobials (Scheme 2.2). The electrophilic halogenation of oxo-AHLs **3** is

hydrogen peroxide dependent and the active site of these enzymes typically relies on vanadium.⁵⁶ The resulting *N*-(2,2-dihalo-3-oxoacyl)-L-homoserine lactones **16** still display QS activity, so the cleavage of the acyl chain to yield a *N*-(2,2-dihaloacetyl)-derivative **22** is the crucial step leading to a complete loss of QS activity.⁵⁷

These enzymes are often encountered in marine organisms, for example in the brown alga *Laminaria digitata*,⁴⁰ the benthic diatom *Nitzschia cf. pellucida*,⁵⁷ and the red alga *Delisea pulchra*,⁵⁸ and are associated with the prevention of microbial fouling by inhibiting QS regulated biofilm formation.⁴⁰ However, haloperoxidases have also been found in terrestrial fungi such as *Curvularia inaequalis*,⁵⁹ although the inactivation of QS signal molecules by these fungal enzymes has yet to be reported.

Oxidoreductases

Reductases will convert the keto functionality of oxo-AHLs **3** to a hydroxy group. The resulting HO-AHL **2** are sometimes still active but often display a strongly reduced activity. The Gram-positive bacterium *Rhodococcus erythropolis* W2 uses such a reductase to convert oxo-AHLs with an acyl chain of at least eight carbon atoms to the corresponding HO-derivatives. This strain also contains an acylase, enabling it to use AHLs as the sole carbon and nitrogen source.⁶⁰

Cytochrome oxidases can be found in bacteria, archaea and eukaryotes and catalyze the oxidation of the acyl chain to form hydroxylated products **20** (Scheme 2.2). Cytochrome P450 monooxygenase from *Bacillus megaterium* efficiently oxidates AHLs at the ω -1, ω -2 or ω -3 carbon atom of the acyl chain. The resulting hydroxylated AHLs **20a–c** still retain QS activity, albeit strongly reduced compared to native AHLs **17**. AHL-degradation products **15** and **18** can be hydroxylated as well by these enzymes.⁶¹

2.1.3 Interkingdom signaling

Prokaryotes and eukaryotes have coexisted and interacted for a very long time, exposed to each other's soluble signal compounds. As a consequence, organisms of both kingdoms have learned to perceive and react to these different compounds in a phenomenon called interkingdom signaling (Figure 2.4). It is an intriguing observation that *Pseudomonas* species found in the plant rhizosphere produce AHLs more often than their counterparts found in bulk soil.⁶² AHL-mediated QS also regulates several traits associated with plant-bacteria interactions such as biofilm formation, virulence factor production, nodulation, synthesis of degradative enzymes, etc.⁶³ As the infection of several eukaryotic hosts often depends on AHL-mediated QS, detecting these AHL molecules could give a distinct advantage.^{47,64} It is therefore not surprising that plants can 'eavesdrop' on the bacterial cross-talk via AHLs and respond in sophisticated ways.

On the other hand, plants can also actively influence this communication via the excretion of compounds with AHL-mimicking or QS-disturbing activity (Figure 2.4).⁶⁴

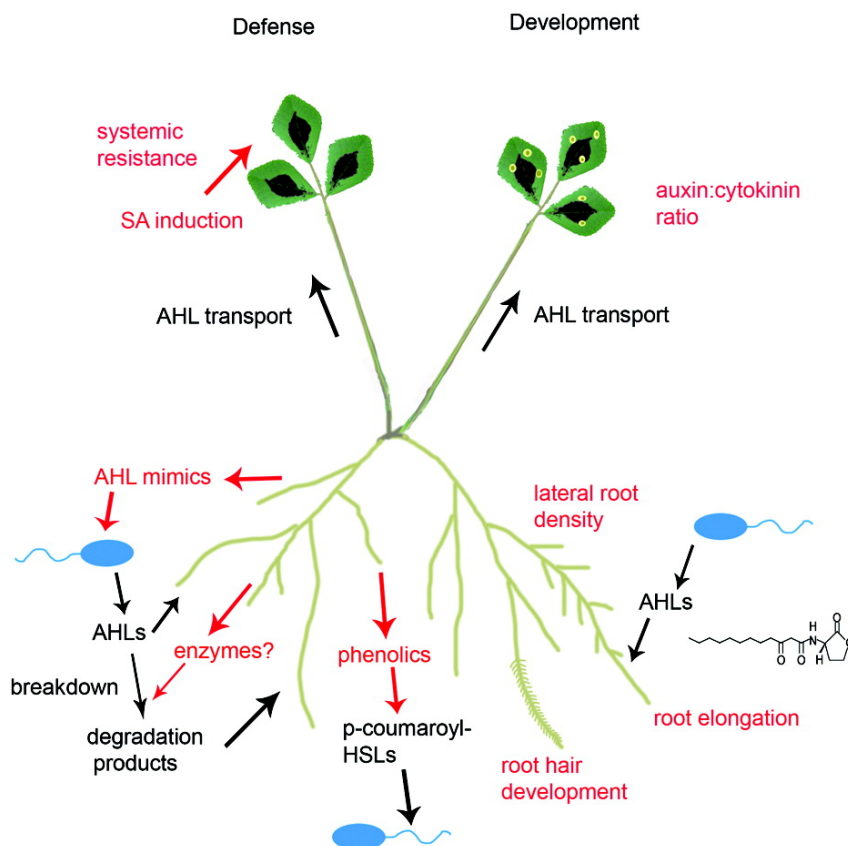


Figure 2.4. Different responses of plants to AHLs. The perception of AHLs can lead to the secretion of AHL-mimics into the rhizosphere. Some compounds out of the exudates, such as *p*-coumaric acid, can be included into bacterial AHLs. Also AHL-uptake and transportation inside the plant, or degradation via enzymes can occur. Alternatively, AHLs can induce salicylic acid (SA) accumulation in roots and shoots, which is suggested to mediate systemic resistance to pathogens. AHLs can also induce morphological changes and influence root elongation, root hair formation, and lateral root density.⁶⁵

2.1.3.1 Effect of AHLs on plants

That plants are able to detect AHLs was confirmed when model legume *Medicago truncatula* was treated with AHLs and more than 150 proteins were differently accumulated. These proteins were linked with stress and plant defense, protein degradation or processing and various primary metabolic activities. Also auxin-inducible and chalcone synthase genes were activated. Exposure to oxo16:1 **3i**, a native AHL of symbiont *Sinorhizobium meliloti*, led to a different response than when oxo12 **3i** was tested (Appendix, Table 8.1).⁶⁶ This specific response to different AHLs was also observed when the effect of AHLs on nodulation was studied. Out of several AHLs tested on *M. truncatula*, only oxo14 **3k**, which is one of the native AHLs of its symbiont *S. meliloti*, could enhance the formation of nodules on the roots. The increased

nodulation caused by oxo14 **3k** was not observed in legumes alfalfa (*Medicago sativa*) and white clover (*Trifolium repens*), showing that the response of plants toward AHLs can be highly specific.⁶⁷

One of the most astonishing effects of AHLs on plants is a clear change in plant morphology. Depending on the structure, AHLs can exert a different effect on the root architecture. When *Arabidopsis thaliana* was treated with 10 μ M of C4 **1a** or C6 **1c** in a floating hydroponic system, a 1.2-fold increase in root length was observed (Appendix, Table 8.1). This root growth promoting effect was linked to a change in the auxin/cytokinin ratio. Application of 10 μ M C8 **1e**, C12 **1i** and C14 **1k** had no effect whereas C10 **1g** had a negative influence on root growth.⁶⁸ When *A. thaliana* was treated with 10 μ M C4 **1a**, C6 **1c**, oxo6 **3c**, C8 **1e** and oxo8 **3e** in an experimental set-up with agar plates, a significant root elongation was observed as well.^{69–72} This promotion was because of increased cell division activity in the meristem zone and enhanced cell elongation in the elongation zone of the roots.⁷³ However, a high (100 μ M) concentration of oxo6 **3c** and oxo8 **3e** resulted in a reduction of the root length.⁷¹ Genetic analysis revealed that GCR1, a G-protein-coupled receptor (GPCR), and G $_{\alpha}$ subunit GPA1 were involved. G-Protein signaling is linked to several plant growth and development processes which transduce environmental signals into the cell.⁷¹ Recent research suggests that the Ca²⁺ binding protein calmodulin participates in the root stimulatory effect of oxo6 **3c** on *A. thaliana* as well.^{72,74} Application of C4 **1a** caused an increase of the cytosolic free Ca²⁺ concentration, supporting this hypothesis.⁷⁴ It was also shown that the root stimulatory effect of oxo6 **3c** depends on an active AtMYB44 protein. This transcriptional factor is associated with plant development and defense responses to pathogens and environmental stress and can induce auxin- and cytokinin-related genes.⁷³ All these data combined led to the hypothesis that GCR1 and GCR2 could be candidate receptors for AHLs in *A. thaliana*. Interaction of AHLs with these GPCRs will activate the heterotrimeric G-protein. Subsequently, the activated G $_{\alpha}$ subunit opens the Ca²⁺ channels which leads to an increase of intracellular free Ca²⁺ which in its turn activates calmodulin. Calmodulin then triggers the downstream cascades leading to the final specific cellular reaction.^{72,74}

Whereas short-chain AHLs seem to stimulate root growth, no effect or a negative effect was observed for AHLs with a longer acyl chain.^{68–72} In a study performed by Ortíz-Castro *et al.*, a dose-dependent inhibitory effect on root length of *A. thaliana* was observed for C8 **1e**, C10 **1g**, C12 **1i** and C14 **1k** (Appendix, Table 8.1).⁵⁴ Compound C10 **1g** had the strongest inhibitory effect (80% reduction at a concentration of 48 μ M) on primary root growth. This reduction is caused by affecting cell division in the meristem and is independent of auxin-signaling.⁵⁴ Also calmodulin was not involved in the inhibition of primary root growth when long-chain

AHLs are applied.⁷² The reduced primary root length was accompanied by a shift toward a more branched root system. This could provide a larger surface area for bacterial colonization. Longer-chain AHLs such as C12 **1i** also stimulated root hair formation.⁵⁴ Remarkably, in their set-up (seeds germinated and grown on AHL-containing agar plates, AHL concentration range 12-192 μM) no effect was observed for C4 **1a**, C6 **1c** or oxo6 **3c**. These differences in activity compared to other studies could be explained by the fact that the *A. thaliana* plants were germinated on AHL-containing medium, unlike other studies where the seeds were germinated first in the absence of AHLs and then transferred to AHL-containing medium. So not only the effect of AHLs on root elongation but also on germination and root development should be taken into account. It is striking that plants produce several compounds with a structural similarity to AHLs, for example *N*-acyl ethanolamines (NAE) **23** and alkamides **24** (Figure 2.5). These plant signals control germination and can alter root and shoot system architecture.^{54,75,76} Therefore, the same AHL-treatment was applied on plants overexpressing a fatty acid amide hydrolase (FAAH) enzyme, responsible for the hydrolysis of NAEs, and a diminished sensitivity toward AHLs was observed as well.⁵⁴ An *A. thaliana* mutant that was resistant to the effect of the alkamide *N*-isobutyl decanamide **24a**, which inhibits primary root growth and stimulates lateral root formation in wild type plants, was resistant as well to the inhibitory effect of C10 **1g**.⁷⁷ This suggests that plants may share a common pathway to perceive NAEs and AHLs for root development.

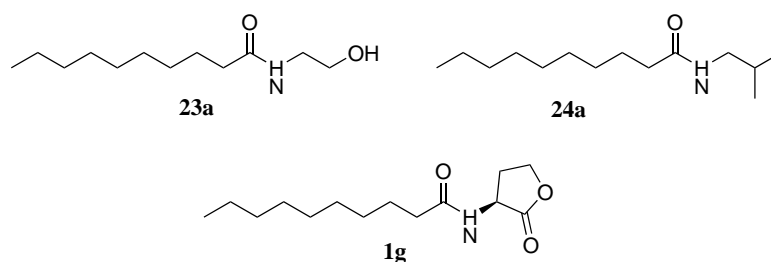


Figure 2.5. Structural similarities between C10 **1g** and plant constituents *N*-ethanol decanamide (NAE10:0) **23a** and *N*-isobutyl decanamide **24a**.

Although C10 **1g** had a strong effect on *A. thaliana*, it is devoid of activity on mung bean (*Vigna radiata*). However, the analogue with the 3-oxo-substituent, oxo10 **3g**, strongly induces the formation of adventitious roots. This compound **3g** stimulates basipetal auxin transport which causes adventitious root formation via hydrogen peroxide- and nitrogen monoxide-dependent cyclic GMP signaling.⁷⁸ In the case of barley (*Hordeum vulgare*), a monocotyledon, both C8 **1e** and C12 **1i** were able to stimulate plant growth and a branched root architecture. This lateral root stimulation was linked to NO-accumulation that was induced by all AHLs. Whereas only 10 μM but not 1 or 100 μM of C6 **1c** and C8 **1e** stimulated K^+ uptake in root cells, the same

effect was observed in all (1, 10 and 100 μM) concentrations tested for C12 **1i** (Appendix, Table 8.1).⁷⁹

Palmer and colleagues found that AHLs elicited a biphasic growth response in *A. thaliana* and *M. truncatula* seedlings. Whereas all (both short and long-chain) AHLs tested caused longer primary roots in submicromolar concentrations, a significant reduction was observed when higher ($> 50 \mu\text{M}$) concentrations were used. The sensitivity of *A. thaliana* to an AHL increased with the acyl chain length, but the functionality did not play an important role, as C12 **1i**, HO12 **2i** and oxo12 **3i** had a very similar effect (Appendix, Table 8.1). Stereochemistry, on the other hand, played a crucial role, shown by the fact that the unnatural D-stereomer of oxo12 **3i** failed to cause any growth effects. Also *p*-coumaryl-HL **4** was devoid of activity. The ring-opened form of oxo12 had a similar activity as oxo12 **3i**, suggesting that an intact lactone ring is not required for AHL-induced plant growth modification. Contrastingly, in bacteria the lactone ring is an absolute requirement for activity. When several AHL-degradation products were tested, a biphasic growth effect similar to the pattern observed for long-chain AHLs, was observed for L-homoserine (HSe) **25**.⁵⁵ The effect of AHL-degradation products on plants was also noted by Joseph *et al.* Whereas no difference in stomatal conductance (a measure for stomatal opening) and transpiration was observed after application of 10 nM oxo6 **3c** to bean plants (*Phaseolus vulgaris*), an increase of 20 to 30% was caused by 10 nM homoserine lactone **19** or HSe **25** (Appendix, Table 8.1). Both bacteria and plant benefit from this effect: while the microorganism gets more access to mineral nutrients carried by soil moisture toward the root, the plant can increase mineral uptake, increase the cooling of leaves and improve photosynthetic efficiency.⁸⁰ HSe **25** is formed after AHL amidolysis by plant-derived fatty acid amide hydrolase (FAAH), followed by lactonolysis (Figure 2.6). FAAH-Deficient seedlings were found to be resistant to the effects of AHLs but showed altered root lengths when L-HSe **25** was applied. This confirms the hypothesis that the growth modulating effect was linked with an AHL-degradation product, although these results contrast with those reported by Ortíz-Casto *et al.*^{54,55} The fact that D-AHLs and short-chain AHLs were not as efficient substrates for FAAH as long-chain AHLs corroborates the difference in activity observed for AHLs with different acyl chain lengths. The second degradation product, the fatty acid **18**, did not have an effect on the root growth. Also the unnatural D-isomer of HSe **25** was inactive. As FAAHs are especially active during the germination and seedling phase, this could explain different results obtained when testing plants in different development phases. At low bacterial and AHL-densities, only low concentrations of L-HSe **25** are present which stimulate plant transpiration and thereby encourage growth, whereas high AHL concentrations lead to high HSe **25** concentrations which may alert the

plant and inhibit growth by stimulating ethylene production.⁵⁵

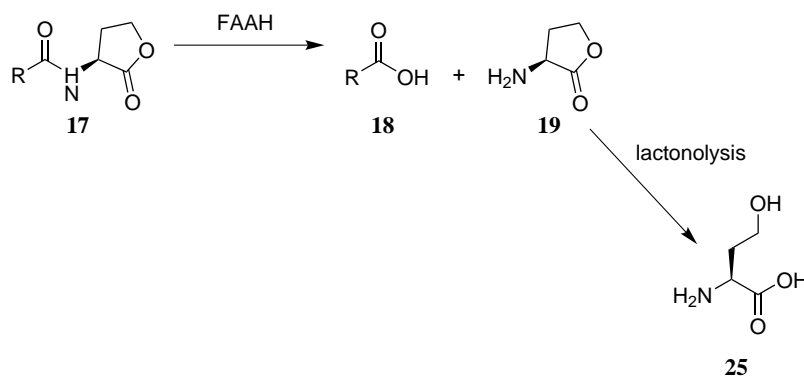


Figure 2.6. FAAH-Catalyzed degradation of AHLs **17** to homoserine lactone **19** (HL) and a fatty acid **18**. The homoserine lactone can hydrolyze to homoserine **25** (HSe).

A stereospecific response of plants toward AHLs was also apparent when two isomers of oxo8 **3e** were applied to sugar cane (*Saccharum officinarum*). Whereas both compounds led to the formation of more stretched root cells, the L-enantiomer caused a larger increase in the sprouting of roots compared to the D-enantiomer (Appendix, Table 8.1).⁸¹

Besides morphological changes, AHLs can also lead to induced systemic resistance (ISR) in plants. This induced systemic resistance causes plants to strengthen their defense mechanisms as a preparation for contact with pathogens or stress. By applying AHLs in a process called priming, plants are brought to this state of increased resistance and can respond stronger and faster to future threats.⁸² When AHL-producing strains were present in the tomato (*Lycopersicon esculentum*) rhizosphere, an enhanced resistance to the fungal leaf pathogen *Alternaria alternata* was observed. AHL-mutants lacked this ability. The effect could be mimicked via the application of synthetic AHL standards.⁸³ This enhanced resistance caused by AHLs relies on the induction of salicylic acid (SA)- and ethylene-dependent defense genes.⁸³ However, no such enhanced resistance was observed when *A. thaliana* was treated with C6 **1c**.⁶⁸ For this plant, mainly longer-chain AHLs (C12 **1i**, oxo14 **3k**) were able to offer such protection.^{69,70} This AHL-induced resistance seems to rely on mitogen-activated protein kinases (MPAKs). These proteins play an important role in the first steps of pathogen perception and induction of defense mechanisms.⁶⁹ When tested on *A. thaliana*, oxo14 **3k** could influence plant defense via an oxylipin/SA-dependent signaling pathway leading to cell wall strengthening by stimulating callose deposition, accumulation of phenolic compounds and lignification. A second effect was the increase of stomatal closure when exposed to a pathogen.^{82,84} The application of AHL-producing bacteria as a soil amendment is currently being investigated.^{84,85}

It is difficult to draw definitive conclusions about the effect of AHLs on plants in general as

most of the studies have been performed with the economically not-important plant *A. thaliana*. As this is a small plant with a short life-cycle and which can easily be grown, *A. thaliana* is perfectly suited to study the effect of AHLs in a profound, standardized manner. However because of the different experimental set-ups (hydroponic system, agar plates, different methods of AHL application) and experimental parameters (age of seedlings, contact time with AHLs, AHL concentration range, stereochemistry of the AHLs used) there are already conflicting results for this one plant species (Appendix, Table 8.1). However, the general trend observed in most cases is that short-chain AHLs (an acyl chain containing six or less carbon atoms) in a concentration lower than 10 μM tend to promote primary root elongation, partially by shifting the hormonal (auxin/cytokinin) balance.^{68,70–72,78} Long-chain AHLs (an acyl chain with ten carbon atoms or more) typically inhibit primary root growth and stimulate the formation of lateral roots and root hairs.^{54,70} Not only the acyl chain length but also the dose and stereochemistry play a crucial role. Short-chain AHLs can also inhibit root growth at higher ($> 10 \mu\text{M}$) concentrations.⁵⁵ On the other hand, AHLs with a longer acyl chain (e.g. C12 **1i**, C14 **1k**) can stimulate induced systemic resistance (AHL-priming).^{69,82,84,86} The exact mechanism by which AHLs exert their effect is not yet fully understood, although for the growth stimulatory effect G-protein receptors seem to be involved. The inhibitory effect seems to be linked with an elevated ethylene concentration, which is caused by the FAAH-mediated AHL-degradation product HSe **25**.

AHLs can also have an influence on the reproductive behavior of some algae. Culture filtrates of several AHL-producing isolates and pure C4 **1a** and C6 **1c** (2–10 μM) standards stimulated the red macroalga *Gracilaria dura* to release its carpospores, whereas longer-chain AHLs C8 **1e**, C10 **1g** and oxo12 **3i** were inactive.⁸⁷ A similar effect was observed for C4 **1a** on the release of spores of red algal epiphyte *Acrochaetium* sp., albeit at high concentrations (100 μM). This effect on spore release was not observed in a second red alga (*Sahlimgia subintegra*).⁸⁸ Zoospores of the green alga of the *Enteromorpha* genus use the presence of AHLs to detect biofilms suited to settle upon. These zoospores only adhere to AHL-liberating strains.⁸⁹

2.1.3.2 Effect of plants on QS signaling

AHLs can influence plants in several ways, but plants can interfere with bacterial signaling as well. Several plant-derived compounds that are able to inhibit quorum sensing are known (Figure 2.7).^{5,13} A true inhibitor disturbs QS without affecting bacterial growth. One of the most studied examples is the production of halogenated furanones **26** by the macro-alga *Delisea pulchra*. These compounds have a certain structural similarity with AHLs and bind to the AHL receptor proteins and enhance degradation of these proteins.^{90,91} Iberin (**27**), an isothiocyanate,

was isolated from horseradish (*Armoracia rusticana*) and is extremely effective in inhibiting QS in *P. aeruginosa*.⁹² Also garlic (*Allium sativum*) contains compounds **28a** and **28b** which solely inhibit QS.⁹³ Cinnamaldehyde (**29**), which can be isolated from the essential oil of cinnamon, interferes at subinhibitory concentrations with the action of short-chain AHLs whereas QS relying on long-chain AHLs is not affected.⁹⁴ The naturally occurring furocoumarins bergamottin (**30a**) and dihydroxybergamottin (**30b**) were isolated from grapefruit juice and inhibit QS without interfering with bacterial growth.⁹⁵ Also the flavan-3-ol catechin (**31**), present in the bark of bushwillow *Combretum albiflorum*, has a negative impact on QS.⁹⁶ As this small selection of plant-derived quorum sensing inhibitors already displays a large structural diversity, different parts of the QS system might be targeted by these compounds, although the exact mechanism is often not yet known.

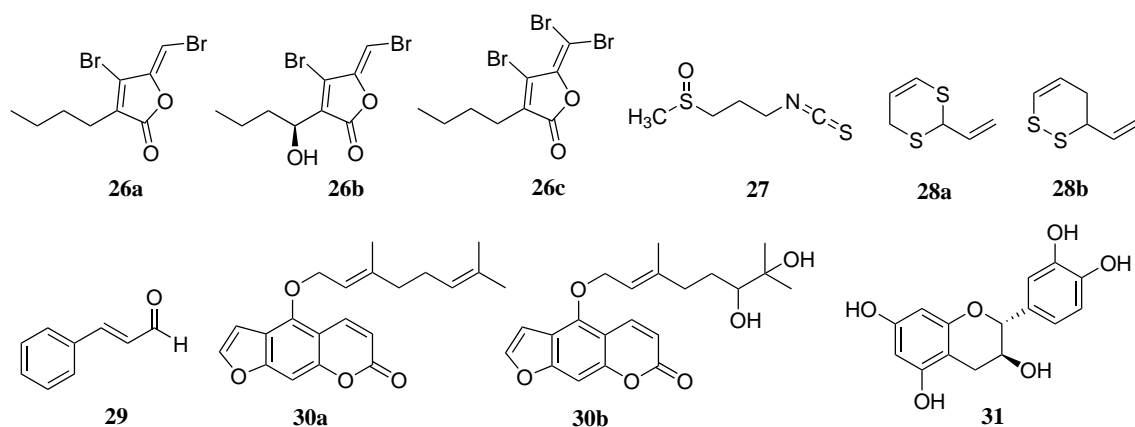


Figure 2.7. Structures of several QS inhibitors isolated from plants and macro-alga.

For several plant extracts, QS inhibiting or stimulating activity has been observed but the active components were not identified yet.^{92,97-99} The methanolic extract of radish (*Raphanus sativus*), tarragon (*Artemisia dracunculus*) and hollyhock (*Althea officinalis*) showed QS inhibition, whereas white clover (*Trifolium repens*) showed QS stimulation.⁹⁸ The extract of several pepper species has QS inhibitory activity as well, but the active compounds have not been identified yet.⁹⁷ Also rice plant (*Oryza sativa*) extracts contain compounds that can activate several AHL reporter strains, although the involvement of certain endophytic bacteria could not be ruled out. These AHL-mimics are sensitive to the AiiA lactonase, so presumably contain an AHL-related lactone core.⁹⁹ Exudates from pea (*Pisum sativum*) seedlings contained several unidentified compounds that could influence AHL-regulated behavior in some reporter strains without altering the bacterial growth. Unlike AHLs, the active compounds from the pea seedling exudate could not be extracted with chloroform or ethyl acetate. The methanol extract on the other hand contained the majority of the QS activity. This difference points to a different chemi-

cal nature of the active compounds compared to bacterial AHLs. Also seedlings of crown vetch (*Coronilla varia*) were able to inhibit a reporter strain, whereas exudates of lettuce (*Lactuca sativa*) and *A. thaliana* proved to be inactive.¹⁰⁰ This presence of QS-influencing compounds was also detected in *M. truncatula* seedlings.¹⁰¹ Importantly, when *M. truncatula* was exposed to AHLs, the excretion of QS signal-mimicking compounds was increased.⁶⁶

To respond to plant signals, several plant-associated bacteria possess LuxR-like proteins with the characteristic AHL-binding domain but without a cognate LuxI-protein. These proteins are called orphan LuxRs or LuxR solos and can be used to eavesdrop on neighboring bacteria but can also bind and respond to plant compounds rather than AHLs. These LuxR solos lack some conserved residues in the AHL-binding pocket compared to classical LuxRs.^{86,102}

In some rare occasion, components of the root exudates can even be incorporated in the AHL-signal. *p*-Coumaric acid is produced by plants as a precursor of lignin and can exert QS-inhibiting activity. The photosynthetic bacterium *Rhodospseudomonas palustris* however relies on plant-derived *p*-coumaric acid to synthesize its *p*-coumaryl-AHL **4** (Figure 1.2).^{4,65}

AHL-Degradation can be effectuated as well by plants. When the root systems of the legumes clover (*Trifolium pratense*) and *Lotus corniculatus* were incubated with C6 **1c**, a rapid degradation of the signal molecule was observed. This disappearance was non-existent when the root system of the monocots corn (*Zea mays*) and wheat (*Triticum aestivum*) was tested. As this degradative activity was absent after boiling, presumably one or more enzymes are involved.³⁷ When barley and yam bean (*Pachyrhizus erosus*) were treated with AHLs, a stronger AHL decrease was observed in the rhizosphere of the legume yam bean compared to barley. This could be explained by the fact that legumes such as bean and clover are naturally exposed to multiple AHLs during their symbiosis with rhizobia, whereas monocots such as barley, corn and wheat do not have such interactions.^{103,104} After treatment of yam bean and barley with C6 **1c**, C8 **1e** and C10 **1g**, all three AHLs were detected in root extracts of both plants. In the shoots of barley on the other hand, only C6 **1c** and C8 **1e** were detectable, whereas only C6 **1c** was found in yam bean shoots. Importantly, AHLs with the unnatural D-configuration showed a reduced uptake by barley and yam bean.¹⁰³ It was found that AHLs with a longer side chain (e.g. C10 **1g**) were degraded faster than their short-chain counterparts.¹⁰⁴ Accumulation of C6 **1c** in shoots and C10 **1g** in roots was also shown for *A. thaliana*.^{68,69} However, when the uptake of C8 **1e** and C10 **1g** was evaluated with more sensitive methods, applying radioactive isotope-labeled AHLs and biosensors, both C8 **1e** and C10 **1g** could be detected in the shoots, albeit in limited amounts for C10 **1g**. It was shown that ABC transporters are involved in the AHL-uptake and

that the transport occurs mainly via the central cylinder.¹⁰⁵ So whereas short-chain AHLs can be transported throughout the plant, long-chains AHL are transported as well but only to a limited extent inside the plant and accumulate mainly in the roots.^{69,105}

2.2 Cyclic lipopeptides

2.2.1 Introduction

The general structure of a cyclic lipopeptide (CLP) consists of a lipid tail connected to an oligopeptide (Figure 2.8 and 2.9). CLPs containing a lactone in the cyclic core are called depsipeptides. These versatile compounds are synthesized by non-ribosomal peptide synthetases (NRPS). The combination of a polar amino acid (AA) head linked to a lipophilic fatty acid tail gives these amphiphilic compounds interesting activities (*vide infra*). The cyclic character is often a prerequisite for the (bio)activity.^{106,107} For example linear analogues of surfactin lack the hemolytic activity that is present in the cyclic analogues.¹⁰⁷ The cyclization itself reduces conformational freedom, constraining the structure and thereby ensuring a proper interaction with the dedicated target.¹⁷ Not only the cyclic character gives these compounds interesting properties, often unusual AAs can be found in CLPs. Several databases containing all the different (> 500) monomers found in non-ribosomal peptides are available.¹⁰⁸ The presence of D-AAs and *N*-methylated AAs constrains the conformation to aid cyclization and furnishes a higher stability against proteolytic digestion, although they can still be degraded by several other microorganisms.^{109,110} The length of the fatty acid tail linked to the oligopeptide moiety can also have a profound effect on the activity of the CLP.¹⁰⁶

CLPs are produced mostly by bacteria belonging to soil-dwelling or plant-associated *Pseudomonas*, *Bacillus*, *Actinomyces*, *Serratia* and *Streptomyces* genera, but CLP-producing organisms have been found in other habitats as well.²⁰ Especially the CLPs produced by the first two genera have been studied extensively.

In this work, first the different types of CLPs are discussed, followed by the biosynthesis. Further on the natural functions and possible commercial applications are mentioned.

2.2.2 Classification

2.2.2.1 *Pseudomonas* CLPs

Based on structural similarities, the CLPs produced by *Pseudomonas* can be divided into six major groups (Figure 2.8 and Table 2.1).¹⁸⁻²⁰

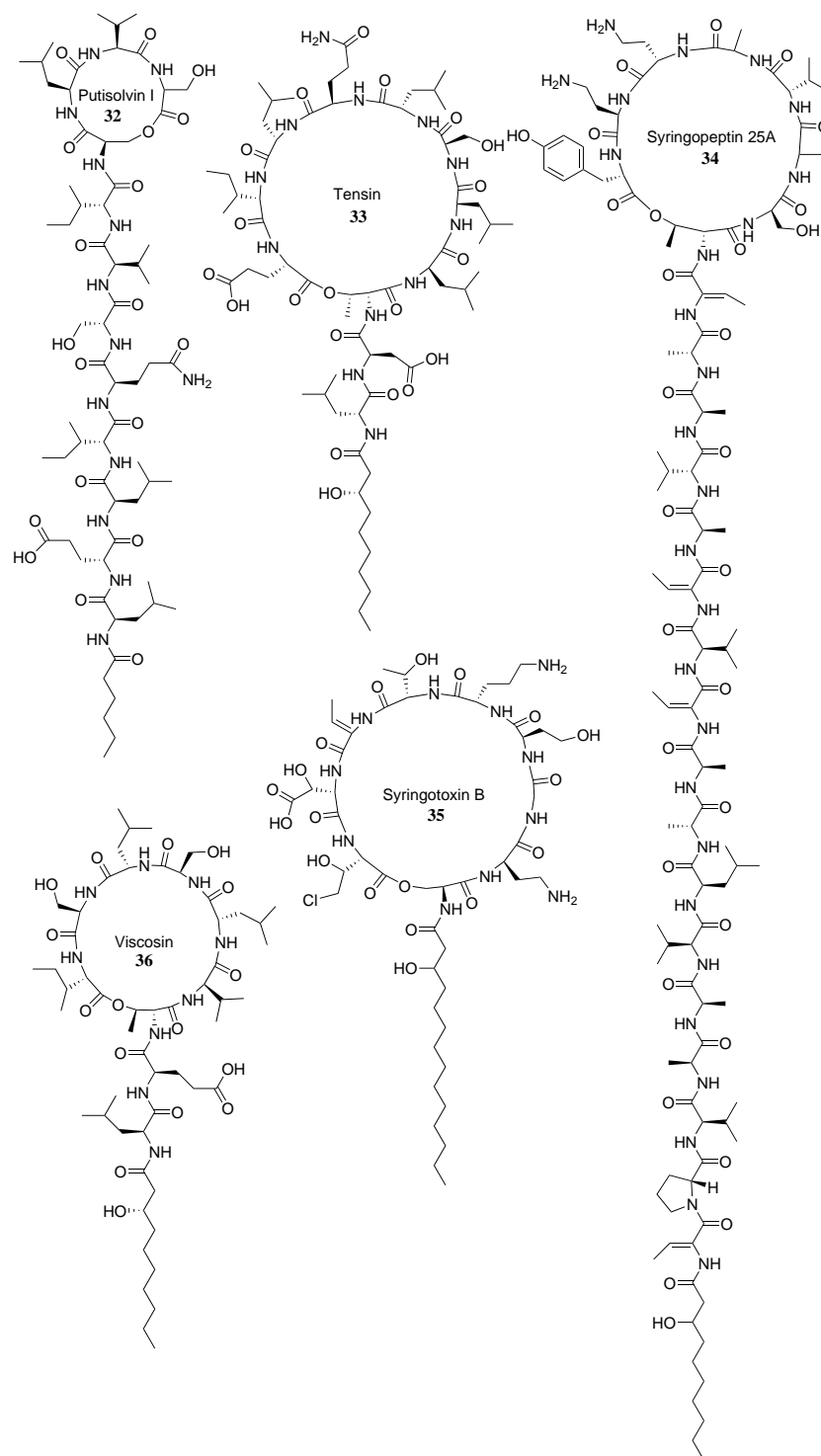


Figure 2.8. Chemical structure of the CLPs putisolvin I (**32**), tensin (**33**), syringopeptin 25A (**34**), syringotoxin B (**35**) and viscosin (**36**) which are produced by *Pseudomonas* sp.^{20,111} The stereochemistry of putisolvin I (**32**) is predicted based upon sequence analysis.²³

Viscosin group

The CLPs of this group are composed out of nine amino acids and are mostly linked to a β -hydroxydecanoyl moiety. The macrolactone is formed via an esterification between the carboxylic acid group of the *C*-terminal amino acid and the hydroxy group of the *D*-*a*Thr residue.^{19,112}

The production of this type of CLP seems to be associated with several fluorescent pseudomonads from different habitats, including rhizosphere, soil, phyllosphere and marine environments.¹¹³ Also the white line-inducing principle (WLIP) belongs to this group. Pseudomonads producing WLIP used to be classified in the ill-defined *P. reactans* group. When a WLIP-producing strain is confronted with tolaasin on a solid medium, a white precipitate originates.¹¹⁴ Besides WLIP, following CLPs belong to the viscosin group: viscosin (**36**), massetolide, viscosinamide, pseudodesmin and pseudophomin (Table 2.1).^{19,112}

Syringomycin group

This group is named after virulence factor syringomycin produced by *P. syringae* pv. *syringae*.¹⁸ CLPs from this heterogenic group contain 9 AAs, including unusual AAs such as homoserine (Hse), 2,4-diaminobutyric acid (Dab), 2,3-dehydroaminobutyric acid (Dhb), ornithine (Orn), 3-hydroxyaspartic acid (Asp(3-HO)) and 4-chlorothreonine (Thr(4-Cl)). The *N*-terminal amino acid is linked to a β -hydroxy or 3,4-dihydroxy fatty acid containing 10, 12 or 14 carbon atoms. The cyclic core of these lipodepsinonapeptides is formed via a cyclization between the *N*-terminal Ser and the *C*-terminal Thr(4-Cl). Examples are the phytotoxic syringomycins, syringostatins and syringotoxin B (**35**) and the antifungal pseudomycin and ecomycin (Table 2.1).^{19,113,115}

Amphisin group

Amphisin, tensin (**33**), lokisin, pholipeptin, hodersin and arthrofactin are members of this group (Table 2.1). The typical structure consists of 11 amino acids coupled to a β -hydroxydecanoic acid tail. The lactone ring of these lipoundecapeptides is formed between the *C*-terminal amino acid and the hydroxy group of the L-Thr or D-*a*Thr residue located at position three.¹⁹

Putisolvin group

These CLPs have a 12 AAs peptide chain coupled to a hexanoic fatty acid tail. The only members of this group are putisolvin I (**32**) and II (Table 2.1).¹⁸

Tolaasin group

CLPs belonging to this group contain 19-25 AAs, often including unusual AAs (e.g. Hse, Dab, Dhb). The lipid moiety is typically β -hydroxydecanoic acid although exceptions are possible in this diverse group. The peptide is cyclized via a lactone formed between the *C*-terminal amino acid and the *a*Thr residue. The cyclic moiety consists of 5-8 AAs.¹¹³ Corpeptin, fuscopeptin and tolaasin are examples of CLPs belonging to this group (Table 2.1). Most of these CLPs possess phytotoxic properties.^{19,113}

Syringopeptin group

CLPs in this group contain 22 or 25 AAs and the *N*-terminal AA is acylated with a β -hydroxydecanoic acid or β -hydroxydodecanoic acid (Table 2.1). The lactone bond is formed between the *C*-terminal Tyr residue and the hydroxy group of *α*Thr.¹¹⁵ The system responsible for the biosynthesis of syringopeptin (**34**) is the largest prokaryotic NRPS described so far (74 kb - 22 modules).^{111,116}

‘Orphan’ CLPs

In recent years, several other CLPs have been discovered with structural features different from the main groups. One example are the orfamides, identified by mining of the *P. fluorescens* Pf-5 genome.¹¹⁷ These depsidecapeptides contain 10 AAs coupled to a β -hydroxydecanoic acid or β -hydroxydodecanoic acid tail and resemble CLPs of the viscosin group (Table 2.1). Another example is entolysin containing 14 AAs with the lactone ring formed between the *C*-terminal carboxy group and the hydroxy group of a Ser residue on the tenth position. Its fatty acid tail consists of a β -hydroxydecanoic acid.¹¹⁸ Very recently the lipotetradecadepsipeptide xantholysin was discovered, with an octacyclic core.¹¹² Sometimes, orfamides and entolysins are regarded as new groups of CLPs, bringing the total number of different groups of *Pseudomonas* CLPs to at least eight.

Table 2.1: Different structural groups of CLPs produced by *Pseudomonas* and primary structures of representatives of each group. Adapted and extended from Gross and Loper.^{18,111,119,120} Residues involved in cyclization are marked with an asterisk (*). Abbreviations used: HOFax: β -hydroxy fatty acid with x the total number of carbon atoms in the chain. diHOFax: 3,4-dihydroxy fatty acid. Asp(3-HO): 3-hydroxyaspartic acid, α Thr: *allo*-threonine, Dab: 2,4-diaminobutyric acid, Dhb: 2,3-dehydroaminobutyric acid, HSe: homoserine, Thr(4-Cl): 4-chlorothreonine, xLeu: Leu or Ile. For the other common AAs the standard three-letter abbreviations are used.

Name	FA	1	2	3	4	5	6	7	8	9	10	11	12	13	14	15	16	17	18	19	20	21	22	23	24	25	
Viscosin group																											
Viscosin (36)	HOFA10	L-Leu	D-Glu	D- α Thr*	D-Val	L-Leu	D-Ser	L-Leu	D-Ser	L-Ile*																	
Viscosinamide	HOFA10	L-Leu	D-Glu	D- α Thr*	D-Val	L-Leu	D-Ser	L-Leu	D-Ser	L-Ile*																	
WLIP	HOFA10	L-Leu	D-Glu	D- α Thr*	D-Val	D-Leu	D-Ser	L-Leu	D-Ser	L-Ile*																	
Massetolide A	HOFA10	L-Leu	D-Glu	D- α Thr*	D- α Ile	L-Leu	D-Ser	L-Leu	D-Ser	L-Ile*																	
Massetolide D	HOFA10	L-Leu	D-Glu	D- α Thr*	D- α Ile	L-Leu	D-Ser	L-Leu	D-Ser	L-Leu*																	
Pseudophorin A	HOFA10	L-Leu	D-Glu	D- α Thr*	D-Ile	D-Leu	D-Ser	L-Leu	D-Ser	L-Ile*																	
Pseudophorin B	HOFA12	L-Leu	D-Glu	D- α Thr*	D-Ile	D-Leu	D-Ser	L-Leu	D-Ser	L-Ile*																	
Pseudodesmin A	HOFA10	L-Leu	D-Gln	D- α Thr*	D-Val	D-Leu	D-Ser	L-Leu	D-Ser	L-Ile*																	
Pseudodesmin B	HOFA10	L-Leu	D-Gln	D- α Thr*	D-Val	D-Leu	D-Ser	L-Leu	D-Ser	L-Val*																	
Syringomycin group																											
Syringomycin SRA 1	HOFA10	L-Ser*	D-Ser	D-Dab	L-Dab	L-Arg	L-Phe	Z-Dhb	L-Asp(3-HO)	L-Thr(4-Cl)*																	
Syringomycin SRE	HOFA12	L-Ser*	D-Ser	D-Dab	L-Dab	L-Arg	L-Phe	Z-Dhb	L-Asp(3-HO)	L-Thr(4-Cl)*																	
Syringosutatin A	HOFA14	L-Ser*	D-Dab	L-Dab	D-HSe	L-Orn	L- α Thr	Z-Dhb	L-Asp(3-HO)	L-Thr(4-Cl)*																	
Syringotoxin B (35)	HOFA14	L-Ser*	D-Dab	Gly	D-HSe	L-Orn	L- α Thr	Z-Dhb	L-Asp(3-HO)	L-Thr(4-Cl)*																	
Pseudomycin A	diHOFA14	L-Ser*	D-Dab	L-Asp	L-Lys	L-Dab	L- α Thr	Z-Dhb	L-Asp(3-HO)	L-Thr(4-Cl)*																	
Comycin A	diHOFA16	L-Ser*	D-Orn	L-Asn	D-HSe	L-His	L- α Thr	Z-Dhb	L-Asp(3-HO)	L-Thr(4-Cl)*																	
Amphisolin group																											
Amphisolin	HOFA10	D-Leu	D-Asp	D- α Thr*	D-Leu	D-Leu	D-Ser	L-Leu	D-Gln	L-Ile	L-Leu	L-Ile	L-Asp*														
Tenasin (33)	HOFA10	D-Leu	D-Asp	D- α Thr*	D-Leu	D-Leu	D-Ser	L-Leu	D-Gln	L-Ile	L-Leu	L-Ile	L-Glu*														
Pholipeptin A	HOFA10	D-Leu	L-Asp	L-Thr*	D-Leu	D-Leu	D-Ser	D-Leu	D-Ser	L-Ile	D-Leu	L-Ile	D-Asp*														
Lokisin	HOFA10	Leu	Asp	D- α Thr*	Leu	Leu	D-Ser	Leu	D-Ser	L-Ile	Leu	L-Ile	Asp*														
Arthrofactin	HOFA10*	D-Leu	D-Asp	D-Thr	D-Leu	D-Leu	D-Ser	L-Leu	D-Ser	L-Ile	L-Ile	L-Ile	L-Asp*														
Puilsolvain group																											
Puilsolvain I (32)	FA6	Leu	Glu	Leu	Ile	Gln	Ser	Val	Ile	Ser*	Leu	Val	Ser*														
Puilsolvain II	FA6	Leu	Glu	Leu	Ile	Gln	Ser	Val	Ile	Ser*	Leu	Val	Ser*														

Table 2.1 Continued.

Name	FA	1	2	3	4	5	6	7	8	9	10	11	12	13	14	15	16	17	18	19	20	21	22	23	24	25	
Tetrasidin group																											
Tetrasidin I	HOFA8	Dhb	D-Pro	D-Ser	D-Leu	D-Val	D-Ser	D-Leu	D-Val	L-Val	D-Gln	L-Leu	-	-	-	-	D-Val	Dhb	D- α -Thr ^a	L-Ile	L-HSe	D-Dab	L-Lys ^a	-	-	-	
Tetrasidin II	HOFA8	Dhb	Pro	Ser	Leu	Val	Ser	Leu	Val	Val	Gln	Leu	-	-	-	-	Val	Dhb	D- α -Thr ^a	Ile	Gly	Dab	Lys ^a	-	-	-	
Tetrasidin A	HOFA5	Dhb	Pro	Ser	Leu	Val	Ser	Leu	Val	Val	Gln	Leu	-	-	-	-	Val	Dhb	D- α -Thr ^a	Ile	HSe	Dab	Lys ^a	-	-	-	
Tetrasidin B	HOFA8	Dhb	D-Pro	L-Leu	D-Ala	D-Ala	D-Ala	D-Ala	D-Val	Gly	D-Ala	D-Val	-	-	-	-	D-Val	Dhb	D- α -Thr ^a	L-Ala	L-Dab	L-Dab	Lys ^a	-	-	-	
FP-B	HOFA8	Dhb	Pro	Ala	Ala	Ala	Val	Val	Dhb	HSe	Val	D-Ile	-	-	-	-	Val	Dhb	D- α -Thr ^a	Ala	Dab	Ser	Ile ^a	-	-	-	
Corcepin A	HOFA10	Dhb	D-Pro	D-Ser	D-Leu	D-Val	D-Gln	D-Leu	D-Val	L-Val	D-Gln	L-Leu	-	-	-	-	D-Val	Dhb	D- α -Thr ^a	L-Ile	L-HSe	D-Dab	L-Lys ^a	-	-	-	
Sessilin	HOFA8	Dhb	D-Pro	D-Ser	D-Leu	D-Val	D-Gln	D-Leu	D-Val	L-Val	D-Gln	L-Leu	-	-	-	-	D-Val	Dhb	D- α -Thr ^a	L-Ile	L-HSe	D-Dab	L-Lys ^a	-	-	-	
Syringopappula group																											
SP22	HOFA10	Dhb	D-Pro	D-Val	D-Val	D-Val	D-Ala	D-Val	D-Val	-	-	D-Val	Dhb	D-Ala	D-Val	L-Ala	D-Ala	Dhb	D- α -Thr ^a	D-Ser	D-Ala	Dhb	L-Ala	L-Dab	D-Dab	L-Tyr ^a	
SP25A (34)	HOFA10	Dhb	D-Pro	D-Val	D-Val	D-Val	D-Ala	D-Leu	D-Val	D-Ala	D-Ala	D-Val	Dhb	Dhb	D-Ala	D-Val	D-Ala	Dhb	D- α -Thr ^a	D-Ser	D-Ala	L-Val	Ala	L-Dab	D-Dab	L-Tyr ^a	
Phe25-SP25A	HOFA10	Dhb	D-Pro	D-Val	D-Val	D-Val	L-Val	D-Leu	D-Val	D-Ala	D-Ala	D-Val	Dhb	Dhb	D-Ala	D-Val	D-Ala	Dhb	D- α -Thr ^a	D-Ser	D-Ala	L-Val	Ala	L-Dab	D-Dab	L-Tyr ^a	
Others																											
Orfamide A	HOFA14	L-Leu	D-Glu	D-Glu	D- α -Ile	L-Leu	D-Ser	L-Leu	L-Leu	L-Leu	D-Ser	L-Val ^a	-	-	-	-	L-Val	Dhb	D- α -Thr ^a	D-Ser	D-Ala	Dhb	L-Ala	L-Dab	D-Dab	L-Tyr ^a	
Orfamide B	HOFA14	L-Leu	D-Glu	D-Glu	D-Val	L-Leu	D-Ser	L-Leu	L-Leu	L-Leu	D-Ser	L-Val ^a	-	-	-	-	L-Val	Dhb	D- α -Thr ^a	D-Ser	D-Ala	Dhb	L-Ala	L-Dab	D-Dab	L-Tyr ^a	
Orfamide D	HOFA12	L-Leu	D-Glu	D-Glu	D-Val	L-Leu	D-Ser	L-Leu	L-Leu	L-Leu	D-Ser	L-Val ^a	-	-	-	-	L-Val	Dhb	D- α -Thr ^a	D-Ser	D-Ala	Dhb	L-Ala	L-Dab	D-Dab	L-Tyr ^a	
Emolyisin A	HOFA10	D-Leu	D-Glu	D-Glu	D-Val	D-Leu	D-Gln	D-Val	D-Leu	D-Leu	D-Gln	L-Val	L-Leu	D-Ser	Ile ^a	-	-	Dhb	D- α -Thr ^a	D-Ser	D-Ala	L-Val	Ala	L-Dab	D-Dab	L-Tyr ^a	
Xanthobolysin A	HOFA10	L-Leu	D-Glu	D-Glu	D-Val	D-Leu	D-Gln	D-Ser ^a	D-Val	L-Leu	D-Gln	Leu	Leu	L-Ile ^a	L-Gln	-	-	Dhb	D- α -Thr ^a	D-Ser	D-Ala	L-Val	Ala	L-Dab	D-Dab	L-Tyr ^a	

2.2.2.2 *Bacillus* CLPs

Most *Bacillus* CLPs are classified in one of the following three groups: the surfactin, iturin and fengycin family (Figure 2.9 and Table 2.2).

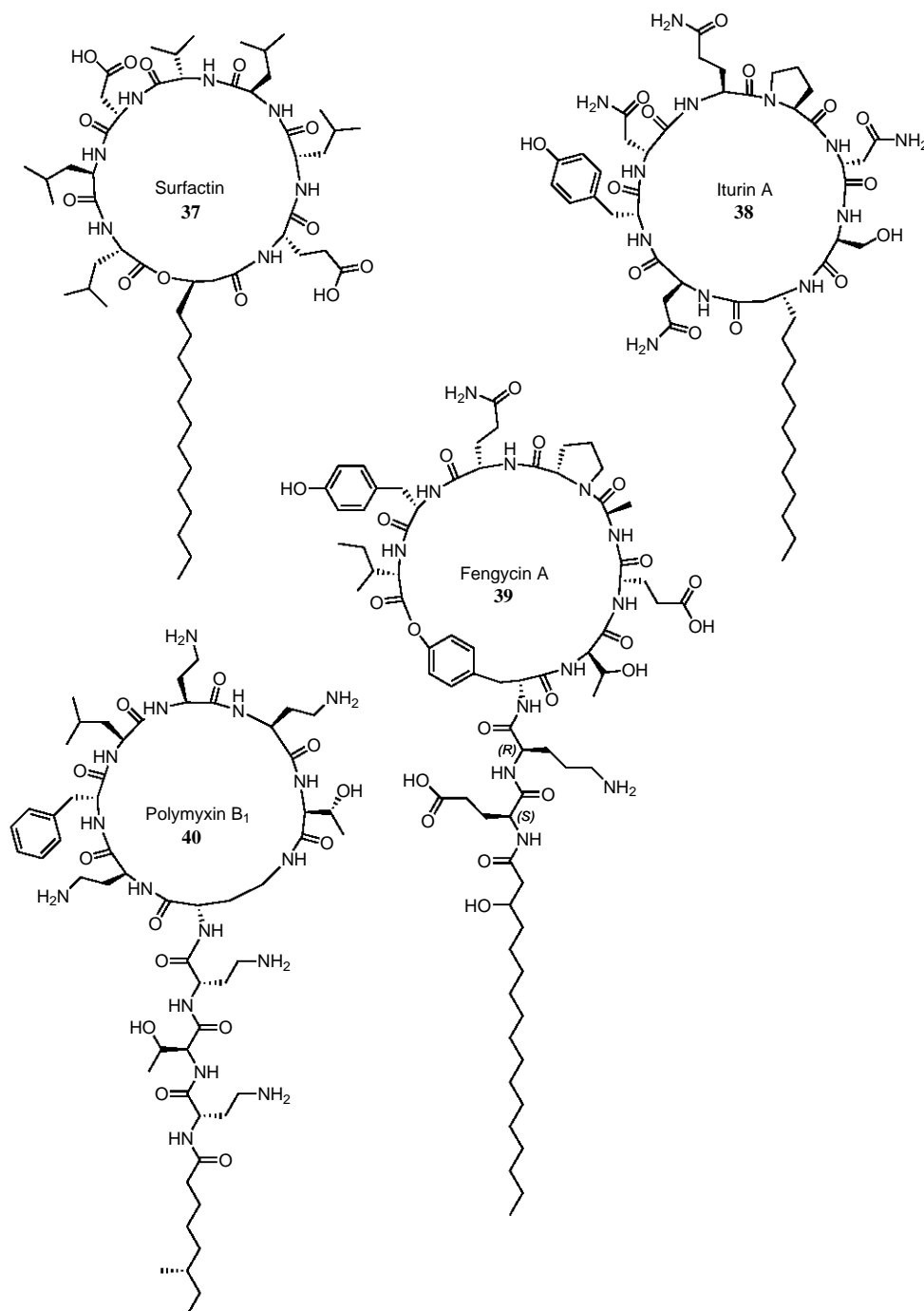


Figure 2.9. Chemical structure of the CLPs surfactin (37), iturin A (38), fengycin A (39) and polymyxin B₁ (40) which are produced by *Bacillus* sp.

Surfactin family

These heptapeptides are interlinked with a β -hydroxy fatty acid containing 12 to 16 carbon atoms and typically have a powerful biosurfactant activity.¹²¹ The macrolactone is formed be-

tween the *C*-terminal peptide and the β -hydroxy fatty acid. The main representative of this family, surfactin (**37**) itself, was discovered in 1968 in the culture broth of a *Bacillus subtilis* and has received a lot of attention since.^{122,123} Other examples of CLPs belonging to this group are esperin, lichenysin and pumilacidin (Table 2.2).

Iturin family

Members of this group are characterized by a β -amino fatty acid moiety of 14 to 17 carbon atoms linked to a cyclic heptapeptide macrolactam. These CLPs are synthesized by a hybrid PKS/NRPS-system. The main variants within this group are iturin A (**38**) and C, bacillomycin D, F, L and LC (also called bacillopeptin) and mycosubtilin (Table 2.2).¹²¹

Fengycin family

This group consists of decapeptides with a β -hydroxytetradecanoic to β -hydroxyoctadecanoic fatty acid tail. The macrolactone is formed between the hydroxy group of a Tyr-residue and the *C*-terminal amino acid. Representative CLPs are fengycin A (**39**) and B (also referred to as plipastins depending on the configuration of the Tyr-residues) (Table 2.2).¹²¹

Others

The antibiotic polymyxins are cationic CLPs with a remarkable Dab-content. Polymyxin B (**40**) and E (also known as colistin) are both produced by the soil bacterium *Bacillus polymyxa*. Polymyxin M (mattacin) on the other hand is produced by *Paenibacillus kobensis* (Table 2.2).¹²⁴

Table 2.2: Different structural groups of CLPs produced by *Bacillus* and primary structures of representatives of each group. Based on Ongena *et al.* and Roongsawang *et al.*^{116,121} Residues involved in cyclization are marked with an asterisk (*). Abbreviations used: *a*Thr: *allo*-threonine, Dab: 2,4-diaminobutyric acid, Orn: ornithine. For the other common AAs the standard three-letter abbreviations are used. aiFA9: *anteiso*-nonanoic acid (6-methyloctanoic acid), iFA8: *iso*-octanoic acid (6-methylheptanoic acid). ^a The major β -hydroxy fatty acids encountered are *iso*- and *anteiso*-HOFA13, *n*- and *iso*-HOFA14, *iso*- and *anteiso*-HOFA15. ^b The major β -hydroxy fatty acids encountered are *anteiso*-HOFA15, *n*- and *iso*-HOFA16, *n*- and *anteiso*-HOFA17. ^c The major β -amino fatty acids encountered are *n*-NH₂FA14, *iso*- and *anteiso*-NH₂FA15 and *n*- and *iso*-NH₂FA16 and *anteiso*-NH₂FA17.¹²¹

Name	FA	1	2	3	4	5	6	7	8	9	10
Surfactin family^a											
Surfactin (37)	HOFA*	L-Glu	L-Leu/Val/Ile	D-Leu	L-Val/Ala/Leu/Ile	L-Asp	D-Leu	L-Leu/Val/Ile*			
Lichenysin	HOFA*	L-Gln/Glu	L-xLeu	D-Leu	L-Val/Ile	L-Asp	D-Leu	L-Ile/Val*			
Surfactant BL86	HOFA*	L-Glx	L-Leu	D-Leu	L-Val	L-Asx	D-Leu	L-Ile/Val*			
Pumilacidin	HOFA*	L-Glu	L-Leu	D-Leu	L-Leu	L-Asp	D-Leu	L-Ile/Val*			
Esperin	HOFA*	L-Glu	L-Leu	D-Leu	L-Val	L-Asp*	D-Leu	L-Leu			
Fengycin family^b											
Fengycin A (39)	HOFA	L-Glu	D-Orn	D-Tyr*	D- α Thr	L-Glu	D-Ala	L-Pro	L-Gln	L-Tyr	L-Ile*
Fengycin B	HOFA	L-Glu	D-Orn	D-Tyr*	D- α Thr	L-Glu	D-Val	L-Pro	L-Gln	L-Tyr	L-Ile*
Plipastatin A	HOFA	L-Glu	D-Orn	L-Tyr*	D- α Thr	L-Glu	D-Ala	L-Pro	L-Gln	D-Tyr	L-Ile*
Plipastatin B	HOFA	L-Glu	D-Orn	L-Tyr*	D- α Thr	L-Glu	D-Val	L-Pro	L-Gln	D-Tyr	L-Ile*
Iturin family^c											
Iturin A (38)	NH ₂ FA*	L-Asn	D-Tyr	D-Asn	L-Gln	L-Pro	D-Asn	L-Ser*			
Iturin C	NH ₂ FA*	L-Asp	D-Tyr	D-Asn	L-Gln	L-Pro	D-Asn	L-Ser*			
Bacillomycin D	NH ₂ FA*	L-Asn	D-Tyr	D-Asn	L-Pro	L-Glu	D-Ser	L-Thr*			
Bacillomycin F	NH ₂ FA*	L-Asn	D-Tyr	D-Asn	L-Gln	L-Pro	D-Asn	L-Thr*			
Bacillomycin L	NH ₂ FA*	L-Asn	D-Tyr	D-Asn	L-Ser	L-Gln	D-Ser	L-Thr*			
Bacillomycin LC	NH ₂ FA*	L-Asn	D-Tyr	D-Asn	L-Ser	L-Glu	D-Ser	L-Thr*			
Mycosubtilin	NH ₂ FA*	L-Asn	D-Tyr	D-Asn	L-Gln	L-Pro	D-Ser	L-Asn*			
Other											
Polymyxin B ₁ (40)	aiFA9	L-Dab	L-Thr	L-Dab	L-Dab*	L-Dab	D-Phe	L-Leu	L-Dab	L-Dab	L-Thr*
Polymyxin B ₂	iFA8	L-Dab	L-Thr	L-Dab	L-Dab*	L-Dab	D-Phe	L-Leu	L-Dab	L-Dab	L-Thr*
Polymyxin E	aiFA8	L-Dab	L-Thr	L-Dab	L-Dab*	L-Dab	D-Leu	L-Leu	L-Dab	L-Dab	L-Thr*
Polymyxin M	aiFA8	L-Dab	L-Thr	L-Dab	L-Dab*	L-Dab	D-Leu	L-Thr	L-Dab	L-Dab	L-Thr*

2.2.2.3 Relevant CLPs produced by other microorganisms

Streptomyces sp.

Daptomycin (**12**) is a semi-synthetic CLP with potent antibacterial activity, produced by *Streptomyces roseosporus* (Figure 2.10). The CLP produced by the microorganism is first deacylated via a deacylase enzyme and then condensed with decanoic acid. Alternatively, decanoic acid can be added to the fermentation medium leading to a direct incorporation.¹²⁵ Daptomycin (**12**) harbors interesting antibiotic activity (*vide infra*). The calcium-dependent antibiotic (CDA) is produced by *Streptomyces coelicolor*.

Serratia sp.

Also *Serratia* produces several CLPs. The best known are serrawettin W2 (**41**) by *Serratia marcescens* MG1 and the antimycobacterial serratamolides (**42**) (Figure 2.10).¹²⁶

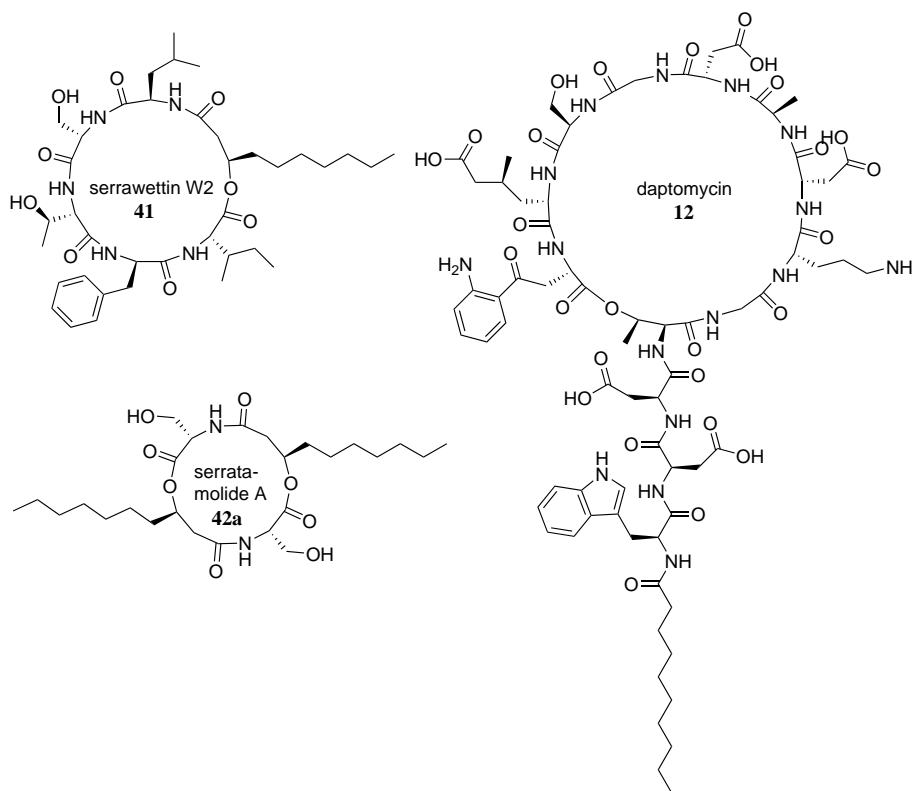


Figure 2.10. Chemical structure of serrawettin W2 (**41**), daptomycin (**12**) and serratamolide A (**42a**).

2.2.3 Biosynthesis

CLPs are synthesized by large, multifunctional enzymes called non-ribosomal peptide synthetases (NRPS). NRPS consist of different sections, called modules, each responsible for the recognition, activation, modification and incorporation of one specific AA building block into the final product. In most cases the sequence and number of modules correlates with the AA sequence of the CLP (colinearity rule). During its synthesis, the elongating peptide moves from

one module to the following, mimicking an assembly-line. A module is further subdivided into different domains effectuating substrate recognition, activation, binding, modification, elongation and release.^{17,18} Ten different types of domains are known.¹⁷ The most important domains are described in detail below.

Overall, three types of modules can be distinguished: initiation, elongation and termination modules. Initiation modules consist of an adenylation and thiolation domain, responsible for the selection and binding of the first amino acid.¹²⁷ Also the *N*-acylation of the first amino acid is typically catalyzed in the initiation module by a condensation domain.¹²⁸ Elongation modules always contain a condensation, adenylation and thiolation domain but editing domains may be present as well. Termination modules contain a condensation, adenylation, thiolation and a thioesterification domain, required for the release and possible cyclization of the oligopeptide.

2.2.3.1 Adenylation (A) domain

The adenylation (A) domain is responsible for AA recognition and activation. The carboxylic acid of the AA is activated via a Mg^{2+} -dependent hydrolysis of ATP, yielding the corresponding amino acyl-*O*-adenylate and pyrophosphate (Figure 2.11).¹⁷ As a consequence of the non-ribosomal synthesis, CLPs can contain not only the 20 common, proteinogenic AAs but different building blocks as well.¹⁷ The large diversity of building blocks of CLPs is explained by the existence of a wide structural variety of A domains.¹⁷ Based on the analysis of the primary sequence of the binding pocket of the A domain, its selectivity can be predicted employing the non-ribosomal code.^{127,129–132} Via selective mutation it is possible to alter the selectivity of the A domain and construct new peptide analogues.^{129,133} The substrate flexibility of certain A domains can give rise to the biosynthesis of several structural variants of a certain CLP or even allow the incorporation of added, unnatural amino acids.^{18,117,134–136}

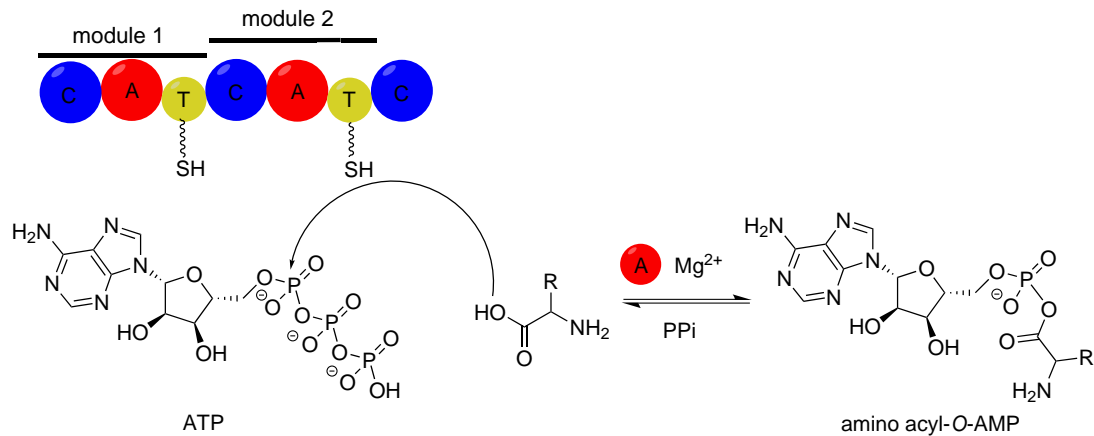


Figure 2.11. A Domain-catalyzed recognition and activation of the selected amino acid at the expense of ATP to yield the amino acyl-*O*-AMP. Figure adapted from Sieber *et al.*¹⁷

2.2.3.2 Thiolation (T) or peptidyl carrier protein (PCP) domain

Downstream of the A domain, the activated amino acyl-*O*-adenylate is covalently bound to the thiol group of the 4'-phosphopantetheinyl (ppant) co-factor, linked to a serine residue of the thiolation (T) domain. Therefore, to activate a T domain, it must be posttranslationally modified to obtain this 20 Å long phosphopantetheinyl arm, derived from coenzyme A. This modification from inactive apo- to functional holo-form is catalyzed by 4'-phosphopantetheinyl transferases (PPTase) and is Mg²⁺-dependent (Figure 2.12).^{127,137,138} The thioesterification between the activated amino acid and the ppant co-factor is catalyzed by the A domain. After this step, the substrate is covalently bound to the enzyme. The T domains are responsible for passing the substrate from one catalytic center to the next throughout the NRPS assembly line.¹⁷ The thioesters employed by NRPS are more reactive than the tRNA-bound ester intermediates which are used in ribosomal peptide synthesis, because of lower mesomeric stabilization of the thioester compared to the ester.¹⁷

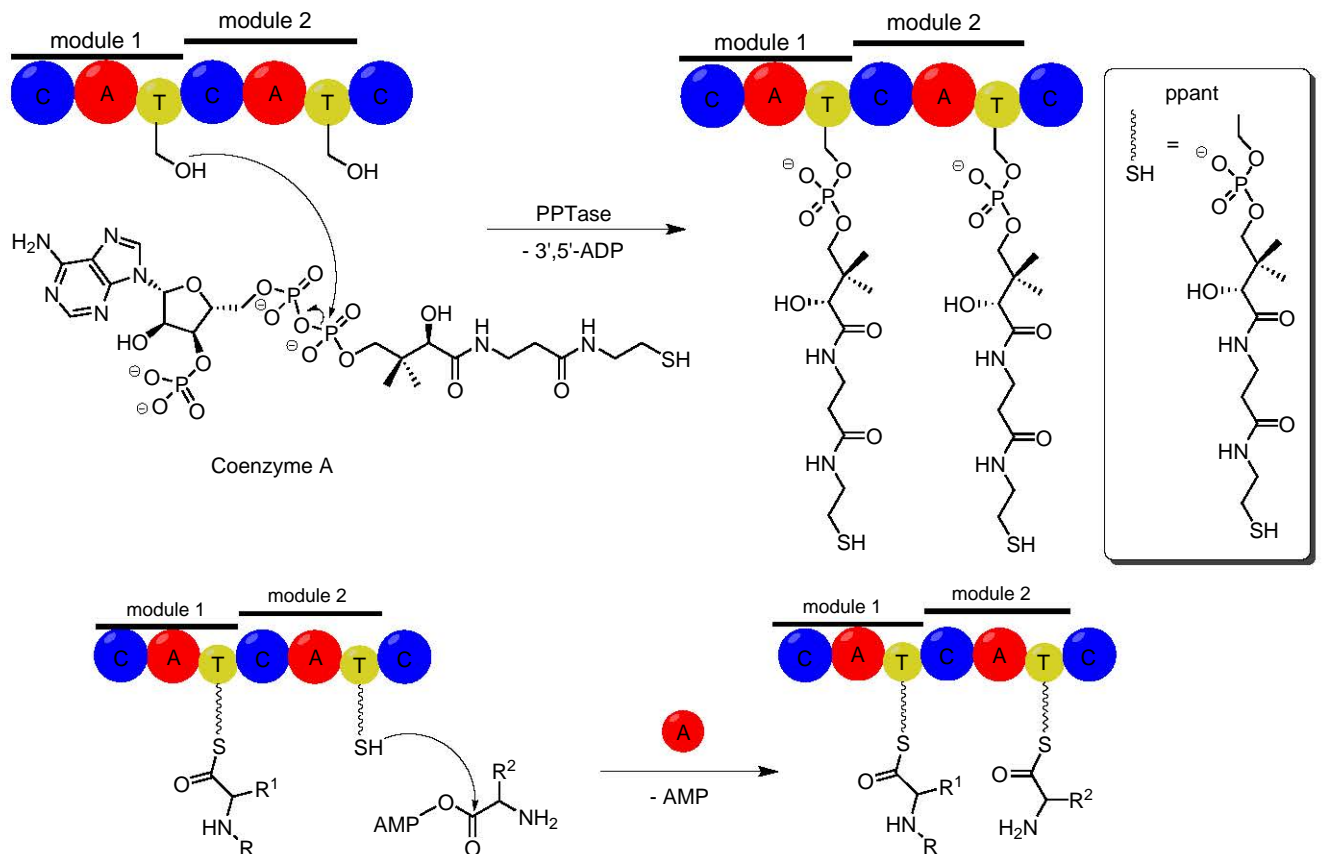


Figure 2.12. Posttranslational modification of the T domain with its ppant co-factor by a phosphopantetheinyltransferase (PPTase). The phosphopantetheine moiety is transferred from coenzyme A to a conserved serine residue of the T domain. Then the activated amino acid moiety is covalently attached to the thiol group of the ppant co-factor of the T domain. This loading of the T domain is catalyzed by the A domain. Figure based on Lambalot *et al.*, Sieber *et al.* and Fischbach *et al.*^{17,137,138}

2.2.3.3 Condensation (C) domain

Condensation (C) domains catalyze the peptide bond formation via nucleophilic attack of the α -amino group of the downstream PCP-bound AA, positioned in the acceptor site, on the as a thioester activated carboxylic acid part of the upstream PCP-bound AA, positioned in the donor site (Figure 2.13). The resulting peptide then serves as the donor substrate in a subsequent condensation catalyzed by the C domain of the next module.^{17,127,128} Although C domains exhibit a high selectivity for the nucleophilic (acceptor) substrate, the electrophilic (donor) substrate is hardly differentiated.¹³⁹ However, when an epimerization domain is present (see section 2.2.3.5), the C domain is responsible for the selection of the donor substrate with the correct stereochemistry.^{128,140}

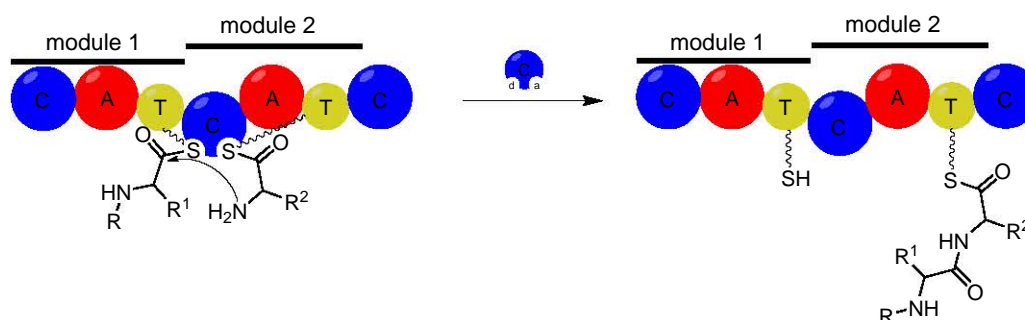


Figure 2.13. Peptide bond formation catalyzed by the C domain. The nucleophilic amine of the amino acid moiety in the acceptor (a) site attacks the electrophilic thioester of the amino acid moiety accommodated in the donor (d) site. The resulting peptide can subsequently act as the electrophile in the donor site of the next C domain. Figure adapted from Sieber *et al.*^{17,127}

2.2.3.4 Thioesterase (TE) domain

Finally, to reactivate the multienzyme complex for another synthetic cycle, the thioesterase (TE) domain cleaves the oligopeptide at the end of the assembly line in the termination module. To achieve this release, a conserved serine residue of the active site of the TE domain attacks the T domain-bound peptidyl thioester, forming a peptide-*O*-TE intermediate.¹²⁷ Subsequently, the peptide can be released from this serine moiety either by hydrolysis, to yield a linear peptide, or by an intramolecular nucleophilic attack, yielding a CLP (Figure 2.14). Whether a cyclic or a linear LP is released is determined by the oxyanion hole. The negatively charged intermediate formed during the release reaction is stabilized by two amide bonds. In the case of a TE domain that is producing CLPs, a rigid proline residue can be found next to one of these amides, whereas for the other type of TE domain, a more flexible glycine residue is present, easing the entry of a water molecule that is required for hydrolysis.¹⁴¹ The cyclization always includes the C-terminal end of the peptide, side-chain to side-chain cyclizations have not been observed.^{17,141} The macrocyclization catalyzed by TE domains occurs stereo- and regioselective.^{142,143} The presence and type of the fatty acid tail can exert a profound effect on the regioselectivity of this cyclization catalyzed by the TE domain.¹⁴³ TE domains also control the oligomerization of identical peptide units during iterative peptide synthesis.¹⁴⁴

Macrocyclization is difficult to achieve via chemical synthesis without the application of many protecting groups, which is often accompanied with low yields. Excised TE domains can be used for chemoenzymatic synthesis. A linear precursor is first synthesized via solid-phase peptide chemistry, followed by selective and efficient cyclization catalyzed by an excised TE domain.^{17,141–143}

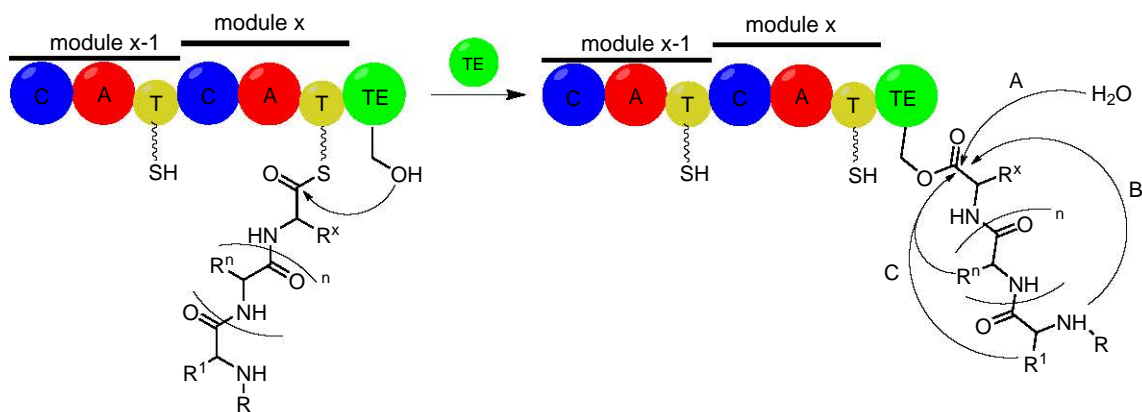


Figure 2.14. Release of the peptide catalyzed by the TE domain. This release can occur via hydrolysis (A), delivering a linear product or via intramolecular cyclization involving (the terminal) amine group (B) or a nucleophilic side chain (C), yielding a lactam or a lactone. Also the fatty acid tail can be involved in this cyclization. Figure adapted from Sieber *et al.*¹⁷

2.2.3.5 Editing domains

When the substrate is linked to the T domain, different modifications can take place, catalyzed by the non-essential editing domains.

Epimerization (E) and condensation/epimerization (C/E) domain

A striking feature of many CLPs is the presence of one or more D-AAAs. A possibility for the inclusion of D-AAAs is selective incorporation by the A domain of D-AAAs provided by an external racemase.¹⁴⁵ A more prevalent way is through the use of E domains. E Domains epimerize the C_{α} -carbon of the amino acid linked to the ppant co-factor of the T domain, delivering a D/L-mixture.^{17,140} Subsequently, the downstream C domain enantioselectively selects the product with the desired stereochemistry.^{127,128,140}

However, sometimes there are discrepancies between the stereochemistry of the final peptide, containing D-AAAs, and the corresponding NRPS, lacking E domains. Typically, these NRPS possess condensation domains with a dual catalytic activity: both condensation and epimerization are effectuated by these domains. These are called C/E domains and epimerize the AA loaded on the T domain of the preceding module. This type of domain can be recognized by the elongated His motif.¹⁴⁶ E Domains have been found in Gram-positive bacteria such as *Bacillus*, but typically not in the Gram-negative *Pseudomonas* species, as they contain C/E domains.

Methyltransferase (MT) domain

Another type of modification is *N*- or *C*-methylation of the substrate. This domain relies on *S*-adenosyl-L-methionine (SAM) as the methyl donor.¹²⁷

(Hetero)cyclization (Cy) domain

This is the only type of editing domain that can replace one of the core domains of the NRPS.¹²⁷ When replacing a C domain, this unit catalyzes the formation of oxazoline and thiazoline rings out of Ser/Thr or Cys respectively.^{17,147}

Oxidation (O) and Reduction (R) domain

The oxidation state of oxazoline and thiazoline rings can be modified via oxidation (Ox) or reduction (R) domains.¹²⁷ In the absence of a TE domain, C-terminal R domains can also reduce the thioester linked to the T domain, thereby releasing the linear oligopeptide as an aldehyde or alcohol.¹⁴⁴

Formyltransferase (F) domain

N-Formylation is effectuated by the *N*-formyltetrahydrofolate-dependent F domain.^{17,148}

2.2.3.6 Fatty acid introduction

An additional condensation (C1) domain preceding the A domain of the initiation module is involved in the *N*-acylation of the first amino acid with the lipid moiety (also known as lipoinitiation).^{128,135,149,150}

In the case of surfactin (**37**), the CoA-activated β -hydroxy fatty acid is transferred with a high specificity to the T domain-bound amino acid. The activation of the β -hydroxy fatty acid itself is catalyzed by a fatty acyl CoA ligase.¹⁴⁹ The calcium-dependent antibiotic (CDA) CLP follows a quite similar mode of fatty acid introduction, only using a fatty acid tethered to ACP instead of CoA.¹⁵⁰ A third mechanism of fatty acid introduction is found in mycosubtilin, produced by a hybrid PKS/NRPS synthase. During its biosynthesis, palmitic acid is loaded onto the first A domain of the polyketide synthase part, then condensed with malonyl-CoA and the resulting β -keto thioester is reductively aminated to give the β -amino fatty acid moiety that is characteristic for CLPs belonging to the iturin group. This fatty acid tail is then presumably passed on to the NRPS part.¹⁵¹ The hydroxy fatty acids themselves could be produced by the primary metabolism (type II fatty acid synthase systems).¹¹⁷

As an example of the complete NRPS-assembly line, the ten modules responsible for the synthesis of the CLP orfamide A are represented in figure 2.15.¹⁸

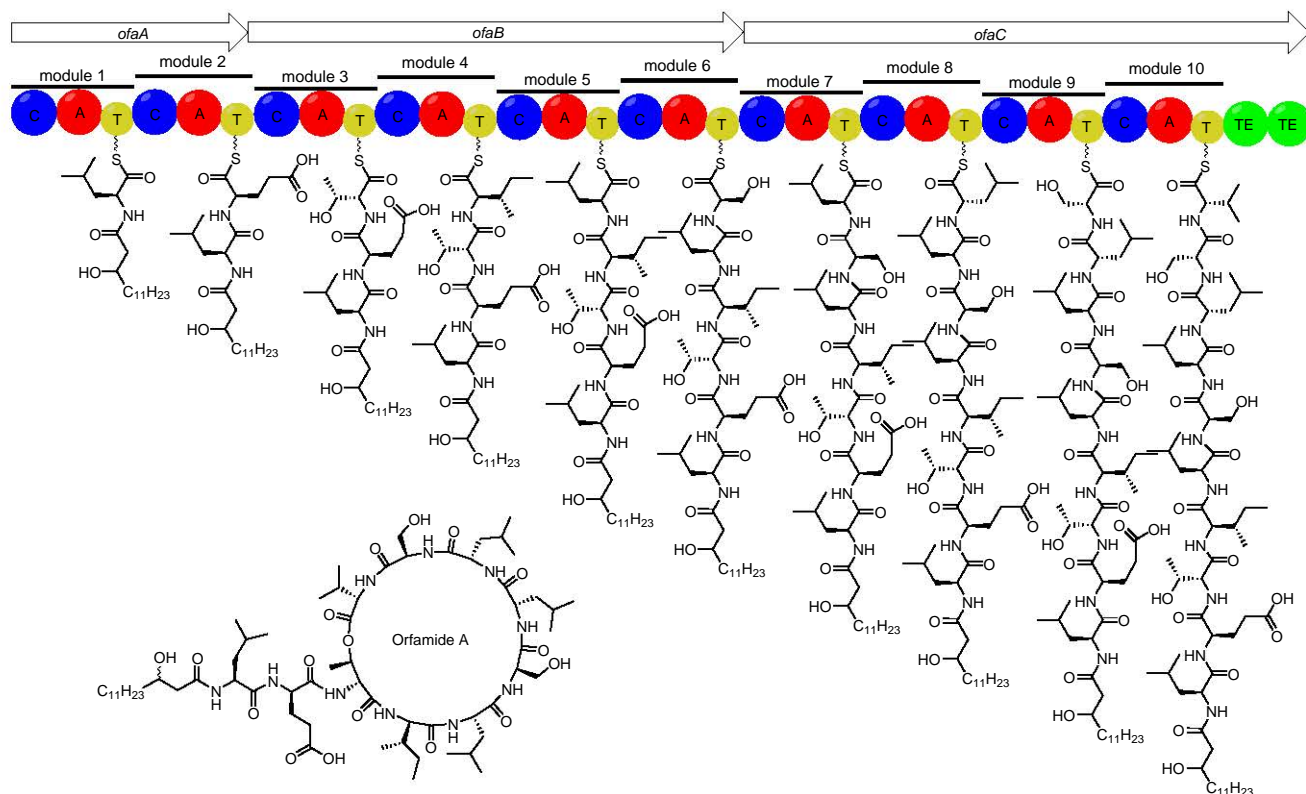


Figure 2.15. NRPS Organization for the biosynthesis of the CLP orfamide A. ¹⁸

2.2.3.7 Comparison ribosomal - non-ribosomal peptide synthesis

In ribosomal peptide synthesis, a tRNA synthetase selects and activates the AA at the expense of ATP, yielding an amino acyl-*O*-adenylate. Although an identical mechanism is followed by the A domains, both type of enzymes evolved independently. In case of the ribosomal peptide synthesis, the activated AA is subsequently loaded onto a tRNA via an ester bond, which then goes to the ribosome for mRNA-directed protein biosynthesis. During non-ribosomal peptide synthesis, the activated AA is transferred to a T domain and then further passed on through the NRPS assembly line. ^{127,152}

Due to the need for precision in primary metabolism, several proofreading mechanisms are included in ribosomal synthesis, which are absent in NRPS. ^{127,152} On the other hand, NRPS can use several hundreds of substrates, whereas ribosomal synthesis is normally restricted to the 20 proteinogenic AAs. ¹²⁷

2.2.4 Regulation of CLP production

In response to several abiotic conditions (temperature, pH, oxygen, etc.), nutritional factors (carbon, nitrogen and trace elements) and sometimes even plant signal molecules, a complex genetic network regulates the CLP production. ¹¹³ Known CLP regulatory genes and mechanisms are discussed below.

2.2.4.1 Regulation of CLP production in *Pseudomonas*

GacS/GacA

The production of CLPs is subjected to complex regulatory circuits. In *Pseudomonas* species, the GacS/GacA (Global activator) two-component system is often a crucial element and functions as a master switch (Table 2.3).^{115,116,118,136,153–159} Nutritional factors and specific plant phenolic glycosides were able to activate the synthesis of syringomycin in *P. syringae* pv. *syringae*.¹¹⁵ Exudates from sugar beet seeds were also able to activate amphisin production in *Pseudomonas* sp. DSS73 via triggering the GacS/GacA two-component system. GacS is a transmembrane protein, functioning as a histidine sensor kinase, which is activated by autophosphorylation in response to environmental stimuli and then phosphorylates its cognate response regulator GacA.^{115,153,154} GacA in its turn activates the expression of certain target genes specifying small noncoding RNAs. These RNAs are characterized by repeated CGA motifs essential for binding small RNA-binding proteins (RsmA) that act as translational repressors of target mRNAs.^{118,160} In this manner, activation of Gac titrates the repressors away. Besides many secondary metabolites, also the production of AHLs is typically GacS/GacA-regulated.¹⁶¹

LuxR-type transcriptional regulators

LuxR-type regulators are found in the flanking regions of most NRPS genes present in *Pseudomonas* (Table 2.3).^{114,157,162} These transcriptional regulators contain a DNA-binding helix-turn-helix motif but lack an AHL-binding or response regulator domain.¹⁶²

LuxR-type regulators SalA and SyrF regulate syringomycin and syringopeptin (**34**) production in *P. syringae* pv. *syringae*. SalA is suspected to interact with the *syrF* promoter and SyrF then binds and activates the promoter of the target NRPS.^{153,157,163} ViscAR and ViscBCR regulate viscosin (**36**) production in *P. fluorescens* SBW25,¹⁶² and the similar MassAR and MassBCR transcriptional regulators control massetolide biosynthesis in *P. fluorescens* SS101.¹³⁶ EtlR controls entolysin biosynthesis in *P. entomophila*,¹¹⁸ and ArfF arthrofactin production in *Pseudomonas* sp. MIS38.¹⁶⁴ Also the production of white line-inducing principle (WLIP), a member of the viscosin CLP group, by rice rhizosphere isolate *P. putida* RW10S2 is activated by the LuxR family regulator WlpR and is not controlled by the present PmrI/PmrR QS system.¹¹⁴

Table 2.3: Regulation of CLP production. Adapted and extended from Raaijmakers *et al.*^{113,162}

CLP	Microorganism	Regulators involved	AHLs
Amphisin ^{154,155}	<i>Pseudomonas</i> sp. DSS73	GacS/GacA	-
Arthrofactin ¹⁶⁴	<i>Pseudomonas</i> sp. MIS38	GacS/GacA, ArfF, heat shock protein HtpG and stress factor spoT	-
Cormycin A ^{24,25}	<i>P. corrugata</i> CFBP5454	QS: PcoI/PcoR, RfiA	C6 1c , C8 1e , oxo6 3c
Corpeptin A & B ^{24,25}	<i>P. corrugata</i> CFBP5454	QS: PcoI/PcoR, RfiA	C6 1c , C8 1e , oxo6 3c
Corpeptins ²⁵	<i>P. mediterranea</i> CFBP5447	QS: PmeI/PmeR, RfiA	C6 1c , C8 1e , oxo6 3c
Entolysin ¹¹⁸	<i>P. entomophila</i>	GacS/GacA, EtlR	-
Massetolide A ^{136,165}	<i>P. fluorescens</i> SS101	GacS/GacA, MassAR and MassBCR, serine protease ClpP	-
Putisolvin I (32) & II ^{22,23,156}	<i>P. putida</i> PCL1445	GacS/GacA, PsoR, heat shock proteins DnaK, DnaJ and GrpE, QS: PpuI/RsaL/PpuR	oxo10 3g , oxo12 3i
Serrawettin W2 (41) ^{126,166}	<i>Serratia marcescens</i> MG1	SwrI/SwrR	C4 1a , C6 1c
Syringopeptin (34) ¹⁵⁷	<i>P. syringae</i> pv. <i>syringae</i> B301D	GacS/GacA, SalA, SyrG, SyrF	-
Syringomycin ^{115,153,157}	<i>P. syringae</i> pv. <i>syringae</i> B301D	GacS/GacA, SalA, SyrG, SyrF	-
Viscosin (36) ²¹	<i>P. fluorescens</i> 5064		HO8 2e
Viscosin (36) ^{131,162}	<i>P. fluorescens</i> SBW25	GacS/GacA, ViscAR and ViscBCR	-
WLIP ¹¹⁴	<i>P. putida</i> RW10S2	GacS/GacA, WlpR	-
Xantholysin ¹¹²	<i>P. putida</i> BW11M11	XtlR	-

Regulation by AHL-mediated QS

AHL-Mediated QS controls several bacterial traits but only in a limited number of cases AHLs play an important regulating role in CLP production (Table 2.3). During the screening for biosurfactant producing strains in the sugar beet rhizosphere, only three out of 80 surfactant-producing isolates were able to synthesize AHLs.¹⁵⁵ True LuxR analogues such as LuxR itself, LasR, RhlR, and PhzR contain an AHL-binding domain.

The involvement of AHL-mediated QS in the control of viscosin (**36**) production by broccoli pathogen *P. fluorescens* 5064 was hinted by the fact that biosurfactant production only started at high cell densities in the late exponential growth phase. The corresponding AHL is HO8 **2e**.²¹ Another example is the PpuI/RsaL/PpuR QS-system regulating putisolvin I (**32**) and II synthesis in *P. putida* PCL1445. These CLPs are produced at late exponential growth phase as well. LuxI and LuxR homologues PpuI and PpuR are responsible for AHL (oxo10 **3g** and oxo12 **3i**) production and recognition, whereas RsaL acts as a repressor of PpuI and PpuR. Mutation in the *ppuI* and *ppuR* genes causes a reduced putisolvin production, whereas *rsaL* mutation gives rise to overproduction of both AHLs and putisolvin.²² Besides the AHL-mediated QS regulation,²² also the LuxR-type regulator PsoR was shown to be involved.²³ Tomato pathogen *P. corrugata* contains the PcoI/PcoR QS-system controlling the synthesis of CLPs corpeptin A

and B and cormycin A as virulence factors.^{24,25} A similar regulation is also found in the closely related *P. mediterranea* (containing the PmeI/PmeR operon).²⁵ *P. corrugata* contains as well a LuxR-family type regulator, designated RfiA, for which the downstream regulatory *rfiA* gene is co-transcribed with *pcoI*.²⁴

Other types of regulators

Besides LuxR analogues or LuxR-type regulators, other proteins can be involved as well. Serine protease ClpP (caseinolytic protease) regulates massetolide biosynthesis via influencing the expression of LuxR-type transcriptional-regulatory genes in the plant-growth stimulating strain *P. fluorescens* SS101. ClpP typically plays a crucial role in intracellular refolding and degradation of proteins. It was postulated that ClpP degrades proteins that repress or interfere with the transcription of the massetolide-regulatory gene. Also an influence on the citric acid cycle and amino acid metabolism cannot be excluded. It was shown that ClpP regulates massetolide biosynthesis independent of the GacA/GacS-controlled regulation.¹⁶⁵

Heat shock proteins DnaK, DnaJ and GrpE were shown to be involved in the regulation of the biosynthesis of putisolvin in *P. putida* PCL1445 at low temperatures. These proteins may be required for proper folding of other positive regulators or the synthetic machinery.¹⁵⁶ Also heat shock protein HtpG is involved in regulating the synthesis of arthrofactin, but the mechanism of its involvement is not entirely clear yet. Also the SpoT stress factor, which is responsible for the hydrolysis of guanosine 3',5'-bispyrophosphate (ppGpp) and synthesis of guanosine 3'-diphosphate,5'-triphosphate (pppGpp), seems to play a role in arthrofactin synthesis.¹⁶⁴

2.2.4.2 Regulation of CLP production in other bacteria

Serratia

Serratia marcescens MG1 (previously designated as *S. liquefaciens*) produces serrawettin W2 (**41**) (Figure 2.10). This production is controlled by the SwrI/SwrR quorum sensing system and its cognate AHLs C4 **1a** and C6 **1c**.^{126,166} In *swrI*-mutant MG44, unable to swarm, the serrawettin W2 (**41**) production and thus the swarming phenotype could be restored by the addition of C4 **1a**.^{126,166} Besides the QS regulated CLP-production, stimulation of the *flhDC* master operon which controls swarmer cell differentiation (cell elongation, multinucleation and hyperflagellation), is needed as well to achieve swarming. Also nutrient status plays a crucial rol.¹⁶⁷

Bacillus

Surfactin (**37**) production is regulated by the two-component system ComA/ComP in a cell-density dependent manner via the peptide pheromone ComX among many other components.

ComA is phosphorylated by protein kinase ComP in response to perception of ComX. The activated ComA then binds to the promoter region.^{20,116,168}

2.2.5 Natural functions

The main natural functions associated with CLPs are antagonism, motility and surface attachment (Figure 2.16).²⁰ The structure of a CLP determines the activity, small structural changes in the peptide core or lipid tail can change the physicochemical properties and interaction with membranes.^{106,123,134,136,162}

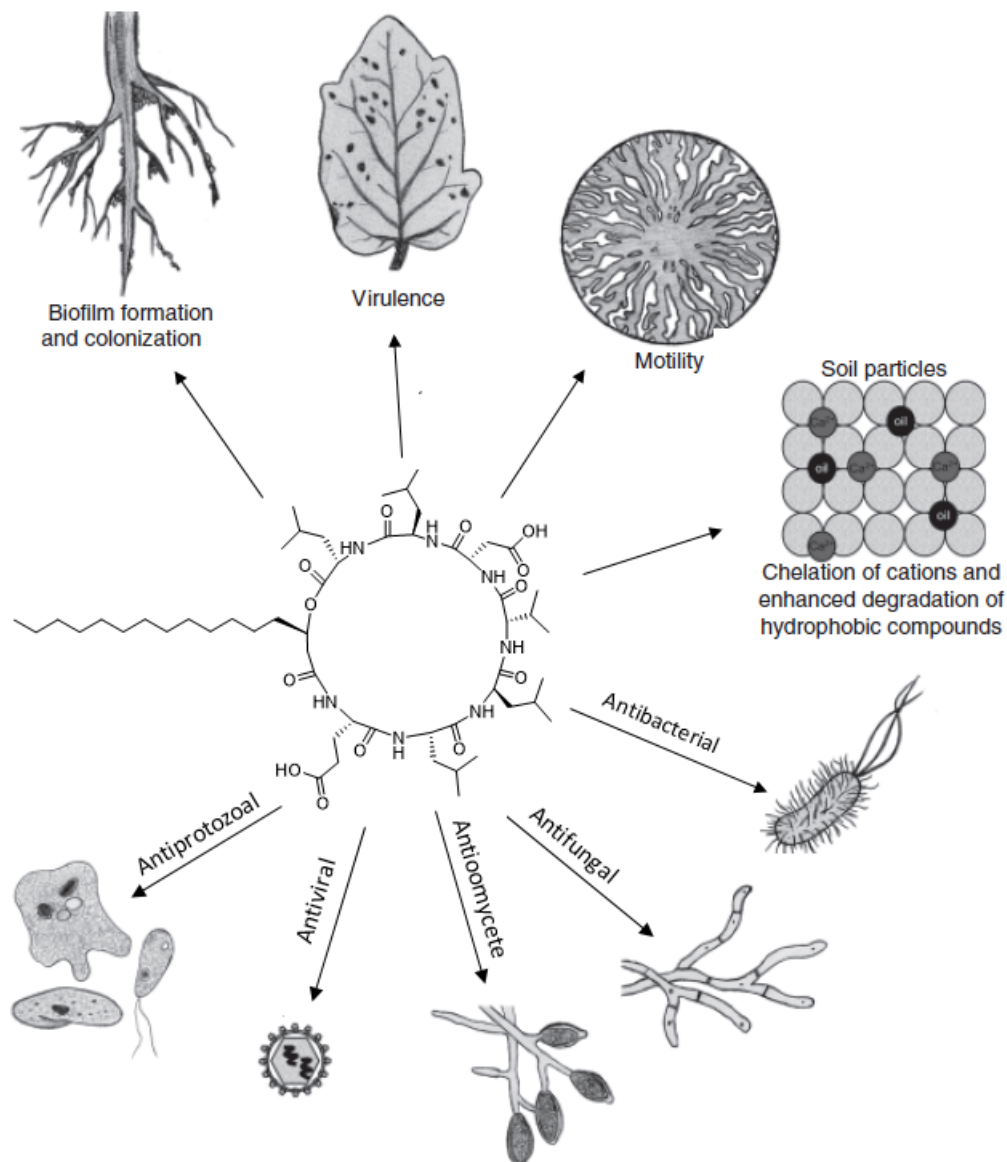


Figure 2.16. Different natural functions of CLPs. Figure from Raaijmakers *et al.*²⁰

Microbial warfare

The antagonistic effects of many CLPs grant a competitive advantage to the producing organism over coexisting microorganisms. By disintegrating membranes, CLPs can exhibit inhibitory ef-

fects against bacteria, viruses, fungi and oomycetes.^{19,20,113,169} The limited activity of CLPs against Gram-negative bacteria has been ascribed to the protective effects of the outer membrane, although there are exceptions.^{19,112,170} The mode of action consists of the formation of channels in the membrane. The resulting pores increase the influx of H⁺ and Ca²⁺ and the efflux of K⁺, causing a collapse of the membrane pH gradient, although some CLPs act rather as a non-specific detergent than as a pore-forming toxin.^{19,115,170,171} To fully assess the antagonistic effect of a CLP, studies with the isolated CLP or with non-producing or overproducing mutants are required, besides the evaluation of the level of CLP-production *in vitro*.¹²¹

Protection against predation

Both surfactin (**37**), produced by *Bacillus*, and serrawettin W2 (**41**), produced by *Serratia marcescens*, were able to fend off the nematode *Caenorhabditis elegans* from feeding on the bacterial colonies.¹⁷² Also viscosin (**36**) produced by *P. fluorescens* SBW25 and massetolide produced by *P. fluorescens* SS101 offer both species protection against predation by the amoeba *Naegleria americana*.¹⁷³

Motility

CLPs can influence the wettability of surfaces, helping the bacteria spread across these surfaces.^{19,113,121,155} Surfactin (**37**) for example can lower the surface tension of water from 71 to 27 mN/m at concentrations as low as 20 μM.¹²³ Viscosin (**36**) has a comparable effect on the surface tension.¹⁹ As a consequence, several CLPs are indispensable for the producing microorganism to swarm, e.g. massetolide A,¹³⁶ amphisin,¹⁵⁵ entolysin,¹¹⁸ and serrawettin W2 (**41**).¹²⁶ Benefits of increased bacterial mobility include better nutrient acquisition, avoiding predators and toxic substances and access to new colonization sites.¹⁵⁵

Biofilm formation

Biofilms can protect the inhabiting bacteria against undesired elements such as antibiotics and predators. CLPs can play an important role during the attachment phase and the formation of biofilm as demonstrated by the tendency of CLP-mutants to form differently structured biofilms. The structure of the CLP plays an important role: whereas some CLPs such as massetolide A, positively stimulate the formation of a thick, structured biofilm,¹³⁶ other CLPs (e.g. putisolvin I (**32**) and II) dissipate existing biofilms.^{22,174,175} The orientation of the CLP plays a crucial role in the final effect. When the hydrophobic moiety of CLP is embedded into the bacterial cell surface, leaving the hydrophilic part of the CLP exposed, only attachment to hydrophilic surfaces is possible. On the other hand, when the hydrophobic part remains exposed, only attachment to hydrophobic surfaces is possible.¹⁷⁶ This effect was suggested by the observation that a rham-

nolipid surfactant increased the cell hydrophobicity of some *P. aeruginosa* strains and hence the rate of octadecane degradation.¹⁷⁷ On the other hand, when a serratamolide (**42**) biosurfactant was added to a *Serratia marcescens* culture, a reduction of cell surface hydrophobicity was observed, presumably caused by blocking the hydrophobic sites.¹⁷⁸ The final effect depends on the initial bacterial surface hydrophobicity as well. Whereas surfactin (**37**) was able to increase the hydrophobicity of a hydrophilic *B. subtilis* strain, a decrease in cell surface hydrophobicity of a hydrophobic strain was observed.¹⁷⁹

Chelation and emulsification

The emulsifying properties of CLPs increase the solubility of hydrophobic nutrients, enhancing the growth.¹⁹ Also several metal ions can be chelated, granting protection against the toxic effects of certain metals or enabling sequestration of trace metals as micronutrients.²⁰ Structural elements play a crucial role, the replacement of a Glu-residue in surfactin (**37**) with Gln yields lichenysin with better chelation properties for Ca^{2+} and Mg^{2+} .¹⁸⁰

Phytotoxicity

Several CLPs have a phytotoxic activity. Syringomycin and syringopeptin (**34**) of *P. syringae* interact with the plant plasma membrane leading to pore formation thereby enabling transmembrane passage of K^+ , H^+ and Ca^{2+} -ions. This eventually induces necrosis of plant tissues.¹¹⁵ Also the biosurfactant properties of CLPs contribute indirectly to the virulence by helping bacteria spread and solubilizing plant protective wax layers, having a synergistic effect with cell wall degrading enzymes.^{19,113} The CLPs corpeptin A and B and cormycin A are the major virulence factors of tomato pathogens *P. corrugata* and *P. mediterranea*.^{24,25}

2.2.6 Commercial applications of bacterial CLPs

Biosurfactants can be applied in a broad range of industrial applications such as oil recovery, bioremediation, wetting and emulsification. The main advantage compared to the synthetic alternatives are their biodegradability and lower toxicity. However, not all CLPs can be used as such. Sometimes the (cyto)toxicity of some CLPs prevents their use for certain (clinical) applications. Also instability can impede industrial application of some CLPs.¹⁰⁹ Another limitation is the rather low level of CLP production. To offer an economically viable alternative for non-renewable, synthetic compounds, CLPs should be produced with a high productivity and on inexpensive substrates. Also the downstream processing should be limited.^{181,182} Surfactin (**37**) is often extracted from the culture broth via acid precipitation, recrystallization and organic solvent extraction. However, several impurities are co-extracted, causing the need for a chromatographic separation step.¹²³ Another option is the foam fractionation technique, exploiting

the surfactant properties of surfactin (**37**). The CLP is recovered from the collapsed foam via acid-induced precipitation.¹⁸³

Cosmetic industry

Besides their environmentally friendly and renewable image, many CLPs possess a low human toxicity, allowing their application for cosmetic products. Several CLPs, such as surfactin (**37**), serrawettin and iturin are suitable to be used as emulsifiers in skin preparations.¹⁸⁴ Surfactin (**37**) can be included in cleansing cosmetics as well. These products show an excellent washability combined with an extremely low skin irritation.^{185,186} The Japanese company Kaneka offers surfactin (**37**) on the market for cosmetic applications.¹⁸⁷ The antimicrobial properties of many CLPs can also aid to increase the product preservation.¹⁸⁶

Soil remediation

Biosurfactants can be applied for soil remediation. By solubilizing the pollutants, their environmental degradation is enhanced. The CLP surfactin (**37**) was able to enhance diesel biodegradation at a concentration of 40 mg/L. On the other hand, a concentration of 400 mg/L halted biodegradation, presumably due to the antibiotic properties of this CLP.¹⁸⁸ Also the biodegradation of the chlorinated pesticide endosulfan was enhanced in the presence of surfactin (**37**).¹⁸⁹ Aliphatic and aromatic hydrocarbons degraded more quickly as well in the presence of this CLP.¹⁹⁰ The increased degradation of aromatic compounds is caused by increasing contact with air to speed up oxidation.¹⁹¹ The solubilizing properties of CLPs toward hydrocarbons can also be exploited for the mobilization of oil, for example entrapped in sandstone cores, thereby enabling oil recovery.^{192,193}

The metal chelating properties of several CLPs can be exploited for the removal of heavy metals from contaminated soil.¹⁹¹ Surfactin (**37**) succeeded in removing Zn and Cu by sorption at the soil interface and metal complexation.¹⁹⁴ Alternatively, blowing with air, causes the metal-CLP complex to foam, allowing easy removal from the soil.¹⁹⁵

Pharmaceutical applications

CLPs represent an underexplored class of natural products with promising antibacterial activity to confront the emergence of multi-resistant human pathogens. Several CLPs with antibiotic activity have been described.¹¹⁰ A strong advantage of CLPs as antimicrobial agents is their rapid bactericidal effect and a minimal induction of resistance because of the fact that the entire membrane is targeted, which is difficult to redesign.¹²⁴ Limitations are the limited solubility and potential toxicity because of the unspecific mode of action.¹²⁴ Most CLPs are only active against Gram-positive bacteria. The Gram-negative outer membrane or peptidoglycan layer presumably

denies the CLP access to the plasma membrane.^{19,170}

A famous example of a CLP-type antibiotic is daptomycin (**12**), produced by the Gram-positive bacterium *Streptomyces roseoporus* and currently used as a last resort antibiotic against methicillin-resistant *Staphylococcus aureus* (MRSA) and vancomycin-resistant *Enterococci* (VRE). This anionic CLP is since its FDA approval in 2003 commercially marketed as Cubicin. The currently accepted mode of action involves Ca²⁺-dependent binding to the cytoplasmic bacterial membrane followed by a perturbation of the membrane in a detergent-like manner.^{124,196,197}

For infections caused by Gram-negative bacteria, polymyxins are an interesting option. These cationic CLPs have an affinity for a lipopolysaccharide (LPS) component of the outer cell membrane of Gram-negative bacteria. Polymyxin B (**40**) and E (= colistin) are already in clinical use, but high doses are accompanied with neurotoxic and nephrotoxic effects.¹⁹⁷ Currently, two polymyxins developed by an optimization program of Northern Antibiotics are undergoing late stage preclinical development.¹²⁴

Another encouraging example is Pseudomycin B. This CLP is effective against the human-pathogenic yeasts *Candida albicans* and *Cryptococcus neoformans* but has an irritating effect and can cause necrosis of the treated tissue, hindering practical applications. However, pseudomycin analogues have been synthesized that retained the antibiotic effect but with a strongly reduced toxicity to the experimental animals.¹⁹⁸

Several other CLPs are known with weak to moderate *in vitro* antibacterial activity.¹¹⁰ Masetolide A and viscosin (**36**) exhibit *in vitro* antimicrobial activity against tuberculosis causative agent *Mycobacterium tuberculosis*.^{18,19,134,136} *B. megaterium* is inhibited by corpeptin and syringopeptin 22A and 25A (**34**).¹⁹ Surfactin (**37**) exhibits antibacterial activity against *Mycoplasma* but its cytotoxicity against erythrocytes hinders its medical application.¹⁶⁹

Some CLPs possess antiviral activity as well. Surfactin (**37**) is active against some enveloped viruses, such as herpes- and retroviruses.^{169,199} Because of its hemolytic activity, clinical application is limited to local treatment.¹⁹⁹ Also viscosin (**36**) has *in vitro* antiviral activity against enveloped human-pathogenic viruses (e.g. infectious bronchitis virus, influenza virus and Newcastle disease virus). The high MIC values suggest a non-specific detergent effect, acting on the lipid envelope of the virus.¹⁹

Other medical applications

Surfactin (**37**) is a valuable inhibitor of fibrin clot formation, but further research is required to determine the applicability of this compound **37**.^{110,122}

Crop protection - fungicides

CLPs have a great potential to be used as environmentally friendly alternatives for chemical plant protection agents currently in use against several agricultural diseases. One option would be to use the CLP as such, whereas another possibility is using the CLP-producing microorganism itself. The spore-forming ability of *Bacillus* is in this point of view a huge advantage.¹²¹ Several CLPs produced by *Pseudomonas* have been reported to play a role in biological control of several plant pathogens as well.²⁰⁰ Some examples are xantholysin against *Xanthomonas* sp. and *Rhizoctonia solani*,¹¹² viscosin (**36**) against *Phytophthora infestans*,¹³¹ and sessilin and orfamide against *R. solani*.^{201,202} Orfamides and massetolides have also a destructive effect on the zoospores of many *Oomycete* plant pathogens (*Pythium ultimum* and *Phytophthora porri*).^{117,131,203}

Antifouling

Several CLPs are able to desintegrate biofilms and prevent biofilm formation. Besides the industrially relevant biofouling, biofilms are medically relevant as well, as they grant resistance against added antibiotics. It was shown that the addition of the *B. subtilis* CLP surfactin (**37**) was able to disperse the biofilm formed in urethral catheters by *Salmonella enterica*, *E. coli*, and *Proteus mirabilis*. Biofilms formed by *P. aeruginosa* remained unaffected.¹⁷⁴

2.3 Concluding remarks

Although a lot of research has been performed on QS, interkingdom signaling is only an emerging field of research. The effect of AHLs on plants, and plants on QS is clear, but there is still a lot of debate about the exact mechanism of action. Sometimes differing (or even contrasting) effects can be observed for one AHL depending on the experimental set-up (plant species, agar plates or liquid medium, duration of the treatment, AHL contact before or after germination, etc.). Careful *in vitro* and *in vivo* experiments with different plant species are required to draw conclusions and perhaps allow the use of AHLs for commercial applications.

CLPs fulfill several crucial functions for the producing organism. As is the case for many secondary metabolites, their production is subjected to many complex regulatory circuits. A better understanding of this regulation could help increase CLP-production to make them even more competitive alternatives for some surfactants used today. Besides the application as pure surfactants, CLPs could be applied in several other markets such as cosmetic industry, pharmaceutical industry, crop protection, soil remediation, etc.

Chapter 3

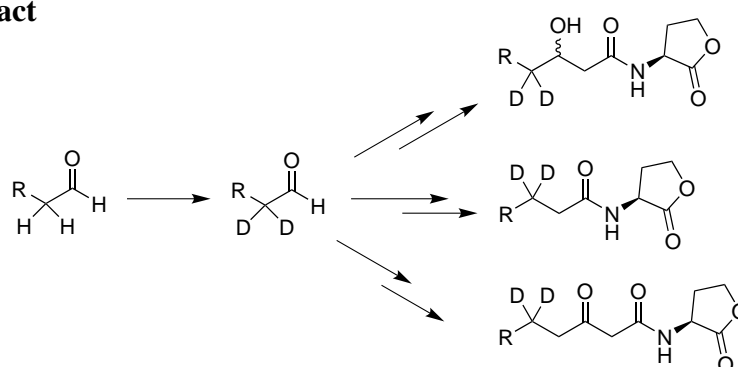
Results and discussion

3.1 Synthesis and analysis of stable isotope-labelled *N*-acyl-L-homoserine lactones

Abstract

Aliphatic aldehydes were deuterated at the α -position via a base-catalyzed exchange reaction with D_2O . These deuterated building blocks were used for the synthesis of labelled analogues of quorum sensing signal molecules belonging to the three major classes of naturally occurring *N*-acylated homoserine lactones (AHLs), with the label on a non-enolizable and therefore stable position. Besides the application of these stable isotope-labelled AHLs as labelled standard for quantitative analysis via isotope dilution mass spectrometry, these compounds can be used to study the metabolic fate of the fatty acid tail of the AHL-molecule. These isotope-labelled compounds were fully characterized and used to synthesize the deuterated analogues of two commonly occurring AHL-degradation products, a tetramic acid and a ring opened *N*-acyl-L-homoserine.

Graphical abstract



Keywords

AHL, quorum sensing, fatty acid, isotope labelling, tetramic acid, isotope dilution, GC-MS

Reference

Ruysbergh, E., Stevens, C. V., De Kimpe, N., Mangelinckx, S. Synthesis and analysis of stable isotope-labelled *N*-acyl homoserine lactones. *RSC Adv.* **2016**, *6*, 73717-73730.

3.1.1 Introduction

Although the AHL-concentration inside a biofilm can reach as high as 600 μM , only concentrations in the nM range are typically encountered in the effluent leaving flow cells covered with biofilm.³⁴ To detect these trace amounts of AHLs, sensitive detection methods are needed. One possible method is via the application of biosensors, such as *Agrobacterium tumefaciens* NT1,²⁰⁴ *Chromobacterium violaceum* CV026,²⁰⁵ and *Escherichia coli* JB523²⁰⁶ (Table 3.1). The detection relies on a phenotypic response such as enzyme secretion, pigment production or bioluminescence when the threshold concentration of AHLs is exceeded.²⁰⁷

Table 3.1: Biosensors commonly used for AHL-detection.

Biosensor	Phenotype	AHL-sensitivity
<i>A. tumefaciens</i> NT1 ²⁰⁴	β -galactosidase production	C6 1c - C14 1k , oxo4 3a - oxo14 3k , HO6 2c - HO10 2g
<i>C. violaceum</i> CV026 ²⁰⁵	purple pigment production	C4 1a - C8 1e , oxo4 3a - oxo8 3e
<i>C. violaceum</i> CV026 ²⁰⁵	inhibition of purple pigment production	C10 1g - C14 1k , oxo10 3g - oxo14 3k
<i>E. coli</i> JB523 ²⁰⁶	gfp-production	C4 1a - C10 1g , oxo6 3c - oxo12 3i

Although detection of sub-picomole amounts of AHLs is feasible, the possible interference by artefacts, such as medium-derived diketopiperazines,²⁰⁸ and the need to use multiple biosensor strains in parallel for complete coverage of all AHLs (Table 3.1), has prompted researchers to develop multiple techniques for instrumental AHL-detection and identification.^{35,38,209,210} To obtain reliable results and exact quantification, an internal standard needs to be included in these analyses. The use of odd-chain AHLs as internal standard was abandoned after the discovery of odd-chain AHL-producing bacteria.^{28,29}

Several groups have reported the synthesis of isotope-labelled AHLs **43-52** (Figure 3.1) which can be used as internal standards.^{34,42,211-217} In the case of isotope dilution mass spectrometry (IDMS), the spike compound should be chemically identical with the analyte. As the isotope-labelled compound acts as an internal standard, compensating for losses during sample isolation and analysis, the mass difference between the isotope and the analyte should not be too high, to avoid possible isotope effects.²¹⁸ Besides the application as a standard, isotope-labelled compounds are often used in absorption, distribution, metabolism and excretion (ADME) studies and to study reaction mechanisms.²¹⁹ Hereby, mostly a 1:1 mixture of non-labelled and isotope-labelled compounds is used, to create a recognizable mass spectral ion pattern to study the *in vitro* and *in vivo* metabolic dispersion.²¹⁹⁻²²² However, no methodology is available to synthesize AHLs belonging to the major different classes with an isotope label in the acyl chain,

starting from one, easily available deuterated building block.

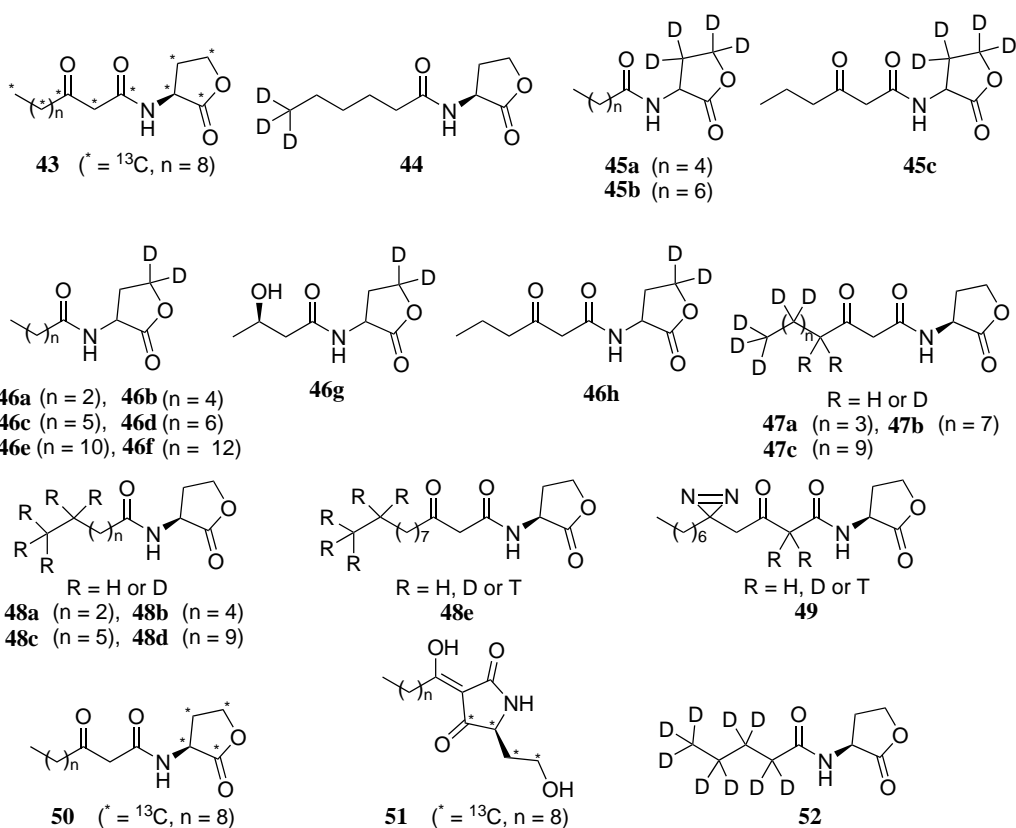
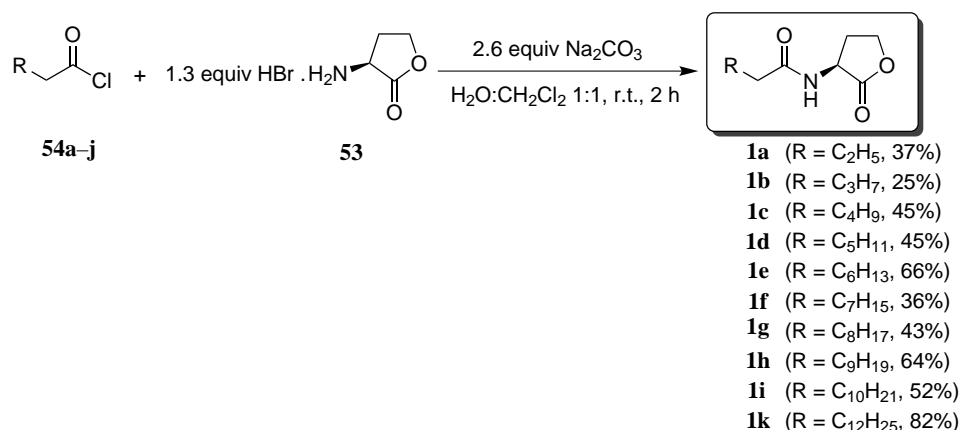


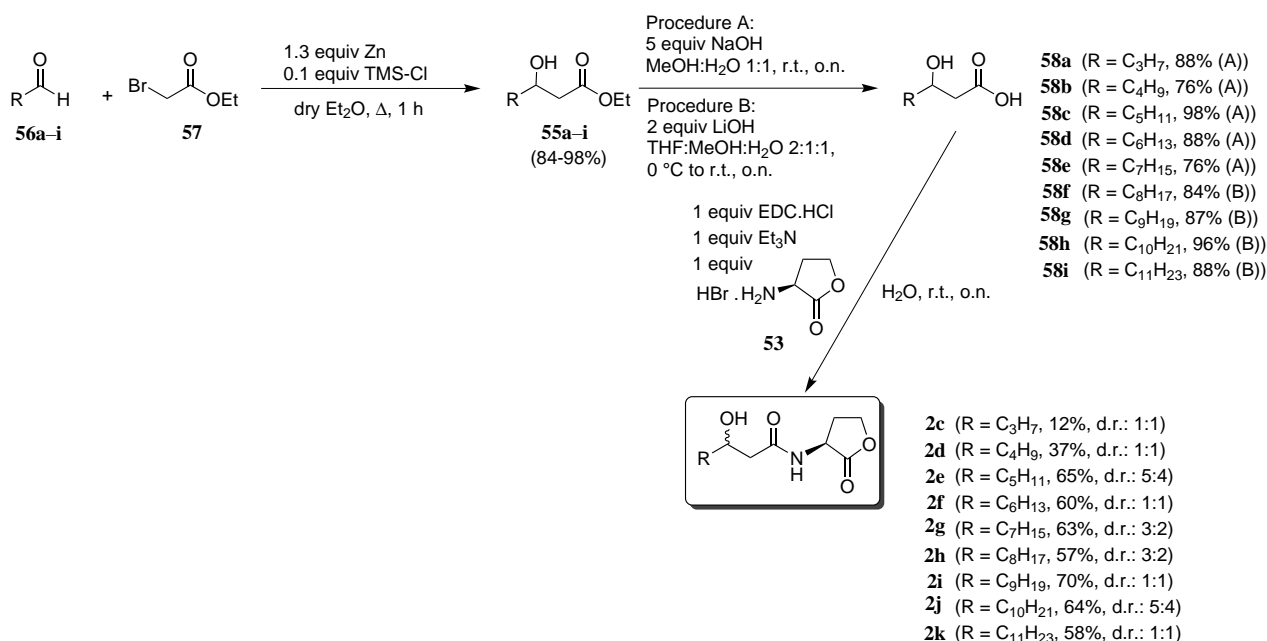
Figure 3.1. Isotope-labelled AHL-analogues **43**,³⁴ **44**,²¹¹ **45a–c**,²¹² **46a–h**,²¹³ **47a–c**,²¹⁴ **48a–e**,²¹⁵ **49**,²¹⁶ **50**, **51**,⁴² and **52**,²¹⁷ described in the literature.

3.1.2 Synthesis of unlabelled AHLs

To be able to compare the chemical properties and spectral data of the labelled analogues with the natural AHLs, a broad library of unlabelled, natural AHLs was synthesized. The common building block of all AHLs, the homoserine lactone unit, was prepared as hydrogen bromide salt **53** via reaction of L-methionine with bromoacetic acid.⁹³ AHLs **1** without a functionality at the 3-position of the *N*-acyl chain were prepared in a straightforward manner by coupling the homoserine lactone hydrobromide **53** with the appropriate acid chloride **54** under Schotten-Baumann reaction conditions (Scheme 3.1).²²³

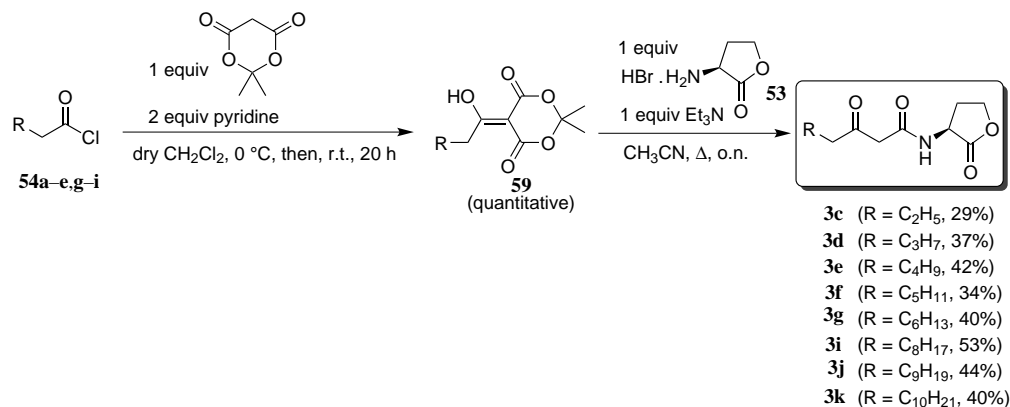
Scheme 3.1. Synthesis of natural AHLs **1a-i,k**.

To synthesize β -hydroxy esters **55a-i**, a Reformatsky reaction between aldehydes **56a-i** and ethyl bromoacetate **57** was performed (Scheme 3.2).²²⁴⁻²²⁶ To obtain β -hydroxy fatty acids **58a-i**, two procedures were used to hydrolyze these esters **55a-i**. Whereas sodium hydroxide in a water:methanol mixture gave satisfying results for the shorter-chain derivatives **58a-e**, too much (up to 25%) of the unreacted ester was remaining for the longer-chain derivatives. Therefore, an alternative procedure with lithium hydroxide in a tetrahydrofuran:methanol:water mixture was used.²²⁵ An 1-ethyl-3-(3-dimethylaminopropyl)carbodiimide (EDC)-mediated coupling reaction of fatty acids **58a-i** with L-homoserine lactone hydrobromide **53** yielded the desired HO-AHLs **2c-k** (Scheme 3.2).²²⁷

Scheme 3.2. Synthesis of natural HO-AHLs **2c-k**.

To prepare oxo-AHLs **3c-g,i-k**, the required acid chloride **54a-e,g-i** was condensed quantitatively with Meldrum's acid, whereafter a nucleophilic attack of L-homoserine lactone, generated from the hydrobromide salt **53** with triethylamine, across the resulting adduct **59** gave

oxo-AHLs **3c–g,i–k**.^{223,228} Alternatively, an EDC-mediated coupling between β -oxo fatty acids and L-homoserine lactone hydrobromide **53** was evaluated to synthesize oxo-AHLs **3**, but only disappointing yields were obtained.



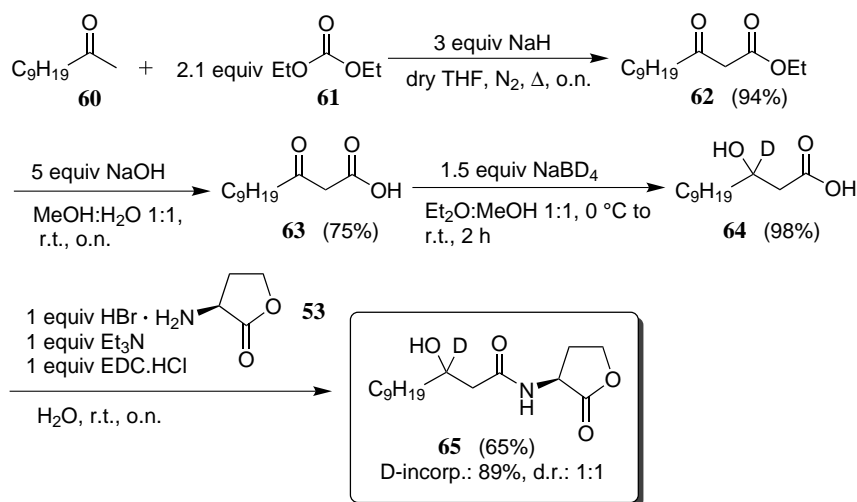
Scheme 3.3. Synthesis of natural oxo-AHLs **3c–g,i–k**.

3.1.3 Synthesis of a monodeuterated HO-AHL

Since secondary metabolites are quite expensive to synthesize in terms of energy and used materials, it is tempting to speculate that certain elements of these metabolites are reused. Several enzymes are known that are able to degrade AHLs.¹⁰ Haloperoxidases for example are able to halogenate *N*-(3-oxoacyl)-L-homoserine lactones **3** in a hydrogen peroxide-dependent manner.^{40,57,58} Subsequent cleavage of the halogenated acyl chain yields *N*-(α,α -dihaloacetyl)-L-homoserine lactone and a fatty acid.⁵⁷ Therefore, to study the metabolic fate of the fatty acid side chains, it was decided to include the isotope label in the acyl side chain of the AHL-molecule. When the isotope label is included in the lactone ring (analogues **45** and **46**), all classes of AHLs can easily be accessed.^{212,213} However, studies to investigate the metabolism of the fatty acid side chain are impossible with these analogues. To include the label in the side chain (analogues **44**, **47** and **52**), most synthetic routes rely on the use of rather expensive deuterated fatty acids.^{211,214,217} A metal-catalyzed reduction of terminally unsaturated AHLs with sodium borodeuteride to include the isotope label (analogues **48**) has been reported as well.²¹⁵

No analogues of *N*-(3-hydroxyacyl)-L-homoserine lactones **2** with an isotope label in the acyl chain have been reported in literature yet. The synthesis of this type of compounds was therefore the first goal. In a first approach, β -ketoester **62** was synthesized in excellent yield by reacting undecanone **60** with diethyl carbonate **61** in the presence of sodium hydride, followed by a sodium hydroxide-mediated hydrolysis to yield β -oxododecanoic acid **63** (Scheme 3.4).²²⁹ The deuterium label was introduced via a reduction of the keto function with sodium borodeuteride

to afford deuterated β -hydroxy fatty acid **64** with a deuterium incorporation of 89% at the carbon atom bearing the hydroxy moiety.²³⁰ An EDC-mediated coupling with L-homoserine lactone hydrobromide **53** yielded the desired *N*-(3-hydroxydodecanoyl-[3-²H])-L-homoserine lactone **65**.²²⁷



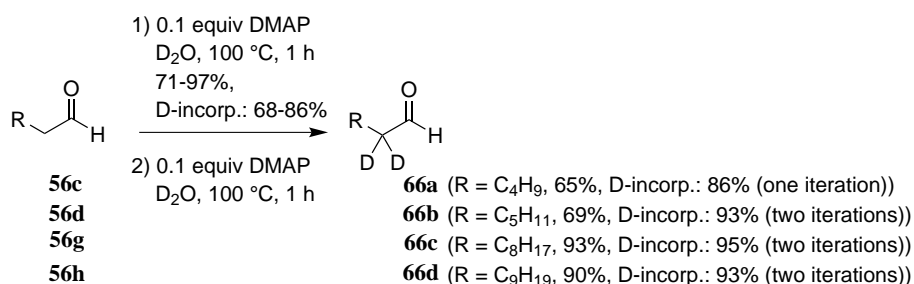
Scheme 3.4. Synthesis of *N*-(3-hydroxydodecanoyl-[3-²H])-L-homoserine lactone **65**. The deuterium content was determined by ESI-MS.

Only the class of AHLs bearing the hydroxy group is accessible via this route. The introduction of only one deuterium atom causes a mass shift of one unit. The natural presence of the heavy isotopes of mainly carbon, oxygen, nitrogen and hydrogen, gives rise to the presence of a mass ($M+1$) one unit higher than the expected parental mass (M). The abundance of this $M+1$ can be as high as 20% of the parental mass M for molecules with a molecular weight of 300 Da, hindering the application of these monodeuterated compounds as standards, but they can be useful to study the fragmentation patterns during GC-MS-analysis. Although $M+2$ is naturally present as well, even for the AHLs with the highest mass, the abundance never exceeds 3% of the presence of the parental mass M , resulting in less interference with peaks of a dideuterated labelled compound. Noteworthy, dideuterated AHL-analogues **46a–h** were applied as internal standards in an isotope dilution tandem mass spectrometric method.²¹³ Therefore, a more general route was developed to gain access to the dideuterated analogues of all different types of AHLs.

3.1.4 Synthesis of dideuterated AHLs

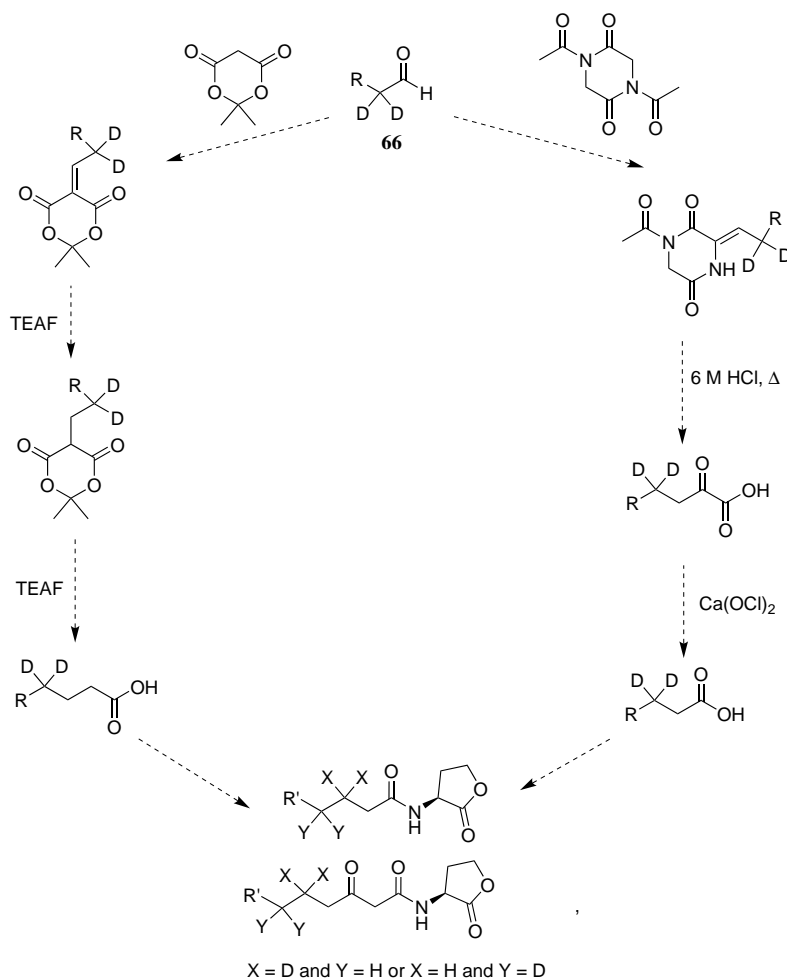
Aliphatic aldehydes **56c,d,g,h** were deuterated at the α -position via a 4-(*N,N*-dimethylamino)pyridine (DMAP)-catalyzed H/D-exchange reaction with D_2O (Scheme 3.5).²³¹ This mild catalysis only allows selective deuterium introduction at the acidic α -position. Due to the formation of HDO and H_2O during this exchange reaction, complete deuteration is impossible. Therefore,

to get a higher degree of deuterium incorporation than 68-86%, obtained after one iteration, a second treatment with D₂O was applied, yielding aldehydes **66b–d** with a satisfactory deuterium incorporation of 93-95%. To achieve a deuterium incorporation higher than 95%, a third iteration with D₂O should be included. However, as in IDMS the focus goes to the alteration of the ratio of two isotopes (labelled compared to non-labelled), the incomplete deuterium incorporation will not hinder the applicability, as long as the isotope ratio of the standard is determined in a parallel analysis.^{218,232,233}



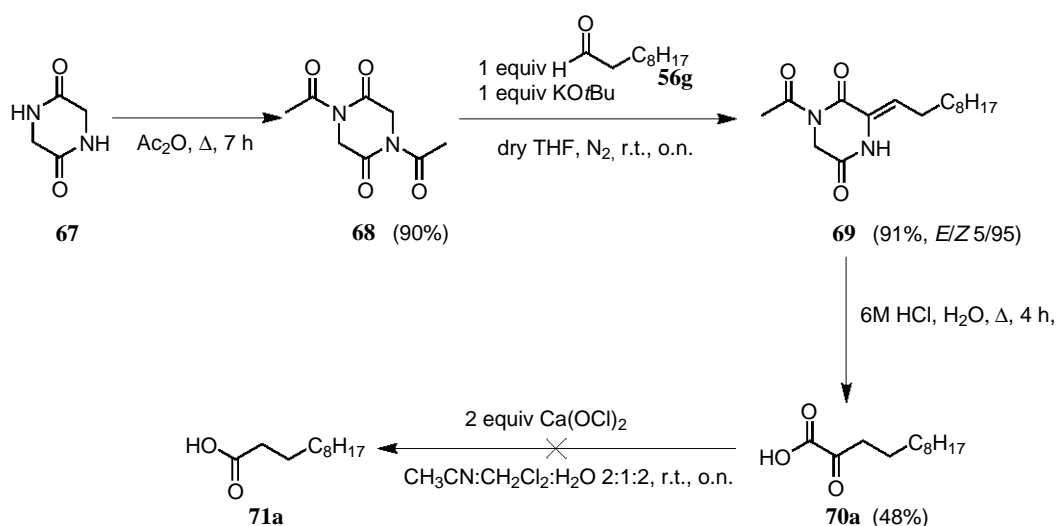
Scheme 3.5. Synthesis of α,α -dideuterated aldehydes **66a–d** as deuterated building blocks. The deuterium content was determined via ¹H NMR.

Further elaboration of these deuterated aldehydes **66** toward unfunctionalized fatty acids was evaluated. Because the α -position of a carbonyl group is quite acidic, a chain extension was needed to shift the deuterium label to the β - or γ -position of the carbonyl and avoid deuterium loss due to a deuterium-hydrogen exchange. At first, two different routes were evaluated (Scheme 3.6).



Scheme 3.6. Proposed routes to synthesize β,β - and γ,γ -dideuterated fatty acids starting from deuterated aldehydes **66**.

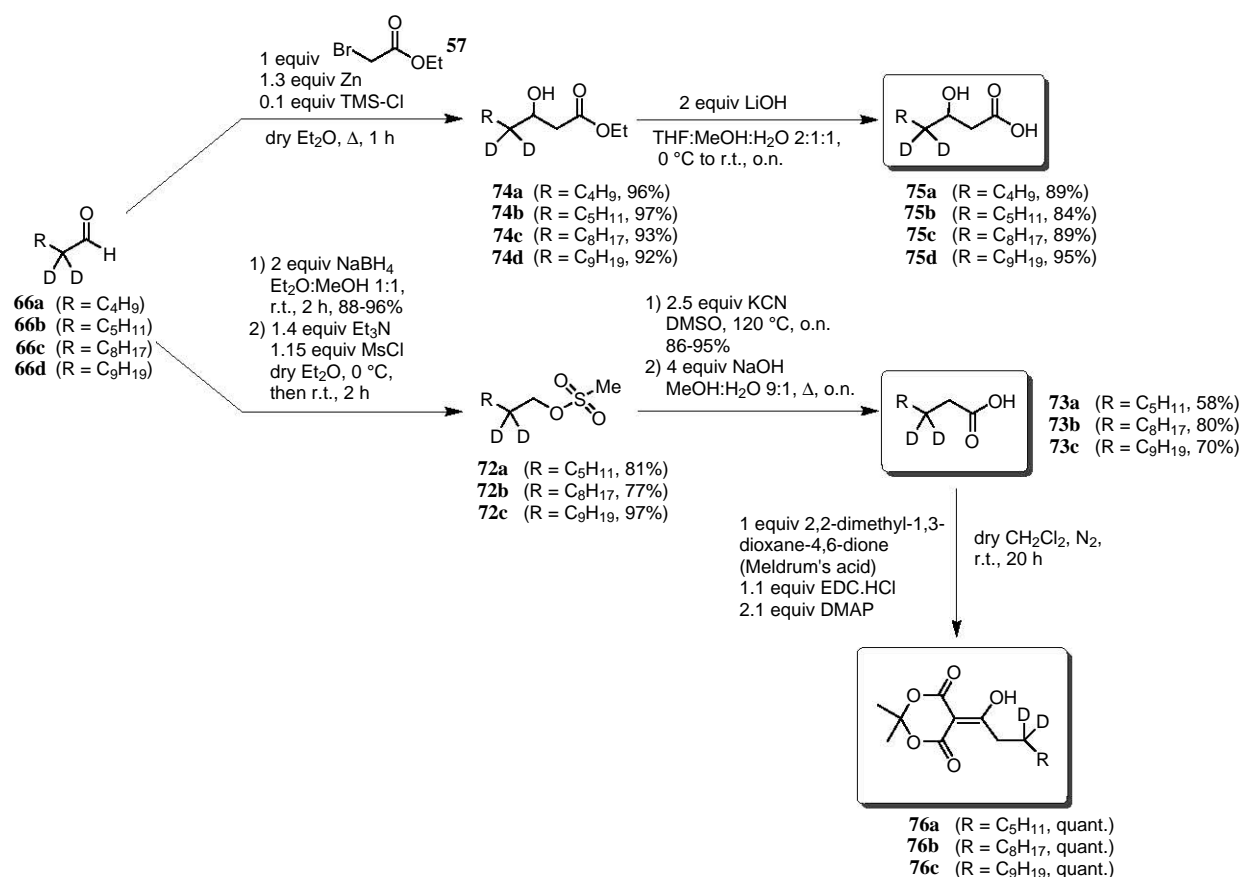
Although the one-pot condensation reaction of the labelled aldehyde **66** with Meldrum's acid in triethylammonium formate (TEAF) led to the fatty acid in high yields,²³⁴ a complete loss of the isotope label was observed. Lowering the reaction temperature from 100 °C to 50 °C failed to retain the deuterium-label in the final product. For the other route, diketopiperazine **67** was efficiently acylated via reaction with acetic anhydride. To test this route without wasting the deuterated aldehyde, the synthesis was first performed with unlabelled decanal **56g** (Scheme 3.7). The acylated precursor **68** was reacted with decanal **56g** in the presence of KO^tBu as a base to give compound **69** in excellent yield. Hydrolysis of **69** with 6M HCl at reflux yielded α -oxododecanoic acid **70a**. However, when the Ca(OCl)₂-mediated oxidative cleavage was attempted,²³⁵ no conversion at all was observed. Therefore, this route was abandoned as well.



Scheme 3.7. Attempt to transform decanal **56g** into undecanoic acid **71a**.

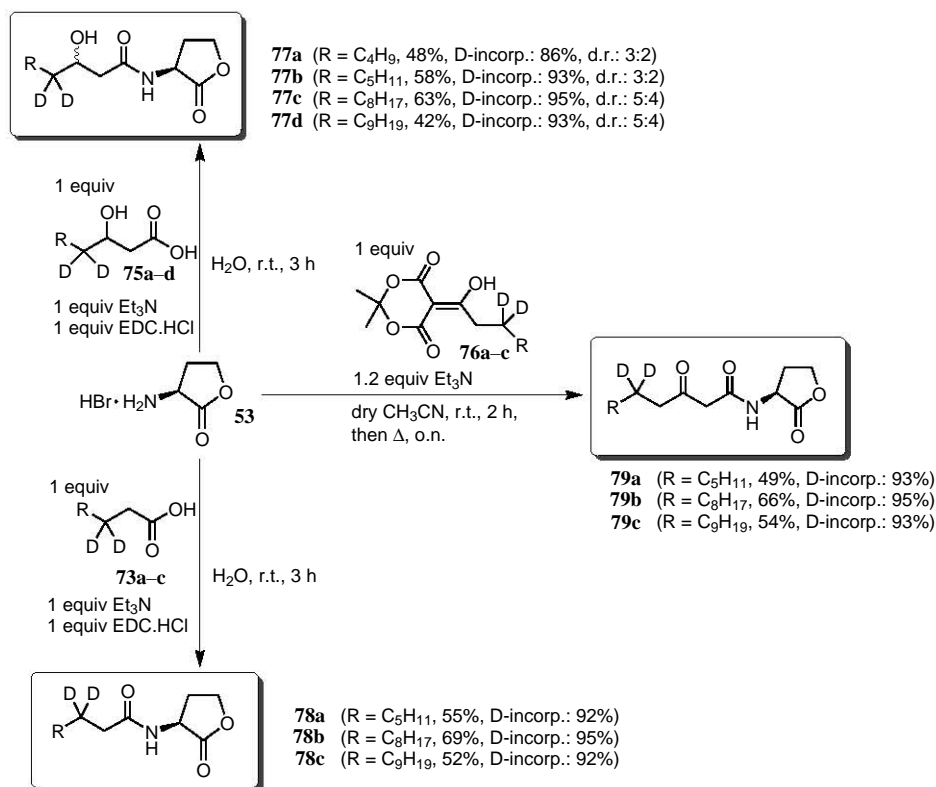
In another attempt, the labelled aldehydes **66b–d** were reduced to the alcohols after reaction with two equivalents of sodium borohydride in ethereal methanol (1:1). Mesylation,²³⁶ followed by substitution with potassium cyanide and alkaline hydrolysis yielded the [3,3-di-²H]-fatty acids **73a–c** (Scheme 3.8).²³⁷

Alternatively, these α,α -dideuterated aldehydes **66a–d** were transformed to the corresponding β -hydroxy esters **74a–d** via a Reformatsky reaction with ethyl bromoacetate **57** (Scheme 3.8). Hydrolysis of β -hydroxy esters **74a–d** gave the [4,4-di-²H]- β -hydroxy fatty acids **75a–d** in excellent yields.²²⁵



Scheme 3.8. Transformation of α,α -dideuterated aldehydes **66a–d** into deuterated fatty acid derivatives **75a–d**, **73a–c** and **76a–c**.

These labelled fatty acids **73a–c** were coupled with L-homoserine lactone hydrobromide **53** to give *N*-(acyl-[3,3-di-²H])-L-homoserine lactones **78a–c** (Scheme 3.9). A similar reaction with [4,4-di-²H]- β -hydroxy fatty acids **75a–d** gave *N*-(3-hydroxyacyl-[4,4-di-²H])-L-homoserine lactones **77a–d**, as a mixture of diastereomers. As expected, no separation of both diastereomers was observed during both HPLC and GC-analysis, allowing this mixture to be used as such as labelled spike for IDMS, utilizing a common analytical equipment. For the *N*-(3-oxoacyl-[5,5-di-²H])-L-homoserine lactones **79a–c**, [3,3-di-²H]-fatty acids **73a–c** were reacted with Meldrum's acid to introduce the oxo function (Scheme 3.8), followed by amidation with L-homoserine lactone hydrobromide **53** (Scheme 3.9).²³⁸ No significant loss of deuterium was observed during this synthetic route.



Scheme 3.9. Synthesis of *N*-(3-hydroxyacyl-[4,4-di-²H])-L-homoserine lactones **77a–d**, *N*-(acyl-[3,3-di-²H])-L-homoserine lactones **78a–c** and *N*-(3-oxoacyl-[5,5-di-²H])-L-homoserine lactones **79a–c** starting from deuterated precursors **75a–d**, **73a–c** and **76a–c**. The deuterium content was determined by ESI-MS.

This methodology allows the convenient and straightforward synthesis of AHLs with different functionalities, starting from one easily available deuterated building block without the use of deuterium gas or expensive catalysts. The presence of two deuterium atoms causes a mass shift of two units, making these isotope-labelled analogues easily distinguishable from the naturally occurring ¹³C-containing AHLs, with a mass one unit higher than the regular AHLs. All deuterated AHLs **77a–d**, **78a–c** and **79a–c** were fully characterized.

The degree of deuterium incorporation in the synthesized AHLs **65**, **77a–d**, **78a–c** and **79a–c** was determined via HPLC-MS. To confirm the position of the isotope label, ¹H and ¹³C NMR spectra were recorded and compared with those of the unlabelled AHLs. The presence of deuterium atoms at the β-position of the acyl chain in *N*-(acyl-[3,3-di-²H])-L-homoserine lactones **78a–c** was confirmed by the transformation of the signal of the α-protons of the acyl chain from a triplet to a singlet and the disappearance of the quintet at δ 1.64 ppm (in CDCl₃). A similar alteration was observed in the spectra of *N*-(3-oxoacyl-[5,5-di-²H])-L-homoserine lactones **79a–c**. For *N*-(3-hydroxydodecanoyl-[3-²H])-L-homoserine lactone **65**, the signal at δ 4.0 ppm (CDCl₃), linked with the *CHOH*-unit logically disappeared, whereas for *N*-(3-hydroxyacyl-[4,4-di-²H])-L-homoserine lactones **77a–d** the signal at δ 1.45 ppm (CDCl₃) was absent. The

expected quintet, associated with a dideuterated carbon atom, was not always clearly visible in the ^{13}C NMR spectrum due to excessive signal splitting and increased relaxation times.²³⁹ A small isotope effect, resulting in an upfield shift of 0.1 to 0.2 ppm, was observed for the flanking carbons, whereas this was negligible for the other carbon atoms.

The presence of deuterium atoms is also obvious from the infrared spectrum by the occurrence of CD-vibrations in the CD_2 moiety. The small peaks around 2200 and 2100 cm^{-1} correspond to antisymmetric and symmetric CD_2 -vibrations. These signals can be used to study the integration of deuterated AHLs in supported bilayers.^{216,240}

3.1.5 GC-MS analysis of deuterated AHLs

Several methods have been developed to analyze AHLs with GC-MS.^{34,241,242} Therefore, the suitability of the synthesized AHLs for this type of analysis was evaluated by studying the electron impact (EI) mass fragmentation pattern (Table 3.2). The retention times of labelled and unlabelled AHL were identical.

Table 3.2: GC-MS data of discussed AHL-molecules.

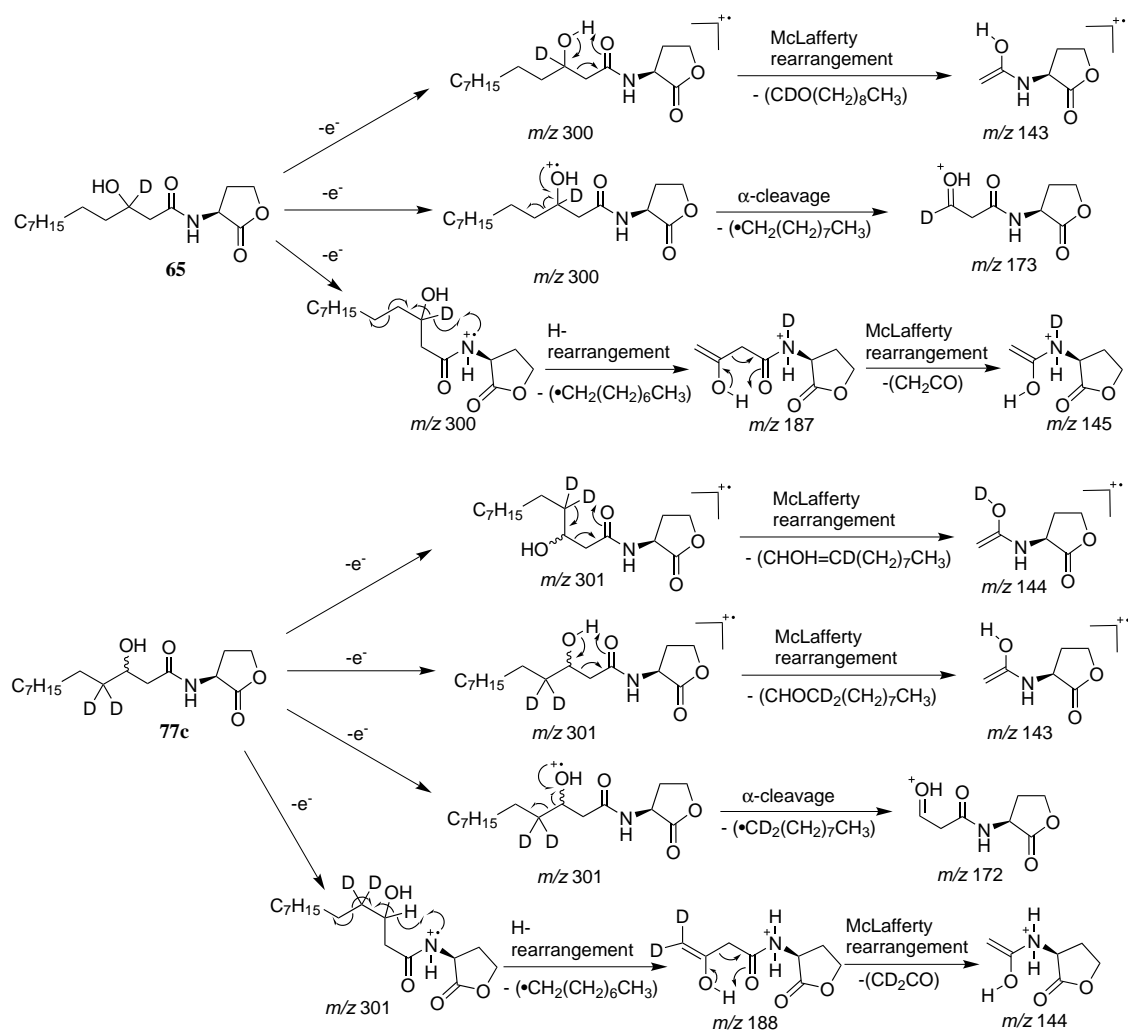
AHL	EI-MS m/z (rel. int.)
<i>N</i> -Dodecanoyl-L-homoserine lactone 1i	283 [M] (4), 156 (21), 143 (100), 125 (17), 102 (18), 83 (15), 57 (41), 55 (19), 43 (21), 41 (17)
<i>N</i> -(Dodecanoyl-[3,3-di- ² H])-L-homoserine lactone 78c	285 [M] (4), 158 (15), 143 (100), 125 (17), 102 (14), 83 (13), 57 (44), 55 (11), 43 (21), 41 (14)
<i>N</i> -(3-Hydroxydodecanoyl)-L-homoserine lactone 2i	299 [M] (2), 281 (3), 214 (11), 197 (19), 172 (100), 144 (18), 143 (40), 125 (11), 102 (85), 83 (18), 69 (12), 57 (51), 56 (19), 55 (21), 43 (36), 41 (21)
<i>N</i> -(3-Hydroxydodecanoyl-[3- ² H])-L-homoserine lactone 65	300 [M] (2), 282 (3), 215 (8), 197 (16), 173 (100), 145 (15), 143 (46), 125 (13), 102 (86), 83 (16), 69 (12), 57 (55), 56 (28), 55 (19), 43 (37), 41 (22)
<i>N</i> -(3-Hydroxydodecanoyl-[4,4-di- ² H])-L-homoserine lactone 77c	301 [M] (2), 283 (2), 216 (11), 199 (17), 172 (100), 144 (24), 143 (28), 125 (9), 102 (79), 83 (12), 69 (9), 57 (48), 56 (22), 55 (14), 43 (33), 41 (17)
<i>N</i> -(3-Hydroxydodecanoyl)-L-homoserine lactone 2i + BSTFA-TMCS	371 [M+TMS] (1), 356 (100), 244 (40), 228 (10), 215 (5), 200 (14), 186 (8), 174 (8), 160 (6), 143 (23), 130 (11), 103 (6), 83 (9), 73 (27), 57 (5), 55 (5), 43 (7), 41 (6)
<i>N</i> -(3-Hydroxydodecanoyl-[3- ² H])-L-homoserine lactone 65 + BSTFA-TMCS	372 [M+TMS] (1), 357 (100), 245 (42), 229 (10), 215 (6), 200 (14), 187 (7), 175 (6), 160 (7), 144 (18), 130 (13), 103 (6), 84 (6), 75 (16), 73 (33), 57 (5), 55 (5), 43 (8), 41 (6)
<i>N</i> -(3-Hydroxydodecanoyl-[4,4-di- ² H])-L-homoserine lactone 77c + BSTFA-TMCS	373 [M+TMS] (1), 358 (100), 244 (40), 228 (11), 215 (5), 200 (14), 186 (8), 174 (8), 160 (6), 143 (18), 130 (9), 103 (6), 85 (6), 73 (31), 57 (5), 55 (4), 43 (7), 41 (6)
<i>N</i> -(3-Oxodecanoyl)-L-homoserine lactone 3g + BSTFA-TMCS	341 [M+TMS] (11), 326 (72), 270 (21), 257 (49), 241 (94), 215 (17), 169 (65), 150 (25), 125 (15), 73 (100), 57 (11), 43 (12)
<i>N</i> -(3-Oxodecanoyl-[5,5-di- ² H])-L-homoserine lactone 79a + BSTFA-TMCS	343 [M+TMS] (9), 328 (60), 272 (16), 257 (44), 243 (81), 215 (16), 171 (57), 152 (24), 125 (12), 73 (100), 57 (11), 43 (15)

The characteristic mass fragment of *N*-acyl-L-homoserine lactones is situated at m/z 143, corresponding to a McLafferty rearrangement. Since the synthesized deuterium-labelled derivatives **78a–c** have the deuterium atoms located at the β -carbon, the label is lost and the ion with m/z 143 is formed as well (Scheme 3.10). To distinguish between the native and labelled AHLs, the higher mass fragments, corresponding to different alkyl chain losses, but retaining the isotope label should be targeted. The ion with m/z 158 (corresponding to m/z 156 in unlabelled AHLs) was detected with sufficient intensity in all *N*-(acyl-[3,3-di-²H])-L-homoserine lactones **78a–c** and can be used in a SIM-method to detect only labelled analogues. In all compounds analyzed, the molecular ion was detected, albeit with low intensities.



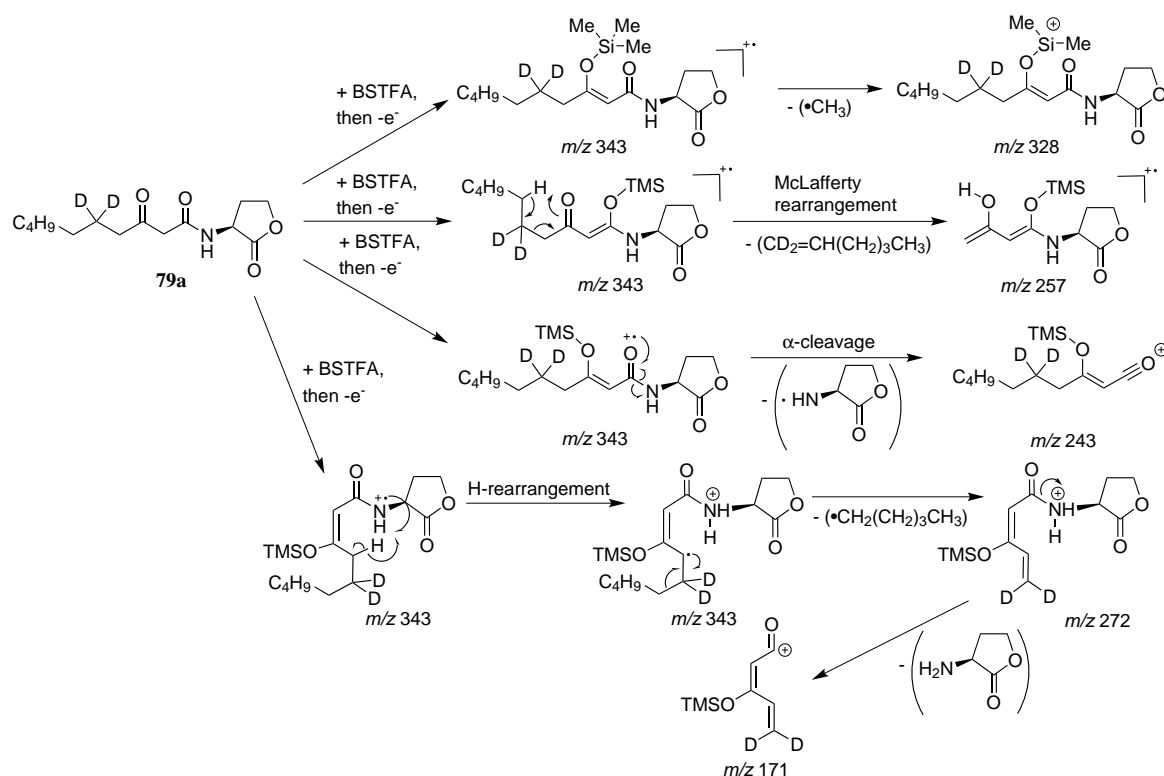
Scheme 3.10. Main mass fragment formed via a McLafferty rearrangement during EI-ionization induced fragmentation of *N*-(acyl-[3,3-di-²H])-L-homoserine lactones **78a-c**.

The characteristic ion formed during fragmentation of *N*-(3-hydroxyacyl)-L-homoserine lactones **2** is located at m/z 172. This fragment arises from an α -cleavage next to the hydroxy group. Not surprisingly, this fragment can be observed in both unlabelled **2** and γ,γ -dilabelled *N*-(3-hydroxyacyl)-L-homoserine lactones **77a-d** (Scheme 3.11). However, in case of the monolabelled analogue **65**, with the deuterium label at the β -position, a fragment with one mass unit higher (m/z 173) results. Another characteristic ion is formed by the McLafferty rearrangement. Whereas the mass fragment of m/z 143 is observed in all *N*-(3-hydroxyacyl)-L-homoserine lactones, the ion with m/z 144 is observed with an elevated intensity in case of the *N*-(3-hydroxyacyl-[4,4-di-²H])-L-homoserine lactones **77a-d**. This can be explained via an alternative McLafferty rearrangement, in which not the proton of the hydroxy group is abstracted, but rather the γ -proton (or deuterium in case of analogues **77a-d**) of the alkyl chain, causing a mass shift of one unit for analogues **77a-d**. As only a minor (37-43%) increase in abundance of m/z 144 is observed, a preference toward abstraction of the hydroxy proton can be concluded. Unfortunately, an alternative fragmentation, a hydrogen rearrangement followed by a McLafferty rearrangement, also leads to m/z 144 in both the unlabelled and dilabelled analogues, rendering this mass fragment not very useful to be targeted in a SIM-method. In the case of the monolabelled analogue **65** this fragmentation leads to a fragment with m/z 145, indicating that mainly the β -hydrogen (or deuterium) atom is abstracted (Scheme 3.11). Once again, the molecular ion itself was detected, albeit with low intensities.



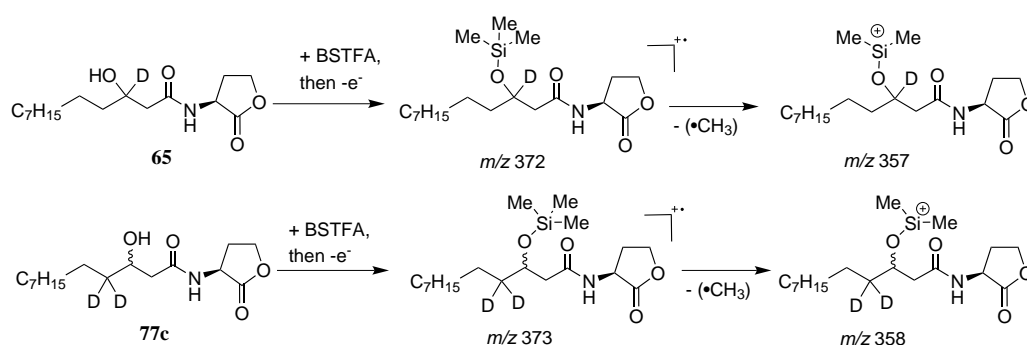
Scheme 3.11. Main mass fragments formed during the fragmentation of isotope-labelled *N*-(3-hydroxyacyl)-*L*-homoserine lactones **65** and **77c**.

Due to the lability of *N*-(3-oxoacyl)-*L*-homoserine lactones **3** during chromatographic analysis, a derivatization step is required. When *N,O*-bis(trimethylsilyl)trifluoroacetamide (BSTFA) is used as silylation agent, detection via GC-MS becomes possible. The molecular ion and the mass fragment resulting from the loss of one methyl group are detected with satisfying intensities. The ion at m/z 257 is formed via a McLafferty rearrangement (Scheme 3.12). α -Cleavage, with loss of the lactone unit, results in an alkyl chain fragment with m/z 243 for *N*-(3-oxodecanoyl)-*L*-homoserine lactone **79a**. A possible marker fragment with m/z 171, common to all *N*-(3-oxoacyl)-[5,5-di- ^2H]-*L*-homoserine lactones **79a–c** and with full retention of the isotope label, is obtained after a H-rearrangement, followed by the expulsion of a neutral homoserine lactone molecule (Scheme 3.12).



Scheme 3.12. Formalisms for the main mass fragments formed during the fragmentation of isotope-labelled *N*-(3-oxodecanoyl)-*L*-homoserine lactone **79a** after derivatization with BSTFA.

When labelled *N*-(3-hydroxyacyl)-*L*-homoserine lactones **65** and **77a–d** are treated with BSTFA, the fragment with the highest intensity observed is the silylated compound minus a methyl group (Scheme 3.13). Due to the high intensity and full retention of the isotope label, this fragment can be used to detect specific labelled *N*-(3-hydroxyacyl)-*L*-homoserine lactones **65** and **77a–d** in a reliable manner.



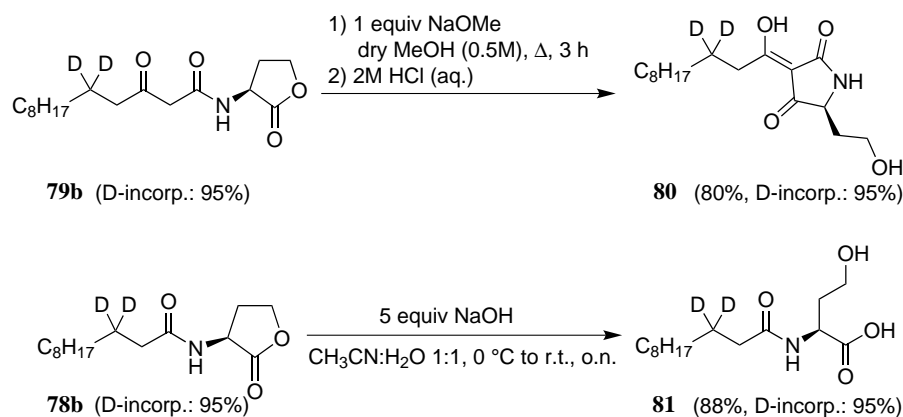
Scheme 3.13. Main mass fragments formed during the fragmentation of isotope-labelled *N*-(3-hydroxyacyl)-*L*-homoserine lactones **65** and **77c** after derivatization with BSTFA.

3.1.6 Synthesis of deuterated AHL-degradation products

To demonstrate and further extend the possible applications of these deuterated compounds, two AHL-degradation products which occur in nature, were synthesized. The hydrolysis of

the lactone ring of AHLs toward *N*-acyl homoserines, occurs in a temperature, pH and chain length dependent way and results in a loss of QS-activity.^{36,243} *N*-(3-Oxoacyl)-L-homoserine lactones **3** can form another type of degradation product. Via an intramolecular Claisen-type rearrangement, a tetramic acid **11** can be formed (Scheme 1.1). Fascinating biological properties such as antibacterial activity and iron chelation are associated with this type of compounds.⁹ Methods have been developed to detect both degradation products as well.^{42,244} However, no deuterium-labelled *N*-acyl homoserines nor deuterated tetramic acids have been reported yet, although these compounds could be used as internal standards for IDMS.

The corresponding tetramic acid **80** and the ring-opened product **81** were synthesized in good yield, and a full retention of the deuterium label was observed during these transformations (Scheme 3.14).



Scheme 3.14. Synthesis of deuterated analogues tetramic acid **80** and ring-opened AHL **81**. The deuterium content was determined by ESI-MS.

3.1.7 Conclusion

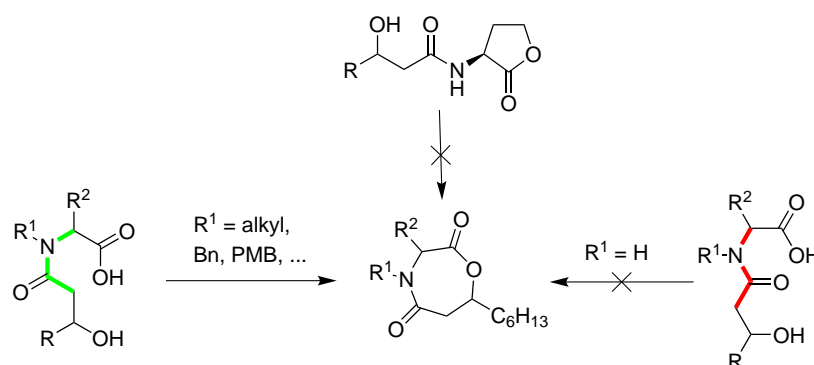
In this part, an easy and reliable method to make suitable, deuterated standards of AHL-molecules belonging to all three important classes of AHLs was described, starting from a cheap and commercially available deuterium source. Deuterium loss via D/H-exchange is avoided by the introduction of the isotope label at a non-enolizable position. All synthesized analogues were fully characterized. These deuterated analogues of the major classes of AHLs can also be used to synthesize the labelled analogues of the naturally occurring degradation products, without a significant loss of deuterium. These labelled AHLs and degradation products can be used to study the metabolization of AHLs in nature.

3.2 Evaluation of the chemical reactivity of *N*-(3-hydroxyacyl)-*L*-homoserine lactones and derivatives

Abstract

It is known that *N*-(3-oxoacyl)-*L*-homoserine lactones can rearrange to tetramic acids with interesting biological properties. In this part, it was evaluated if *N*-(3-hydroxyacyl)-*L*-homoserine lactones can participate in such a similar rearrangement toward 1,4-oxazepane-2,5-diones. However, due to the preference of an amide for a *trans*-conformation, such a spontaneous rearrangement proved to be very unlikely. It was shown for such a reaction to occur that a third substituent at the amide nitrogen atom is required. Several *N*-protecting groups were evaluated for this challenging cyclization reaction. With the use of the removable PMB-group, a *N*-unsubstituted 1,4-oxazepane-2,5-dione was synthesized. Via the application of pseudo-prolines, *i.e.* serine-derived oxazolidines as another type of protecting group, a compound with the presumed structure of the natural product serratin was obtained. Due to the differences in spectral data, the incorrect structural assignment of the natural product serratin was identified. Instead of the predicted seven-membered heterocycle, a symmetrical serratamolide analogue is proposed to be the correct structure of serratin.

Graphical abstract



Keywords

natural product, cyclization, heterocycle, pseudo-proline, 1,4-oxazepane, HO-AHL, photochemistry

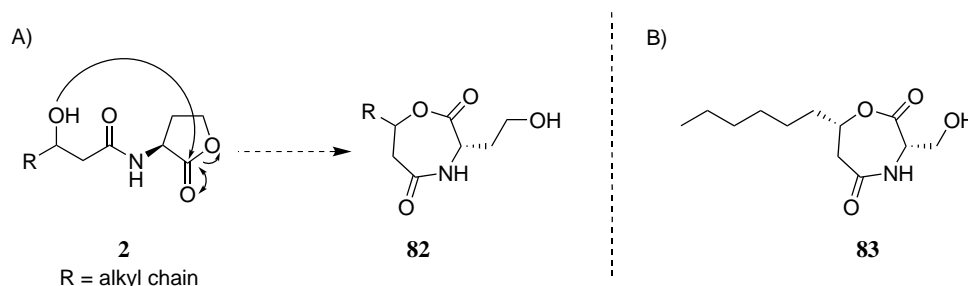
Reference

Ruysbergh, E., Van Hecke, K., Stevens, C. V., De Kimpe, N., Mangelinckx, S. Synthesis of 1,4-Oxazepane-2,5-diones via Cyclization of Rotationally Restricted Amino Acid Precursors and Structural Reassignment of Serratin. *J. Org. Chem.*, **2017**, *82*, 6210-6222.

3.2.1 Introduction

AHLs **17** can be degraded in many ways in nature. Bacteria produce several classes of quorum quenching enzymes. Acylases cleave the fatty acid from the homoserine lactone unit,^{50,51} whereas lactonases hydrolyze the ester bond of the lactone ring (See Literature overview).^{5,7,10} Alternatively, lactonolysis can also occur non-enzymatically (See Literature overview).^{7,36} Many bacterial secondary metabolites perform more than one function for the producing organism. This is also the case for the *N*-(3-oxoacyl)-L-homoserine lactones **3**. The tetramic acid type degradation product **11** of this class of quorum sensing signals, formed by an intramolecular Claisen-type condensation (Scheme 1.1), has not only a bactericidal effect against Gram-positive bacteria, but can also bind iron and serve as a primordial siderophore.⁹

One could wonder if a similar rearrangement could happen to the *N*-(3-hydroxyacyl)-L-homoserine lactones **2**, where the hydroxy group could act as a nucleophile and open the lactone ring to form a new, seven-membered ring-containing compound **82** (Scheme 3.15).²⁴⁵ This type of behavior is suggested by the difference in heat stability of the autoinducers of *Aliivibrio fischeri* (previously designated as *Vibrio fischeri*), oxo6 **3c**, and the autoinducer of *Vibrio harveyi*, HO4 **2a**. Heating a medium containing the autoinducer **3c** of *A. fischeri* at 100 °C for 5 minutes did not have an effect on the bioluminescence-inducing activity of this quorum sensing signal molecule **3c**. Applying the same treatment to a medium containing the autoinducer **2a** of *V. harveyi*, caused a complete deactivation of the bioluminescence inducing activity.²⁴⁶ Not surprisingly, both autoinducers lost their QS stimulating properties at high pH.



Scheme 3.15. A) Possible rearrangement of *N*-(3-hydroxyacyl)-L-homoserine lactones **2** toward seven-membered ring **82**. B) Reported structure of bacterial metabolite serratin (**83**).²⁴⁷

This type of rearrangement of *N*-(3-hydroxyacyl)-L-homoserine lactones **2** has not been reported in literature. However, the reported compound serratin (**83**) (Scheme 3.15), isolated from the bacteria *Serratia marcescens*, resembles this type of rearrangement product quite well.²⁴⁷ The main difference is the presence of a hydroxymethyl substituent rather than a hydroxyethyl substituent.²⁴⁷ Bacteria belonging to the *Serratia* genus are known to produce the cyclodep-

sipeptides serratamolide A-F (**42a–f**) (Figure 3.2) which are composed out of similar building blocks as serratin (**83**).^{248,249} These macrocyclic compounds do not only possess antimycobacterial activity, but can induce cell cycle arrest and proapoptotic effects in breast cancer cells.²⁵⁰ Also the lipoamino acid serratamic acid (**84**) has been isolated from alkaline extracts of *S. marcescens* cultures (Figure 3.2),^{251,252} presumably formed by the hydrolysis of serratamolides (**42**).^{248,249}

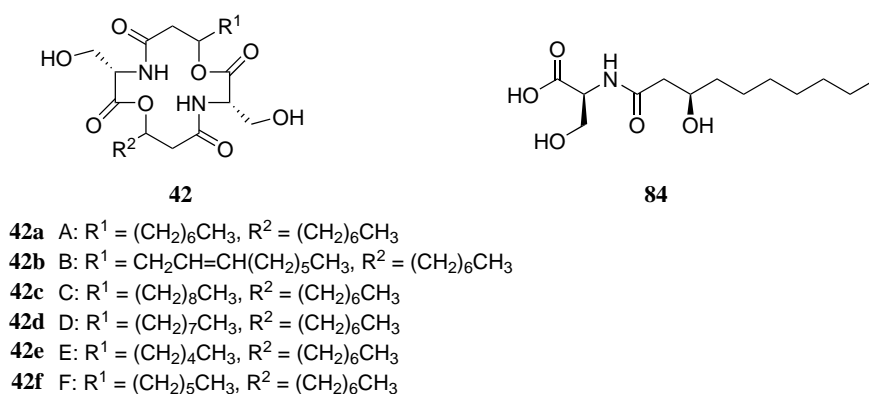


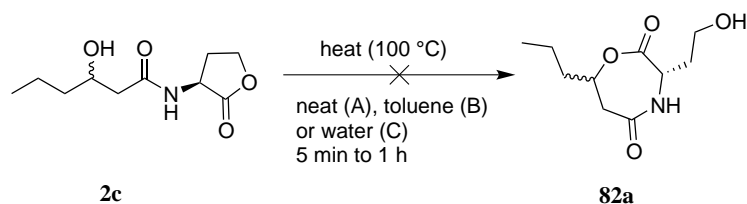
Figure 3.2. Serratamolides A-F (**42a–f**),²⁴⁸ and serratamic acid (**84**),^{251,252} produced by *Serratia* sp.

The most common AHLs occurring in *Serratia* sp. cultures are the rather short chain AHLs C4 **1a** and C6 **1c**.¹⁶⁷ However, also HO6 **2c** and HO8 **2e** have been detected in a *Serratia* strain, albeit in limited amounts.²⁵³ Therefore, it could be tempting to speculate that an incorrect structure was assigned to serratin (**83**) and that it results from the rearrangement of HO8 **2e**.

3.2.2 Rearrangement of *N*-(3-hydroxyacyl)-*L*-homoserine lactones

As the exact biosynthetic origin of serratin (**83**) is unknown, the possibility was evaluated that the seven-membered ring indeed arises from a spontaneous rearrangement of a bacterial HO-AHL **2**. Eberhard observed that the autoinducer of *V. harveyi*, HO4 **2a** lost its activity after heating it for five minutes at 100 °C in minimal medium.²⁴⁶ Later on, it was hypothesized that this was caused by the nucleophilic attack of the β -hydroxy group of this AHL.²⁴⁵ By mimicking the described reaction conditions (heating at 100 °C for 5 min),²⁴⁶ followed by attempts with other solvents and longer reaction times, this route was evaluated. However, the formation of the desired seven-membered ring **82a** was never observed (Scheme 3.16). The starting material **2c** was fully recovered. When the reaction time was prolonged, elimination and hydrolysis products were observed as well.

Reaction conditions suited for the nucleophilic attack of the β -hydroxy group might give rise to cyclic compound **82a**, but then the resulting primary hydroxy group could reattack the seven-



Scheme 3.16. Attempt to form serratin-like compound **82a** via a heat-induced rearrangement of HO6 **2c**.

membered lactone, forming the more stable five-membered lactone ring, and once again yielding starting material **2c**. This difference in stability results from a combination of entropy and energy terms and was studied by the group of Mandolini (Figure 3.3).^{254–256} The energy term represents the increase in ring strain and unfavorable interactions needed to be overcome when the open-chain form approaches the ring-shaped transition state. The entropy term is linked with the probability of the two chain terminals coming close enough to interact.²⁵⁷ Therefore, it is very unlikely that a significant amount of serratin-like structures **82** will result from the spontaneous rearrangement of *N*-(3-hydroxyacyl)-L-homoserine lactones **2**.

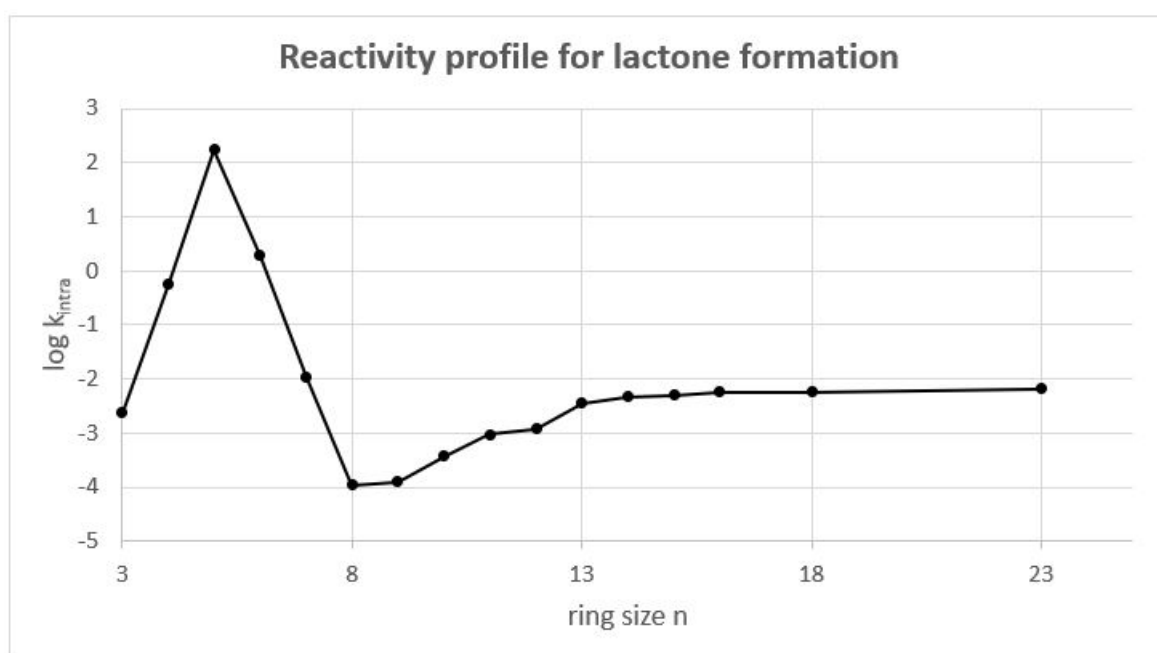
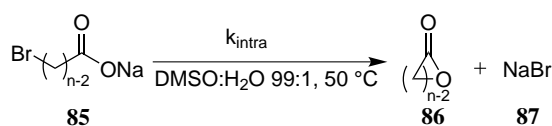
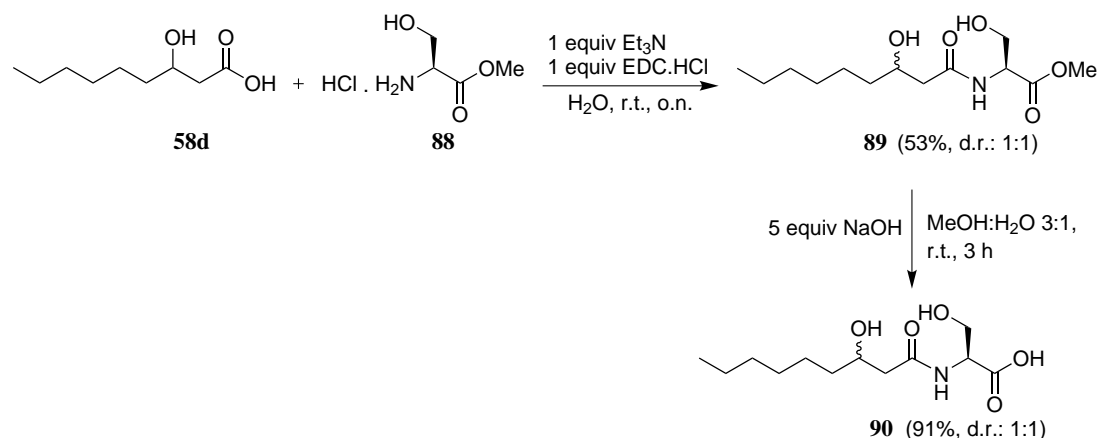


Figure 3.3. Reactivity plot for the cyclization of sodium ω -bromo carboxylates **85** in 99% aqueous DMSO at 50 °C.^{254–256}

3.2.3 Rearrangement of *N*-(3-hydroxynonanoyl)-L-serine

In a next step, it was evaluated if a serratamic acid-like compound, *N*-(3-hydroxynonanoyl)-L-serine (**90**) could lie at the origin of serratin (**83**). This compound **90** was synthesized via an

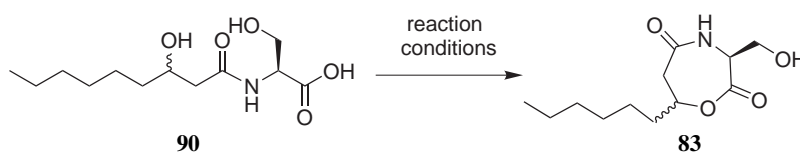
EDC-mediated coupling reaction of β -hydroxynonanoic acid **58d** with serine ester **88**, followed by alkaline hydrolysis (Scheme 3.17). When the free hydroxy group of serratin would attack the seven-membered lactone, a four-membered lactone would be formed. As this type of lactone is less stable than a five-membered lactone, it can be expected that at least some of the seven-membered lactone ring should remain or can be reformed.^{254–256}



Scheme 3.17. Synthesis of *N*-(3-hydroxynonanoyl)-L-serine **90**.

For the ring-closure, reaction of amino acid derivative **90** with 1 equiv of EDC and 1 equiv of Et₃N in water was tested but no reaction was observed. Repeating this reaction with EDC with a catalytic amount of DMAP in dichloromethane yielded a complex reaction mixture.²⁵⁸ Stirring the reaction mixture overnight in acetic anhydride also failed to yield any of the desired ring-closed product **83** (Table 3.3).²⁵⁸

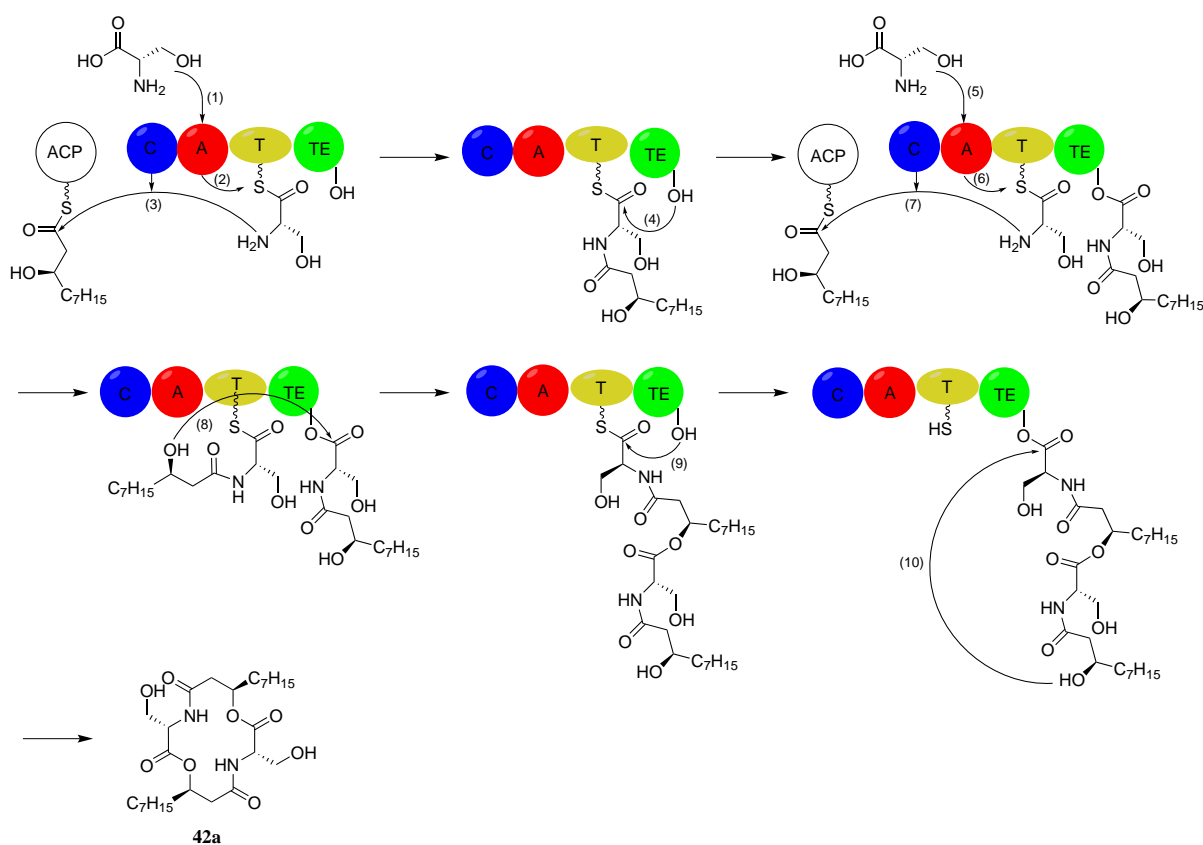
Table 3.3: Attempts to cyclize *N*-(3-hydroxynonanoyl)-L-serine **90**.



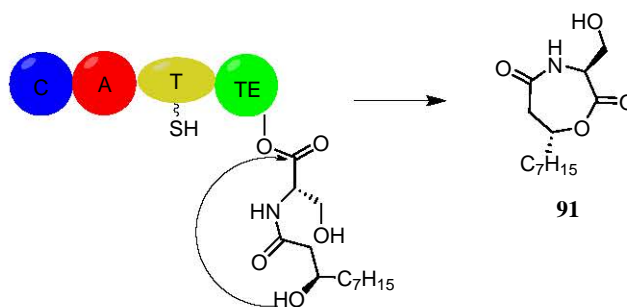
Entry	Reaction conditions	Result
1	1 equiv EDC.HCl, 1 equiv Et ₃ N, H ₂ O, r.t., o.n.	No reaction
2	1 equiv EDC.HCl, cat. DMAP, dry CH ₂ Cl ₂ , r.t., o.n.	Complex reaction mixture
3	Ac ₂ O, r.t., o.n.	Complex reaction mixture

As both HO-AHLs **2** as serratamic acid analogue **90** failed to yield serratin (**83**), another explanation for the origin of this cyclic compound **83** was sought. Serratamide A (**42a**) is synthesized by the action of non-ribosomal peptide synthetases (NRPS) (Scheme 3.18), which explains the fact that the most likely precursor, serratamic acid (**84**), was not found in serratamide-

deficient mutants. Alkaline extracts of the wild type do contain serratamic acid (**84**), but this should be considered as a hydrolytic product of serratamolide **42**. The NRPS SwrW, responsible for the synthesis of serratamolide A (**42a**), is the simplest unimodular NRPS and consists of a condensation (C), adenylation (A), thiolation (T) and thioesterase (TE) domain, responsible for the activation and coupling of serine and a β -hydroxydecanoic acid derivative.²⁵⁹ If however, the serratamic acid linked to the TE-domain, is not transferred to the T-domain linked serratamic acid, but undergoes a cyclization instead, cyclic compound **91** could be formed (Scheme 3.19). So far, only serratin (**83**) has been reported in the literature, which points out the unlikeliness of this type of cyclization. Perhaps the presence of the unusual β -hydroxynonanoic acid **58d** causes a disruption in the normal course of this biosynthetic route.



Scheme 3.18. Biosynthesis of serratamolide A (**42a**) via the NRPS SwrW, consisting of a condensation (C), adenylation (A), thiolation (T) and thioesterase (TE) domain. First, serine is adenylated by the A domain (1), then the activated serine binds as a thioester to the T domain (2). The amine group of the bounded serine will react with an ACP-linked β -hydroxydecanoyl moiety (3), followed by a transfer to the TE domain (4). Subsequently, a second serine molecule passes through the same steps (5-7), resulting in two differently linked serratamic acids. Then the hydroxy group of the β -hydroxydecanoyl moiety of the molecule linked to the T domain, will attack the TE domain ester bond (8). A final transfer to the TE domain (9), followed by a cyclization, releases serratamolide A (**42a**) (10).^{259,260}



Scheme 3.19. Possible explanation for the formation of serratin-like compound **91** via a deviation from the standard biosynthetic route.

3.2.4 Cyclization of *N*-(3-hydroxyacyl)amino acids

Although several methods are available for the synthesis of 1,4-diazepane-2,5-diones,^{261–265} no general method is known for the synthesis of 1,4-oxazepane-2,5-diones. Besides serratin (**83**), several natural products have been isolated containing this seven-membered core. One example is callipeltin L (**92**) (Figure 3.4), belonging to a group of antifungal peptides, produced by the marine sponge *Latrunculia* sp.²⁶⁶ Compound **93** with a similar lactone core was isolated from the methanolysis mixture of the marine immunosuppressant lipopeptide microcolin A and shows relatively potent immunosuppressive activity as well.²⁶⁷ Also inducamide C (**94**), isolated from a chemically induced mutant strain of *Streptomyces* sp. and exhibiting modest cytotoxicity, contains the same 1,4-oxazepane-2,5-dione core.²⁶⁸ Because of the instability of the lactone bond, it is often difficult to isolate sufficient amounts of these natural products to fully assess their biological activities. However, the same lactone bond offers the distinct advantage of rendering the compound neutral by masking the carboxylic acid unit, allowing better membrane permeability whereafter degradation or nucleophilic attack within the cell releases the active compound.^{269,270} It was therefore decided to continue the synthetic efforts toward serratin (**83**) in this work.

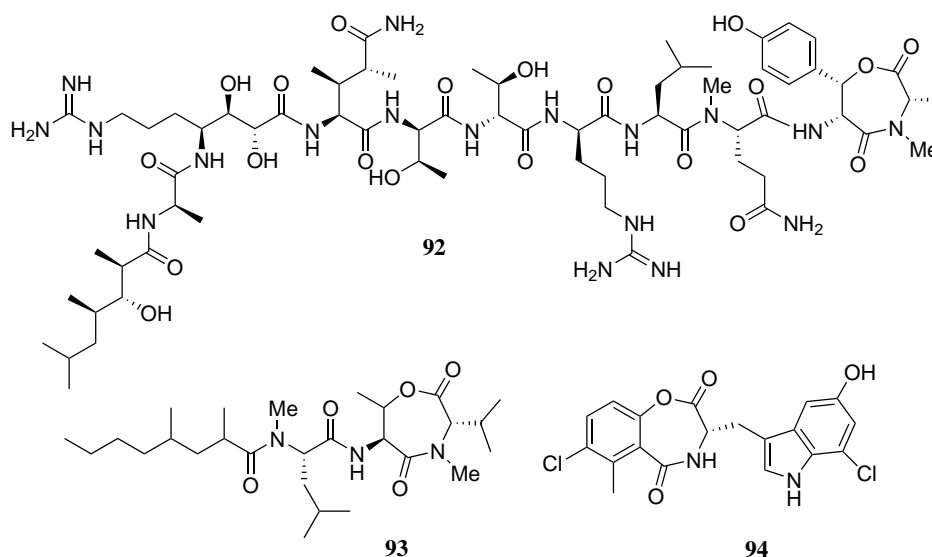


Figure 3.4. 1,4-Oxazepane-2,5-dione core-containing natural products **92**,²⁶⁶ **93**,²⁶⁷ and **94**.²⁶⁸

However, the synthesis of medium-sized heterocycles still represents a synthetic challenge. A head-to-tail cyclization often fails to yield the desired seven- or eight-membered heterocycles because of a combination of energy and entropy terms (*vide supra*).²⁵⁷ The resistance toward cyclization is even more prevalent when a carboxylic amide bond is present. The preference of an amide for a *trans*-conformation removes both termini of the linear precursor from each other's proximity, impeding cyclization.^{271,272} As medium-sized lactams constitute a class with a great potential for drug applications, many synthetic efforts have been devoted to this type of medium-sized heterocycles. *N*-Substitution of the amide and dilute reaction conditions are often applied,²⁶¹ but methods using solid support,^{273,274} or those that rely on a Staudinger ligation for ring closure,^{262,263} are described as well. Another possibility is the use of pincer auxiliaries, fulfilling both a tethering and templating role.²⁶⁴

The apparent lack of cyclization that was observed for serine derivative **90** (Table 3.3), can be explained by the fact that the amide bond strongly prefers a *trans*-conformation, whereas for the desired cyclization to occur, a *cis*-amide bond is needed (Figure 3.5). The 2D-NOESY analysis of methyl ester **89** revealed that indeed only the *trans*-conformer was present (Figure 3.6).²⁷⁵

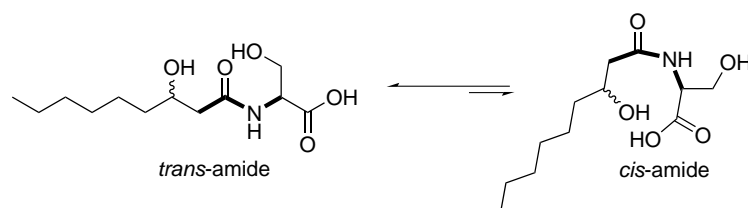


Figure 3.5. *Trans* and *cis*-conformation of *N*-(3-hydroxynonanoyl)-L-serine **90**.

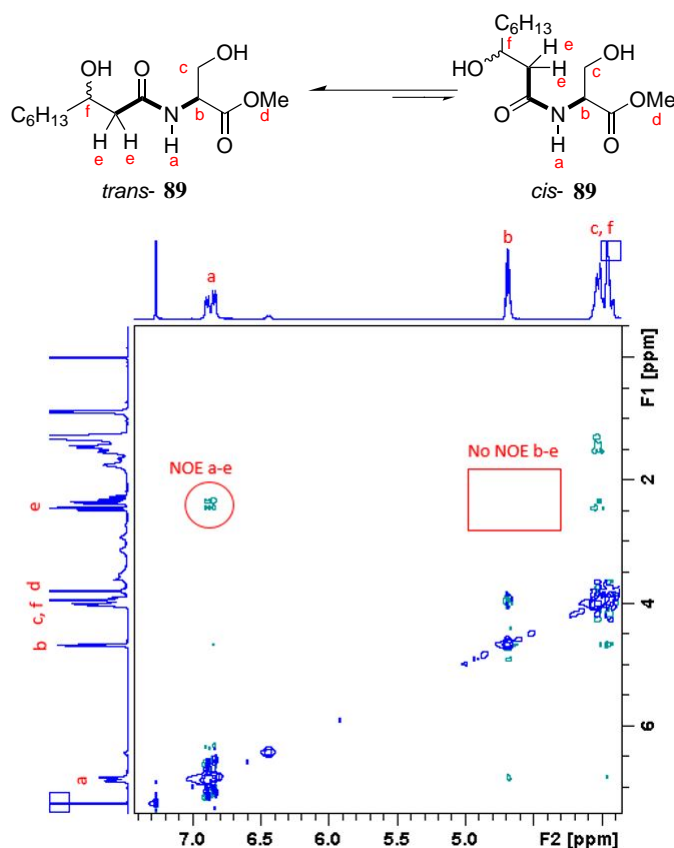
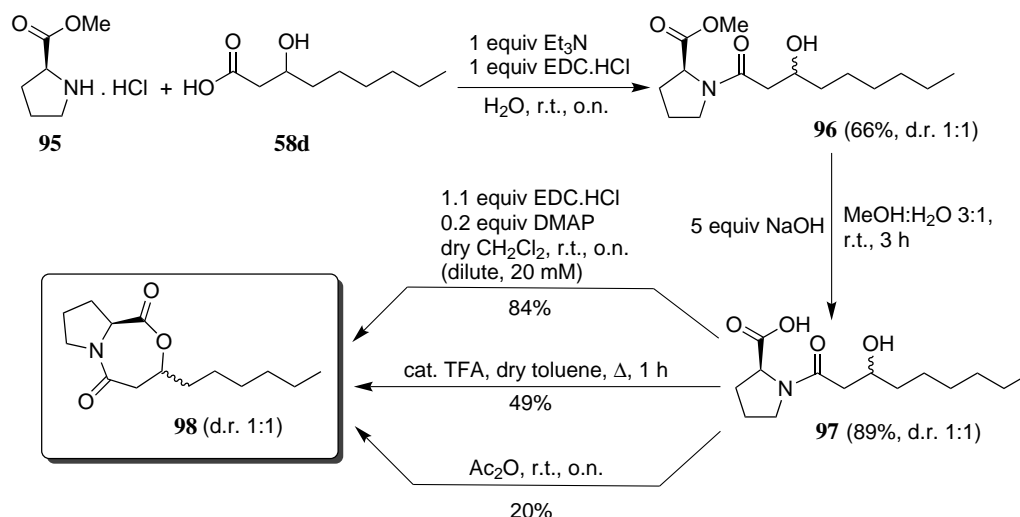


Figure 3.6. Zoom in of the 2D-NOESY spectrum of **89**. In this spectrum, a clear interaction between NH (a) and CH₂CON (e) was observed. No such interaction was present between CHN (b) and CH₂CON (e), indicating that the amide exists as the *trans*-conformer.

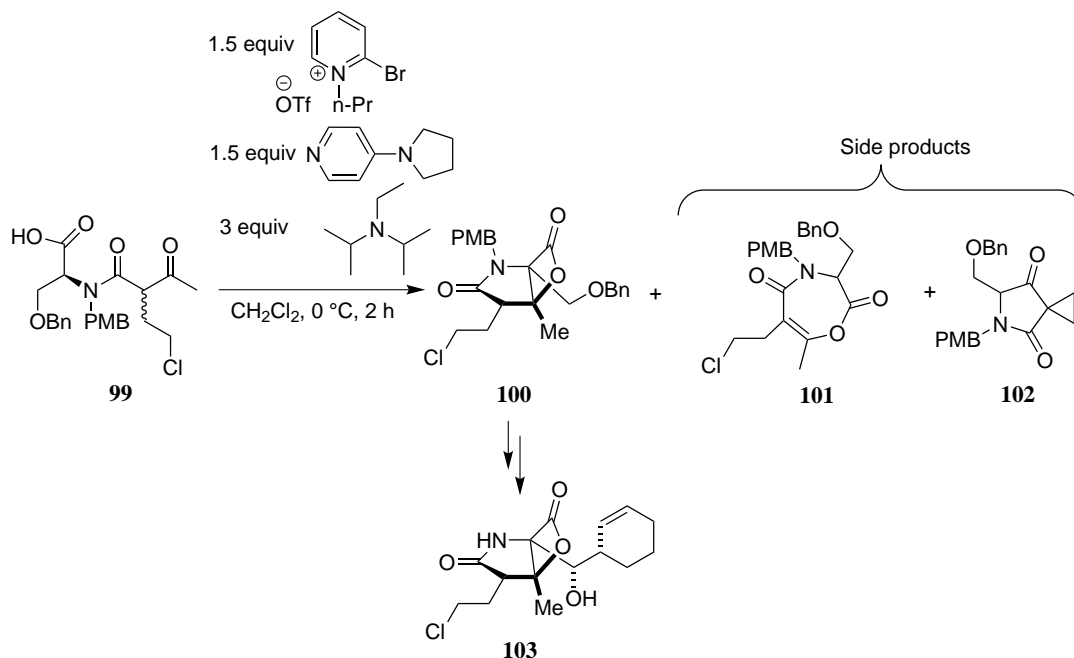
The partial double bond character of the amide C-N bond, caused by the delocalization of the lone pair on nitrogen, only allows slow internal rotation.^{271,272,276} In the case of larger heterocycles, such as fourteen-membered rings, *trans*-amides can be included. This was used for the synthesis of a serratamolide analogue. Noteworthy, during this synthesis seven-membered rings were never observed.²⁷⁷

However, it is known that proline-containing peptides typically contain an elevated amount of *cis*-amide bonds.^{278,279} Therefore, the proline-containing analogue **97** was synthesized and three different conditions for cyclization were evaluated (Scheme 3.20).²⁵⁸ As intramolecular cyclization is a first order reaction and dimerization is second order, dilute conditions were applied to avoid the latter, unwanted, reaction. The bicyclic structure **98** was observed in all cases, albeit in different amounts.



Scheme 3.20. Synthesis and cyclization of *N*-(3-hydroxynonanoyl)-L-proline **97**.

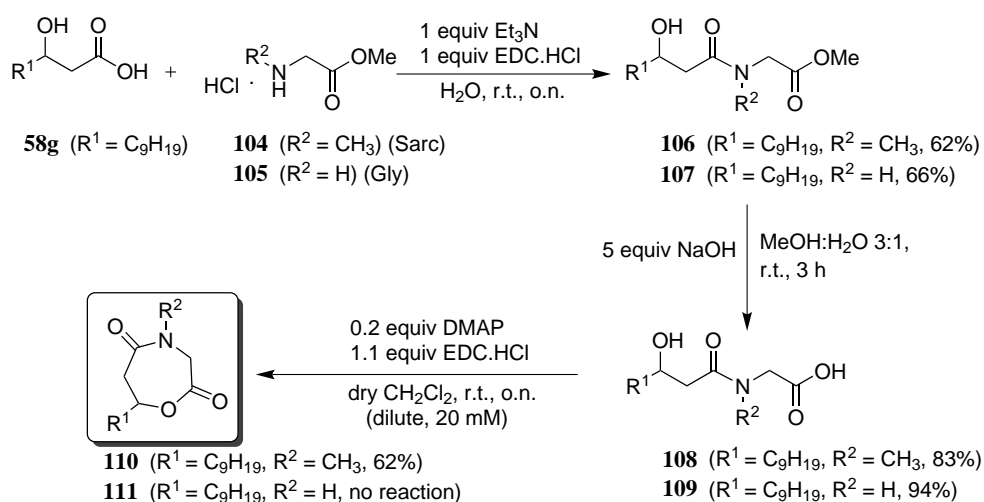
That the application of *N,N*-disubstituted amides could be useful to obtain cyclic products, was also hinted by the appearance of a seven-membered ring containing side product **101** during the bis-cyclization of acid **99** (Scheme 3.21).^{280,281} Bicyclic compound **100** is a precursor in the synthesis of salinosporamide A (**103**), a secondary metabolite of the marine actinomycete *Salinispora tropica* and a highly potent and selective inhibitor of the 20S proteasome which has received a lot of attention for the treatment of cancer.²⁸²



Scheme 3.21. Formation of the seven-membered ring containing side product **101** during the bis-cyclization of **99**.^{280,281}

To decide if the imposed rigidity, caused by the cyclic side chain of proline, was really necessary for the cyclization, the highest yielding cyclization conditions were applied to sarcosine

derivative **108** (Scheme 3.22). The existence of both *cis* and *trans*-isomers of this compound in solution was apparent by the presence of both conformers being observed in ^1H NMR and ^{13}C NMR (in CDCl_3 , Figure 3.7 A and 3.8 A).²⁸³ No such conformers were observed in the ^1H NMR and ^{13}C NMR spectra of derivative **90**. The *cis/trans*-ratio of isomers of **108** in a CDCl_3 solution is 1:3. A similar ratio is observed for *N*-dodecanoylsarcosine, although solvent and concentration can play an important role.^{284–286} The cyclic product **110**, with a similar seven-membered core as callipeltin L (**92**), was obtained in 62% yield. In the ^1H and ^{13}C NMR spectrum, different isomers were not observed (CDCl_3 , Figure 3.7 B and 3.8 B), which is consistent with the formation of a more rigid, cyclic structure lacking the possibility of *cis/trans*-isomerization. As a proof of concept, the reaction was repeated with the glycine derivative **109** under identical conditions, but no cyclization was observed (Scheme 3.22). As the ring-closing reaction only proceeds with great difficulty, a spontaneous, non-enzymatical rearrangement can be excluded for the origin of serratin (**83**).



Scheme 3.22. Synthesis of *N*-(3-hydroxyacyl)amino acids **108** and **109** and ring closure toward 1,4-oxazepane-2,5-dione **110**.

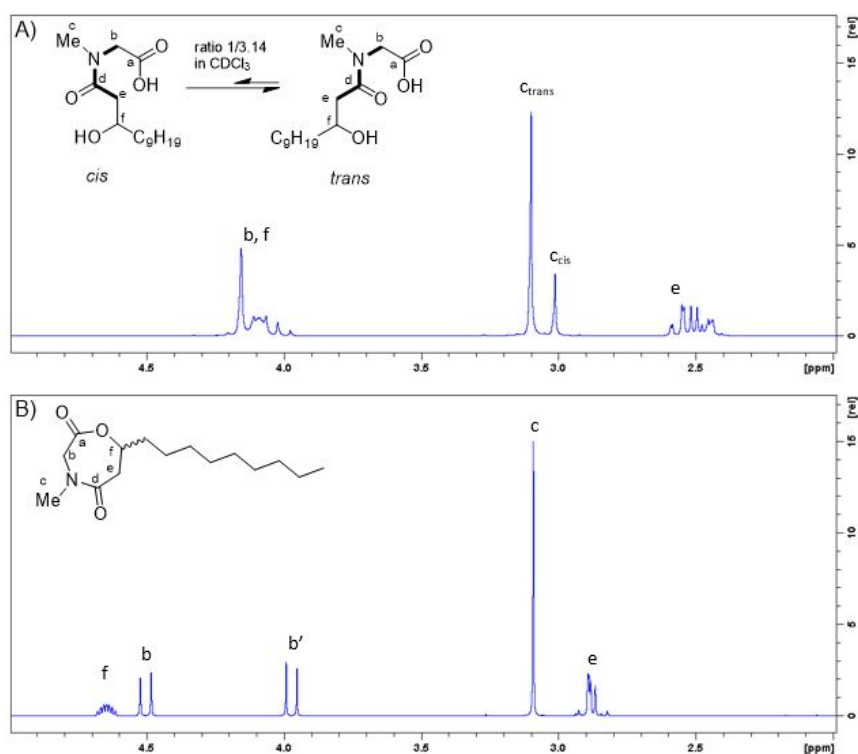


Figure 3.7. Zoom in of the ^1H NMR spectrum of *N*-(3-hydroxydodecanoyl)sarcosine (**108**) (spectrum A) and the cyclic derivative **110** (spectrum B). The existence of two rotamers in spectrum A is indicated by the presence of two singlets around 3 ppm, corresponding to the *N*-methyl group. In spectrum B, only one signal is present for the *N*-methyl group.

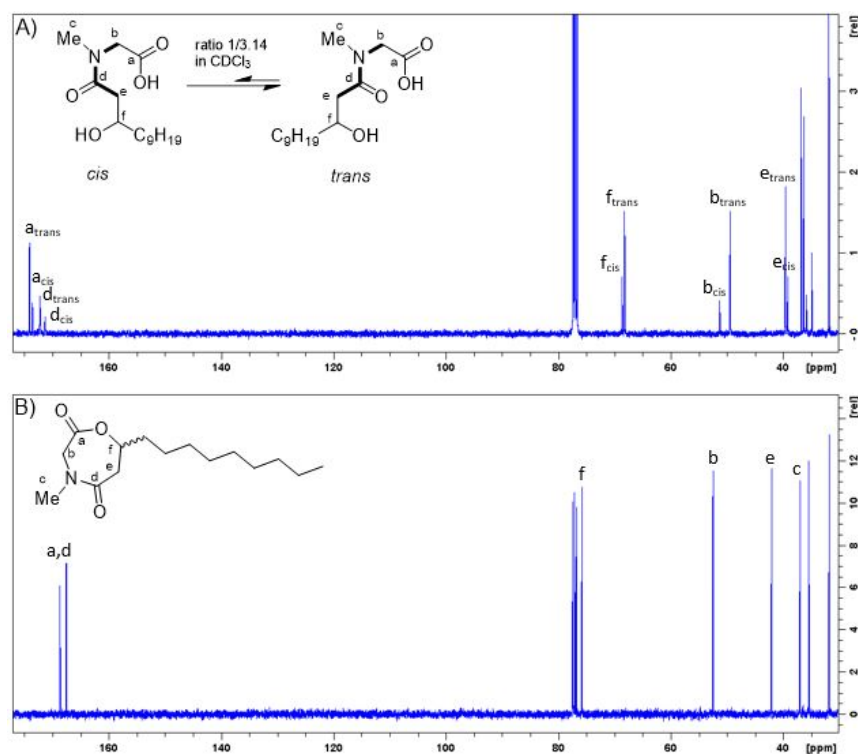
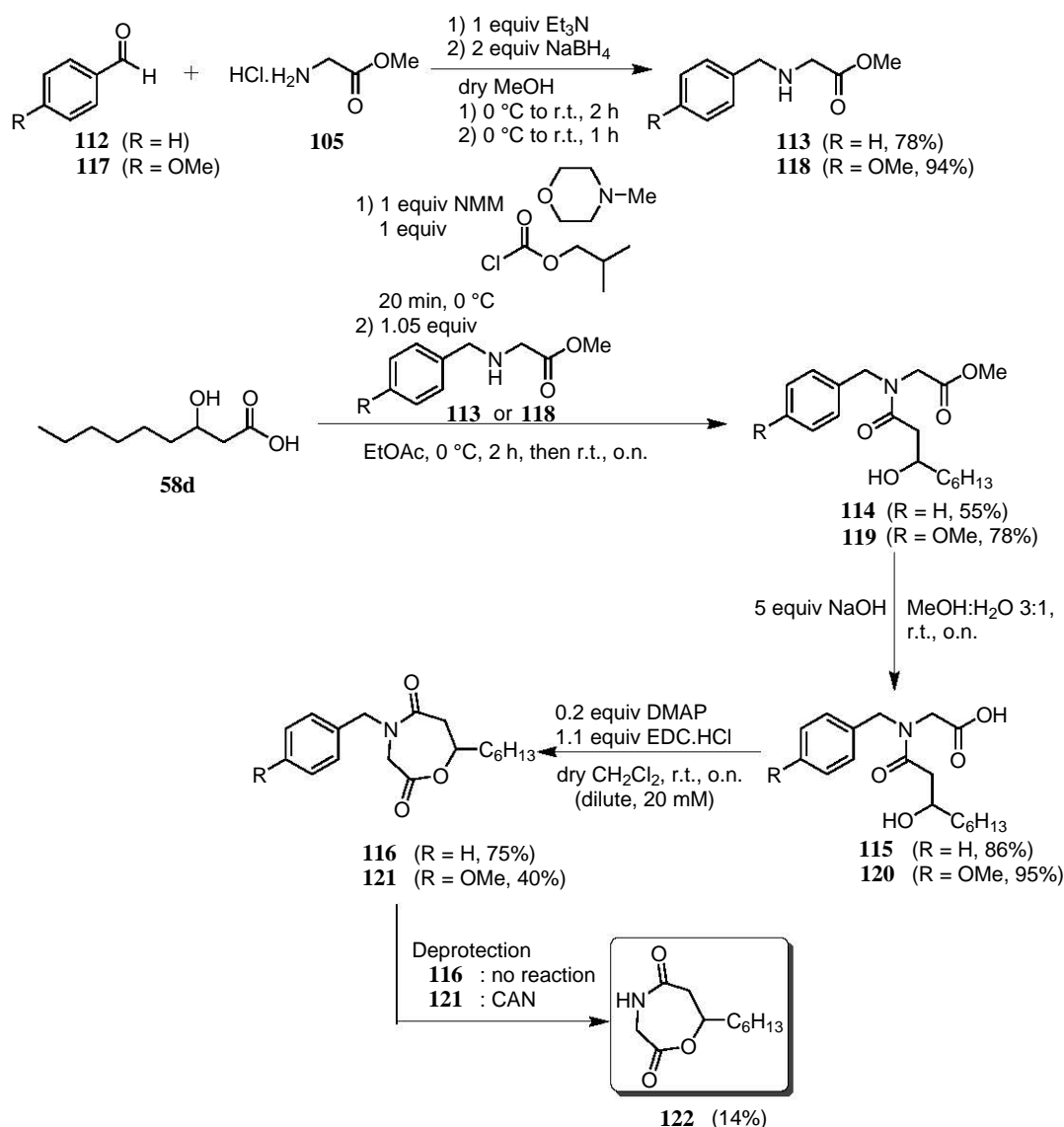


Figure 3.8. Zoom in of the ^{13}C NMR spectrum of *N*-(3-hydroxydodecanoyl)sarcosine (**108**) (spectrum A) and cyclic derivative **110** (spectrum B). The existence of two rotamers can clearly be observed in spectrum A whereas only one conformer exists in spectrum B.

3.2.5 Cyclization of *N*-(3-hydroxyacyl)amino acids with a deprotectable group at nitrogen

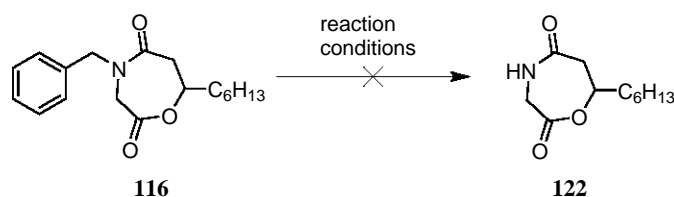
From the above-mentioned results, it is obvious that the *N*-(3-hydroxyacyl)amino acid derivative needs to be forced in the correct conformation for cyclization to occur. This necessity was also observed during the synthesis of 1,4-oxazepan-5-ones.²⁷⁵ The introduction of a third substituent at nitrogen, as is the case for the proline and sarcosine derivatives **97** and **108**, altered the *cis/trans*-ratio, and resulted in cyclization. To obtain the natural product serratin (**83**), this additional group at nitrogen should be a removable one. Because of the lability of the desired lactone, many protecting groups, that can be applied for the synthesis of seven-membered lactams, cannot be used for this cyclization as the reaction conditions needed for their removal after the cyclization step, will destroy the lactone bond.

As a benzyl group can be removed via hydrogenolysis, this *N*-protecting group was evaluated as a possible solution. Reductive amination of benzaldehyde **112** with methyl glycinate **105**, used as hydrochloride and released with the aid of triethylamine, yielded the *N*-benzyl-protected methyl ester of glycine **113**, which was coupled to β -hydroxynonanoic acid **58d**. Alkaline hydrolysis in aqueous methanol, followed by cyclization in dilute reaction conditions gave the desired *N*-benzyl-protected seven-membered ring-containing compound **116** (Scheme 3.23).



Scheme 3.23. Synthesis of *N*-benzyl and *N*-PMB-protected seven-membered lactones **116** and **121** and CAN-mediated deprotection of **121** to 7-hexyl-1,4-oxazepane-2,5-dione (**122**).

To remove the *N*-protecting group, several reaction conditions were tested but none was able to deliver the desired deprotected compound **122** (Table 3.4).^{287–291} Either there was no reaction at all (except for solvolysis of the lactone ring, Table 3.4, entries 1, 2 and 6) or a complex reaction mixture was obtained (Table 3.4, entry 5). The only condition giving debenzilation, albeit in moderate yield, was accompanied by ethanolysis of the lactone ring (Table 3.4, entry 3). Replacement of ethanol by ethyl acetate as a solvent, halted the deprotection, even when the reaction time was significantly prolonged (Table 3.4, entry 4). Similar difficulties to remove a benzyl group from a carboxamide were also encountered by Williams *et al.* during the debenzilation of a diketopiperazine.²⁹²

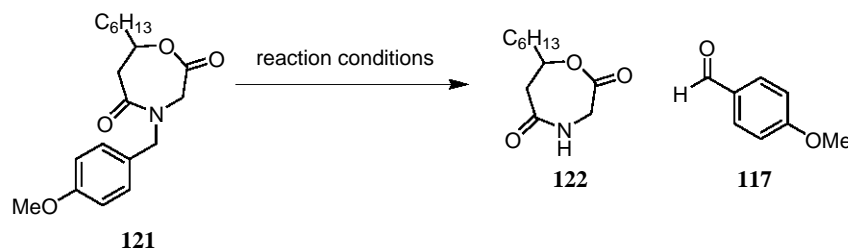
Table 3.4: Reaction conditions evaluated for the *N*-deprotection of compound **116**.^{287–291}

Entry	Reaction conditions	Result
1	3 bar H ₂ , 1 wt. equiv 10% Pd/C, MeOAc, r.t., 48 h ²⁸⁷	–[a]
2	3 bar H ₂ , 0.5 wt. equiv 10% Pd/C, EtOH, r.t., 16 h ²⁸⁸	–[b]
3	3 bar H ₂ , 0.5 wt. equiv 20% Pd(OH) ₂ /C, EtOH, r.t., 4 h ²⁸⁹	–[c]
4	3 bar H ₂ , 0.5 wt. equiv 20% Pd(OH) ₂ /C, EtOAc, r.t., 24 h	–[a]
5	1 equiv NBS, 0.2 equiv AIBN, EtOAc, Δ, 4 h ²⁹⁰	–[d]
6	2.5 equiv NBS, 0.1 equiv NMA, dry CH ₂ Cl ₂ , r.t., o.n. ²⁹¹	–[a]

[a] No reaction. [b] No deprotection, degradation of starting material **116**. [c] Deprotection followed by solvolysis or solvolysis followed by deprotection. [d] Complex reaction mixture.

As the synthesis of the *N*-benzyl-protected seven-membered core-containing compound **116** was successful, whereas the *N*-deprotection proved to be problematic, the *p*-methoxybenzyl (PMB) protecting group was evaluated as a more labile protecting group. Reductive amination of glycine methyl ester hydrochloride **105** with anisaldehyde **117** gave *N*-PMB-protected methyl glycinate **118** in a good yield (Scheme 3.23).²⁹³ The same *N*-acylation and cyclization conditions used for the synthesis of the *N*-benzyl derivative **116** were applied to yield the *N*-PMB-protected seven-membered ring-containing compound **121** (Scheme 3.23).

For the removal of the PMB-protecting group, several conditions were tested (Table 3.5). Both 2,3-dichloro-5,6-dicyano-1,4-benzoquinone (DDQ) and ceric ammonium nitrate (CAN), the reagents commonly used for PMB-deprotection, were evaluated under different reaction conditions, alongside other reagents.^{281,294–298}

Table 3.5: Reaction conditions evaluated to remove the PMB-protecting group of *N*-PMB-1,4-oxazepane-2,5-dione **121**.^{281,294–298}

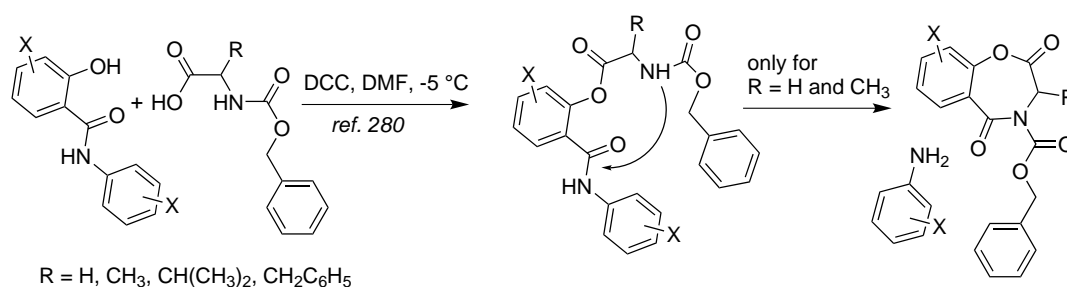
Entry	Reaction conditions	Result
1	2 equiv DDQ, CH ₂ Cl ₂ :H ₂ O 9:1, r.t., 8 h	– ^[a]
2	5 equiv CAN, CH ₃ CN:H ₂ O 4:1, 0 °C to r.t., 2 h	122 (15%) ^[b]
3	5 equiv CAN, CH ₃ CN:H ₂ O (NaOAc/HOAc buffer, pH 5.2), 0 °C, 2 h	122 (18%) ^[b] and 121 (41%) ^[b]
4	10 equiv CAN, CH ₃ CN:H ₂ O 4:1, 0 °C, 1 h	122 (30%) ^[b] and 121 (6%) ^[b]
5	5 equiv CAN, EtOAc:H₂O 4:1, 0 °C, 2 h	122 (36%) ^[b] and 121 (28%) ^[b]
6	10 equiv CAN, EtOAc:H ₂ O 4:1, 0 °C, 2 h	122 (32%) ^[b] and 121 (33%) ^[b]
7	5 equiv CAN, <i>t</i> BuOH:CH ₂ Cl ₂ 4:1, r.t., 2 h	– ^[c]
8	5 equiv CAN, CH ₃ CN:H ₂ O 99:1, r.t., o.n.	122 (10%) ^[b] and 121 (70%) ^[b]
9	4 equiv PhI(OAc) ₂ , MeOH, r.t., o.n.	– ^[a]
10	BF ₃ .OEt ₂ , r.t., o.n.	– ^[d]
11	BF ₃ .OEt ₂ , 128 °C, 6 h	– ^[e]

[a] Solvolysis of **121**. [b] Quantitative data were obtained after the extraction of the reaction mixture with ethyl acetate, followed by a washing step with a saturated aq. sodium bicarbonate solution to remove ring-opened degradation products. The crude yield of the different products was determined via integration of the ¹H NMR spectrum. [c] Deprotection followed by solvolysis or solvolysis followed by deprotection. [d] No reaction. [e] Complex reaction mixture.

As the deprotection with 5 equivalents of CAN in a solvent mixture of ethyl acetate and water in a 4:1-ratio gave the best result (Table 3.5, entry 5), this reaction was repeated on a larger scale to give the pure, fully deprotected, seven-membered lactone **122** in 14% yield after purification via column chromatography. This rather low yield can be attributed to several factors. First, the reaction duration is too short to allow complete conversion, which is obvious from the recovery of the *N*-PMB-protected lactone **121**. Second, when the product **122** is formed, lactonolysis can occur by the water present as a co-solvent, which is needed for the deprotection. This

lactonolysis also can open the starting material **121**, but this route seems to be slower. Third, reactions with CAN often give rise to a laborious work-up because of the difficult separation of the turbid aquatic phase and the organic phase.

The synthesis of the deprotected seven-membered core **122** was successfully completed, so the focus was put on the synthesis of serratin (**83**), which differs from lactone **122** only by the presence of a hydroxymethyl group. However, when the *N*-acylation reaction was repeated with methyl *N*-PMB-serinate, *O*-acylation instead of *N*-acylation was observed. To avoid this undesired reaction, the reaction sequence was repeated with *O*-benzylserine, but when the cyclization was attempted in the final step, a complex reaction mixture was obtained, instead of the desired heterocycle. This lack of cyclization could be caused by steric factors. A similar observation was made by Imramovský *et al.* during a coupling reaction of *N*-benzyloxycarbonyl-protected amino acids with a salicylanilide.²⁹⁹ When *N*-Cbz-glycine and *N*-Cbz-alanine were used, a seven-membered ring was formed. This type of cyclization was not observed when valine or phenylalanine were used (Scheme 3.24).



Scheme 3.24. Difference in cyclization behavior observed by Imramovský *et al.* during a salicylanilide esterification.²⁹⁹

3.2.6 Application of photoremovable protecting groups (PPGs)

In an attempt to improve the low yield of the PMB-deprotection step, photolabile or photoremovable protecting groups (PPGs) were tested. Their removal is solely based upon irradiation with light, so the presence of water, which can cause lactonolysis, can be avoided. The efficiency of photoconversion is determined by the quantum yield ϕ (proportion of molecules that undergoes photolysis after absorption of a photon) and the absorption coefficient ϵ (proportion of incident light absorbed).^{300–302} PPGs are commonly applied in biochemistry to control the release of certain bioactive compounds in living tissues. A caged compound is administered and irradiated to release the bioagent at certain target sites. A PPG should have a strong absorption at wavelengths above 300 nm to avoid absorption by and to minimize damage to the biological system.³⁰⁰ PPGs have been used to force the cyclization of peptides via a ring contraction as

well. In this case a 2-hydroxy-6-nitrobenzyl group is typically used. This PPG is introduced at the *N*-terminus of the peptide and then the hydroxy group of this PPG forms a (macro)cyclic ester with the *C*-terminus of the peptide. A subsequent *O*- to *N*-acyl transfer delivers the desired cyclic compound, whereafter the PPG is removed via photolysis.³⁰³ To synthesize highly strained cyclic peptides, it can be necessary to introduce two PPGs: one at the *N*-terminus to fulfill a ring closure/contraction role and one in the middle of the peptide sequence to promote a *cis*-amide bond to facilitate the cyclization.³⁰⁴

One of the most commonly used PPGs are the 2-nitrobenzyl derivatives **123**. Some disadvantages of this class are the slow rate of release after excitation and the toxic and strongly absorbing by-products.³⁰⁰ Sometimes a protective thiol group is added to cope with this, or reduced glutathione present within cells can give the same protection.³⁰¹ Other commonly used groups are the benzoin group **124**, the *p*-hydroxyphenacyl group **125** and the coumarinyl group **126** (Figure 3.9).^{300,302}

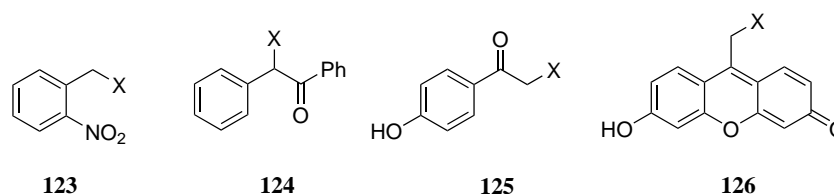
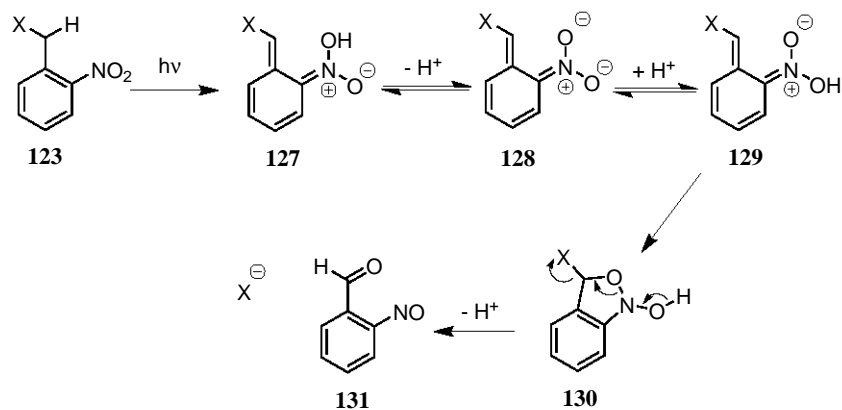


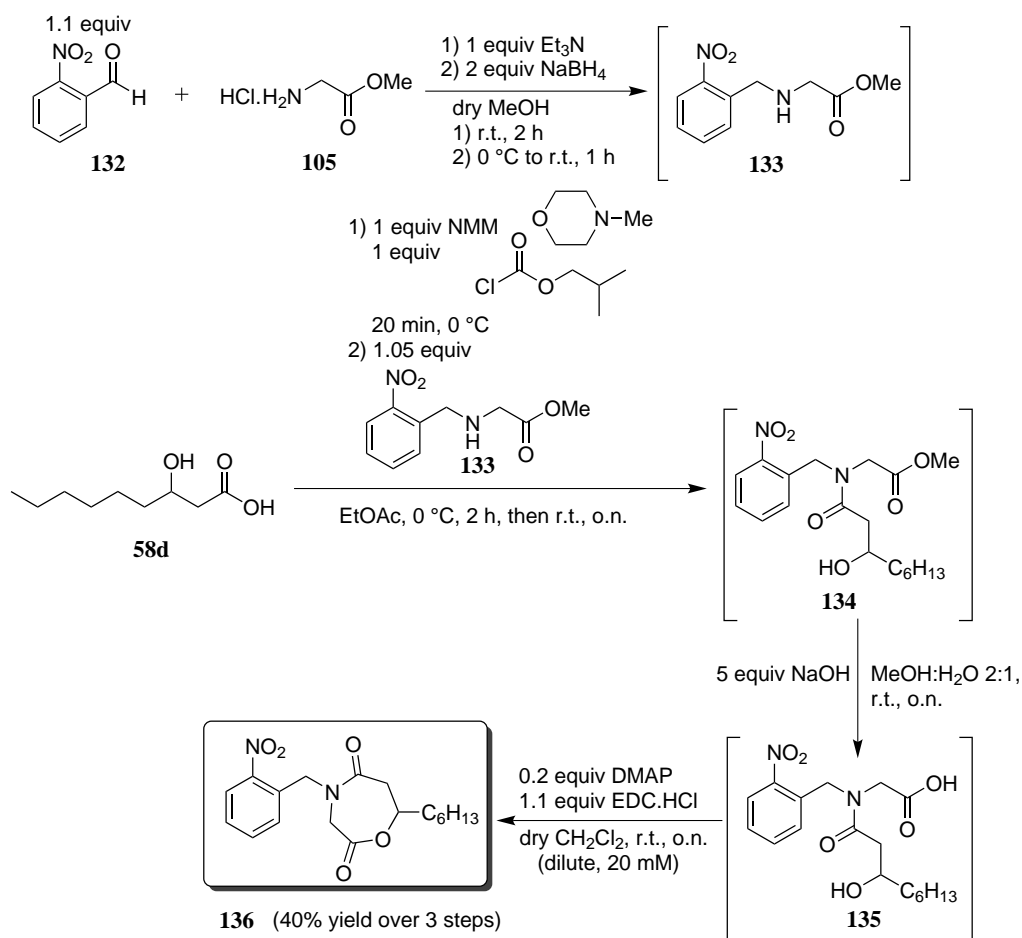
Figure 3.9. General structure of some PPGs, with X representing the caged compound.

Electronic excitation of 2-nitrobenzyl compounds **123** generates very quickly their *aci*-nitrotautomers **127** (Scheme 3.25). The *Z*-nitronic acid **127** is formed via transfer of a benzylic hydrogen to an oxygen of the nitro group. Deprotonation followed by reprotonation gives the *E*-nitronic acid **129** and allows cyclization to *N*-hydroxybenzisoxazoline **130**, which then decays to compound **131**, hereby releasing the caged compound X.^{300,301} The quantum yield ϕ is not readily manipulated but the absorption coefficient ϵ can be varied, e.g. in case of the aromatic nitro compounds by adding electron-donating groups to the aromatic ring, causing an increase of absorbance at longer wavelengths (bathochromic shift). Substituents on the benzylic carbon also have a profound effect, with a higher photolytic cleavage rate linked to a more electron rich benzylic carbon atom.^{301,302,305,306} However, it is very difficult to predict the reaction rate or efficiency. Solvent plays an important role in determining the half life of the PPGs as well.³⁰⁵



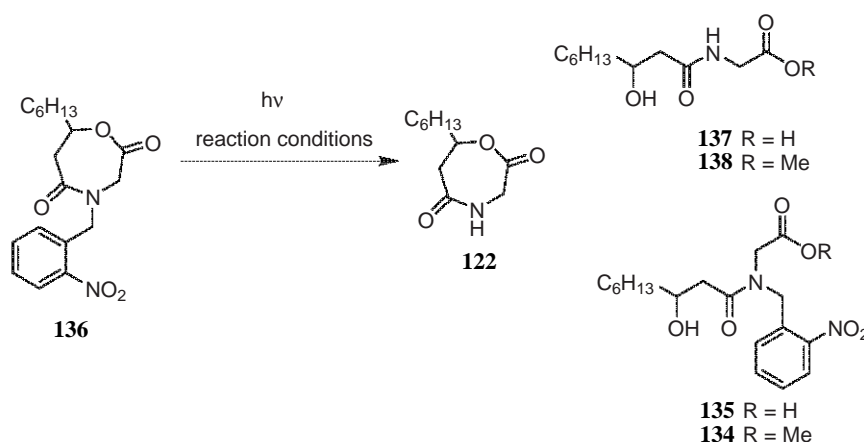
Scheme 3.25. Mechanism of photolysis of 2-nitrobenzyl derivatives **123**, with X representing the caged compound.³⁰¹

The first PPG that was evaluated was the 2-nitrobenzyl group.^{307,308} Commercially available 2-nitrobenzaldehyde **132** was reacted with glycine methyl ester hydrochloride **105** (Scheme 3.26). The obtained PPG-protected amino acid methyl ester **133** was coupled to β -hydroxynonanoic acid **58d**. Hydrolysis and cyclization yielded seven-membered ring **136**. To avoid premature photolysis, all reactions were shielded from light and purification via column chromatography was only performed on the final product.



Scheme 3.26. Synthesis of *N*-2-nitrobenzyl-protected seven-membered ring **136**.

For the photolysis, two UV-light sources were evaluated: the OSRAM Ultra-Vitalux 300W - 230V E27 lamp (radiated power 315-400 nm (UVA) 13.6 W/m² - radiated power 280-315 nm (UVB) 3.0 W/m²) fitted with a UV-light transmitting, visible light absorbing Hoya U-360 filter, and the UVLS-28 EL Series UV Lamp 8W - 230V (wavelength 366 nm), commonly used in laboratories to visualize TLC-plates. Although several reaction conditions and times were evaluated, *N*-deprotection was never observed (Table 3.6). It seems that both lamps were unable to deliver the needed intensity unlike the pulsed laser (pulse width 8 ns, energy 38 mJ, wavelength 355 nm) which was reported in literature to promote the photodeprotection of a 2-nitrobenzyl group from a peptide chain.³⁰⁷ However, a hand-held UV lamp used for TLC visualization was successfully employed to deprotect *N*-2-nitrobenzylglycine,³⁰⁸ showing the difference in ease of photodeprotection between an amine and an amide.

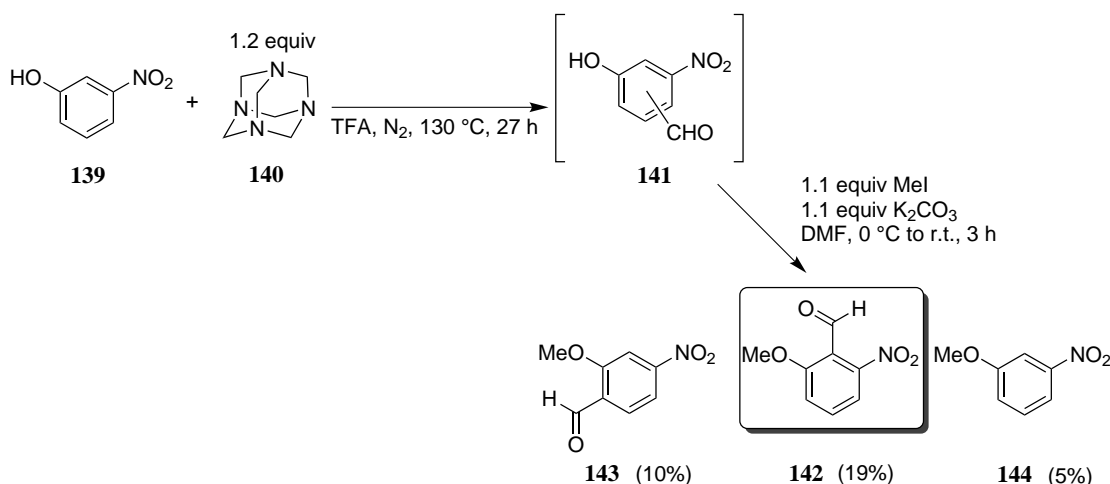
Table 3.6: Reaction conditions evaluated to remove the 2-nitrobenzyl group of **136**.^{303–305,307}

Entry	Reaction conditions	UV-Source	Result
1	1% DMSO in MeOH, r.t., 40 min	OSRAM Ultra-Vitalux 300W - 230V	- [a]
2	1% AcOH in MeOH, r.t., 40 min	OSRAM Ultra-Vitalux 300W - 230V	- [a]
3	CH ₂ Cl ₂ :CF ₃ CH ₂ OH 4:1, r.t., 6 h	UVLS-28 EL Series UV Lamp 8W - 230V, long wavelength, 366 nm	- [b]
4	1% DMSO in MeOH, r.t., 6 h	UVLS-28 EL Series UV Lamp 8W - 230V, long wavelength, 366 nm	- [a]
5	1% DMSO in <i>p</i> -dioxane, r.t., 6 h	UVLS-28 EL Series UV Lamp 8W - 230V, long wavelength, 366 nm	- [b]
6	1% AcOH in MeOH, r.t., 6 h	UVLS-28 EL Series UV Lamp 8W - 230V, long wavelength, 366 nm	- [a]
7	2.5 mM TES (<i>N</i> -[tris-(hydroxymethyl)methyl]-2-aminoethanesulfonic acid) in H ₂ O:CH ₃ CN 3:2, r.t., 6 h	UVLS-28 EL Series UV Lamp 8W - 230V, long wavelength, 366 nm	- [b]
8	0.1% TFA in H ₂ O:CH ₃ CN: 1:1, r.t., 6 h	UVLS-28 EL Series UV Lamp 8W - 230 V, long wavelength, 366 nm	- [a]

[a] Complete solvolysis of **136** without photodeprotection. [b] No reaction.

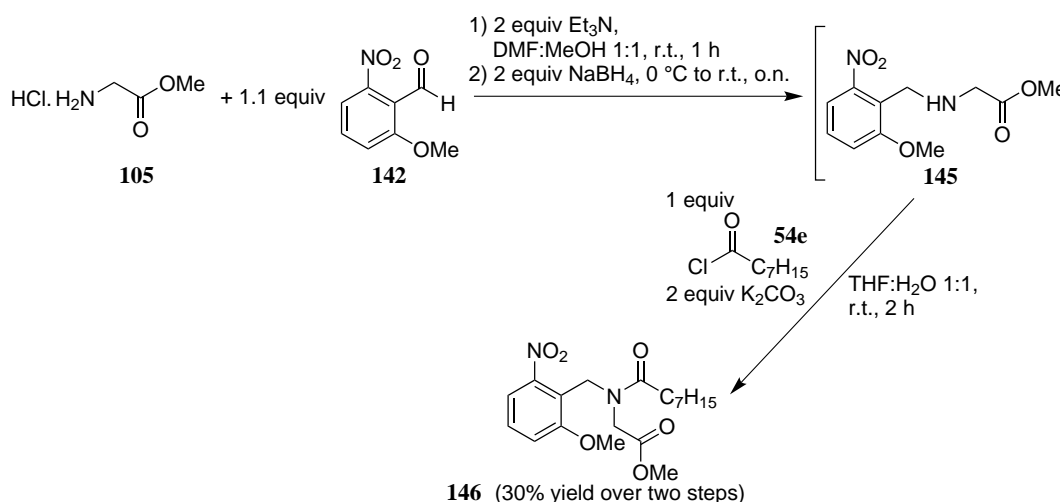
As the introduction of electron-donating groups causes an increase of absorbance at longer wavelengths,³⁰⁵ 2-methoxy-6-nitrobenzyl was evaluated as a PPG. 2-Hydroxy-6-nitrobenzaldehyde **141** was synthesized via a Duff reaction with *m*-nitrophenol **139** and hexamethylenete-

tramine **140** (Scheme 3.27).^{309,310} The crude mixture was methylated with iodomethane. Purification via column chromatography yielded the desired 2-methoxy-6-nitrobenzaldehyde **142** in 19% yield. The main side products that were isolated were 2-methoxy-4-nitrobenzaldehyde **143** and the methylated starting material 3-nitroanisole **144** in 10% and 5% yield, respectively.



Scheme 3.27. Synthesis of the PPG-precursor 2-methoxy-6-nitrobenzaldehyde **142**.

The reductive amination procedure used for the synthesis of methyl *N*-(2-nitrobenzyl)glycinate **133** (Scheme 3.26) did not yield the desired compound **145** when using 2-methoxy-6-nitrobenzaldehyde **142**, so a slightly modified procedure was used and the target compound **145** was obtained (Scheme 3.28).³¹¹ This compound was reacted with octanoyl chloride **54e** under Schotten-Baumann conditions to obtain *N*-protected compound **146**.

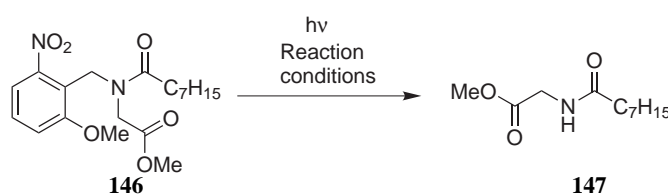


Scheme 3.28. Synthesis of PPG-protected *N*-octanoyl glycine methyl ester **146**.

The PPG-protected *N*-octanoyl glycine methyl ester **146** was synthesized as a model compound to evaluate several photolysis conditions (Table 3.7). A blacklight bulb - E27 - 20W/230V was used as a light source and both flow (reactor volume: 24 mL, flow rate: 0.3 mL/min) and batch

set-ups were evaluated. This time, photolysis was observed in all cases. Performing the reaction in flow gave a better conversion and required a shorter reaction time compared to the same reaction conditions in batch (Table 3.7, entries 2 and 5). The reaction conditions which gave the best result (Table 3.7, entry 3) were also applied on 2-nitrobenzyl protected substrate **136**, but once again no photolysis was observed.

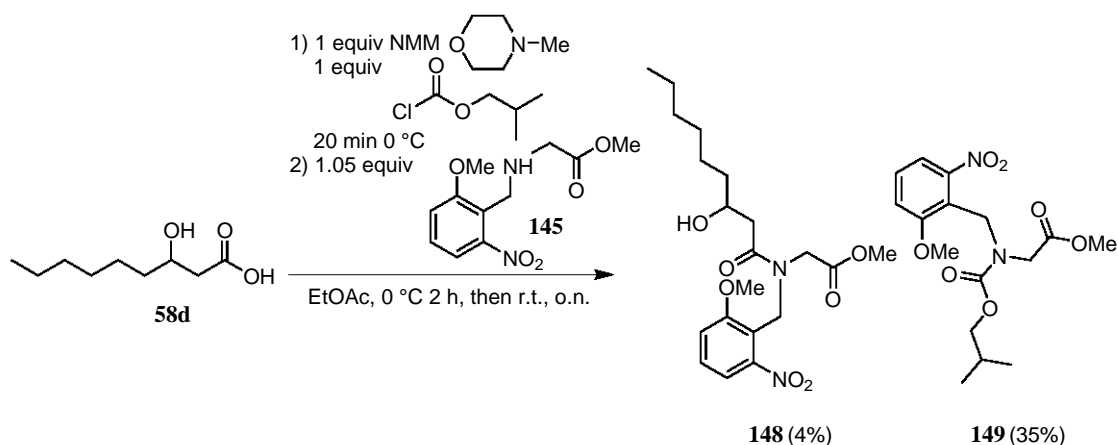
Table 3.7: Reaction conditions evaluated to remove the 2-methoxy-6-nitrobenzyl group of **146** with a blacklight bulb - E27 - 20W - 230V as a source of UV-light.^{303,305,309,311}



Entry	Batch/Flow	Solvent	Reaction time (min)	Result
1	Flow	MeOH	80	42% conversion
2	Flow	1% AcOH in MeOH	80	57% conversion
3	Flow	1% DMSO in MeOH	80	67% conversion
4	Batch	1% DMSO in <i>p</i> -dioxane	480	27% conversion
5	Batch	1% AcOH in MeOH	480	35% conversion

Previous tests had shown that the seven-membered lactone **136** was stable in 1% DMSO in *p*-dioxane (Table 3.6, entry 5) and these conditions were able to bring about the photolysis of the 2-methoxy-6-nitrobenzyl group of an amide nitrogen (Table 3.7, entry 4). Therefore, to obtain a high yielding deprotection procedure for the desired 1,4-oxazepane-2,5-dione core, an attempt was made to synthesize the *N*-(2-methoxy-6-nitrobenzyl)-protected lactone (Scheme 3.29).

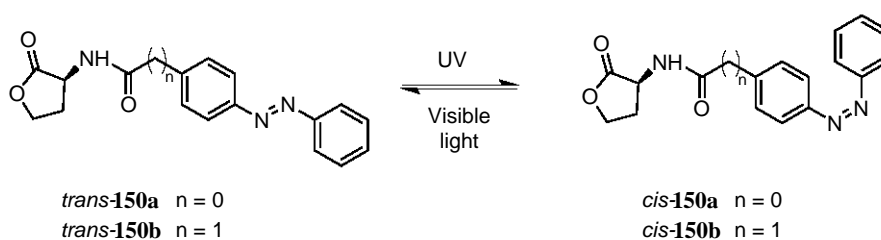
Unlike previous *N*-acylation reactions that were performed using the same reaction conditions, the *N*-acylation product **148** of the PPG-protected amino acid derivative **145** was only obtained as the minor product (Scheme 3.29). The main isolated product **149** was the adduct of the PPG-protected amino acid derivative **145** and isobutyl chloroformate. Alkaline hydrolysis of the minor product **148**, followed by a cyclization reaction, failed to yield the *N*-(2-methoxy-6-nitrobenzyl)-protected seven-membered ring.



Scheme 3.29. Attempt to *N*-acylate methyl *N*-(2-methoxy-6-nitrobenzyl)glycinate **145**.

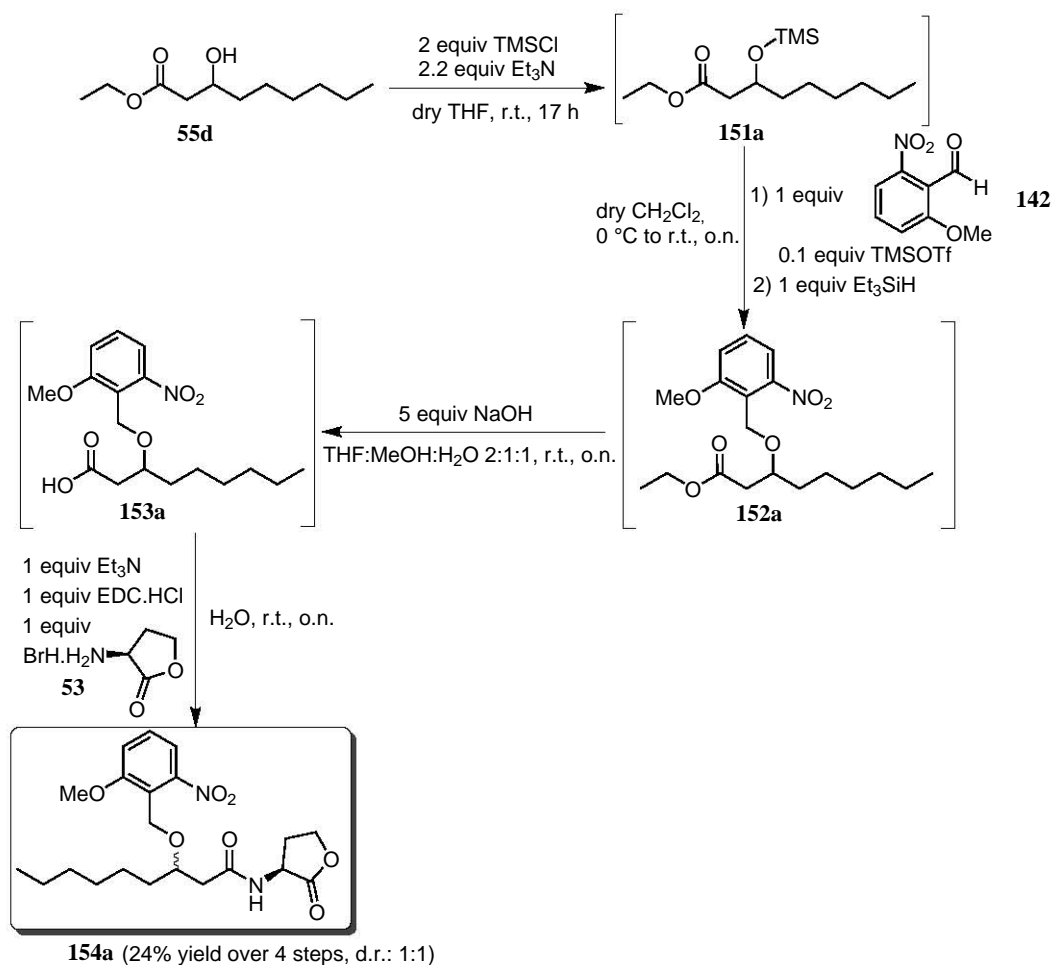
3.2.7 PPG-protected *N*-(3-hydroxyacyl)-*L*-homoserine lactones

As the UV-light driven removal of the 2-methoxy-6-nitrobenzyl PPG proved to be successful (Table 3.7), it was decided to employ this group to synthesize a PPG-protected *N*-(3-hydroxyacyl)-*L*-homoserine lactone. This type of compounds allows the non-invasive, external interference with the bacterial communication system by using light. In a previous study by Van der Berg *et al.*, researchers were able to temporarily modulate QS-regulated traits via photoswitchable compounds **150**, which relied on the *trans* to *cis*-isomerization of the azobenzene photochromic unit upon UV-light irradiation. Exposure to visible light changes the conformation back to mainly the *trans*-isomer (Scheme 3.30).³¹² Both compounds **150** had a QS-activating effect but upon UV-light irradiation, compound **150a** showed a drop in efficacy whereas compound **150b** had a fivefold increase in activity.



Scheme 3.30. Photoswitchable QS-molecules **150**.³¹²

To obtain the PPG-protected hydroxy-AHL **154a**, ethyl 3-hydroxynonanoate **55d** was benzylated via a reductive etherification,^{313,314} based upon Noyori's TMSOTf-catalyzed acetalization,³¹⁵ followed by a triethylsilane-reduction of the acetal (Scheme 3.31).³¹⁶ Alkaline hydrolysis of the *O*-PPG-protected ester **152a** to the acid **153a**, followed by EDC-mediated coupling with *L*-homoserine lactone **53** yielded *O*-PPG-protected hydroxy-AHL **154a**.



Scheme 3.31. Synthesis of *N*-(3-((2-methoxy-6-nitrobenzyl)oxy)nonanoyl)-*L*-homoserine lactone **154a**.

For the removal of the PPG-group, a solution of AHL **154a** dissolved in 1% acetic acid in methanol in an open beaker was irradiated with a blacklight bulb (E27 - 20W/230V) and samples were analyzed at regular time intervals via LC-MS (Figure 3.10). After 3 h, already more than half of the caged AHL was released. When the experiment was repeated with 1% ethanol in water as solvent mixture, to mimic biotesting conditions, photolysis was already complete within 2 h. Remarkably, in both conditions tested, no solvolysis of the lactone ring was observed during the monitoring via LC-MS.

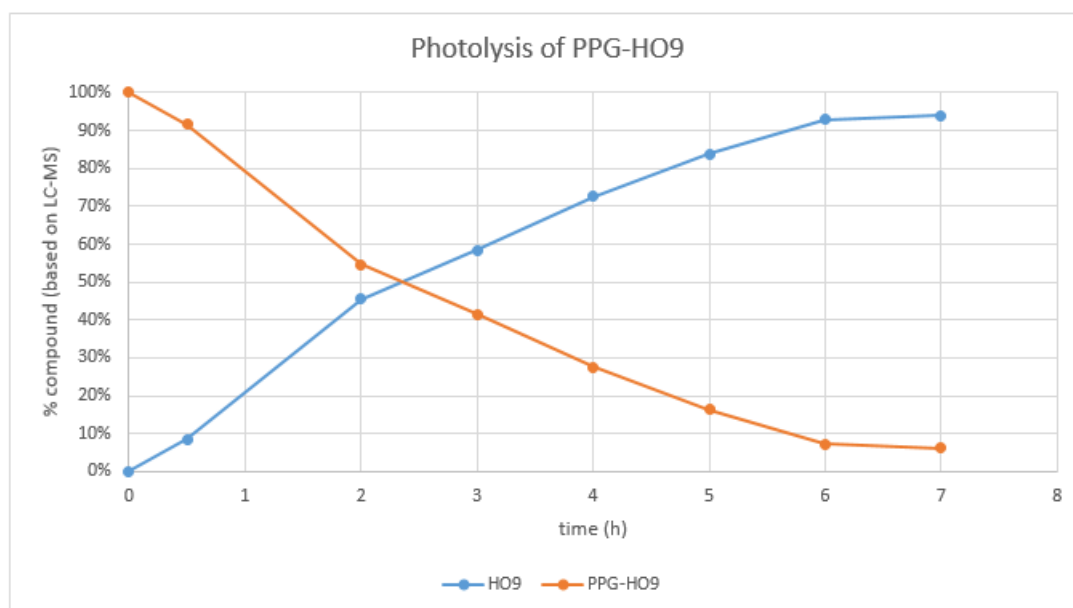


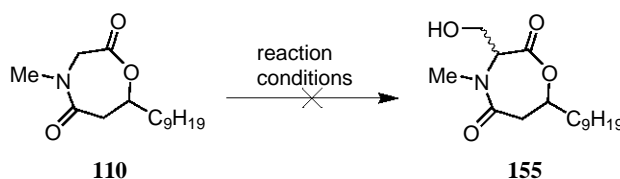
Figure 3.10. Photolysis of *N*-(3-((2-methoxy-6-nitrobenzyl)oxy)nonanoyl)-L-homoserine lactone **154a** with a blacklight bulb (E27 - 20W/230V) in 1% AcOH in MeOH.

A disadvantage of photolysis is the need for UV-radiation to release the caged compound. Although peptides are relatively stable toward >350 nm UV light, this may not be the case for complex heterocycles. Also methionine is sensitive toward photooxidation.³⁰⁵ However, the two-photon irradiation technique can help to overcome the toxicity linked with UV-light irradiation. Because at high light intensity, chromophores may simultaneously absorb two red/NIR photons, producing higher-energy excited states, similar to those accessible by direct excitation with UV photons of about twice the frequency.³⁰² As this requires very high light intensities, only ultrafast pulsed lasers are suitable for this application. Using this approach, Neveu *et al.* studied the effect of retinoic acid on zebrafish embryogenesis via the *o*-nitrobenzyl moiety protected derivative, which was photolysed via one- or two-photon excitation.³¹⁷

3.2.8 Post-cyclization modification

As the route which led to the *N*-PMB-protected seven-membered ring **121** failed when serine was used instead of glycine, the introduction of a hydroxymethyl group on the *N*-PMB-protected seven-membered ring **121** was evaluated.

Both reactions with paraformaldehyde as such and with paraformaldehyde as a source of formaldehyde via thermal cracking, were unable to introduce the desired hydroxymethyl group on the *N*-methyl derivative **110**, which was used as a test substrate (Table 3.8).^{318–320}

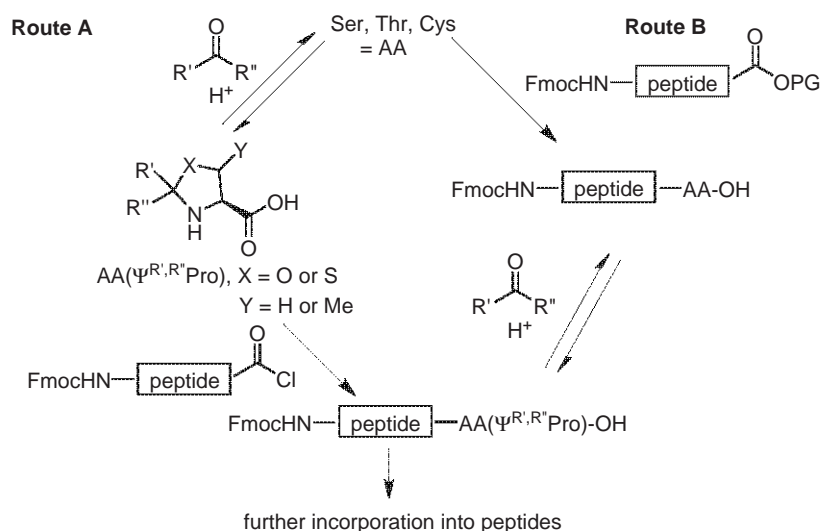
Table 3.8: Reaction conditions evaluated to introduce a hydroxymethyl group in cyclic compound **110**.^{318–320}

Entry	Reaction conditions	Result
1	15 equiv KHCO ₃ , 11 equiv paraformaldehyde, DMF, r.t., 1 h to o.n.	- ^[a]
2	1) 1 equiv LDA, dry THF, N ₂ , -78 °C, 1 h 2) 6 equiv paraformaldehyde, dry THF, N ₂ , -78 °C, 3 h to r.t., o.n.	After 3 h at -78 °C: - ^[a] After o.n. at r.t.: - ^[b]
3	1) 2 equiv LDA, dry THF, N ₂ , -78 °C, 1 h 2) 6 equiv paraformaldehyde, dry THF, N ₂ , -78 °C, 3 h to r.t., o.n.	After 3 h at -78 °C: - ^[a] After o.n. at r.t.: - ^[b]
4	1) 1 equiv LDA, dry THF, N ₂ , -78 °C, 1 h 2) formaldehyde (g) (formed by dry heating 10 equiv paraformaldehyde at 170 °C), dry THF, N ₂ , -78 °C, 3 h to r.t., o.n.	After 3 h at -78 °C: - ^[a] After o.n. at r.t.: - ^[b]

[a] No reaction. [b] Complex reaction mixture.

3.2.9 Pseudo-prolines (Ψ Pro)

As the synthesis of the deprotected seven-membered ring **122** was performed well, but its application using the same reaction conditions to the serine derivative in order to synthesize serratin (**83**) failed, an alternative synthetic route was sought. Serine (and threonine) can react with aldehydes or ketones to form oxazolidines (Scheme 3.32). These cyclic structures are unstable in acidic environment, but can be acylated in an alkaline environment and isolated as such.³²¹ Pseudo-prolines are commonly used to alter the solubility of peptides by disrupting secondary structure formation or to facilitate the cyclization of small peptides.^{322,323} There are two ways to introduce such a pseudo-proline moiety: either the pseudo-proline is synthesized separately by reacting serine, threonine or cysteine with an aldehyde or ketone, and then included into the peptide chain (Figure 3.32, route A), or the peptide chain is synthesized and then the pseudo-proline is formed afterwards (post-insertion method, Figure 3.32, route B).^{322,324,325}



Scheme 3.32. The two different routes to introduce a pseudo-proline moiety in a peptide chain.³²⁵

Variation of the C-2 ring substituents of a pseudo-proline has a profound effect on the ring stability. Whereas dilute TFA affected ring opening of a 2,2-dimethyloxazolidine-peptide (Ser($\Psi^{\text{Me, Me}}$ Pro)) within minutes, a treatment with trifluoromethanesulfonic acid for several hours was needed to deprotect the rather stable C-2-unsubstituted oxazolidine (Ser($\Psi^{\text{H, H}}$ Pro)).³²⁵ The C-2 substitution pattern also has an influence on the conformational properties (Figure 3.11). Whereas for peptides containing the unsubstituted serine-derived oxazolidines (Ser($\Psi^{\text{H, H}}$ Pro)) the *trans*-isomer is the dominant one (66% *trans* in DMSO, determined via ^1H NMR at 17 °C), peptides containing the 2,2-dimethyl derivative (Ser($\Psi^{\text{Me, Me}}$ Pro)) have a clear preference for the *cis*-conformer (less than 5% *trans* in DMSO, determined via ^1H NMR at 17 °C). The *cis/trans*-ratio of the C-2 monosubstituted oxazolidines lies somewhere in between.^{326–328}

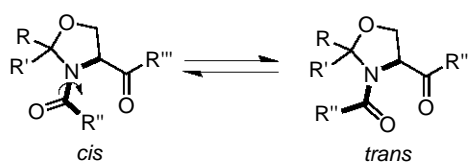
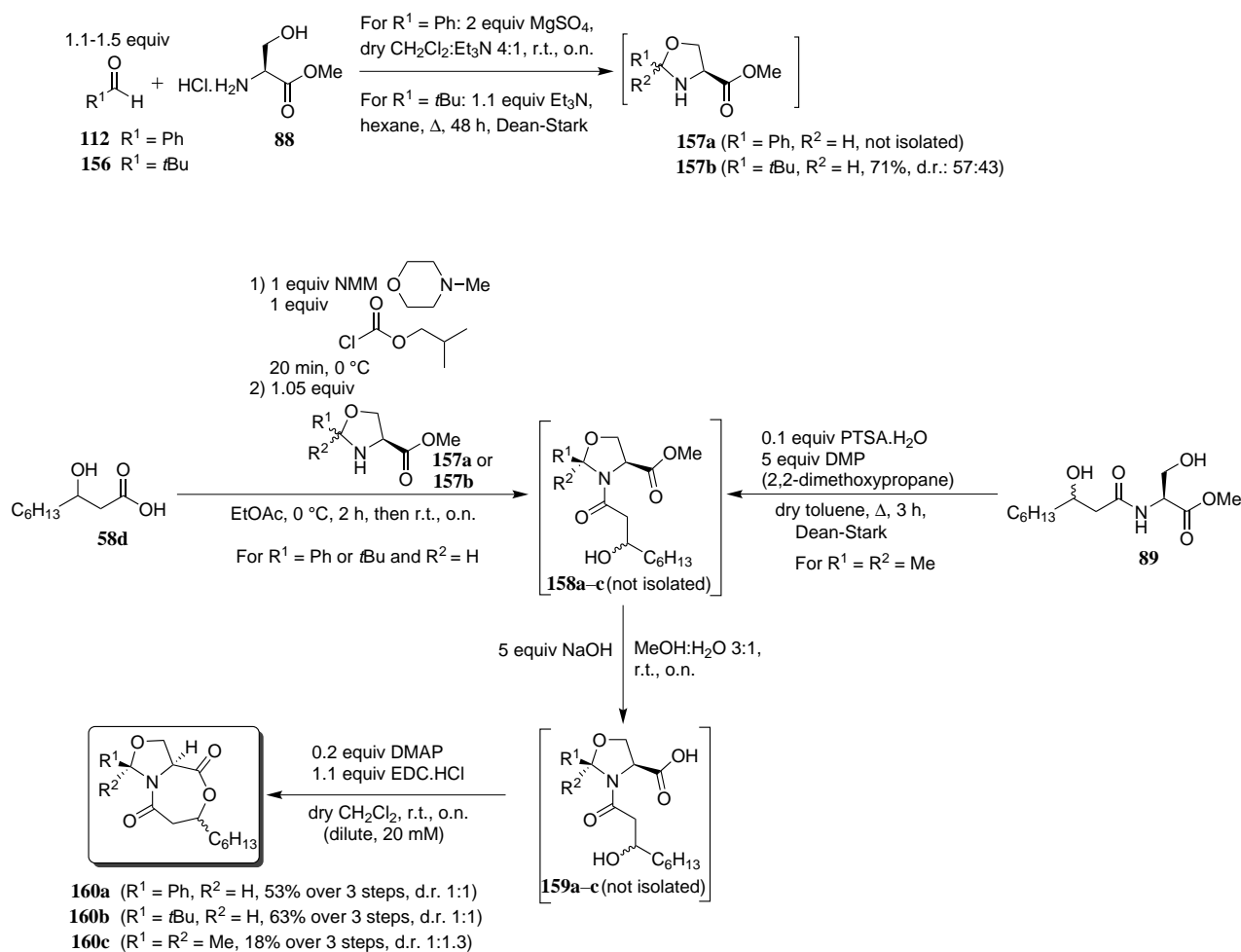


Figure 3.11. *Cis* and *trans*-conformers of a pseudo-proline.³²⁶

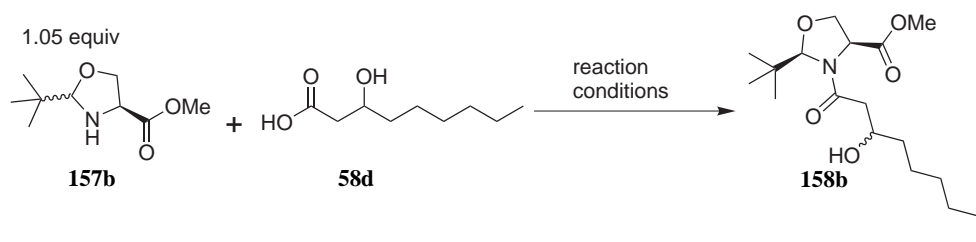
Oxazolidine **157b** was synthesized by heating the hydrochloride of the methyl ester of L-serine **88** with pivaldehyde **156** and triethylamine with continuous removal of water (Scheme 3.33). This crude oxazolidine **157b** was obtained as a 3:2-mixture of diastereomers in 71% yield.^{322,329}

Several procedures were evaluated for the *N*-acylation of oxazolidine **157b** (Table 3.9). The formation of the mixed anhydride of β -hydroxynonanoic acid **58d** via reaction with isobutyl chloroformate, followed by reaction with the methyl ester of oxazolidine **157b** proved to be the best procedure to obtain compound **158b** (Table 3.9, entry 4).³³⁰ The *N*-acylated 2-*t*Bu-oxazolidine **158b** possessed a C2,C4-*cis*-relation, although the starting oxazolidine **157b** was

obtained as a 3:2 diastereomeric mixture. Ring-chain tautomerism allows equilibration to the more stable product with the *t*Bu-group on a quasi-axial position. The amide nitrogen in the five-membered-ring is considerably pyramidalized, allowing some overlap of the nitrogen lone pair with the amide carbonyl group.^{331–333} Subsequent alkaline hydrolysis of the *N*-acylated 2-*t*Bu-oxazolidine **158b**, followed by cyclization in dilute reaction conditions yielded the bicyclic structure **160b** (Scheme 3.33).



Scheme 3.33. Synthesis of oxazolidine-containing bicyclic structures **160a–c**.

Table 3.9: Reaction conditions evaluated for the *N*-acylation of 2-*t*-butyloxazolidine **157b**.

Entry	Reaction conditions	Result
1	1 equiv EDC.HCl, 1 equiv Et ₃ N, CH ₂ Cl ₂ , r.t., 2 d	-[a]
2	0.1 equiv DMAP, 1 equiv DCC, r.t., o.n.	-[a]
3	1 equiv DMAP, 1 equiv DCC, r.t., 2 d	-[b]
4	1 equiv <i>N</i> -methylmorpholine (NMM), 1 equiv isobutyl chloroformate, EtOAc, 2 h at 0 °C, r.t., o.n.	158b (63%) ^[c]
5	1 equiv <i>N</i> -methylmorpholine (NMM), 1 equiv isobutyl chloroformate, dry THF, 2 h at 0 °C, r.t., o.n.	158b (42%) ^[c]

[a] No reaction. [b] Complex reaction mixture [c] Crude yield after work-up determined via integration of the ¹H NMR spectrum.

Bicyclic compound **160b** was obtained as a 1:1 mixture of diastereomers. The diastereomers (*RSS*)-**160b** and (*RRS*)-**160b** were separated via column chromatography followed by recrystallization. One of the two diastereomers remained an amorphous powder, whereas the other one formed needle-like crystals, allowing structure confirmation and stereochemistry determination via X-ray diffraction analysis (Figure 3.12). The crystals belong to the orthorhombic Sohnke space group *P*2₁2₁2₁ and hence contain only one enantiomer, being (*RSS*)-**160b** with a *cis*-relationship of the substituents. The C₆H₁₃-alkyl chain was disordered over two positions in the crystal due to its flexibility.

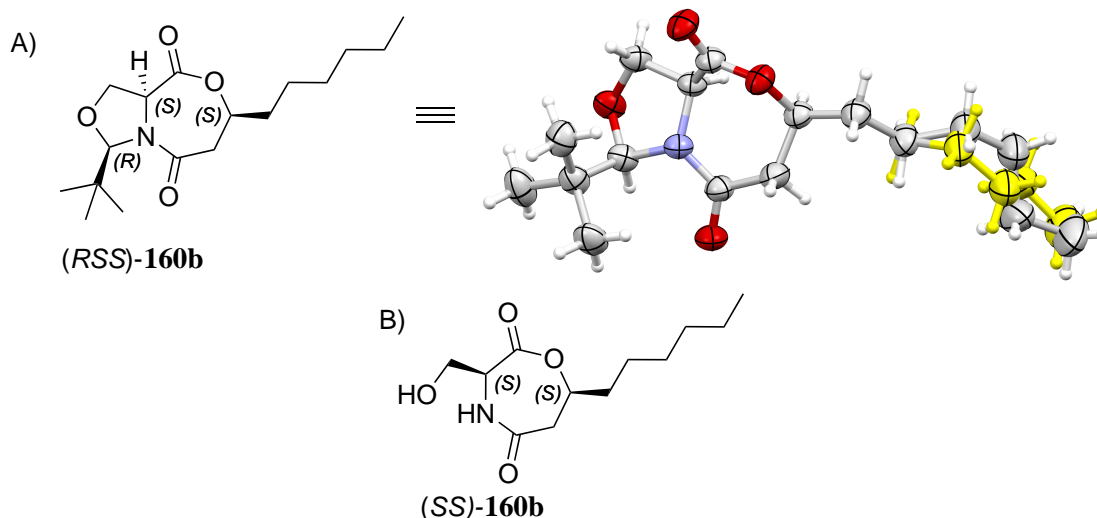


Figure 3.12. A) Molecular structure of (*RSS*)-**160b**, showing thermal displacement ellipsoids, drawn at the 30% probability level. The positional disorder of the C_6H_{13} -alkyl chain is shown in yellow. B) Stereochemistry of serratin ((*SS*)-**83**) based upon comparison with theoretical calculations of the ^{13}C NMR chemical shift.²⁴⁷

Both diastereomers showed quite different chemical shifts. The crystalline diastereomer (*RSS*)-**160b** has both its substituents in a *cis*-relationship. This *RSS*-diastereomer showed a signal for $CH-O$ at 75.2 ppm ($CDCl_3$) in the ^{13}C NMR spectrum and the attached hydrogen atom $CH-O$ showed a multiplet at 4.71-4.83 ppm ($CDCl_3$) in the 1H NMR spectrum. For the other diastereomer (*RRS*)-**160b**, with a *RRS*-stereochemistry, the corresponding signals were at 79.7 ppm ($CDCl_3$, ^{13}C NMR) and 4.68-4.79 ppm ($CDCl_3$, 1H NMR). The signal around 70 ppm in the ^{13}C NMR spectrum is quite characteristic and is present in all 1,4-oxazepane-2,5-diones described in literature (Figure 3.13 and Table 3.10).^{247,258,266–268,299,334,335} Another difference was the shift of the CH_2 adjacent to the $CH-O$ moiety. For diastereomer (*RSS*)-**160b** the corresponding signals were a dd at 2.85 ppm ($CDCl_3$) and a dd at 2.97 ppm ($CDCl_3$), whereas for the other diastereomer (*RRS*)-**160b** a d at 2.72 ppm ($CDCl_3$) and a dd at 3.14 ppm ($CDCl_3$) were observed. For serratin (**83**), Luna *et al.* noticed signals for the CH_2 at 2.42 ppm (dd, $CDCl_3$) and 2.62 ppm (dd, $CDCl_3$) and a signal for $CH-O$ at 72.4 ppm ($CDCl_3$) in the ^{13}C NMR spectrum.²⁴⁷ These values seem to be consistent with our observations for diastereomer (*RSS*)-**160b**.

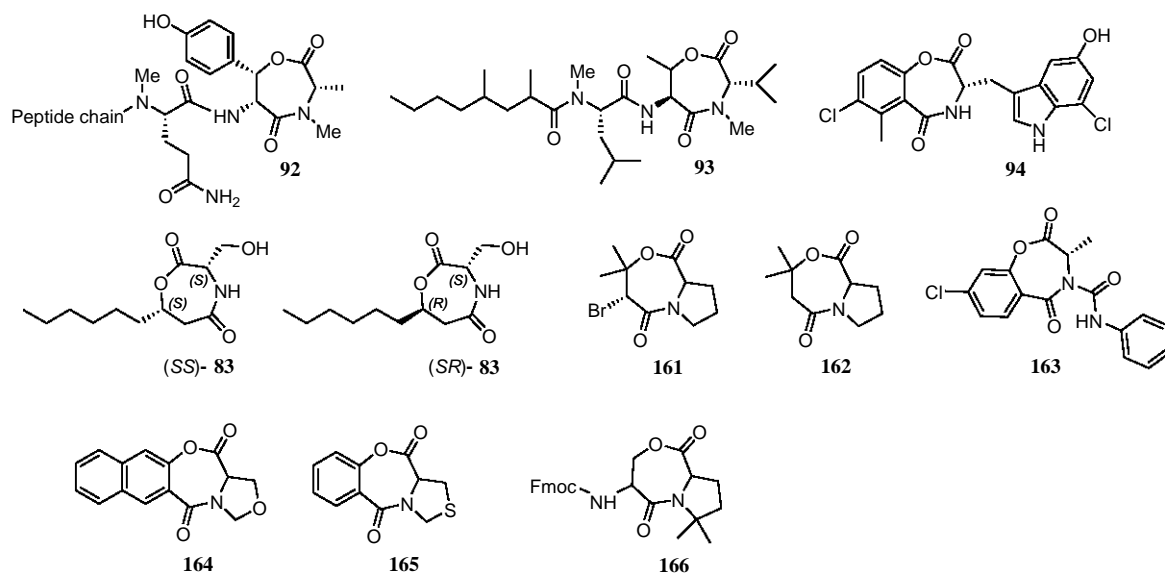


Figure 3.13. 1,4-Oxazepane-2,5-diones described in literature.^{247,258,266–268,299,334,335}

Table 3.10: Spectral data of 1,4-oxazepane-2,5-diones described in literature. NA: not applicable, NM: not mentioned.^{247,258,266–268,299,334,335}

Structure (NMR solvent)	B		C		E	F		G	
	δ_C	δ_H	δ_C	δ_C	δ_C	δ_H	δ_C	δ_H	δ_C
Callipeltin L (92) (CD ₃ OD) ²⁶⁶	169.4	3.92	56.6	164.8	4.35	60.3	6.17	77.7	
93 (CDCl ₃) ²⁶⁷	166.2	3.59	68.4	163.2	3.87	59.7	5.25	72.6	
Inducamide C (94) ((CD ₃) ₂ SO) ²⁶⁸	170.8	4.3	59.2	164.1	NA	NA	NA	NA	
Serratin 83 (CDCl ₃) ²⁴⁷	169.4	4.65	54.4	169.2	2.42 and 2.62	40.5	5.3	72.4	
Serratin 83 (SR Theoretical) ²⁴⁷	165.7	NM	57.3	174.5	NM	45.4	NM	79.1	
Serratin 83 (SS Theoretical) ²⁴⁷	167.7	NM	53.5	167.8	NM	44.9	NM	73.8	
161 (CDCl ₃) ³³⁴	NM	4.47	NM	NM	4.98	NM	NA	NM	
162 (CDCl ₃) ³³⁴	NM	4.46	NM	NM	2.56 and 3.20	NM	NA	NM	
163 ((CD ₃) ₂ CO) ²⁹⁹	167.8	5.57	53.4	160.4	NA	NA	NA	NA	
164 (CDCl ₃) ²⁵⁸	NM	4.82	NM	NM	NA	NM	NA	NM	
165 (CDCl ₃) ²⁵⁸	NM	4.46	NM	NM	NA	NM	NA	NM	
166 (CDCl ₃) ³³⁵	162.7	4.19	58.8	170.0	4.28	54.8	4.38 and 4.8	70.5	

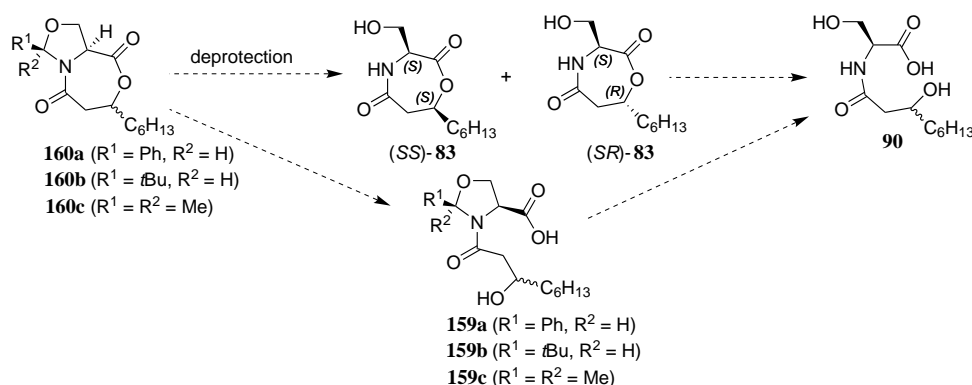
As the 2-*t*Bu-oxazolidine is a rather stable type of oxazolidine, it was decided to synthesize two different types of oxazolidines as well. The first type was the more labile 2,2-dimethyloxazolidine (Ser($\Psi^{\text{Me,Me}}$ Pro)), which undergoes rapid deprotection in dilute TFA.³²⁵ Unlike the Ser(Ψ^{tBu} Pro) **157b**, this type of oxazolidine cannot be isolated as such and is commonly introduced via the post-insertion route (Scheme 3.32, route B). Therefore, methyl *N*-(3-hydroxynonanoyl)-serinate **89** was reacted with 2,2-dimethoxypropane (DMP) with continuous removal of water to yield compound **158c** (Scheme 3.33).³³⁶ As ¹H NMR analysis revealed that this *N*-acylated

oxazolidine **158c**, obtained after column chromatography, was less pure than the crude compound after work-up because of degradation during purification, it was decided to proceed with the reaction sequence without further purification. Hydrolysis of compound **158c** with NaOH in a water:methanol (ratio 1:3) mixture, followed by cyclization gave 2,2-dimethyloxazolidine protected oxazepane-2,5-dione **160c** in a total yield of 18% after purification. Once again, the CH-O and CH₂ of both diastereomers gave distinct signals in NMR spectroscopy.

For the 2-phenyloxazolidine derivative, L-serine methyl ester hydrochloride **88** was neutralized with Et₃N and allowed to react with benzaldehyde **112** to produce oxazolidine derivative **157a** (Scheme 3.33).³³⁷ This compound was *N*-acylated with β -hydroxynonanoic acid **58d** and the ester functionality was hydrolyzed under alkaline conditions to furnish compound **159a**. The 2-phenyloxazolidine protected oxazepane-2,5-dione **160a** was obtained in 53% total isolated yield after the DMAP-catalyzed cyclization under dilute reaction conditions (Scheme 3.33).

Several reaction conditions were evaluated to deprotect the oxazolidine unit without opening the seven-membered lactone (Table 3.12). A catalytic amount of bismuth(III) bromide was successfully employed by Cong *et al.* to deprotect a cyclic *N,O*-aminal under mild reaction conditions.³³⁸ However for substrates **160a–c**, no reaction was observed (Table 3.12, entries 1A–C). This could be explained by the fact that the reactivity of the oxazolidine ring is dramatically reduced upon amidation.³³⁹ When a catalytic amount of water was added to the reaction mixture, the 2-phenyloxazolidine moiety of the *trans*-diastereomer (*RRS*)-**160a** was deprotected to the ring-opened structure **90** (Table 3.12, entry 2B). As traces of the ring-opened, oxazolidine-containing, product **159a** were detected during the course of the reaction, unlike the deprotected compound **83**, hydrolysis probably preceded deprotection. The other diastereomer (*RSS*)-**160a** could be recovered from the crude reaction mixture, albeit in a severely reduced amount. For the two other types of oxazolidines, all stereoisomers seemed to react at a similar rate and only the deprotected and hydrolyzed product **90** was isolated (Table 3.12, entries 2A and C). In an alternative procedure, mild acidic conditions for deprotection were used by employing formic acid in a THF:H₂O-mixture (Table 3.12, entries 3A and B).³⁴⁰ In the case of the *t*Bu-containing oxazolidine **160b**, a quick hydrolysis of both diastereomers to **159b** was observed. Interestingly, for the 2-phenyloxazolidine **160a** the *trans*-diastereomer (*RRS*)-**160a** hydrolyzed significantly faster than the *cis*-diastereomer (*RSS*)-**160a**: whereas the starting compound had a d.r. of 1:1, this changed to 1:2.7 for the recovered starting material. Treatment with an acidic resin also failed to deliver the desired compound (Table 3.12, entries 4A and B).³⁴¹ 5% TFA in dichloromethane left the 2-*t*Bu-oxazolidine **160b** intact, even after a reaction time of 48 h (Table 3.12, entry 5A).³²³ Under the same conditions, the *trans*-diastereomer of the 2,2-dimethyloxazolidine **160c**

was successfully deprotected (Table 3.12, entry 5C). The ^1H NMR of the crude reaction mixture, obtained after washing with a saturated aqueous NaHCO_3 -solution to remove the TFA and the ring-opened product, revealed the presence of only the *cis*-diastereomer. The deprotected *trans*-isomer (*SR*)-**83** however was not detected. When the same treatment was applied on the 2-phenyloxazolidine-protected seven-membered ring **160a** a similar observation was made: the *trans*-diastereomer (*RRS*)-**160a** seemed to react faster, but none of the deprotected serratin (**83**) could be isolated (Table 3.12, entry 5B and Figure 3.14). When 4M of HCl (g) in dioxane was evaluated for the removal of the oxazolidine moiety,³²³ a difference in reactivity was observed between the 2-*t*Bu- and the 2-phenyloxazolidine moiety: in the case of the *t*Bu-compound **160b**, the *cis*-diastereomer (*RSS*)-**160b** was deprotected faster whereas for the latter compound **160a**, the *trans*-diastereomer (*RRS*)-**160a** was deprotected faster. In both cases none of the deprotected seven-membered ring **83** could be isolated (Table 3.12, entries 6A and B). When the reaction time was prolonged, all of the starting material was converted to the deprotected, hydrolyzed compound **90**. The protocol with 1,3-propanedithiol in acidic trifluoroethanol, *i.e.* containing 2% HCl, developed by Corey,³⁴² also caused a faster deprotection of the *trans*-diastereomer of both the *t*Bu- and the 2-phenyloxazolidine compared to the *cis*-isomers. Once again, no deprotected serratin (**83**) could be isolated.

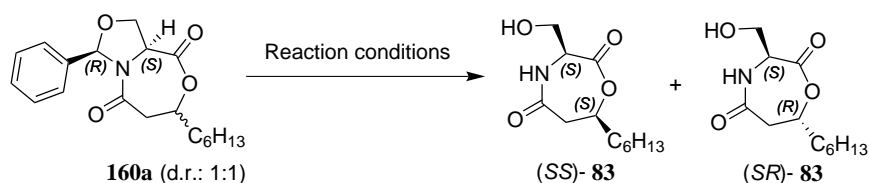
Table 3.12: Reaction conditions evaluated to achieve the deprotection of the different oxazolidine moieties of seven-membered rings **160a**, **160b** and **160c**.^{328,338,340–342}

Entry	Reaction conditions	Ψ Pro derivative	Result ^[a]
1A	0.1 equiv BiBr ₃ , CH ₃ CN, r.t., 1 h to o.n. ³³⁸	<i>t</i> Bu	- ^[b]
1B	Idem	Ph	- ^[b]
1C	Idem	DiMe	- ^[b]
2A	1 equiv BiBr ₃ , cat. H ₂ O, CH ₃ CN, r.t., 1 h to 48 h	<i>t</i> Bu	- ^[c]
2B	Idem	Ph	Conversion of <i>trans</i> -diastereomer (<i>RRS</i>)- 160a to 90 . No isolation of (<i>SR</i>)- 83 . Slower reaction of <i>cis</i> -diastereomer (<i>RSS</i>)- 160a .
2C	Idem	DiMe	- ^[c]
3A	THF:H ₂ O:HCOOH 3:1:1, r.t., 1 h to 48 h ³⁴⁰	<i>t</i> Bu	Ring-opening to 159b
3B	Idem	Ph	Ring-opening to 159a ; <i>trans</i> -diastereomer (<i>RRS</i>)- 160a reacts faster than (<i>RSS</i>)- 160a
4A	Amberlyst 15, acetone:H ₂ O 9:1, r.t., 1 h to 24 h ³⁴¹	<i>t</i> Bu	- ^[b]
4B	Idem	Ph	- ^[b]
5A	5% TFA in dry CH ₂ Cl ₂ , 0 °C, 3 h, then r.t., 48 h ³²⁸	<i>t</i> Bu	- ^[b]
5B	Idem	Ph	No reaction of <i>cis</i> -diastereomer (<i>RSS</i>)- 160a ; deprotection of <i>trans</i> -diastereomer (<i>RRS</i>)- 160a to 90
5C	Idem	DiMe	No reaction of <i>cis</i> -diastereomer (<i>SS</i>)- 160c ; deprotection of <i>trans</i> -diastereomer (<i>RS</i>)- 160c to 90
6A	4M HCl in dioxane, 0 °C to r.t., 1 h to 24 h ³²⁸	<i>t</i> Bu	Formation of 90 ; faster reaction of the <i>cis</i> -diastereomer (<i>RSS</i>)- 160b
6B	Idem	Ph	Formation of 90 ; faster reaction of the <i>trans</i> -diastereomer (<i>RRS</i>)- 160a
7A	3 equiv 1,3-propanedithiol, 2% HCl in 2,2,2-trifluoroethanol, r.t., 1 h to 24 h ³⁴²	<i>t</i> Bu	Formation of 90 ; faster reaction of the <i>trans</i> -diastereomer (<i>RRS</i>)- 160b
7B	Idem	Ph	Formation of 90 ; faster reaction of the <i>trans</i> -diastereomer (<i>RRS</i>)- 160a

[a] Based on LC-MS analysis during the course of the reaction and ¹H NMR analysis of the crude reaction mixture after work-up. [b] No reaction. [c] Deprotection and ring-opening or ring-opening and deprotection. Only recovery of **90**.

As deprotection was observed but isolation of serratin (**83**) failed, either because of deprotection followed by immediate ring-opening or by first ring-opening and then deprotection, another route for the 2-phenyloxazolidine **160a** was evaluated. In a first attempt to remove the 2-phenyloxazolidine unit from **160a**, hydrogenolysis with Pd/C in ethyl acetate and in methanol was evaluated, but no reaction (Table 3.13, entry 1) or only a limited conversion, combined with degradation (Table 3.13, entry 2), were obtained. When Pd(OH)₂/C was employed in ethanol, a complete debenzoylation was observed, unfortunately combined with ethanolysis of the deprotected product (Table 3.13, entry 3). When the reaction was repeated in ethyl acetate, deprotection without solvolysis was observed (Table 3.13, entry 4). Remarkably, both diastereomers behaved differently: only the seven-membered ring (*SS*)-**83** with both substituents in a *cis*-relationship was obtained and isolated in 22% yield (based on the total amount of starting material). The diastereomeric ratio of the recovered, oxazolidine-containing starting material **160a** had consequently changed from 1:1 to 1:3, favoring the (*RRS*)-diastereomer (Figure 3.14). This observed selectivity for (*RSS*)-**160a** could be explained by steric factors. The (*RSS*)-isomer of **160a** has the phenyl and alkyl substituent on the same side of the bicyclic ring system (see Figure 3.12 for (*RSS*)-**160b**), allowing a relatively unhindered interaction of the opposed side with the palladium catalyst. As the (*RRS*)-isomer has the bulky phenyl substituent on one side and the alkyl substituent on the other side, it is expected that such an interaction with the catalyst proceeds with more difficulty.

Table 3.13: Reaction conditions evaluated for the removal of the 2-phenyloxazolidine moiety of **160a**.



Entry	Reaction conditions	Result
1	4 atm H ₂ , 25 wt% Pd/C, EtOAc, r.t., o.n.	– ^[a]
2	4 atm H ₂ , 25 wt% Pd/C, MeOH, r.t., o.n.	– ^[b]
3	4 atm H ₂ , 25 wt% Pd(OH) ₂ /C, EtOH, r.t., o.n.	– ^[c]
4	1 atm H ₂ , 50 wt% Pd(OH) ₂ /C, EtOAc, r.t., 6 h	(<i>SS</i>)- 83 (22%). No reaction of the other diastereomer; recovery of starting material 160a (67%) with a d.r. of 1:3

[a] No reaction. [b] Solvolysis of starting material **160a**. [c] Deprotection and solvolysis or solvolysis and deprotection.

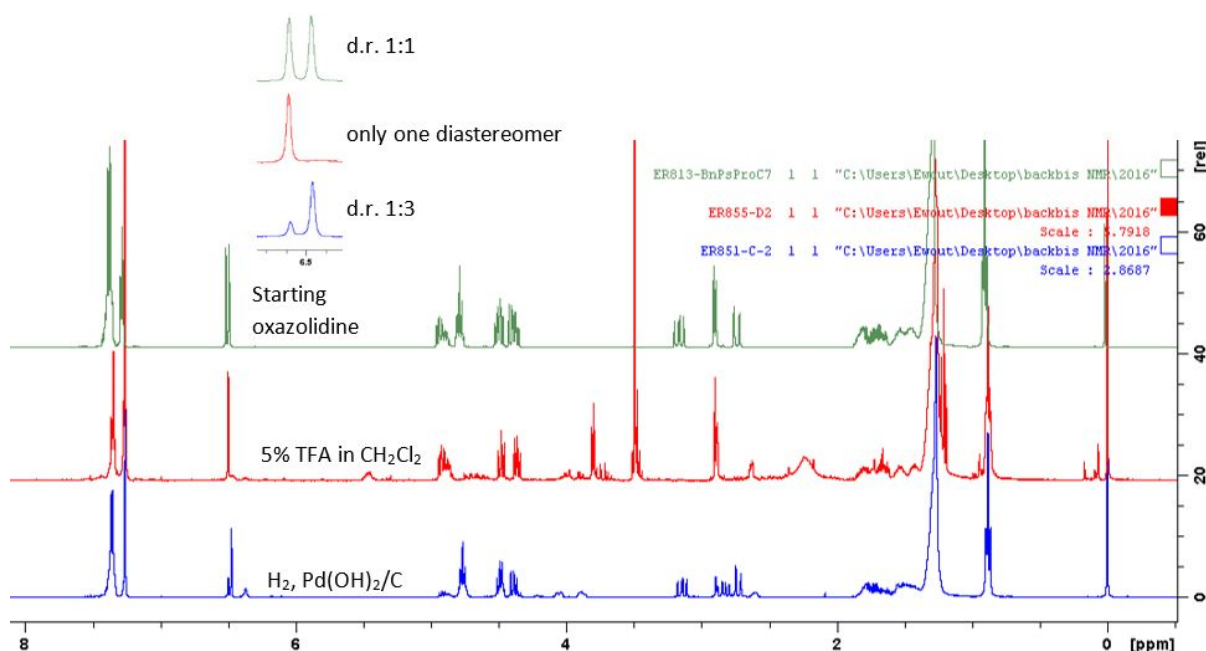


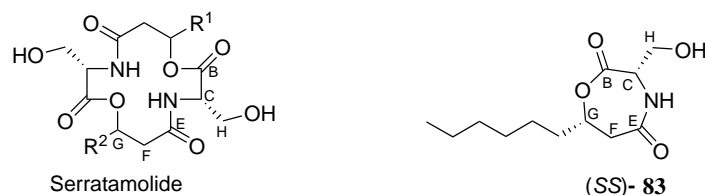
Figure 3.14. Overlay of the ^1H NMR spectra of 2-phenyloxazolidine protected compound **160a** (in CDCl_3) and the crude ^1H NMR spectra (in CDCl_3) of the same compound **160a** recovered after treatment with 5% TFA in CH_2Cl_2 or H_2 gas and $\text{Pd}(\text{OH})_2/\text{C}$ in EtOAc.

The (*RSS*)-diastereomer that was deprotected, however, had the correct stereochemistry to deliver serratin (*SS*)-**83**. In the ^1H NMR spectrum (CDCl_3), a signal for *NH* became visible, which is consistent with a successful deprotection. The *CH-O*-signal at 73.7 ppm (CDCl_3) was also present, indicating that the seven-membered heterocycle was still intact. However, unlike the value around 5.30 ppm (CDCl_3) reported by Luna *et al.* for *CH-O*, a multiplet around 4.73–4.81 ppm (CDCl_3) was observed. A big difference for the adjacent *CH*₂ was also apparent: whereas Luna *et al.* reported two dd at 2.42 and 2.62 ppm (CDCl_3), we detected the corresponding signals at 2.79 and 2.87 ppm (CDCl_3).

The values reported by Luna *et al.* show a lot of similarities with the spectral data of the compound serratamolide A (**42a**) (Table 3.14). This antimycobacterial cyclodepsipeptide is produced by *Serratia* sp. and has the *CH-O* signal at 5.33 ppm (^1H NMR, CD_3OD), the *CH-O* signal at 73.2 ppm (^{13}C NMR, CD_3OD) and the adjacent *CH*₂ at 2.39 and 2.72 ppm (^1H NMR, CD_3OD).²⁴⁸ That the actual structure of serratin (**83**) could be a serratamolide analogue is also suggested by the observed vicinal coupling constants of the *O-CHCH*₂*C(=O)* moiety. Whereas for the compound synthesized in this study vicinal coupling constants of 11.3 Hz and 3.0 Hz were observed, which corresponds to a conformation as depicted in figure 3.12 with one large and one small dihedral angle of the coupling protons, values of 4.9 Hz and 2.0 Hz were reported by Luna *et al.*²⁴⁷ These small vicinal coupling constants were also reported for serratamolide A (**42a**) (5.0 Hz and 2.6 Hz), which correspond with a more flexible structure and smaller di-

hedral angles (Table 3.14).³⁴³ Serratamolide A (**42a**) is a symmetrical molecule composed of two serine units and two times β -hydroxydecanoic acid as the fatty acid moiety. However, the asymmetrical analogue serratamolide F (**42f**) has a β -hydroxydecanoic acid moiety but also a β -hydroxynonanoic acid moiety in its structure.²⁴⁸ It is known that during the biosynthesis of cyclic lipopeptides, a relaxed substrate specificity can give rise to the production of several analogues of one main cyclic lipopeptide compound.^{134,248} Therefore, if a symmetrical serratamolide exists with two β -hydroxynonanoic acid tails, the corresponding NMR spectra would contain only a limited number of signals with values nearly identical to those reported by Luna *et al.* for serratin (**83**) (Table 3.14).

Table 3.14: Comparison of the spectral data of serratamolide (**42**) and serratin (**83**).^{247,248,250,343,344}



42a A: R¹ = (CH₂)₆CH₃, R² = (CH₂)₆CH₃

42b B: R¹ = CH₂CH=CH(CH₂)₅CH₃, R² = (CH₂)₆CH₃

42c C: R¹ = (CH₂)₈CH₃, R² = (CH₂)₆CH₃

42d D: R¹ = (CH₂)₇CH₃, R² = (CH₂)₆CH₃

42e E: R¹ = (CH₂)₄CH₃, R² = (CH₂)₆CH₃

42f F: R¹ = (CH₂)₅CH₃, R² = (CH₂)₆CH₃

Structure (NMR solvent)	B		C		E	F		G		H	
	δ_C	δ_H	δ_C	δ_C	δ_C	δ_H	δ_C	δ_H	δ_C	δ_H	δ_C
Serratamolide A (42a) (CD ₃ OD) ³⁴³	NM	4.49 (t, <i>J</i> = 3.6 Hz)	NM	NM	NM	2.34 (dd, <i>J</i> = 13.6 Hz, 2.6 Hz) and 2.68 (dd, <i>J</i> = 13.6 Hz, 5.0 Hz)	NM	5.39 (m)	NM	3.82 (dd, <i>J</i> = 10.8 Hz, 3.3 Hz) and 4.08 (dd, <i>J</i> = 10.8 Hz, 3.8 Hz)	NM
Serratamolide A (42a) (CD ₃ OD) ²⁵⁰	NM	4.47 (m)	NM	NM	NM	2.33 (dd) and 2.67 (dd)	NM	5.28 (m)	NM	3.82 (dd) and 4.07 (dd)	NM
Serratamolide A (42a) (CD ₃ OD) ²⁴⁸	171.3	4.53 (dd, <i>J</i> = 3.8 Hz, 3.2 Hz)	56.3	172.0	172.0	2.39 (dd, <i>J</i> = 13.5 Hz, 2.7 Hz) and 2.72 (dd, <i>J</i> = 13.5 Hz, 4.9 Hz)	41.2	5.33 (m)	73.2	3.87 (dd, <i>J</i> = 10.8 Hz, 3.2 Hz) and 4.11 (dd, <i>J</i> = 10.8 Hz, 3.8 Hz)	63.2
Serratamolide B (42b), C10:0 alkyl chain (CD ₃ OD) ²⁴⁸	171.3	4.52 (dd, <i>J</i> = 3.9 Hz, 3.4 Hz)	56.4	171.8	171.8	2.40 (dd, <i>J</i> = 13.6 Hz, 2.9 Hz) and 2.73 (dd, <i>J</i> = 13.6 Hz, 4.8 Hz)	41.2	5.33 (m)	73.2	3.87 (dd, <i>J</i> = 10.8 Hz, 3.4 Hz) and 4.11 (dd, <i>J</i> = 10.8 Hz, 3.9 Hz)	63.1
Serratamolide B (42b), C12:1 alkyl chain (CD ₃ OD) ²⁴⁸	171.0	4.53 (dd, <i>J</i> = 4.1 Hz, 3.4 Hz)	56.4	172.0	172.0	2.44 (dd, <i>J</i> = 13.6 Hz, 2.9 Hz) and 2.70 (dd, <i>J</i> = 13.6 Hz, 4.8 Hz)	40.4	5.24 (m)	73.1	3.87 (dd, <i>J</i> = 10.8 Hz, 3.4 Hz) and 4.08 (dd, <i>J</i> = 10.8 Hz, 4.1 Hz)	63.1
Serratamolide A (42a) (CDCl ₃) ³⁴⁴	169.6	4.40 (m)	54.6	169.4	169.4	2.30 (d) and 2.55 (d)	40.4	5.20 (m)	72.4	3.70 (m) and 4.05 (m)	63.0
Serratin (83) (CDCl ₃) reported by Luna <i>et al.</i> ²⁴⁷	169.4	4.65 (dt, <i>J</i> = 8.1 Hz, 2.8 Hz)	54.4	169.2	169.2	2.42 (dd, <i>J</i> = 14.1 Hz, 2.0 Hz) and 2.62 (dd, <i>J</i> = 14.1 Hz, 4.9 Hz)	40.5	5.30 (m)	72.4	3.85 (d, <i>J</i> = 8.8 Hz) and 4.22 (d, <i>J</i> = 8.8 Hz)	63.4
Serratin (83) (CDCl ₃) reported in this study	171.6	4.49 (m)	52.8	169.5	169.5	2.79 (dd, <i>J</i> = 18.7 Hz, 3.0 Hz) and 2.87 (dd, <i>J</i> = 18.6 Hz, 11.3 Hz)	41.7	4.77 (m)	73.7	3.89 (ddd, <i>J</i> = 12.3 Hz, 8.3 Hz, 4.3 Hz) and 4.06 (ddd, <i>J</i> = 12.0 Hz, 5.0 Hz, 5.0 Hz)	61.1

3.2.10 Conclusion

In this chapter, the evaluation of HO-AHLs **2** in an intramolecular rearrangement leading to 1,4-oxazepane-2,5-diones, resembling the rearrangement of oxo-AHLs **3** to tetramic acids **11**, was performed. One compound, serratin (**83**), with such a structure, has been isolated from a bacterial culture broth, hinting the possibility of such a rearrangement. However, both HO-AHLs **2** as *N*-(3-hydroxynonanoyl)-L-serine (**90**) refused to participate in such a cyclization. As analogues with a third *N*-substituent cyclized readily, it was concluded that the preference of a secondary carboxylic amide for a *trans*-conformation hinders such reactivity for HO-AHLs **2**, pointing out the unlikeliness that such a spontaneous rearrangement of a *N*-mono- or disubstituted compound could lie at the origin of serratin (**83**).

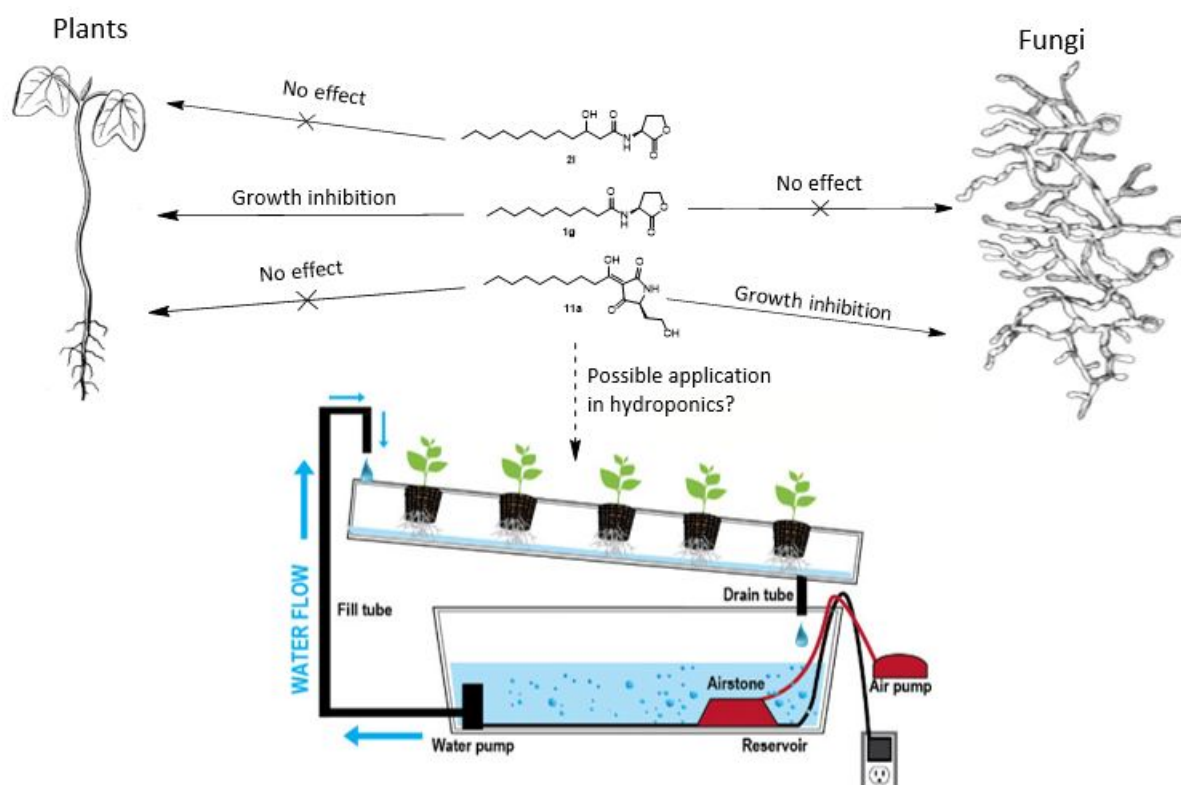
As several natural products containing a 1,4-oxazepane-2,5-dione-core are known, and few methods have been described to synthesize this type of compounds, a method for the synthesis of such 1,4-oxazepane-2,5-diones was developed. Because of the presence of an amide, which has a preference for a *trans*-conformation, and the presence of a labile lactone moiety in this core, many synthetic methodologies commonly used for the cyclization toward medium-sized heterocycles cannot be applied. Therefore, several *N*-protecting groups were tested and PMB was applied as a protecting group to force the linear amino acid precursor in a correct conformation for cyclization to occur. Via the application of pseudo-prolines as another type of protecting group for serine derivatives, a compound with the presumed structure of the natural product serratin (**83**) was obtained. As a result of the differences in spectral data, the incorrect structural assignment of the natural product serratin (**83**) was identified. Instead of the alleged seven-membered heterocycle, a symmetrical serratamolide **42** analogue is proposed to be the correct structure of serratin.

3.3 The influence of quorum sensing signal molecules on plants and fungi

Abstract

Pseudomonas sp. CMR12a is a strain which could potentially be applied as a biocontrol agent against the cocoyam root rot disease caused by *Pythium myriotylum*. To better understand the role of QS in the biocontrol activity of this strain, the influence of one of its QS signal molecules, HO12, on plant growth was studied. The influence of this compound on two plant species, lettuce (*Lactuca sativa*) and *Arabidopsis thaliana*, was evaluated but no direct effects were observed. The bioactivity of a degradation product of oxo-AHLs, a tetramic acid, was evaluated as well. Neither plant growth stimulating nor inhibiting effects were observed, but a significant growth reduction of the agriculturally relevant plant pathogen *Rhizoctonia solani* was observed. As tetramic acids display algicidal effects as well, these compounds might have the potential to be used as an algicide or fungicide or a combination of both in hydroponics.

Graphical abstract



Keywords

AHL, quorum sensing, AHL-plant interactions, biocontrol, tetramic acid, fungi

3.3.1 Introduction

The production of bioactive metabolites has attracted scientific interest in order to use microorganisms as biocontrol agents. In this approach an organism is applied that exerts an antagonistic effect on an agricultural plague. As fungicides are often not sufficiently effective anymore due to resistance development and both an economically non-viable and environmentally unfriendly option, the use of a biocontrol agent could often form a sustainable alternative.³⁴⁵ The production of many secondary metabolites is regulated by QS. Some of these metabolites are required for biofilm formation whereas other exert antimicrobial effects. Not surprisingly, a mutation of the QS system often gives rise to mutants which are impaired in bioactivity and habitat colonization.³⁴⁶ Therefore, if one wants to apply a microorganism as a biocontrol agent, a thorough understanding of the (QS) regulation of its secondary metabolite production is required.

In an attempt to find a biocontrol agent against the cocoyam root rot disease, several fluorescent *Pseudomonas* ssp., characterized by the production of fluorescent green-yellow siderophores called pyoverdins, were isolated from the rhizospheres of healthy cocoyam plants (*Xanthosoma sagittifolium*) (Figure 3.15) in Cameroon and evaluated as biocontrol agents.³⁴⁷ This tropical tuber crop is an important constituent of the human diet in (sub)tropical regions as the tubers are rich in carbohydrates and contain a substantial amount of essential amino acids, fats and vitamins.³⁴⁸ Of all existing cocoyam varieties, white cocoyam is the highest yielding and most tasteful, and therefore the preferred variety. However, this variety is also the most susceptible to the cocoyam root rot disease.³⁴⁷ This disease is caused by the oomycete *Pythium myriotylum* and can reduce the harvested tuber yield with more than 90%.³⁴⁹



Figure 3.15. Left: cocoyam (*Xanthosoma sagittifolium*) plant; right: harvested cocoyam tubers.³⁴⁸

Out of all the isolates, *Pseudomonas* sp. CMR12a proved to be an efficient *Py. myriotylum* antagonist. It was found that the biological activity of this strain was linked with the production of antifungal phenazines **167** and cyclic lipopeptide (CLP)-type biosurfactants **168** and **169** (Figure 3.16).³⁴⁷ Besides *Py. myriotylum*, *Pseudomonas* sp. CMR12a also succeeded in suppressing

root rot disease on bean (*Phaseolus vulgaris*) caused by *Rhizoctonia solani* AG 2-2 and AG 4-HGI as well as the damping-off disease caused by *R. solani* AG 2-1 on Chinese cabbage (*Brassica chinensis*).^{201,202}

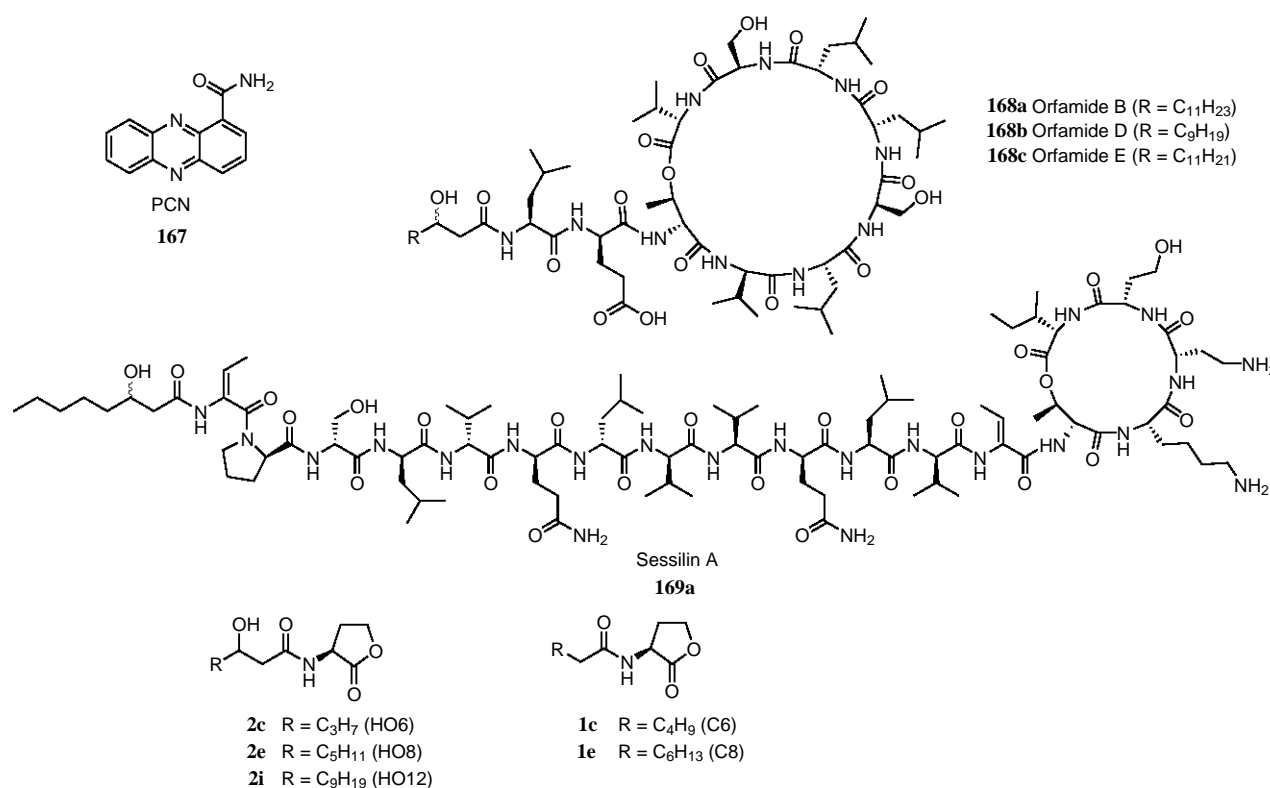


Figure 3.16. Secondary metabolites and QS signal molecules produced by *Pseudomonas* sp. CMR12a: phenazine-1-carboxamide (PCN) **167**, the CLPs orfamide B, D, E (**168a–c**) and sessilin A (**169a**), and the AHLs *N*-(3-hydroxyhexanoyl)-L-homoserine lactone (HO6) **2c**, *N*-hexanoyl-L-homoserine lactone (C6) **1c**, *N*-(3-hydroxyoctanoyl)-L-homoserine lactone (HO8) **2e**, *N*-octanoyl-L-homoserine lactone (C8) **1e** and *N*-(3-hydroxydodecanoyl)-L-homoserine lactone (HO12) **2i**.³⁵⁰

In previous research the antagonistic effect of *Pseudomonas* sp. CMR12a against the cocoyam root rot pathogen was ascribed to the phenazine and CLP-production of this strain.³⁴⁷ It was shown that phenazine production was QS regulated and a role of QS in CLP-production could not be excluded as well.³⁵⁰ A thorough understanding of the QS pathways could help to fine-tune the secondary metabolite production and strongly enhance the efficacy of *Pseudomonas* sp. CMR12a as a biocontrol agent. However, there was also a plant growth stimulatory effect of QS signal molecule HO12 **2i** observed. The two other HO-AHLs, HO6 **2c** and HO8 **2e** did not display such activity.^{351,352} Therefore, to fully assess the role of QS on the biocontrol activity of strain CMR12a, the effect of compound **2i** on plant growth was studied further.

3.3.2 Evaluating the effect of AHLs on the growth of lettuce

A lot of research has been carried out on the influence of AHLs on plants (see Literature overview). In most cases these studies are limited to the economically non-important plants *Arabidopsis thaliana* and *Medicago truncatula*. Most of these studies apply 10 μM of the AHL to evaluate the effects (Appendix, Table 8.1).^{54,68,70,73,74,79,83} In the supernatant of planktonic *P. aeruginosa* cultures, concentrations of 5-15 μM of oxo12 **3i** are detected.^{34,35} However, concentrations higher than 600 μM of oxo12 **3i** have been detected in *P. aeruginosa* biofilms, whereas outside the biofilm only nM concentration of AHLs were found.³⁴ In a 6 days old subtidal biofilm, concentrations exceeding 3000 μM of C12 **1i** were detected.³⁵³ These observations point out the strong spatial heterogeneity regarding AHL concentrations but as well the existence of AHL hotspots with local concentrations exceeding the micromolar range, making 10 μM a biologically relevant concentration. It was therefore decided to use a concentration of 10 μM as well.

In previous research, a root growth stimulating effect of 10 μM HO12 **2i** on lettuce (*Lactuca sativa*) was observed, whereas shorter-chain analogues HO6 **2c** and HO8 **2e** were inactive.^{351,352} Unsubstituted AHL C14 **1k** was added as well as the strongest growth influencing effect are associated with long-chain AHLs.⁵⁵ However, in an exploratory experiment, a huge growth difference between the control plates (MS plant agar medium with 0.01% ethanol) was observed, depending on the position in the growth chamber (Figure 3.17).



Figure 3.17. Two control plates with lettuce seedlings.

A second attempt with a more randomized distribution of the plates in the growth chamber revealed again a clear effect of the position in the growth chamber but no clear effect of the added compounds on root growth could be observed, even when comparing within the same line of the growth chamber (Figure 3.18 and 3.19).

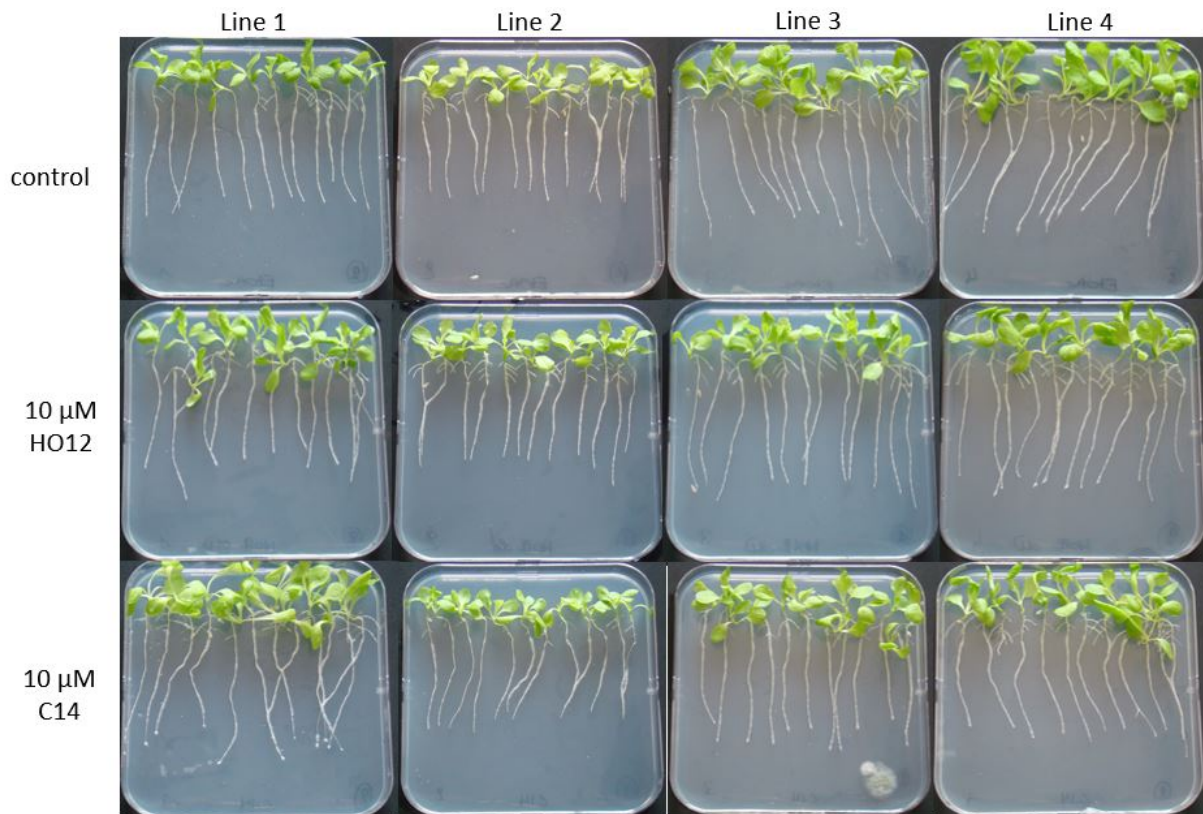


Figure 3.18. Effect of HO12 **2i** and C14 **1k** on the growth of lettuce seedlings.

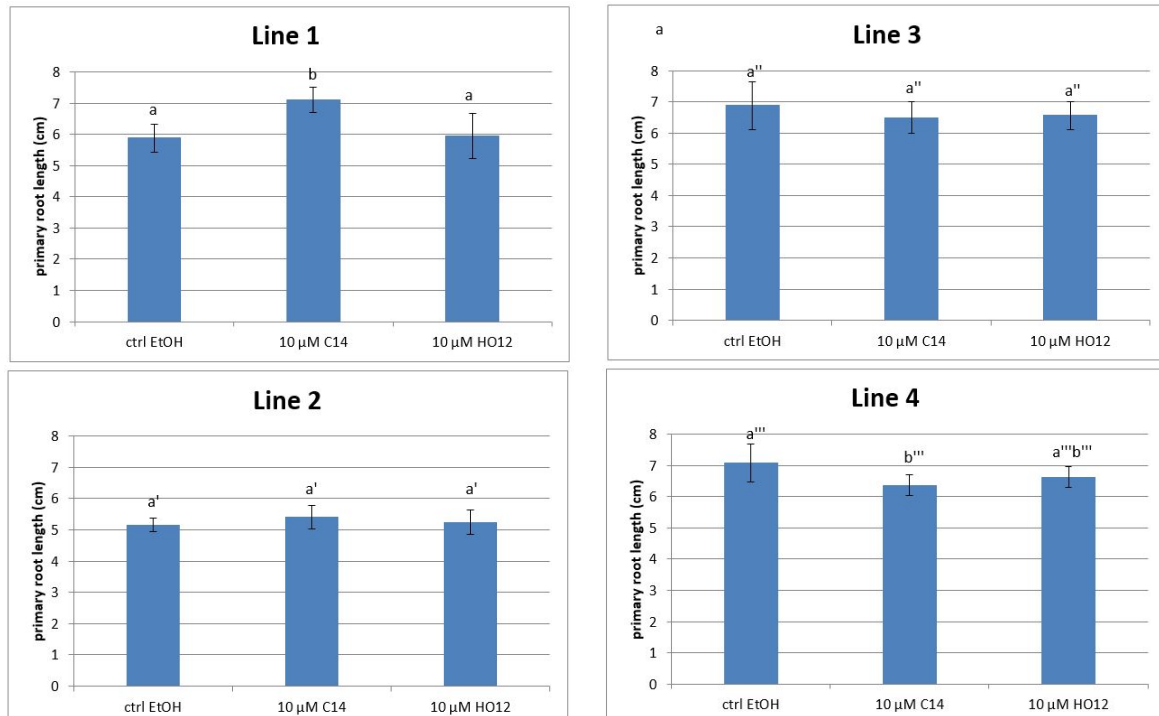


Figure 3.19. Measured primary root length of lettuce seedlings after exposure to C14 **1k** and HO12 **2i**. Represented values are the mean of twelve plants. Bars with a different letter are statistically different according to Tukey's *post-hoc* test ($p = 0.05$).

To exclude possible concentration effects, several concentrations of HO12 **2i** were tested but no

growth stimulating effect could be observed for the concentrations under study (Figure 3.20).

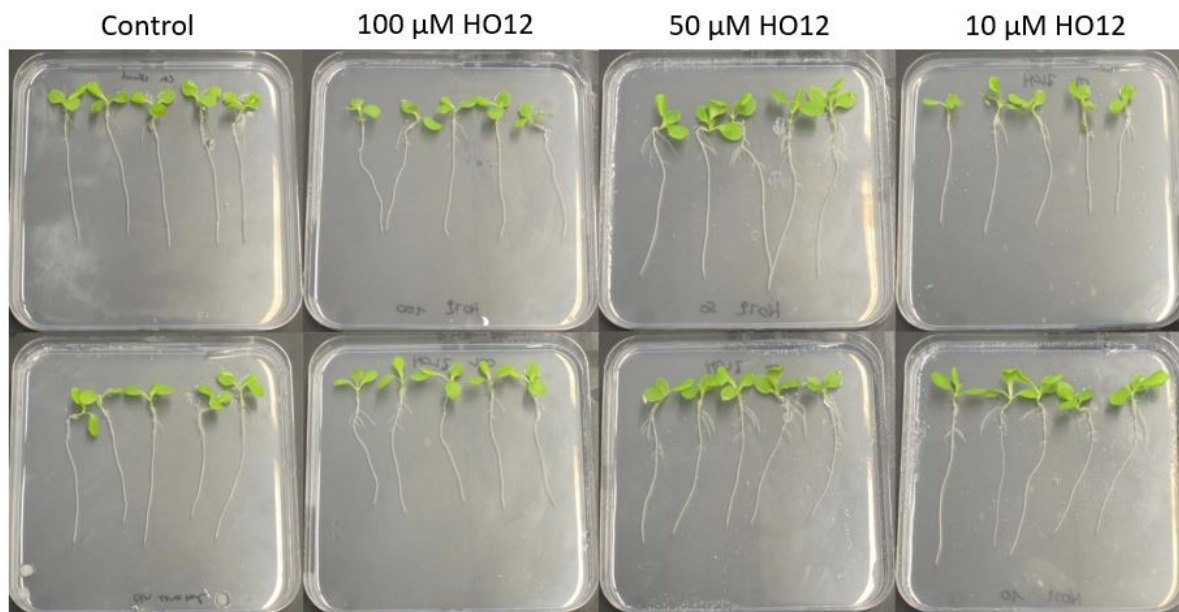


Figure 3.20. Effect of different HO12 **2i** concentrations on the growth of lettuce seedlings.

Due to the difficulties to control the interplate variability linked with the light incidence in the growth chamber and the apparent absence of growth influencing effects, this experimental set-up was abandoned and a switch to *A. thaliana*, which displays less variability, was made.

3.3.3 Evaluating the effect of AHLs and TA on the growth of *Arabidopsis thaliana*

As it is known that C10 **1g** inhibits root growth in *A. thaliana*,⁵⁴ this AHL **1g** was included as a negative control. Several plant-associated bacteria use oxo-AHLs **3** (e.g. *Pseudomonas syringae* pv. *syringae* produces oxo6 **3c** and oxo8 **3e**, *Agrobacterium tumefaciens* produces oxo8 **3e**, *Sinorhizobium meliloti* produces oxo14 **3k** and oxo16 **3m**).^{62,63} These oxo-AHLs **3** can rearrange to tetramic acids **11** (see Literature overview),^{9,42} suggesting these TA can occur in the rhizosphere. It is known that TA12 **11a** exhibits strong algicidal effects (Michail Syrpas, PhD thesis).³⁵⁴ Therefore, the tetramic acid **11a**, derived from the intramolecular rearrangement of oxo12 **3i** was tested as well (Figure 3.21).

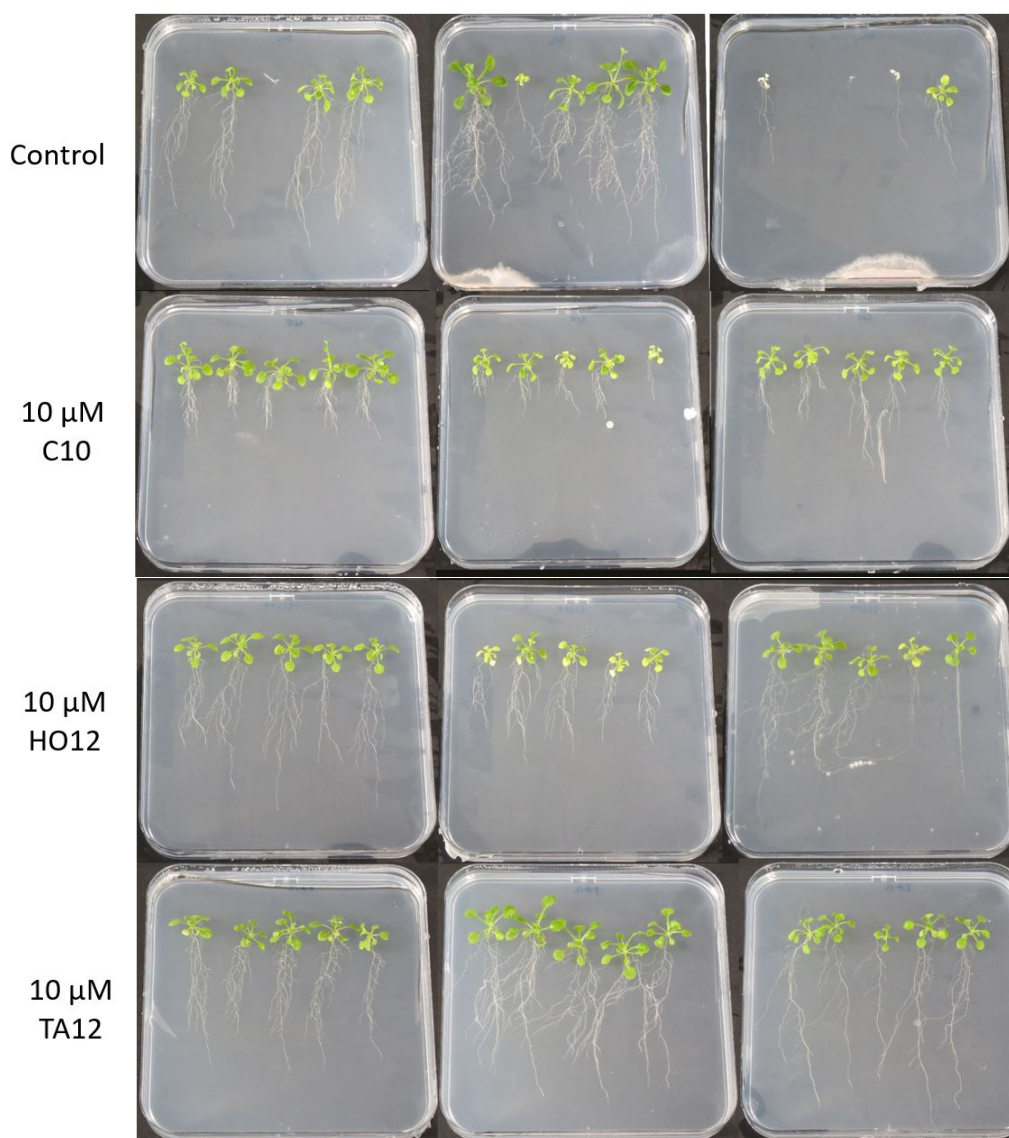


Figure 3.21. Effect of C10 **1g**, HO12 **2i** and TA12 **11a** on the growth of *A. thaliana* seedlings.

In this assay, no clear effect of the position in the growth chamber was observed. The primary root growth inhibitory effect of C10 **1g** on *A. thaliana* was confirmed.⁵⁴ However, no such inhibitory (or stimulatory) effect was observed for HO12 **2i**. Also TA12 **11a** did not display a growth inhibitory effect. As it is known that TA12 **11a** exhibits strong algicidal effects (Michail Syrpas, PhD thesis),³⁵⁴ this compound could be used in hydroponics.

However, when tetramic acid-containing fungal metabolite trichosetin (**170**) (Figure 3.22) was added to seedlings (3-27 μM), it inhibited root and shoot growth of the five plant species (*Vigna radiata*, *Lycopersicon esculentum*, *Oryza sativa*, *Medicago sativa* and *Capsicum frutescens*) evaluated.³⁵⁵ This inhibition was caused by damaging the cell membrane.³⁵⁵ On the other hand, 1-10 μM harzianic acid (**171**) (Figure 3.22), a secondary metabolite produced by *Trichoderma*, promotes the growth of tomato seedlings (*Solanum lycopersicum* cv. Roma) presumably due to its iron-binding activity.^{356,357} No such growth promotion of tomato seedlings

was observed using a concentration of 100 μM harzianic acid (**171**), although a higher germination percentage was observed for the treated tomato seeds.^{356,357} The growth of canola (*Brassica napus*) seedlings was inhibited by high (10-100 μg per seed) harzianic acid (**171**) concentrations whereas low (1, 10 and 100 ng harzianic acid (**171**) per seed) doses stimulated the growth of the seedlings, stressing the importance of the applied concentration of a compound.³⁵⁸ Therefore, to fully understand the bioactivity of TA12 **11a** a dose-response study should be performed.

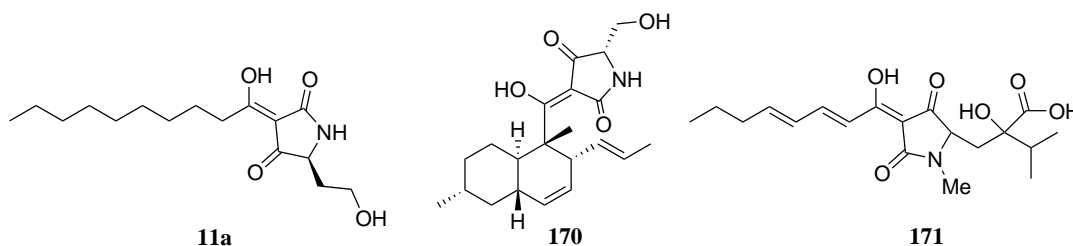


Figure 3.22. Chemical structure of bacterial TA12 **11a**, used in this study, and fungal tetramic acids trichosetin (**170**) and harzianic acid (**171**).

3.3.4 Evaluating the effect of AHLs and TA on the growth of fungi

Several natural products containing a tetramic acid core display antifungal activity.³⁵⁹ It was also shown by Hogan *et al.* that oxo12 **3i** influences the morphology of the yeast *Candida albicans* at concentrations of 200 μM . This could be caused by the formation of TA12 **11a** but is less likely as the unsubstituted AHL C12 **1i** had a similar effect.³⁶⁰ Therefore, to further explore the potential of TA12 **11a**, the effect of this compound on two agriculturally relevant plant pathogenic fungi, *Botrytis cinerea* and *Rhizoctonia solani*, was tested. As the minimum inhibitory concentration of TA12 **11a** on the diatom *Phaeodactylum tricornerutum* was between 20 and 50 μM (Michail Syrpas, PhD thesis),³⁵⁴ 50 μM was selected to test the effect of TA12 **11a** on these economically relevant fungi. Whereas no significant effect was observed on *B. cinerea*, up to 13% growth reduction was observed when tested on the soil-borne pathogen *R. solani* (Figure 3.23). Previously, bactericidal activity was already reported for this compound **11a**.^{9,41}

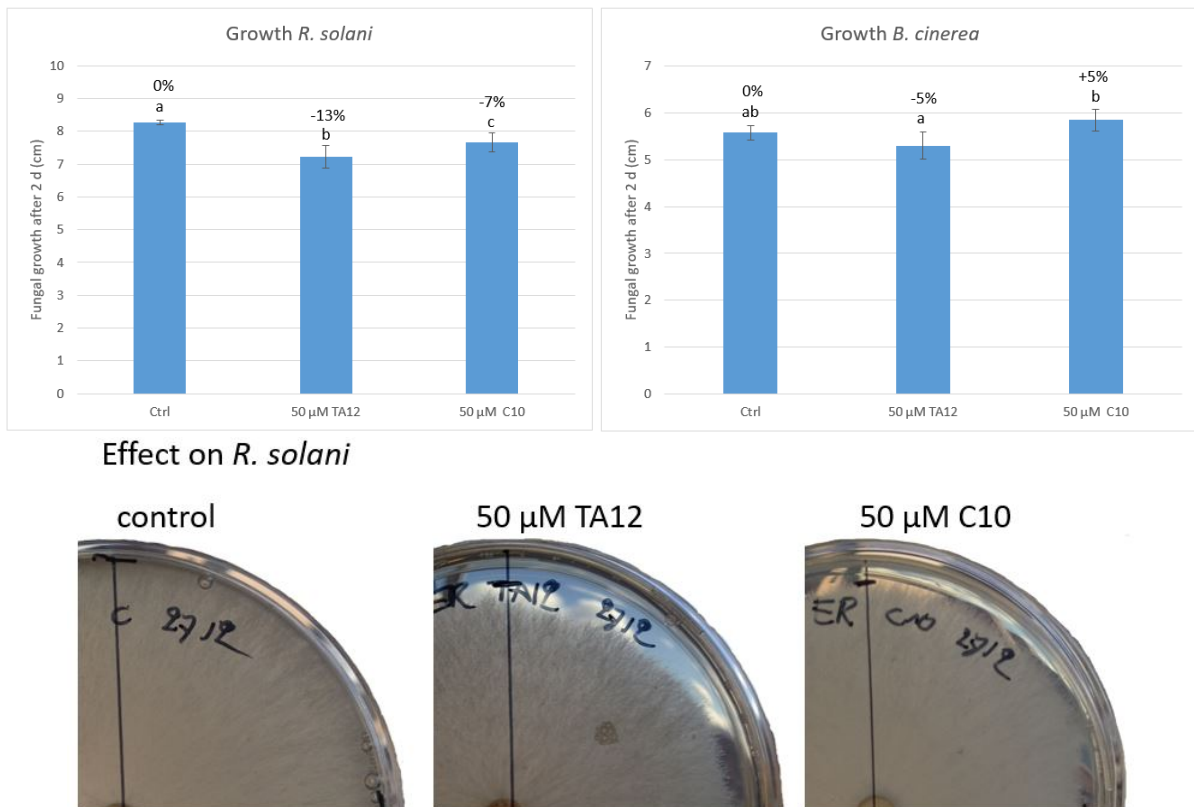


Figure 3.23. Top: Effect of TA12 **11a** and C10 **1g** on the growth of fungi *B. cinerea* and *R. solani*. Represented values are the mean of eight repetitions. Bars with a different letter are statistically different according to Tukey's *post-hoc* test ($p = 0.05$). Bottom: Photographs of the mycelium of *R. solani* obtained after the different treatments.

3.3.5 Conclusions

In this part, the effect of QS molecules and a TA on the growth of plants and fungi was assessed. Because of the high variability associated with the assay utilizing lettuce, no reliable conclusions could be obtained for this plant. For *A. thaliana* the root growth inhibiting effect of C10 **1g** was confirmed, but no effect of HO12 **2i** nor TA12 **11a** was observed under the conditions tested. However to fully disclose the effect of the QS signal molecules as such in the biocontrol capacity of *Pseudomonas* sp. CMR12a, contact studies with a pathogen after AHL-treatment should be evaluated, as it is known that several AHLs are able to induce systemic resistance to plants.

Although algicidal effects are associated with TA12 **11a**, this compound did not inhibit the growth of *A. thaliana*. On the other hand, in a preliminary experiment TA12 **11a** was able to significantly reduce the growth of the agriculturally relevant pathogen *R. solani* but showed only limited activity against *B. cinerea*. Therefore, further research should be carried out to evaluate the potential of this tetramic acid **11a** to be used as an algicide or fungicide in hydroponics. Different concentrations, different pathogens and the effect on different plants should be carefully

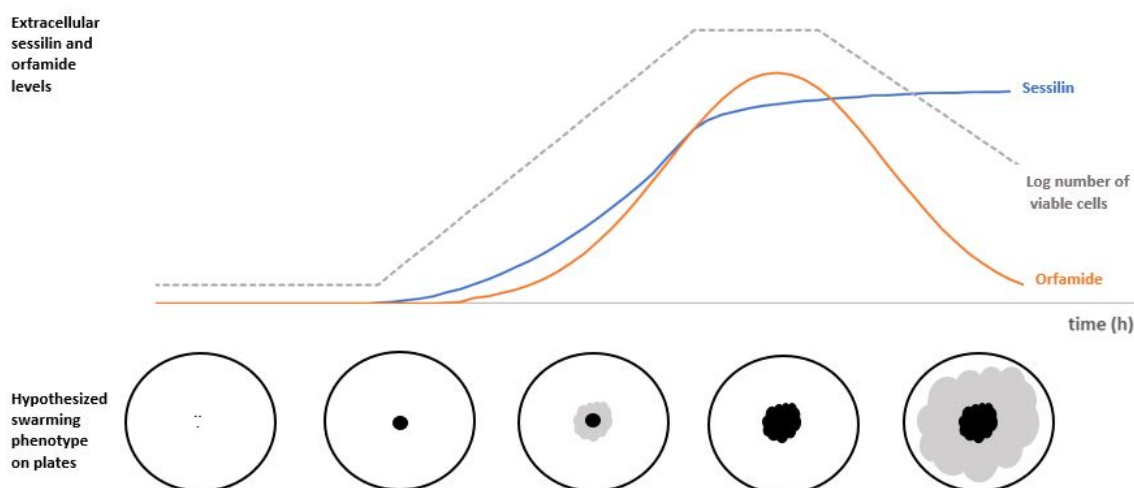
evaluated to fully assess the potential of this compound.

3.4 The influence of the quorum sensing signal molecule *N*-(3-hydroxy-octanoyl)-L-homoserine lactone on the regulation of cyclic lipopeptide production by *Pseudomonas* sp. CMR12a

Abstract

In this part the influence of a QS signal molecule, HO8 **2e**, on the swarming behavior of *Pseudomonas* species CMR12a was studied. It was shown that this QS signal could stimulate orfamide production via activation of the PhzI/PhzR-operon. No effect on sessilin production was observed. After a comparison of the effect of this compound **2e** with the swarming phenotype on agar plates, it was hypothesized that both CLPs, orfamide and sessilin, which are produced by this bacterium fulfill a crucial role in its swarming behavior. It is believed that QS controls the final swarming phenotype. This control depends on an elegant fine-tuning of the ratio of the two produced CLPs, orfamide and sessilin, via the control of the orfamide production. When the cell density and thus the concentration of HO8 **2e** increases, more orfamide is produced. It is hypothesized that the decrease of the sessilin/orfamide ratio causes a sessile behavior in a structured biofilm. On the other hand, when the sessilin/orfamide ratio increases, a switch to swarming behavior might be made once more.

Graphical abstract



Keywords

AHL, quorum sensing, CLP, swarming, metabolite regulation

3.4.1 Introduction

In previous research, it was shown that *Pseudomonas* sp. CMR12a needs to produce either phenazines **167**, or CLPs **168** and **169** to exert its biocontrol activity (Figure 3.16).^{201,202,347} However, the regulatory mechanisms controlling CLP-production and the possible influence of QS are far from being understood in this promising biocontrol strain.

Pseudomonas sp. CMR12a produces two types of CLPs: orfamides and sessilins (Figure 3.16). Orfamides B, D and E (**168a–c**) are produced in similar amounts and consist of a peptide containing 10 amino acids coupled to a β -hydroxytetradecanoyl, β -hydroxydodecanoyl or β -hydroxytetradecenoyl fatty acid tail. Sessilins are made up out of an 18 amino acid peptide core, linked to a β -hydroxyoctanoyl fatty acid moiety and differ only one amino acid from the toxic tolaasins, produced by mushroom pathogen *P. tolaasii*. Sessilin A (**169a**) is the main compound produced, but sessilin B and C are detected in minor amounts as well.³⁵⁰ The two types of CLP seem to fulfill a different role: whereas orfamide is indispensable for swarming, sessilin seems to oppose swarming and stimulate biofilm formation.^{117,350}

Quorum sensing (QS) regulates different bacterial phenotypes such as swarming, virulence expression, biofilm formation, bioluminescence, etc. in a population density-dependent manner (see Literature overview).^{2,3} Strain *Pseudomonas* sp. CMR12a possesses two QS systems, both controlled by the GacS/GacA two-component regulatory system. The first, designated PhzI/PhzR, uses *N*-(3-hydroxyhexanoyl)-L-homoserine lactone (HO6) **2c**, *N*-hexanoyl-L-homoserine lactone (C6) **1c**, *N*-(3-hydroxyoctanoyl)-L-homoserine lactone (HO8) **2e** and *N*-octanoyl-L-homoserine lactone (C8) **1e** as signal molecules (Figure 3.16) and regulates phenazine production. The second system, CmrI/CmrR, uses the uncommon *N*-(3-hydroxydodecanoyl)-L-homoserine lactone (HO12) **2i** but its function is yet unknown.³⁶¹

The production of CLPs is subjected to complex regulatory circuits. The GacS/GacA two-component system is often a crucial element (see Literature overview).^{153–156,158,159} The biosynthesis gene clusters of sessilin and orfamide of *Pseudomonas* sp. CMR12a were only recently fully characterized (Figure 3.24).³⁶² As in many other NRPS genes, LuxR-type regulators are present in the flanking regions.^{114,162} Whereas LuxR-type regulators OfaR1 and OfaR2 control both sessilin and orfamide production in *Pseudomonas* sp. CMR12a, no apparent function was found for SesR.³⁶²

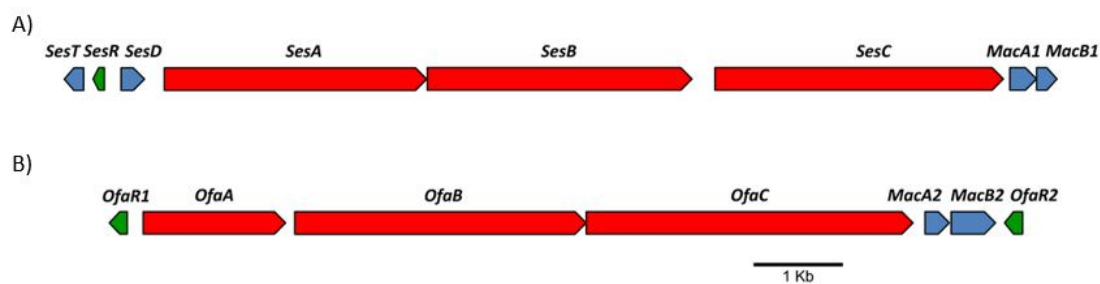


Figure 3.24. Schematic representation of A) sessilin and B) orfamide gene clusters of *Pseudomonas* sp. CMR12a. SesR, OfaR1 and OfaR2: LuxR-type transcriptional regulators. SesT: NodT-like outer membrane lipoprotein. SesD: SyrD-like ABC transporter protein. MacA: periplasmatic membrane protein. MacB: inner membrane protein. Figure from Olorunleke *et al.*³⁶²

In only a limited number of cases AHLs play an important regulating role in CLP production (see Literature overview).^{21–25,126,167,363} However, previous research hinted the involvement of QS in the CLP production of *Pseudomonas* sp. CMR12a. The aim of this study was therefore to obtain a better understanding of the complex regulation of CLP-production in the promising biocontrol strain *Pseudomonas* sp. CMR12a.

3.4.2 Recycling of the fatty acid tail of HO-AHLs into CLPs

It is an intriguing observation that *Pseudomonas* sp. CMR12a uses only a limited number of different β -hydroxy fatty acid moieties for its secondary metabolite production. Whereas one of the AHLs of the PhzI/PhzR QS system, HO8 **2e**, shares the same fatty acid moiety with sessilin A (**169a**), this overlap is also present between orfamide D (**168b**) and the AHL HO12 **2i** used by the CmrI/CmrR system. Therefore, a first goal of this study was to investigate if the fatty acid tails of AHLs are recycled into the CLPs. This hypothesis was based on several observations. First, it is known that several pseudomonads contain an AHL-acylase, enabling them to metabolize AHLs and use the acyl chain.^{5,52,53} Second, when decanoic acid is added to the fermentation medium of *Streptomyces roseosporus*, this fatty acid is incorporated, leading to the production of daptomycin (**12**) instead of the natural analogues with a branched fatty acid side chain.¹²⁵ This experimental result shows the possibility to influence the fatty acid incorporation of the NRPS. Third, in previous research it was observed that a sessilin mutant of *Pseudomonas* sp. CMR12a displayed a remarkably higher phenazine production than the wild type.²⁰¹ Phenazine production is influenced by the QS signal HO8 **2e**. As sessilin has the same β -hydroxyoctanoyl fatty acid side chain, abolishment of sessilin production could give rise to a higher HO8 **2e** concentration and hence more phenazine production. Finally, as long-chain AHLs rely on active transport to be secreted,³³ these compounds can accumulate in starving cells. *Pseudomonas* sp. CMR12a produces such a long-chain AHL, HO12 **2i**. Using

this β -hydroxydodecanoyl chain from this AHL **2i** to produce orfamide D (**168b**), which has the same β -hydroxy fatty acid chain, could enable *Pseudomonas* sp. CMR12a to start swarming and escape the nutrient-depleted environment. As orfamide and sessilin production only starts in the late exponential phase,³⁶² AHLs are expected to be present in abundant concentrations.

To evaluate the effect of QS on the swarming behavior, three AHLs with a different chain length were synthesized (see section 3.1) and added to the wild type and to two QS mutants (for a list of mutants used in this study, see Experimental part, section 5.5).²²⁵ The first mutant, $\Delta\text{phzI}\Delta\text{cmrI}$, lacks active LuxI-analogues and therefore displays no AHL-production at all. The other mutant, $\Delta\text{phzR}\Delta\text{cmrR}$, has no active LuxR-type proteins and as a consequence is unable to detect AHLs. One of the added compounds was a native AHL of PhzI, HO8 **2e**. This AHL is the major AHL produced by this strain. The production of the CLP viscosin by *P. fluorescens* 5064 is regulated via this QS signal molecule HO8 **2e** as well.²¹ The other two added AHLs had an acyl chain containing one carbon atom less (HO7 **2d**) or more (HO9 **2f**). These unnatural AHLs were tested to monitor the specificity of the LuxR-analogue.

The typical swarming phenotype observed for the wild type consisted of the formation of a thick central structure with swarming at the edges (Figure 3.25). This type of swarming was present without the addition of AHLs and with addition of HO7 **2d** and HO8 **2e**. The $\Delta\text{phzR}\Delta\text{cmrR}$ -mutant covered the entire plate in all conditions tested. As this mutant does not possess active LuxR-type proteins it cannot respond to the added AHL molecules. Interestingly, a distinct difference was observed after addition of HO7 **2d** and HO8 **2e** to the $\Delta\text{phzI}\Delta\text{cmrI}$ -mutant. While in the absence of AHLs, swarming similar to the $\Delta\text{phzR}\Delta\text{cmrR}$ -mutant was observed, the addition of 10 μM HO7 **2d** or HO8 **2e** halted the swarming, and a similar phenotype as the wild type was observed. The application of HO9 **2f** on the other hand was unable to stop swarming, and caused a full coverage of the plates, as observed for the other strains. This type of AHL-controlled behavior seems to suggest that an activated LuxR-type protein can act as a brake for swarming.

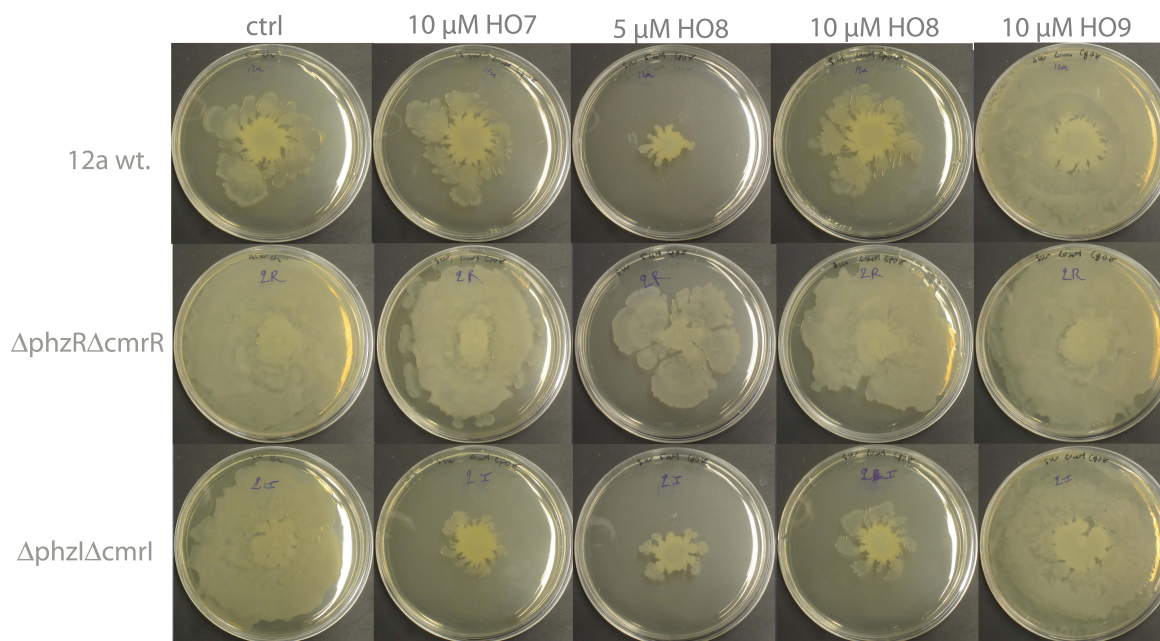


Figure 3.25. Observed swarming behavior of *Pseudomonas* sp. CMR12a and its QS mutants on 0.6% LB agar with and without the exogenously added AHLs HO7 **2d**, HO8 **2e** and HO9 **2f**. Cell density of inoculum: 10^5 CFU/mL. Pictures taken after 41 h of incubation at 28 °C.

As sessilin, the CLP linked with biofilm formation and swarming inhibition, also contains the same β -hydroxyoctanoyl fatty acid moiety, it is tempting to speculate that at least a part of the HO8 AHLs **2e** is recycled for the biosynthesis of sessilin. However, analysis of the produced CLPs after addition of HO7 **2d** to the Δ phzI Δ cmrI-mutant, did not reveal the presence of a sessilin analogue with a β -hydroxyheptanoyl fatty acid tail. This experiment was also repeated with isotope-labelled HO8 **77a** (see section 3.1.4),³⁶⁴ but once again no recycling of the labelled fatty acid part into sessilin could be observed. Scraping off the cells and quantification of the produced CLPs after extraction did not reveal an increase in sessilin after the addition of HO8 **2e**. Unexpectedly, the amount of orfamide did increase (Figure 3.26). These results led to abandoning the recycling hypothesis. The origin of the β -hydroxy fatty acid side chain could be sought in the poly- β -hydroxyalkanoates (PHA), which are typically composed of β -hydroxy fatty acids with 4 to 12 carbon atoms and which are accumulated in several pseudomonads.³⁶⁵ Alternatively, the β -hydroxy fatty acid tail could also originate from the primary metabolism.¹¹⁷

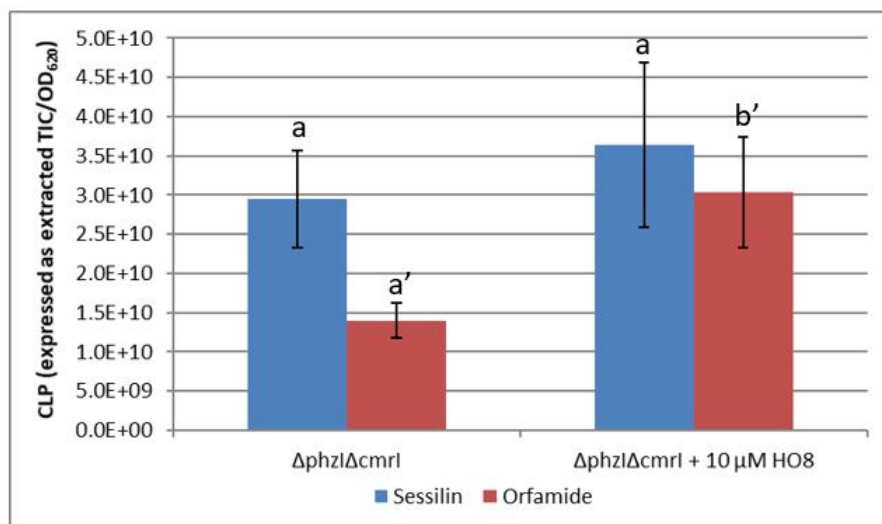


Figure 3.26. Sessilin and orfamide levels of the *Pseudomonas* sp. CMR12a $\Delta\text{phzI}\Delta\text{cmrI}$ -mutant, without and with the addition of 10 μM of HO8 **2e**. Cell density of inoculum: 10^5 CFU/mL. Cultures were inoculated on 0.6% LB agar plates and after 41 h of incubation at 28 °C, all cells were scraped off and ultrasonicated. Represented values are the mean of three repetitions. Bars with a different letter are statistically different according to a two sample *t*-test ($p = 0.05$).

The fact that the shorter-chain AHLs HO7 **2d** and HO8 **2e**, unlike the slightly longer HO9 **2f**, had a clear phenotypic effect, suggests mainly involvement of the PhzI/PhzR operon, which produces and detects the shorter-chain AHLs HO6 **2c**, HO8 **2e**, C6 **1c** and C8 **1e**. To evaluate if the PhzI/PhzR QS system was activated differently by the applied HO-AHLs **2d–f**, phenazine production which is controlled by the PhzI/PhzR operon,^{18,366} was monitored spectrophotometrically after the addition of the AHLs (Figure 3.27). As expected, phenazine production was observed in all cases for the wild type. Because of the absence of active LuxR-type proteins in the $\Delta\text{phzR}\Delta\text{cmrR}$ -mutant, no phenazine production was observed in all conditions evaluated for this mutant. For the $\Delta\text{phzI}\Delta\text{cmrI}$ -mutant on the other hand, the absence of phenazine production could be restored to wild type levels by the addition of HO7 **2d** or HO8 **2e**. The longer-chain analogue HO9 **2f** failed to evoke phenazine production. As the CmrI/CmrR system does not lead to a distinct phenotype upon (de)activation,³⁶¹ it was not possible to perform a similar assay to evaluate the activation of this QS operon by the different AHLs.

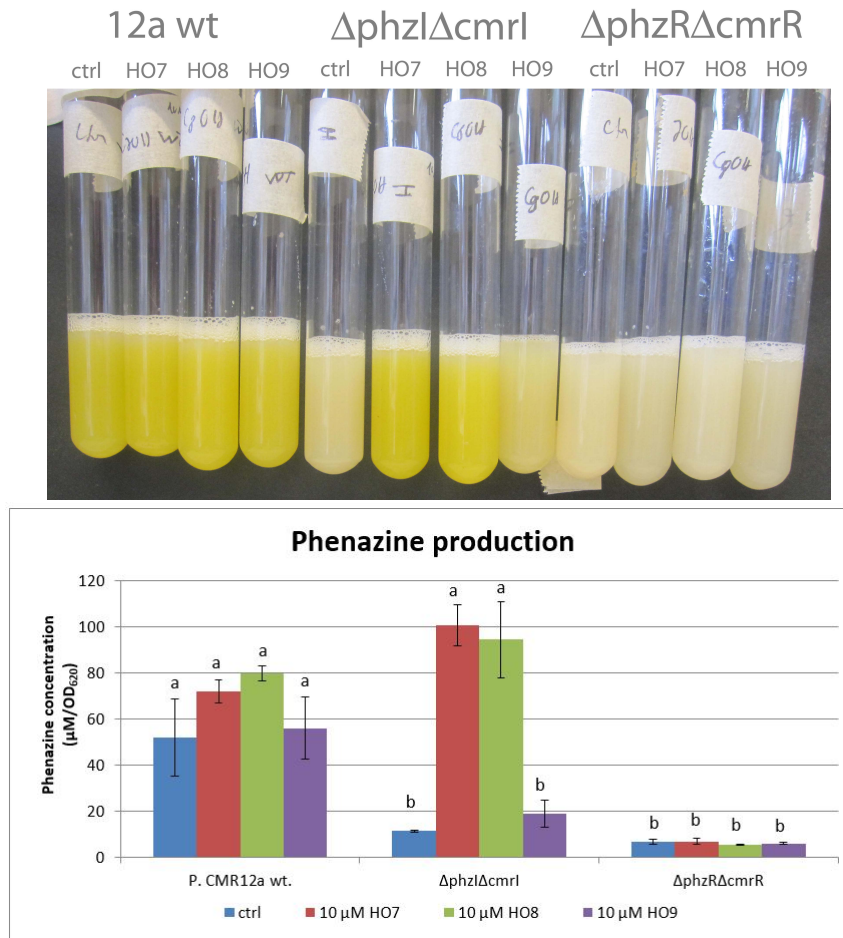


Figure 3.27. Observed phenazine production of *Pseudomonas* sp. CMR12a and its QS mutants Δ phzI Δ cmrI and Δ phzR Δ cmrR with and without the exogenously added AHLs HO7 **2d**, HO8 **2e** and HO9 **2f** after 24 h of incubation on a shaker at 28 °C. Represented values are the mean of two repetitions. Bars with a different letter are statistically different according to Tukey's *post-hoc* test ($p = 0.05$).

3.4.3 Effect of HO8 on the swarming phenotype of *Pseudomonas* sp. CMR12a and its QS mutants

To further assess the effect of HO8 **2e** and the role of the two different QS systems, the swarming assay was repeated with the wild type, the Δ phzR Δ cmrR-mutant (unable to detect AHLs), the Δ phzI Δ cmrIR-mutant (with only *phzR* active) and the Δ phzIR Δ cmrI-mutant (with only *cmrR* active) (Figure 3.28). One striking observation is the difference in colony morphology between the Δ phzR Δ cmrR-mutant (without active LuxR-analogues) and the other strains with at least one active LuxR-analogue. Whereas the latter strains formed a central sun-like structure and started swarming via the edges, the Δ phzR Δ cmrR-mutant immediately started to swarm in a disorganized manner. For the wild type and the Δ phzI Δ cmrIR-mutant, the addition of HO8 **2e** intensified the formation of the central structure. Elevated amounts of HO8 **2e** delayed the swarming out of the edges. The central, sun-shaped structure was also present in the

$\Delta\text{phzIR}\Delta\text{cmrI}$ -mutant albeit less pronounced. The influence of the addition of HO8 **2e** seemed to be negligible as well.

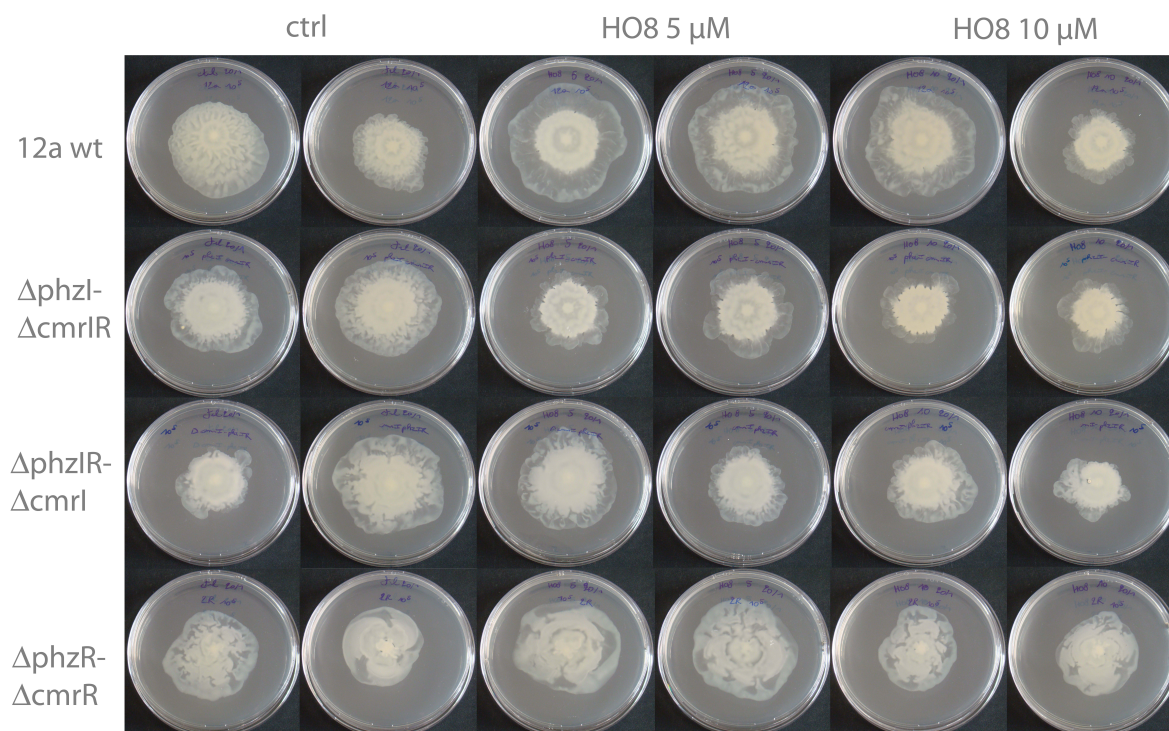


Figure 3.28. Observed swarming behavior of *Pseudomonas* sp. CMR12a and its QS mutants on 0.6% LB agar with and without exogenously added HO8 **2e**. Cell density of inoculum: 10^5 CFU/mL. Pictures taken after 41 h of incubation at 28 °C.

As for a given strain, several distinct swarming patterns were observed varying from one assay to the other, the influence of the number of viable bacterial cells was evaluated by performing a swarming assay employing an inoculum with a different cell density (Figure 3.29). At high cell densities, swarming behavior was observed for all strains tested. However, both the wildtype and the ΔcmrIR -mutant showed only limited swarming behavior at an inoculum of less than 10^7 CFU/mL, but deletion of the PhzI/PhzR-operon (mutants ΔphzIR and $\Delta\text{phzIR}\Delta\text{cmrIR}$) led to a swarming phenotype, even at low starting cell densities. These results stress the importance of the PhzI/PhzR-operon for controlling the swarming behavior and show that cell density can play a crucial role. Alternatively, different factors could also play a role. Swarming is flagellum-dependent and typically strictly regulated. On the other hand, the presence of CLPs could also give rise to flagellum-independent sliding by wetting the surface. These two types of motility might be impacted differently by QS, hence complicating the interpretation of these swarming assays.

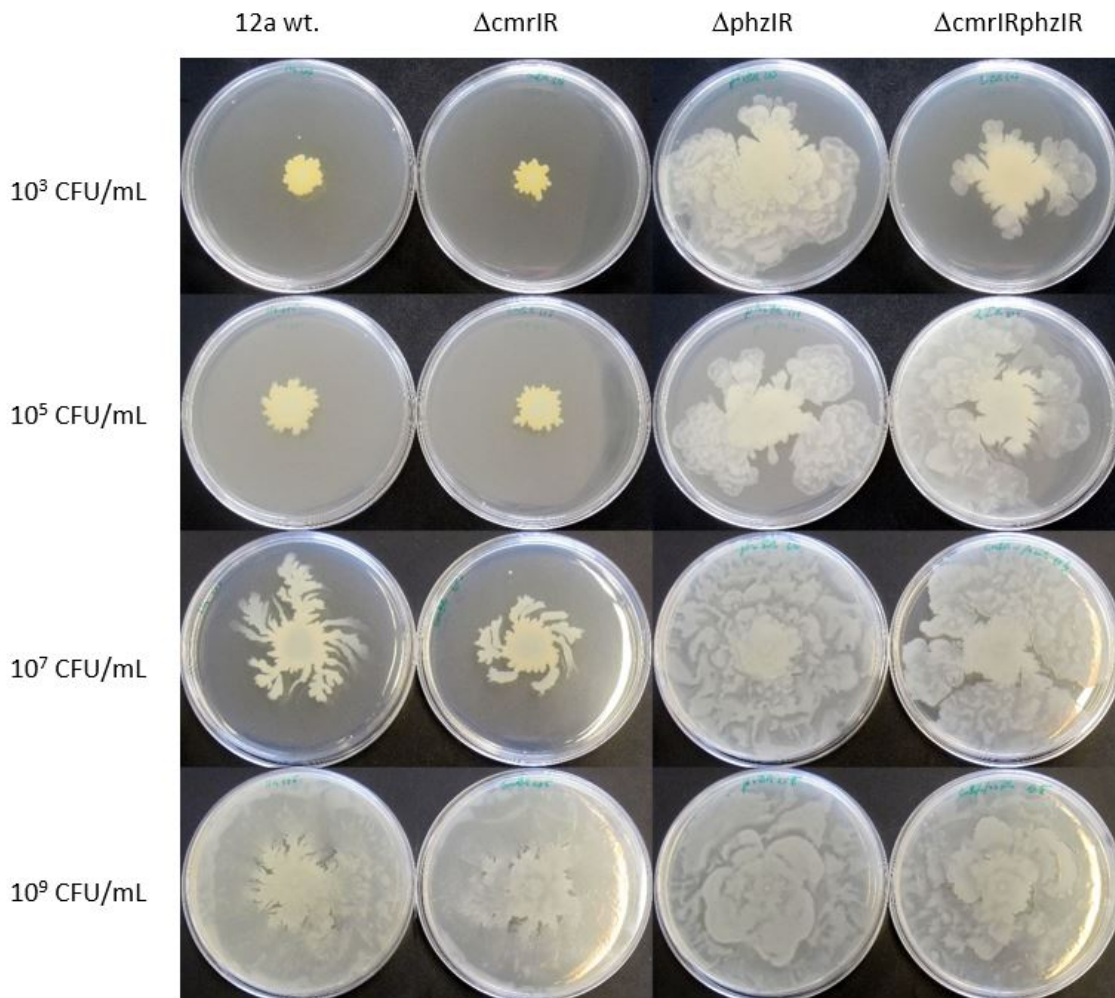


Figure 3.29. Observed swarming behavior of *Pseudomonas* sp. CMR12a and its QS mutants on 0.6% LB agar starting from an inoculum with a different cell density. Pictures taken after 41 h of incubation at 28 °C.

3.4.4 Possible QS-regulated secretion of CLPs

CLPs are secreted by ABC transporters. These are similar to the macrolide efflux transporter MacA-MacB-TolC found in *E. coli*. The corresponding MacA-MacB genes are found downstream of the orfamide and sessilin biosynthetic genes (Figure 3.24). SesT is annotated as a NodT family efflux transporter. As the orfamide gene cluster is not preceded by a NodT family efflux transporter it was previously hypothesized that the MacA-MacB transporters of sessilin and orfamide both use the same outer membrane efflux transporter upstream of the sessilin biosynthetic cluster.^{350,362}

To evaluate if QS could stimulate the secretion of CLPs via the activation of an alternative efflux transporter, the different native AHLs of *Pseudomonas* sp. CMR12a were added to a NodT2-mutant. This mutant lacks an active NodT2-transport protein and as a consequence fails to secrete sessilin efficiently. The cytotoxic properties of this CLP cause a significant growth impairment. However, no significant increase in growth, measured as optical density (OD),

was observed after the addition of the AHLs to the strains in liquid LB medium (Figure 3.30). Compared to the wild type, no growth differences were observed for the $\Delta\text{phzI}\Delta\text{cmrI}$ -mutant (Figure 3.30).

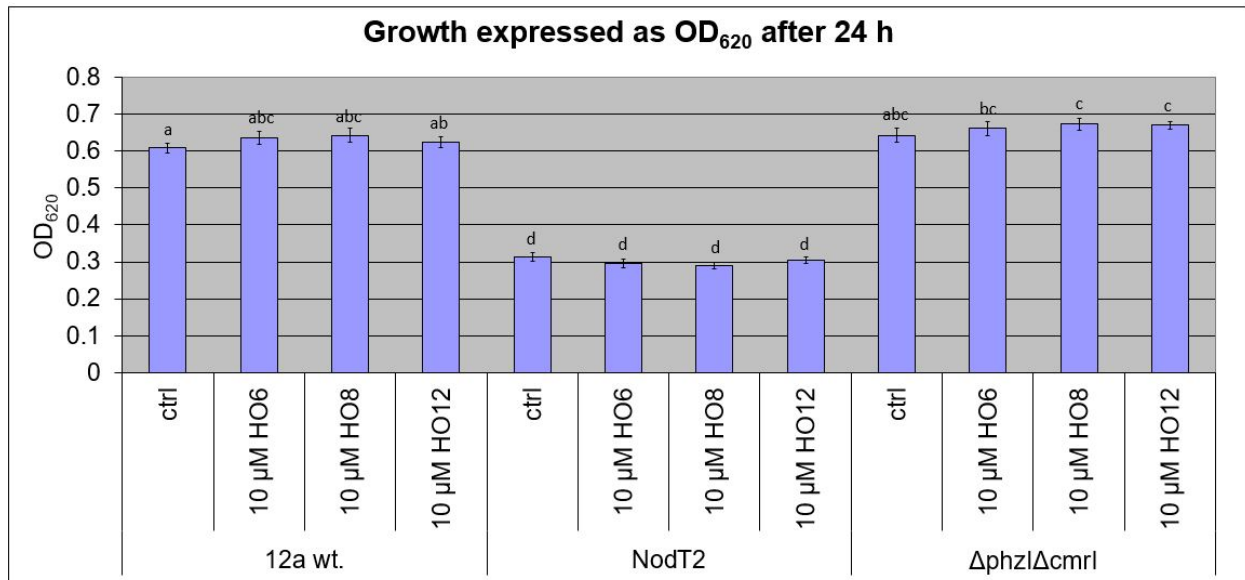


Figure 3.30. Optical densities observed for *Pseudomonas* sp. CMR12a wt. and its mutants NodT2 and $\Delta\text{phzI}\Delta\text{cmrI}$ with and without added AHLs HO6 **2c**, HO8 **2e** and HO12 **2i**. Cultures were inoculated (inoculum: 10^4 CFU/mL) in liquid LB medium and incubated for 24 h on a shaker at 28 °C. Represented values are the mean of three repetitions. Bars with a different letter are statistically different according to Tukey's *post-hoc* test ($p = 0.05$).

3.4.5 Quantification of CLPs

To enhance the standardization and quantification of the CLP production, it was decided to continue using liquid medium instead of agar plates. Via this approach it was possible to compare the CLP production between different strains with or without the addition of AHLs in a quantitative way via HPLC analysis. However, CLP production also strongly depends on the incubation conditions, for example in agitated cultures *Pseudomonas* sp. CMR12a produces more biomass but the cells remain planktonic and have strongly reduced intracellular sessilin levels compared to still cultures in the same medium.^{350,362} Therefore, a comparison of results obtained on agar plates with those obtained in still, liquid cultures should always be made with great caution. Importantly, insufficient amounts of pure sessilin have been isolated to develop a calibration curve to convert chromatographic peak areas to molar concentrations. As several factors influence the detection of a compound, a larger peak area on a chromatogram for a certain compound does not necessarily corresponds to a higher concentration of that compound compared to another compound. Therefore, the data represented below can only be used for relative comparisons

between the different strains.

To evaluate the effect of the two different QS systems, mutants lacking either the PhzI/PhzR (ΔphzIR) or the CmrI/CmrR (ΔcmrIR) QS system were employed. There were no differences in growth observed between the different strains under study, except a slower initial growth for the ΔphzIR -mutant (data not shown). Orfamide and sessilin are coproduced starting in the late exponential phase.³⁶² One important observation was that the relative extracellular orfamide concentration was tenfold lower than the relative sessilin concentration (Figure 3.31). On the other hand, inside the cells orfamide was the dominant CLP, indicating a preferential secretion of the cytotoxic sessilin. The amount of sessilin secreted by the ΔphzIR -mutant was slightly lower than the wild type and this reduction was also visible inside the bacterial cells. This slight reduction of intracellular sessilin levels was also observed in the ΔcmrIR -mutant, but was less clear extracellular (Figure 3.31). For orfamide, a significantly reduced production was observed for the ΔphzIR -mutant (Figure 3.31). The intracellular orfamide concentration was on average two times higher in the wild type, and the extracellular concentration seven times higher. The fact that the extracellular concentration is more strongly reduced than the intracellular concentration points to a certain intracellular accumulation. However, as the intracellular concentration was significantly reduced as well, it is clear that rather the orfamide production than the secretion is affected. This trend was not observed for the ΔcmrIR -mutant.

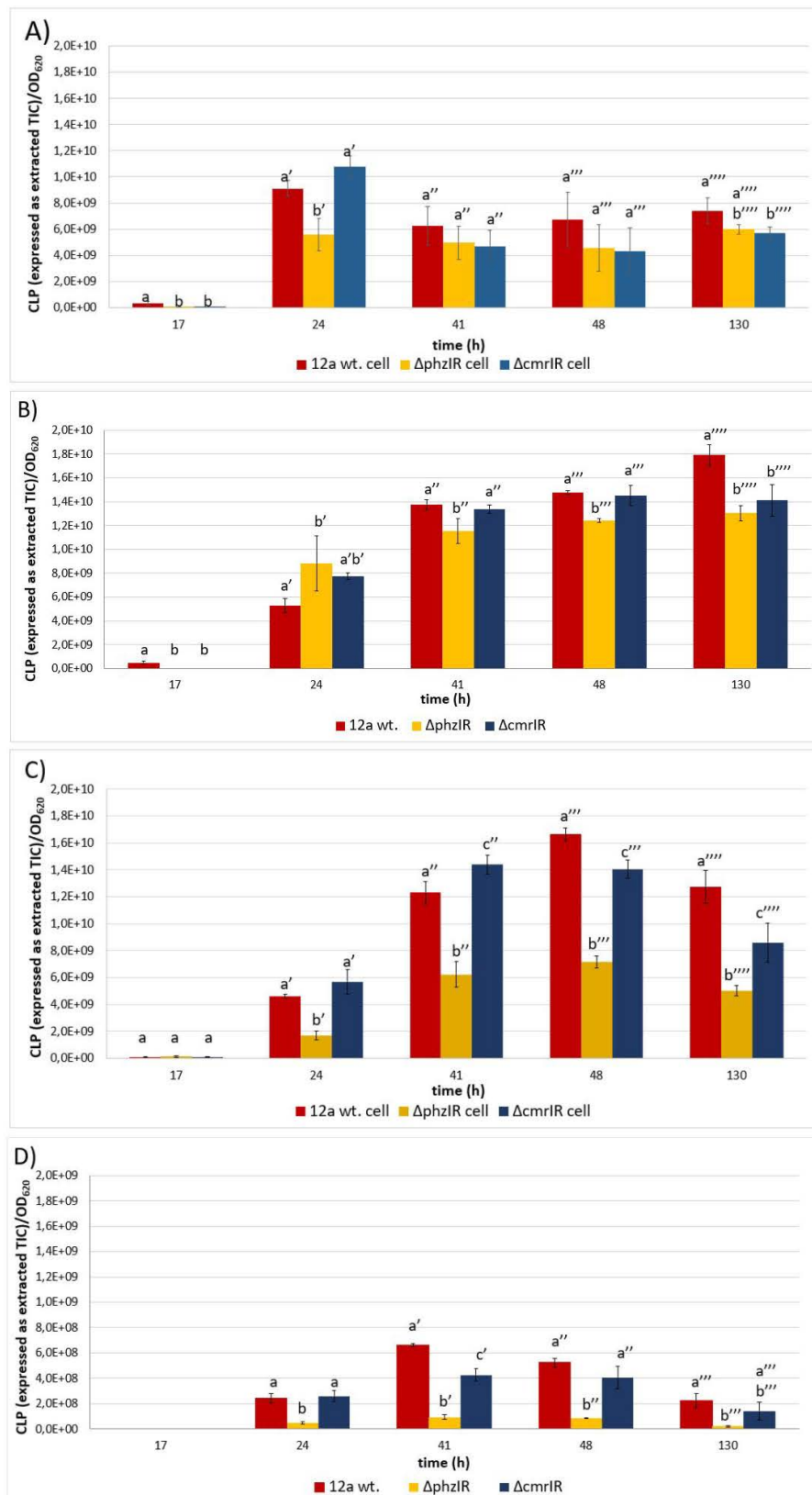


Figure 3.31. Observed CLP levels in *Pseudomonas* sp. CMR12a and its QS mutants in LB-medium under still growth conditions at 28 °C. Cell density of inoculum: 10⁵ CFU/mL. A) Intracellular sessilin. B) Extracellular sessilin. C) Intracellular orfamide. D) Extracellular orfamide. Data expressed as the peak area of total extracted ions of the LC-MS spectrum and corrected for cell density (measured as OD₆₂₀). Represented values are the mean of three repetitions. Bars with a different letter are statistically different according to Tukey's *post-hoc* test (*p* = 0.05).

As a confirmation, this assay was repeated with the wild type and the Δ phzIR-mutant, and the Δ phzI-mutant was included as well (Figure 3.32). This mutant does not contain active PhzI-proteins, and as a consequence cannot produce C6 **1c**, C8 **1e**, HO6 **2c** and HO8 **2e**. The PhzR-proteins on the other hand are present so this strain can respond to added AHLs. Therefore it is possible to complement this Δ phzI-mutant with HO8 **2e** to assess the effect of this QS signal molecule. Once again the Δ phzIR-mutant had significantly reduced orfamide levels, both intra- and extracellularly. The orfamide levels for the Δ phzI-mutant are lower than the wild type but higher than the Δ phzIR-mutant. This increased production level compared to the Δ phzIR-mutant suggests a residual effect of the present PhzR-proteins, possibly by binding with AHLs produced by the CmrI/CmrR-operon. Alternatively, the PhzR proteins could also act AHL-independently. As in the case of the PcoI/PcoR QS operon of *P. corrugata*, where the absence of AHLs causes the PcoR-protein to act as an activator of different virulence genes, while in the presence of AHLs, this activation goes via co-transcription of *rfa*.²⁴

Interestingly, the reduction in orfamide could be fully restored to wild type levels via the addition of 10 μ M of the native AHL HO8 **2e** (Figure 3.32). This clearly indicates an important regulatory effect of this QS signal molecule. In previous research, it was shown that a mutation in LuxR-type regulator genes *ofaR1* or *ofaR2* led to a weaker transcript of the genes *sesABC*, *MacA1B1*, and *ofaBC*. On the other hand, the transcription of *ofaA* and *macA2B2* was only marginally affected.³⁶² Therefore, another promoter which enables transcription of *ofaA* and *macA2B2* might form a target of the QS regulation of the orfamide production. The reactivation of the Phz-operon upon addition of HO8 AHL **2e** was also obvious by the reappearance of the yellow-colored phenazines in the cell pellet obtained after centrifugation of the culture broth (Figure 3.33), which can be used as a quick visual check to evaluate if the PhzI/PhzR-operon is active.

The fact that orfamide production and not sessilin production can be influenced by the addition of HO8 **2e**, confirms the analysis of the swarming assay on the agar plates where an increase of orfamide was observed but not of sessilin (see section 3.4.2). As orfamide is associated with swarming and sessilin inhibits swarming and stimulates biofilm formation,³⁵⁰ these results seem to contradict the observed swarming behavior on agar plates, where the addition of HO8 **2e** seemed to oppose swarming (Figure 3.25 and 3.28).

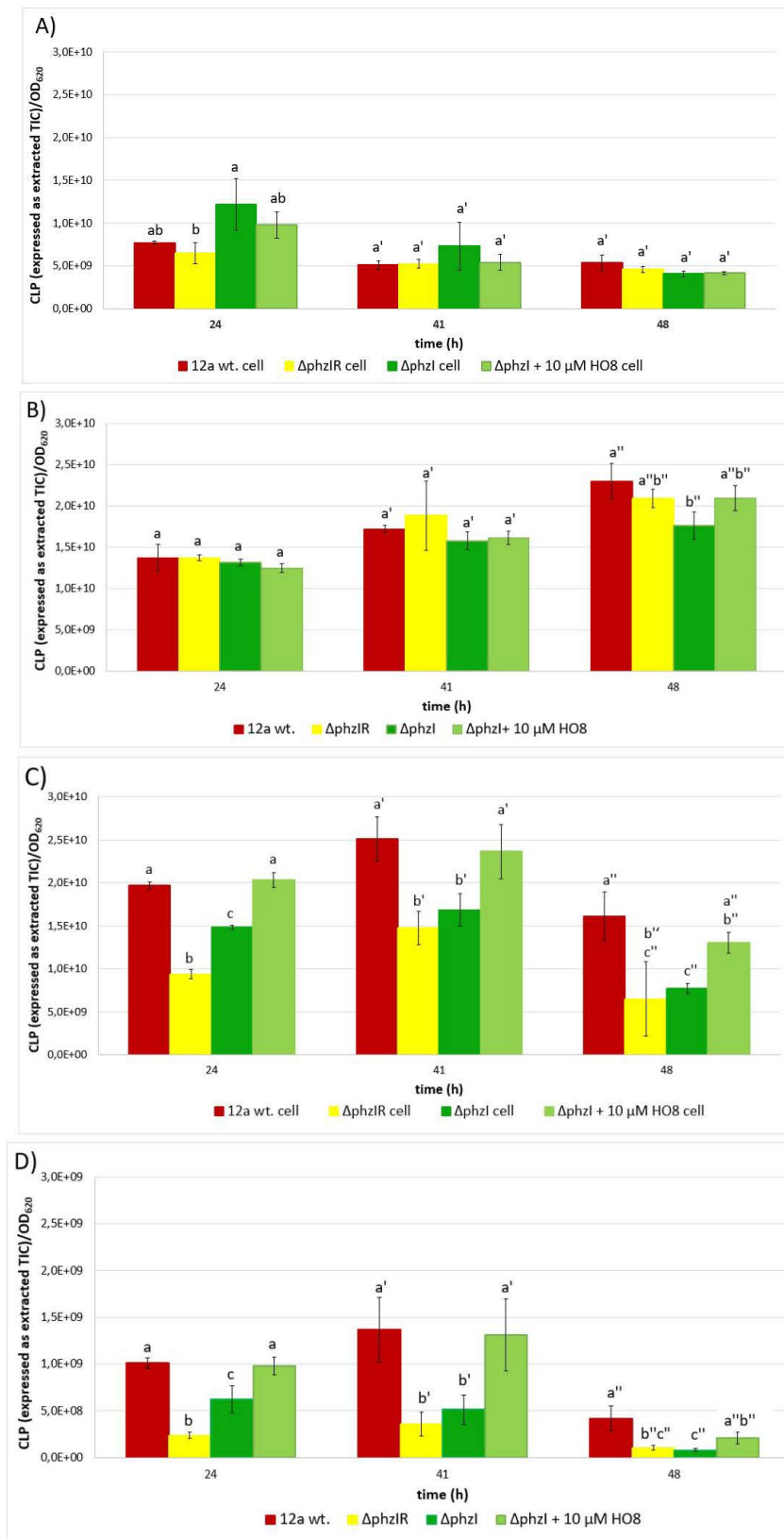


Figure 3.32. Observed CLP levels in *Pseudomonas* sp. CMR12a and its QS mutants in LB-medium under still growth conditions at 28 °C. Cell density of inoculum: 10^5 CFU/mL. A) Intracellular sessilin. B) Extracellular sessilin. C) Intracellular orfamide. D) Extracellular orfamide. Data expressed as the peak area of total extracted ions of the LC-MS spectrum and corrected for cell density (measured as OD_{620}). Represented values are the mean of three repetitions. Bars with a different letter are statistically different according to Tukey's *post-hoc* test ($p = 0.05$).



Figure 3.33. Cell pellet obtained after 24 h incubation in LB medium under still growth conditions at 28 °C, followed by centrifugation and removal of the supernatant. Cell density of inoculum: 10^5 CFU/mL. From left to right: 12a wt., Δ phzIR-mutant, Δ phzI-mutant, Δ phzI-mutant + 10 μ M HO8 **2e**.

In a subsequent assay the Δ phzR Δ cmrR-mutant was included, lacking any active LuxR-type proteins, and 10 μ M HO8 **2e** was added to all the strains under investigation. Surprisingly, a small reduction in orfamide production was observed for the wild type when HO8 **2e** was added, perhaps by disturbing the normal regulatory circuit due to the addition of the AHL (Figure 3.34). As expected, the exogenously added HO8 **2e** failed to increase the orfamide production in the Δ phzIR-mutant, because of the absence of the corresponding PhzR receptor proteins. Therefore it can be concluded that the added HO8 **2e** should interact with the PhzR receptor and not any alternative receptor to influence orfamide production. The Δ phzR Δ cmrR-mutant showed a reduced production of orfamide similar to the Δ phzIR-mutant after 24 h although after 41 h near wild type levels were observed (Figure 3.34). As this strain displays a slower growth, it could be that its orfamide production peaks at a different time as compared to the wild type.

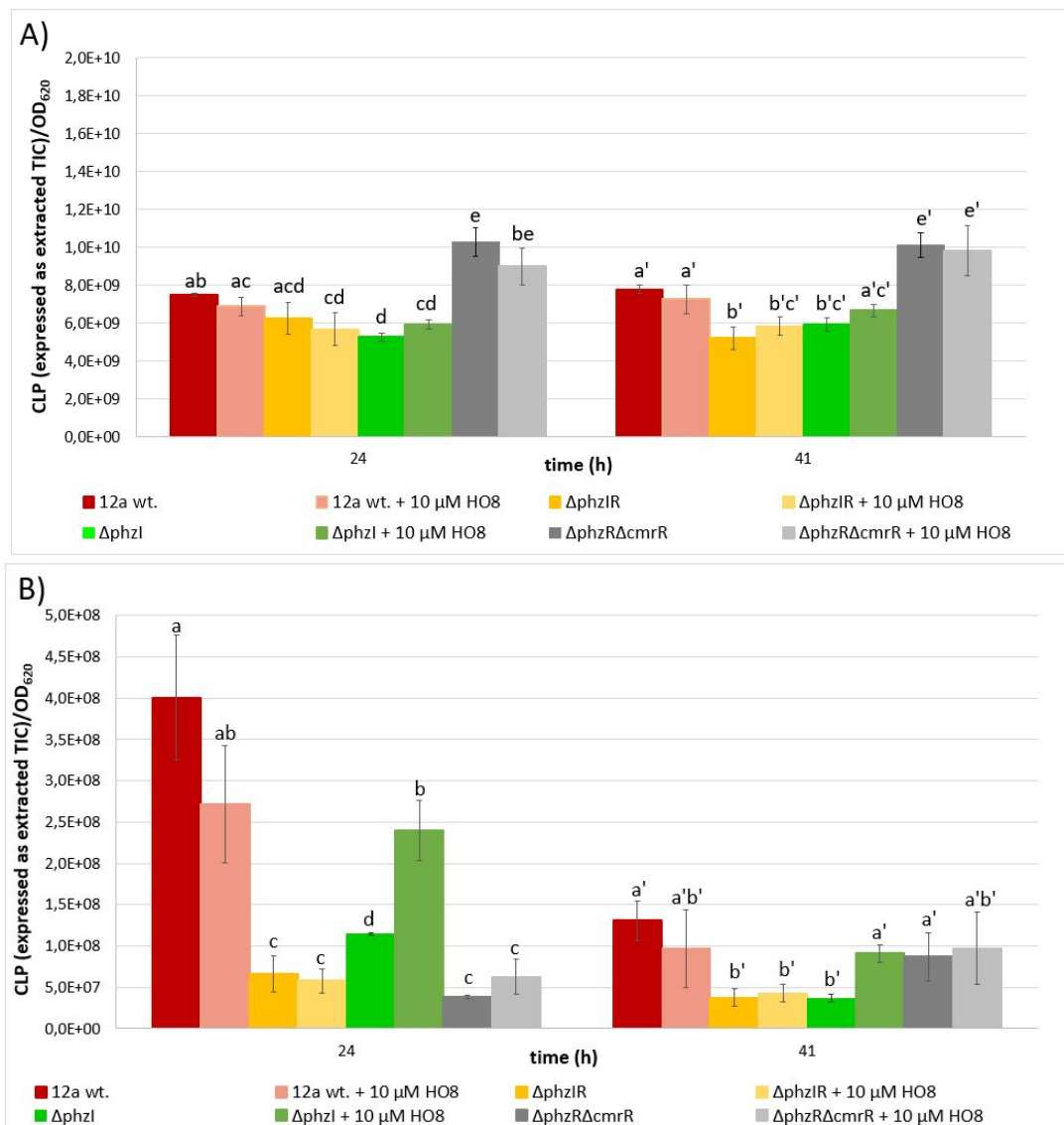


Figure 3.34. Observed CLP levels in *Pseudomonas* sp. CMR12a and its QS mutants in LB-medium under still growth conditions at 28 °C. Cell density of inoculum: 10^5 CFU/mL. A) Intracellular orfamide. B) Extracellular orfamide. Data expressed as the peak area of total extracted ions of the LC-MS spectrum and corrected for cell density (measured as OD_{620}). Represented values are the mean of three repetitions. Bars with a different letter are statistically different according to Tukey's *post-hoc* test ($p = 0.05$).

For the sessilin production no clear effect of the addition of 10 μ M HO8 **2e** could be observed in any strain (Figure 3.34). The Δ phzR Δ cmrR-mutant however showed a distinct higher sessilin production than the wild type and the other QS mutants. The cause of this increase is not clear yet. Although sessilin is linked with biofilm formation, these results indicate that a higher sessilin versus orfamide ratio might shift the bacterial motility toward swarming in an unstructured manner as observed in the Δ phzR Δ cmrR-mutant (Figure 3.35) and stimulation of orfamide production via the addition of HO8 **2e** to the Δ phzI-mutant might cause the formation of the central round structure and swarming from the edges.

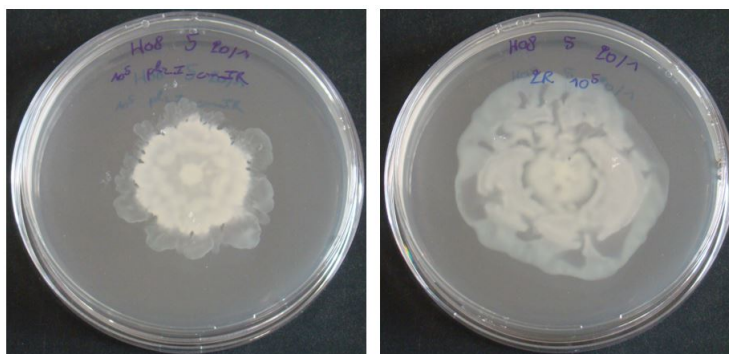


Figure 3.35. Left: typical swarming phenotype observed on 0.6% LB agar with an active Phz-operon. Right: typical swarming phenotype observed on 0.6% LB agar with an inactive Phz-operon. Cell density of inoculum: 10^5 CFU/mL. Pictures taken after 41 h of incubation at 28 °C.

3.4.6 Interaction orfamide-sessilin

It is known that different CLPs can interact with each other. One well-described example is the white line-inducing principle (WLIP), which causes the production of a white precipitate when confronted with a CLP of the tolaasin group.¹¹⁴ The same reaction has also been observed for sessilin and orfamide: when they are both secreted they interact to form a white precipitate.³⁵⁰ As a sessilin mutant shows a clear swarming behavior, and as an orfamide mutant is unable to swarm it was believed that orfamide is required for swarming and sessilin opposes swarming.³⁵⁰ Therefore, sessilin can hinder swarming by co-precipitating with orfamide. In the *Pseudomonas* sp. CMR12a wt. only sessilin is secreted in high amounts and orfamide is retained close to or inside the bacterial cells, avoiding such a precipitation reaction under normal circumstances. Alternatively, sessilin can also block orfamide secretion as they both rely on the same outer membrane protein, SesT, to be secreted.³⁶²

However, in this study it was observed that a decrease in orfamide production, as is the case for mutants lacking an active Phz-operon, stimulates swarming. A restoration of orfamide production to wild type level, for example by the addition of HO8 **2e**, halted swarming (Figure 3.25 and 3.28). It was therefore hypothesized that both sessilin and orfamide can be responsible for swarming and that the interaction between those two CLPs determines the final phenotype. Orfamide alone is sufficient to swarm but sessilin requires a minimal amount of orfamide to evoke swarming. The reason for this dependence of sessilin on orfamide to swarm is yet unknown.

When sessilin is the major CLP present and orfamide only as a minor component, sessilin is the putative causal agent of the swarming. This swarming has a rather unstructured appearance (for example figure 3.28, strain $\Delta\text{phzR}\Delta\text{cmrR}$). Remarkably, the amount of extracellular sessilin significantly increases in time, whereas the amount of extracellular orfamide peaks and then

decreases. This increase of the sessilin/orfamide ratio could shift the cells to swarming when nutrients are exhausted. When besides sessilin, also an increased amount of orfamide is present, they might impede each other's swarming inducing activity and it is hypothesized that then the characteristic sun-shaped structure is formed and no swarming is observed (Figure 3.28, strain $\Delta\text{phzI}\Delta\text{cmrIR}$ + HO8 2e). When only orfamide is present, as is the case in a sessilin mutant, orfamide is the driving force for the swarming phenotype.

To confirm this hypothesis, a strain that secretes orfamide in the culture medium and a strain that has a high sessilin to orfamide ratio and secretes sessilin in the culture medium were mixed. Sessilin mutant ΔCLP1 does not produce sessilin and releases orfamide in the medium. This strain shows a strong swarming phenotype.³⁵⁰ Mutant ΔPhzIR has a strongly reduced orfamide production but produces sessilin at wild type levels (Figure 3.31, 3.32 and 3.34). This strain also has a strong swarming behavior. When cultured separately both ΔCLP1 and ΔPhzIR display a swarming phenotype (Figure 3.36). ΔCLP1 swarms due to the high levels of extracellular orfamide, whereas ΔPhzIR relies on sessilin for swarming. When cultured together, resulting in high levels of both sessilin and orfamide in the extracellular environment which then interact, a more sessile phenotype is observed (Figure 3.36). However when one of the CLPs takes the upper hand, as is the case for sessilin in the $\Delta\text{CLP1}:\Delta\text{PhzIR}$ 1:2 mix, swarming is reactivated. This effect is less clear for orfamide in the $\Delta\text{CLP1}:\Delta\text{PhzIR}$ 2:1 mix as sessilin has a stronger deactivating effect on orfamide. The small difference in swarming phenotype observed between the co-culture of ΔCLP1 and ΔPhzIR ($\Delta\text{CLP1} + \Delta\text{PhzIR}$) versus the 1:1 mixture of both strains ($\Delta\text{CLP1}:\Delta\text{PhzIR}$ 1:1) could be explained by a different ratio of both CLPs as both mutants might have a different growth pattern.

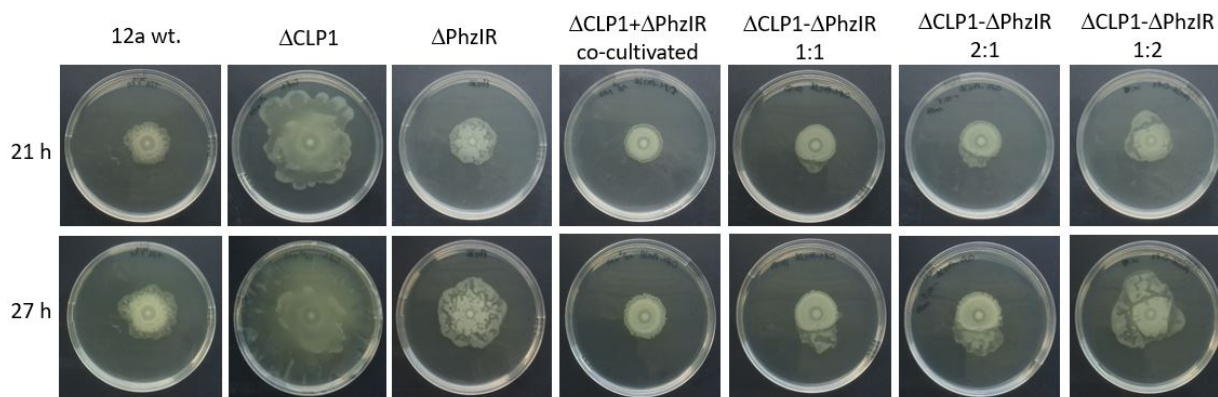


Figure 3.36. Swarming phenotypes obtained for strains *Pseudomonas* sp. CMR12a wt., Δ CLP1, Δ PhzIR and mixtures of these strains on 0.6% LB agar. Cell density of inoculum: 10^5 CFU/mL. Pictures taken after 21 and 27 h incubation at 28 °C. For the Δ CLP1+ Δ PhzIR treatment, the bacteria were co-cultivated in liquid LB culture medium and plated as such. For the Δ CLP1- Δ PhzIR 1:1, 2:1 and 1:2 swarming plates, separate cultures of both bacteria were added together in the specified ratio/concentration and then plated. Experiment performed by Dr. Feyisara Olorunleke (Department of Crop protection, Faculty of Bioscience Engineering, Ghent University).

3.4.7 Conclusions

In this work the influence of a QS signal molecule, HO8 **2e**, on the swarming behavior of *Pseudomonas* sp. CMR12a was studied. Via studies with several QS-mutants in liquid LB medium, it was shown that this QS signal could stimulate orfamide production via activation of the PhzI/PhzR-operon. Orfamide is associated with a swarming phenotype. However, in swarming assays on agar plates, a more sessile phenotype was observed after application of this QS signal **2e**. It is therefore hypothesized that the other CLP sessilin, which was associated with biofilm formation and the inhibition of swarming, also plays a role in swarming and that the final phenotype depends on the ratio of both CLPs. It is believed that QS can fine-tune the ratio of the two produced CLPs, orfamide and sessilin, via the control of orfamide production (Figure 3.37). The swarming pattern of *Pseudomonas* sp. CMR12a is hypothesized to proceed as follows. At first, when only sessilin is secreted no swarming is observed and the colony is established via the formation of a biofilm. Subsequently, a minute amount of orfamide is secreted, causing a swarming phenotype which expands the colony size. When the quorum and thus the concentration of HO8 **2e** increases, orfamide production goes up and swarming is inhibited. When the orfamide production starts to decrease, and as a consequence the sessilin/orfamide ratio increases, a switch to swarming behavior is made once more to anticipate nutrient depletion.

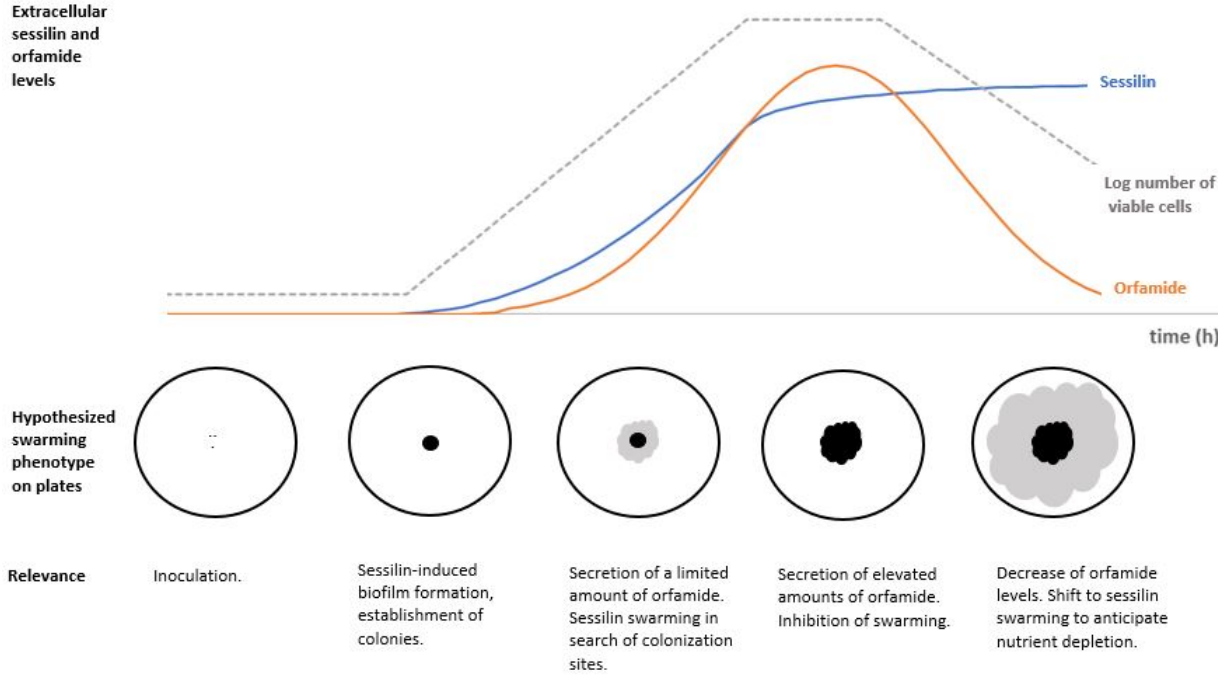


Figure 3.37. Hypothetical influence of different extracellular orfamide and sessilin ratios on the swarming behavior of *Pseudomonas* sp. CMR12a.

Chapter 4

Perspectives

The deuterated fatty acids **64**, **73** and **75** (Figure 4.1), which were synthesized in the first part of this PhD research in good yields, or more generally the application of the developed methodology allowing the design and synthesis of tailor-made deuterated fatty acids, can be used as a powerful tool to elucidate the biosynthetic origin of several metabolites containing a fatty acid tail by feeding these compounds to bacterial cultures and evaluating if the isotope-label appears in the compound of interest. Besides their application as internal standard in isotope-dilution mass spectrometry to quantify AHLs, the isotope-labelled AHLs **65**, **77**, **78** and **79** and AHL-degradation products **80** and **81** (Figure 4.1) can be employed to study the metabolization (and perhaps recycling) of the AHL acyl chain.

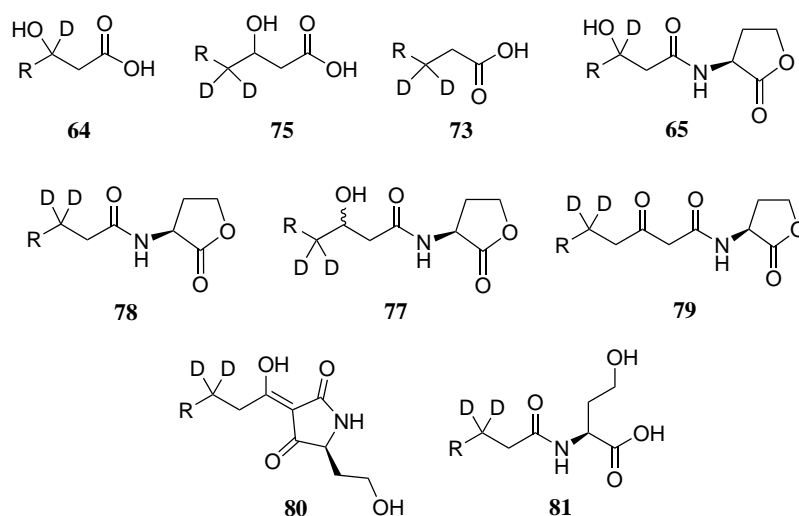
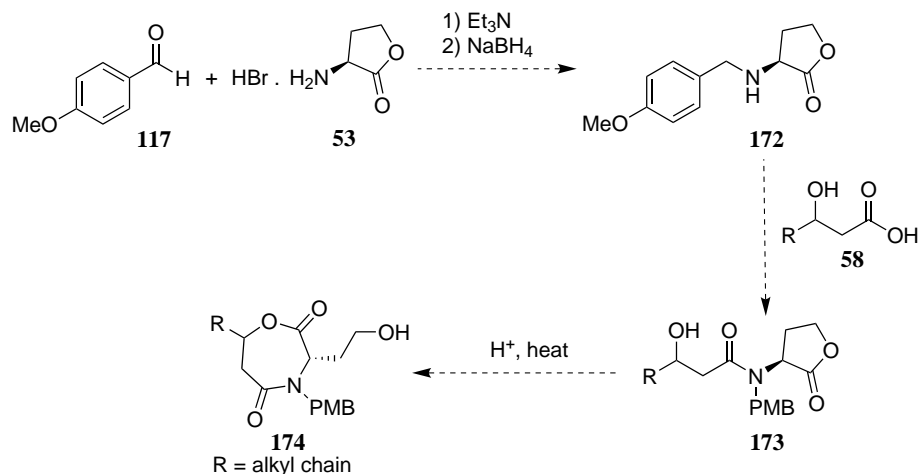


Figure 4.1. General structure (R = alkyl chain) of the synthesized deuterated fatty acids **64**, **73**, and **75**, AHLs **65**, **77**, **78** and **79** and AHL-degradation products **80** and **81**.

In the second part, the spontaneous rearrangement of *N*-(3-hydroxyacyl)-L-homoserine lactones **2** toward 1,4-oxazepane-2,5-diones **82** was excluded because of the absence of the correct conformation for cyclization to proceed. However, it was shown that the introduction of a third substituent at the amide nitrogen atom gave rise to an elevated amount of the amide in the *cis*-conformation, allowing cyclization. Therefore, it could be of interest to synthesize *N*-(3-hydroxyacyl)-L-homoserine lactones with a third substituent at nitrogen (e.g. PMB for **173**) and

to re-evaluate the cyclization. These compounds could be accessed via a reductive amination of L-homoserine lactone hydrobromide **53**, followed by the developed coupling protocol with a β -hydroxy fatty acid **58** (Scheme 4.1). As no such *N*-protected *N*-(3-hydroxyacyl)-L-homoserine lactones have been reported yet, it would also be interesting to evaluate their bioactivity, although the introduction of a bulky substituent often leads to a loss of QS activity.



Scheme 4.1. Proposed synthetic route toward *N*-PMB-protected *N*-(3-hydroxyacyl)-L-homoserine lactones **173**, followed by a heat- or acid-induced rearrangement to 1,4-oxazepane-2,5-dione **174**.

As no synthetic route toward the 1,4-oxazepane-2,5-diones **175** existed, the biological activities of this class compounds has not been studied yet. A first interesting area to test these seven-membered ring structures **175** is as QS modulators. Several AHL-analogues with an alteration of the lactone ring have been tested, with differing activities (Figure 4.2).¹² Some AHL-analogues mimic the AHL-structure very closely, whereas others only show distant (or no) similarities. Typically, modifications of the AHL lactone ring are tolerated but result in compounds with a reduced QS activity. The retainment of hydrogen bond acceptors seems to be important.¹³ The 1,4-oxazepane-2,5-diones **175** would not be susceptible to degradation by specific AHL-degrading enzymes. However, these compounds **175** can be broken down by abiotic degradation as they still contain the lactone moiety.

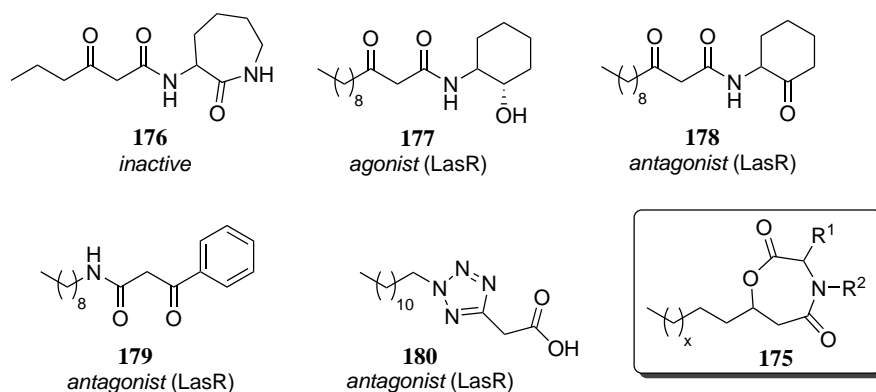


Figure 4.2. A small selection of QS modulators **176–180** with an alteration of the lactone ring,¹² and the general structure of the synthesized 1,4-oxazepane-2,5-diones **175**.

Small cyclic peptides have interesting biological properties and are a promising class of drug candidates.³⁶⁷ The comparison of the seven-membered bislactams with the 1,4-oxazepane-2,5-dione-analogues **175**, which have one lactam and one lactone bond instead of two lactam bonds, could therefore help developing interesting structure-activity relationships. One important aspect of cyclic peptides is their resistance toward enzymatic degradation. It is expected that 1,4-oxazepane-2,5-dione-analogues **175** also possess this resistance as the enzyme-catalyzed hydrolytic breakdown of peptides usually starts at the *C*- or *N*-terminus. The 1,4-oxazepane-2,5-dione-analogues **175** contain a lactone moiety, so these compounds are sensitive to alkaline hydrolysis. These compounds **175** could therefore be used to study the temporary activation of a target receptor.

Also bicyclic structures **98** (Scheme 3.20) and **160a–c** (Scheme 3.33) could be interesting scaffolds to test for bioactivity. For example, bicyclic compounds **181** and **182** (Figure 4.3) can bind to X-linked inhibitors of apoptosis proteins (XIAPs), which are central regulators of both death-receptor-mediated and mitochondria-mediated apoptosis pathways and have potential application in cancer treatment.³⁶⁸ Also analogues **183** and **184** (Figure 4.3) are able to inhibit human immunodeficiency virus type-1 integrase (HIV-1 IN), albeit with relatively low potency.^{258,369}

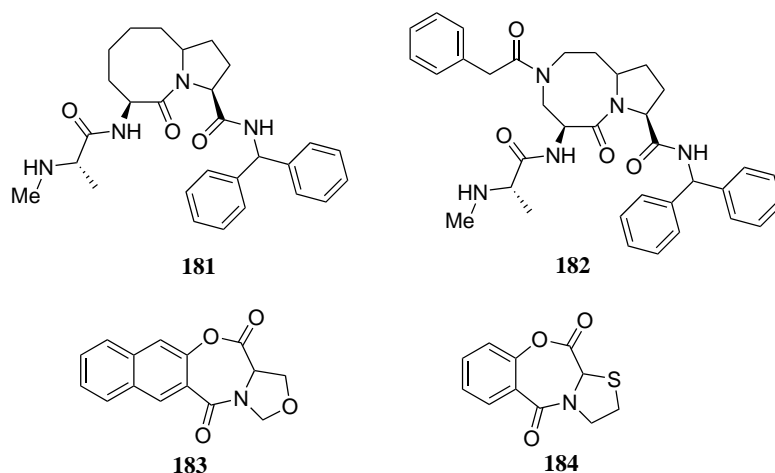
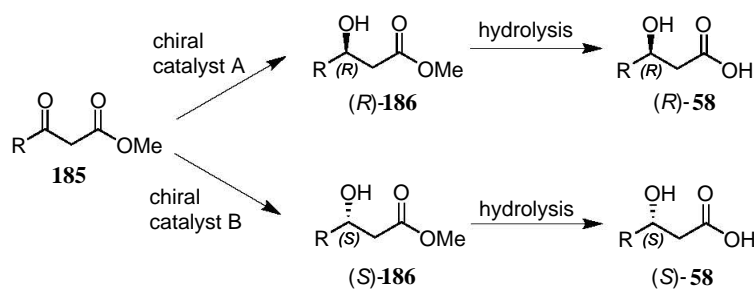


Figure 4.3. Bioactive bicyclic compounds **181**, **182**, **183** and **184**.^{258,368}

As mentioned before, the lability of the lactone moiety might seem a disadvantage at first, but can be used to temporarily influence certain receptors without the risk of accumulation of the cyclic compound. A second distinct advantage is that the cyclization renders the compound neutral by masking the carboxylic acid unit, allowing a better membrane permeability whereafter hydrolysis releases the charged *N*-(3-hydroxyacyl)amino acid derivative. As a lot of interest exists in *N*-acyl amino acids, for example as biosurfactants or feed additives, the cyclic analogues could be used to temporarily inactivate these *N*-(3-hydroxyacyl)amino acids, followed by a release after hydrolysis. However for such application, a stability study of the synthesized 1,4-oxazepane-2,5-diones **175** at different pH-ranges is required.

During the hydrogenolytic deprotection of serratin precursor **160a**, it was observed that only the (*RSS*)-diastereomer got deprotected (Table 3.13). Because of this selectivity, the maximum yield that can be obtained after the deprotection step when starting from oxazolidine-containing bicyclic structure **160a** with a d.r. of 1:1 is 50% of compound **83**, combined with the recovery of the unreacted (*RRS*)-isomer of **160a**. Therefore, to ameliorate this yield, the (*S*)-enantiomer of β -hydroxynonanoic acid **58d** should be used for the synthesis to obtain only (*RSS*)-**160a**.

Several methods have been described for the enantioselective synthesis of β -hydroxy fatty acids. Typically, the corresponding β -keto methyl esters **185** are stereoselectively reduced via the use of a chiral catalyst (Scheme 4.2).^{370–372}



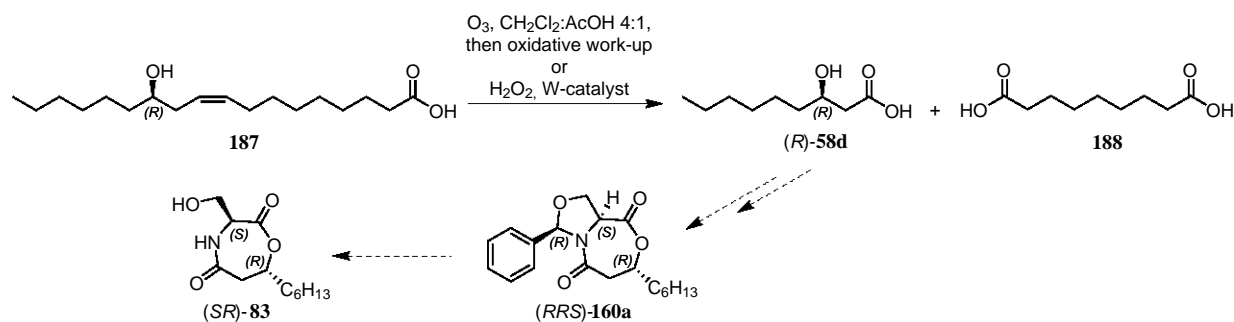
Scheme 4.2. Stereoselective reduction of β -keto esters **185** to β -hydroxy esters **186**, followed by a hydrolysis step to yield enantiomerically pure β -hydroxy fatty acids **58**.

To enantioselectively synthesize the (*RRS*)-isomer of **160a**, for example for biotesting or to further evaluate deprotection conditions for this compound, the (*R*)-enantiomer of β -hydroxynonanoic acid **58d** is required. This (*R*)-enantiomer of β -hydroxynonanoic acid **58d** could also be obtained from castor oil (Figure 4.4). Because of the presence of ricin, a water-soluble toxin, castor oil is inedible. Because of its unique, high ricinoleic acid (**187**) level (up to 90% of the fatty acid content in castor oil), it has received a lot of attention from the chemical industry.^{373,374}



Figure 4.4. Mature castor oil plant (*Ricinus communis*) (left) and the oil-containing castor beans (right). Image source: www.arkive.org/castor-oil-plant/ricinus-communis/.

Ricinoleic acid (**187**) can be transformed into (*R*)-3-hydroxynonanoic acid **58d** via ozonolysis,³⁷⁵ or via reaction with hydrogen peroxide over a tungsten catalyst (Scheme 4.3).^{376,377}



Scheme 4.3. Proposed application of castor oil-derived (*R*)-3-hydroxynonanoic acid **58d** for the enantioselective synthesis of (*RRS*)-**160a**.

During the search for a suitable *N*-protecting group to force the linear precursors in the correct conformation for cyclization to proceed, 2-methoxy-6-nitrobenzyl was evaluated. Although unsuccessful for the synthesis of the desired 1,4-oxazepane-2,5-dione, this photoremovable group was used for the synthesis of photolabile AHL **154a**. The photolysis was complete within 2 h in 1% ethanol in water. However, to allow the application of this compound in biological experiments, the harmfulness of the UV-radiation (360 nm) on the microorganisms should be studied. Alternatively, the possibility of two-photon excitation could be evaluated, as this process can proceed with red or NIR light (720 nm), but this requires high light intensities.

During biotesting, no direct effect of the QS signal HO12 **2i** on the growth of lettuce and *A. thaliana* was observed. However, to fully understand the role of HO12 **2i** in the biocontrol activity of *Pseudomonas* sp. CMR12a, the effect of this compound in pathogen contact studies should be evaluated as it might lead to induced systemic resistance of the plants. For tetramic acid **11a**, a degradation product of oxo-AHL **3i**, no negative effects on the growth of *A. thaliana* were observed as well. However, this lack of growth inhibiting effect could be an advantage as this compound has known algicidal properties. In a preliminary screening, an antifungal effect against the pathogenic fungus *Rhizoctonia solania* was observed. To fully grasp the antifungal potential of this tetramic acid, several concentrations should be tested and the effect on several fungal pathogens should be evaluated. Because of the algicidal and antifungal effects, it was suggested that this compound could be used in hydroponics. To test this hypothesis, such an experimental hydroponics set-up should be developed and the effect of tetramic acid **11a** on several plants with and without the addition of algae and fungi should be assessed.

In this thesis, the effect of QS signal molecule HO8 **2e** on the swarming behavior of promising biocontrol strain *Pseudomonas* sp. CMR12a was clarified. The hypothesis that the fatty acid tail of this QS signal might be reused for the synthesis of CLPs was refuted. However, it could be interesting to add labelled β -hydroxy fatty acids **75** to evaluate if these compounds

get incorporated in the CLPs. One could also add β -hydroxy fatty acids with a slightly different chain length or substitution pattern in an attempt to obtain several CLP-analogues with a modified fatty acid tail. Our results led to the hypothesis that HO8 **2e** controls the swarming by stimulating the orfamide production and hence controlling the sessilin/orfamide ratio. The typical course of the extracellular orfamide and sessilin levels in liquid LB medium is represented in figure 4.5. The orfamide level peaks at the beginning of the stationary phase and then drops whereas the extracellular sessilin levels keep increasing. Based on the CLP-quantification in liquid medium and comparison with swarming phenotypes on agar plates, a hypothesis for the typical course of the swarming was developed. However, orfamide and sessilin levels were quantified in only a limited number of swarming plates. To confirm the proposed effect of the ratio of these CLPs on the swarming behavior, CLP quantification on swarming plates is required, preferably at different stages of the swarming. It would also be interesting to monitor the HO8 **2e** concentration to see if it follows a similar pattern as orfamide (Figure 4.5, dashed line HO8-1). Alternatively, it could be that the amount of HO8 **2e** keeps increasing (Figure 4.5, dashed line HO8-2) and that a high concentration of HO8 **2e** exerts a different effect on the orfamide production compared to low concentrations.

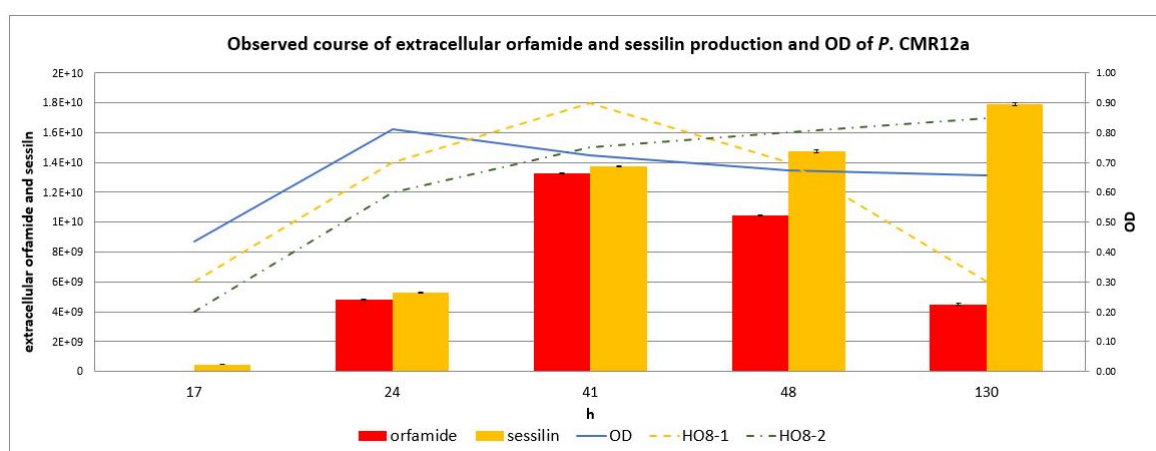


Figure 4.5. Observed course of extracellular orfamide and sessilin (bars not on scale) and OD₆₂₀ of *Pseudomonas* sp. CMR12a. The dashed lines gives two hypothetical courses (HO8-1 and HO8-2) of the QS signal molecule HO8 **2e**.

Also the dependence of sessilin on orfamide to cause a swarming behavior rises many questions. As an orfamide mutant is unable to swarm it was first thought that sessilin only inhibited swarming. However, the present results have shown that sessilin is mostly the causal agent for swarming but requires at least some orfamide to exert its effect. This phenomenon could be further studied in depth by mixing an orfamide mutant with different concentrations of orfamide to see at which concentration swarming reappears.

In this work the focus was on the effect of HO8 **2e** on swarming as this is the main AHL produced by this strain. However, it would be interesting to evaluate the effect of the other produced AHLs. It is expected that the short-chain AHL HO6 **2c** will display a similar effect as HO8 **2e**. This might also be the case for unfunctionalized AHLs C6 **1c** and C8 **1e**, although a drop in activity might be present. The role of longer-chain AHL HO12 **2i** can only be guessed for so far, as the role of the second QS operon Cmr which produces this AHL is not clear yet. In general, a better understanding of the regulation of CLP-production in *Pseudomonas* sp. CMR12a could tremendously aid the application of this strain as a biocontrol agent for tropical regions, either by being able to stimulate metabolite production on desired moments, or by targeted genetical engineering of this strain.

Chapter 5

Experimental part

5.1 General methods

Flame-dried glassware was used for all non-aqueous reactions. Commercially available solvents and reagents were purchased from common chemical suppliers and used without further purification, unless stated otherwise. Sodium borodeuteride (98% D) and D₂O (99.9% D) were purchased from Sigma-Aldrich.

Solvents

Diethyl ether, tetrahydrofuran and toluene were dried by distillation over sodium/ benzophenone ketyl. Methanol was reacted in the presence of magnesium and iodine, distilled and kept over molecular sieves. Dichloromethane was distilled from calcium hydride prior to use. Petroleum ether refers to the 40-60 °C boiling fraction. Acetonitrile was kept over molecular sieves at least 24 hours prior to use.

Column chromatography

The purification of the reaction mixtures was performed by column chromatography with silica gel (Acros, particle size 0.035-0.070 mm, pore diameter ca. 6 nm). Solvent systems were determined via thin layer chromatography (TLC) on glass plates coated with silica gel (Merck, Kieselgel 60 F254, precoated 0.25 mm) using standard visualization techniques or agents: UV fluorescence (254 nm and 366 nm) and coloring with iodine vapors or with potassium permanganate solution.

Liquid chromatography

Liquid chromatography analysis was performed by a reverse phase LC-column (Eclipse plus C18 column). The LC column has dimensions of 50 x 4.6 mm and has a particle size of 3.5 μm. Gradient elution was used (30% acetonitrile in water to 100% acetonitrile over 6 minutes).

Gas chromatography mass spectrometry

GC-MS Spectra were recorded on an Agilent HP 6890 series with a DB-5 MS fused-silica capillary column (30 m; 0.25 mm, film thickness = 0.25 μm) connected to an Agilent HP 5973 series Mass Selective Detector mass spectrometer.

Mass spectrometry

Low-resolution mass spectra were recorded using a direct inlet system with an Agilent 1100 series LC/MSD type SL with a UV detector and mass spectrometer with electrospray ionisation geometry (ESI 70 eV) using a Mass Selective Detector (quadrupole). High-resolution mass spectra were obtained using an Agilent 1100 series HPLC coupled to an Agilent 6210 TOF-Mass Spectrometer, equipped with ESI/APCI-multimode source.

NMR spectroscopy

^1H (300 or 400 MHz) and ^{13}C (75 or 100.6 MHz) NMR spectra were recorded on a Jeol Eclipse FT 300 NMR spectrometer or a Bruker Avance III Nanobay 400 MHz spectrometer at room temperature. Peak assignments were obtained with the aid of DEPT, COSY, HSQC and/or HMBC spectra. The compounds were diluted in deuterated solvents, quoted in parts per million (ppm) with tetramethylsilane as internal standard.

Infrared spectroscopy

IR spectra were recorded with a Perkin-Elmer Spectrum One FTIR spectrometer with an ATR (Attenuated Total Reflectance) accessory in neat form.

Melting point

Melting points were measured using a Kofler bench, type WME Heizbank of Wagner & Munz.

X-ray analysis

For the structure of (*RSS*)-**160b**, X-ray intensity data were collected at room temperature on an Agilent Supernova Dual Source (Cu at zero) diffractometer equipped with an Atlas CCD detector using ω scans and $\text{CuK}\alpha$ ($\lambda = 1.54178 \text{ \AA}$) radiation. The images were interpreted and integrated with the program CrysAlisPro.³⁷⁸ Using Olex2,³⁷⁹ the structure was solved by direct methods using the ShelXS structure solution program and refined by full-matrix least-squares on F² using the ShelXL program package.^{380,381} Non-hydrogen atoms were anisotropically refined and the hydrogen atoms in the riding mode and isotropic temperature factors fixed at 1.2 times $U(\text{eq})$ of the parent atoms (1.5 times for methyl groups).

CCDC 1541166 contains the supplementary crystallographic data for compound (*RSS*)-**160b** and can be obtained free of charge via www.ccdc.cam.ac.uk/conts/retrieving.html (or from the Cambridge Crystallographic Data Centre, 12, Union Road, Cambridge CB2 1EZ, UK; fax: +44-1223-336033; or deposit@ccdc.cam.ac.uk).

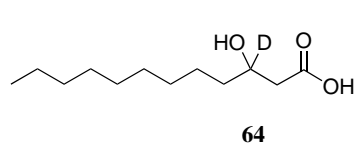
All X-ray diffraction analyzes were performed in collaboration with Prof. Dr. K. Van Hecke, XStruct, Department of Inorganic and Physical Chemistry, Ghent University, Belgium.

5.2 Synthesis of deuterated AHLs

Synthesis of [3-²H]-3-hydroxydodecanoic acid **64**

Diethyl carbonate **61** (2.1 equiv, 22 mmol, 2.5 mL) and sodium hydride (60% dispersion in mineral oil, 3 equiv, 30 mmol, 1.2 g) in 20 mL of dry THF were stirred at reflux under a nitrogen atmosphere. 2-Undecanone **60** (1 equiv, 10 mmol, 2.1 mL) was added dropwise and the resulting mixture was stirred at reflux overnight. After cooling down to r.t., the suspension was poured into a mixture of saturated aq. NH₄Cl, 5% aq. HCl and ice. Extraction (three times 50 mL of diethyl ether) and washing of the combined organic phases, followed by drying over MgSO₄ and removal of the solvent *in vacuo*, afforded 2.3 g of ethyl 3-oxododecanoate **62** (9.4 mmol) as a yellow oil in 94% yield. This crude β-ketoester **62** was used for the next step without further purification.

To a stirred solution of ethyl 3-oxododecanoate **62** (1 equiv, 8.5 mmol, 2.0 g) in 25 mL of methanol was added 22 mL of 2M aq. NaOH (5 equiv, 44 mmol, 1.7 g). The resulting mixture was stirred overnight at room temperature, after which it was extracted with 50 mL of diethyl ether. The organic phase was discarded and the aqueous phase was acidified to pH 2 by addition of 2M aq. HCl, and extracted three times with 50 mL of diethyl ether. The combined organic phases were dried over MgSO₄ and the solvent was removed *in vacuo*. Recrystallization from hexane afforded 3-oxododecanoic acid **63** as a colorless powder (1.37 g, 6.4 mmol, 75% yield). Sodium borodeuteride (1.5 equiv, 7.5 mmol, 0.31 g) was added to a solution of 3-oxododecanoic acid **63** (1 equiv, 5 mmol, 1.1 g) in diethyl ether:methanol 1:1 (10 mL) at 0 °C. The ice bath was removed and the mixture was stirred at room temperature for 2 h. The mixture was diluted with 10 mL of 2M aq. HCl and 10 mL of diethyl ether. After phase separation, the aqueous phase was extracted twice with 10 mL of diethyl ether. The combined extracts were washed with 20 mL of brine and dried over MgSO₄. Filtration and evaporation of the solvent *in vacuo* yielded pure [3-²H]-3-hydroxydodecanoic acid **64** (98%, 1.1 g, 4.95 mmol) as a colorless powder.



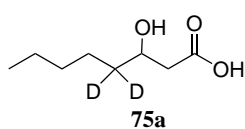
[3-²H]-3-Hydroxydodecanoic acid **64** (89% D). ¹H NMR (400 MHz, CDCl₃): δ = 0.88 (3H, t, *J* = 6.9 Hz, CH₃), 1.20-1.61 (16H, m, (CH₂)₈CH₃), 2.47 (1H, d, *J* = 16.6 Hz, CHH'COOH), 2.58 (1H, d, *J* = 16.6 Hz, CHH'COOH), 4.00-4.11 (0.1H, m, CHOH) ppm. ¹³C NMR (100 MHz, CDCl₃): δ = 14.1 (CH₃), 22.7, 25.4, 29.3, 29.5, 29.6 (2C), 31.9, 36.3 ((CH₂)₈CH₃), 41.0 (CH₂COOH), 67.4-68.3 (m, CDOH), 68.2 (CHOH), 177.8 (COOH) ppm. MS (ESI): *m/z* (%): 218 (M+H⁺, 7), 235 (M+NH₄⁺, 100). HRMS mass calcd.: C₁₂H₂₂DO₃⁻ 216.1715; found: 216.1721. IR (cm⁻¹): ν_{max} 913, 1226 (C-O), 1680 (C=O), 2130 (C-D), 2848, 2915, 2953, 3050 (COO-H), 3534 (O-H). Melting point: 72-74 °C. Colorless powder. Yield: 98%.

General procedure for the synthesis of deuterated aldehydes 66a–d

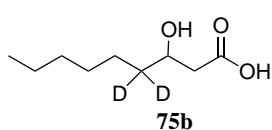
As described by Ariza *et al.*,²³¹ freshly distilled aldehyde **56c,d,g,h** (1 equiv, 13 mmol), 4-(*N,N*-dimethylamino)pyridine (0.1 equiv, 1.3 mmol, 0.16 g) and D₂O (10 equiv, 130 mmol, 2.3 mL) were added to a septum sealed flask and heated at 100 °C for 1 h. Then 20 mL of dichloromethane and 5 mL of 1M aq. HCl were added. The organic phase was washed with 15 mL of saturated aq. NaHCO₃ and 15 mL of brine. Drying over MgSO₄, filtration and removal of the solvent *in vacuo* yielded the deuterated aldehyde **66a–d** (71-97% yield). To obtain a higher degree of deuterium incorporation, the obtained deuterated aldehyde was subjected to a second iteration with fresh D₂O.

General procedure for the synthesis of deuterated β -hydroxy fatty acids 75a–d

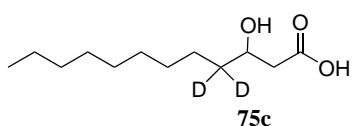
To a stirred suspension of activated zinc dust (acid-washed and dried) (1.3 equiv, 6.5 mmol, 0.43 g) in 20 mL of anhydrous diethyl ether in a flame-dried bulb, was added chlorotrimethylsilane (0.1 equiv, 0.5 mmol, 65 μ L). The mixture was stirred at room temperature for 15 min and then heated at reflux for 10 min. The suspension was allowed to cool down to r.t. and a mixture of ethyl bromoacetate **57** (1 equiv, 5 mmol, 0.57 mL) and deuterated aldehyde **66a–d** (1 equiv, 5 mmol) was added dropwise in such a rate that a gentle reflux was obtained. The resulting mixture was further heated at reflux for 1 h, after which it was cooled down and 20 mL of 2M aq. HCl was added. After stirring for 15 min, the layers were separated and the aqueous phase was extracted two times with 20 mL of diethyl ether. The combined organic phases were washed with 20 mL of saturated aq. NaHCO₃ and 20 mL of brine. Drying over MgSO₄ and removal of the solvent *in vacuo* yielded the desired β -hydroxy ethyl ester **74a–d** as a colorless oil in 92-97% yield. The obtained ester **74a–d** was dissolved in 30 mL of a 2:1 mixture of tetrahydrofuran:methanol and placed in an ice bath. Then, 10 mL of 1M aq. LiOH (2 equiv, 10 mmol, 0.24 g) was added and the stirring was continued for 2 h at 0 °C. Subsequently, the ice bath was removed and the hydrolysis continued at room temperature overnight. The mixture was extracted once with 20 mL of diethyl ether to remove unreacted ester. The aqueous phase was acidified with 2M aq. HCl to pH 2 and extracted three times with 20 mL of diethyl ether. Drying over MgSO₄, filtration and rotary evaporation *in vacuo* of the solvent yielded crude β -hydroxy fatty acid **75a–d**. Recrystallization from diethyl ether gave the pure fatty acid **75a–d** as a colorless powder (84-95% yield).



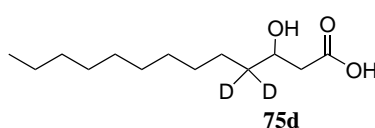
[4,4-di-²H]-3-Hydroxyoctanoic acid **75a** (86% D). ¹H NMR (400 MHz, CDCl₃): δ = 0.89 (3H, t, *J* = 6.7 Hz, CH₃), 1.22-1.48 (6H, m, (CH₂)₃CH₃), 2.46 (1H, dd, *J* = 16.4 Hz, 8.9 Hz, CHH'COOH), 2.58 (1H, dd, *J* = 16.6 Hz, 3.0 Hz, CHH'COOH), 4.04 (1H, dd, *J* = 8.7 Hz, 3.1 Hz, CHOH) ppm. ¹³C NMR (100 MHz, CDCl₃): δ = 14.1 (CH₃), 22.4, 25.1, 31.7 ((CH₂)₃CH₃), 35.1-35.9 (m, CD₂), 41.1 (CH₂COOH), 68.1 (CHOH), 177.9 (COOH) ppm. MS (ESI): *m/z* (%): 163 (M+H⁺, 25), 180 (M+NH₄⁺, 100). HRMS mass calcd.: C₈H₁₄D₂O₃⁻ 161.1152; found: 161.1154. IR (cm⁻¹): ν_{max} 911, 1218 (C-O), 1678 (C=O), 2105 (CD₂), 2180 (CD₂), 2858, 2918, 2952, 3025 (COO-H), 3536 (O-H). Melting point: 48-50 °C. Colorless powder. Yield: 89%.



[4,4-di-²H]-3-Hydroxynonanoic acid **75b** (93% D). ¹H NMR (400 MHz, CDCl₃): δ = 0.88 (3H, t, *J* = 6.8 Hz, CH₃), 1.21-1.50 (8H, m, (CH₂)₄CH₃), 2.48 (1H, dd, *J* = 16.6 Hz, 8.8 Hz, CHH'COOH), 2.58 (1H, dd, *J* = 16.6 Hz, 3.1 Hz, CHH'COOH), 4.03 (1H, dd, *J* = 8.8 Hz, 3.1 Hz, CHOH) ppm. ¹³C NMR (100 MHz, CDCl₃): δ = 14.1 (CH₃), 22.6, 25.2, 29.1, 31.8 ((CH₂)₄CH₃), 35.7 (quintet, *J*_{C-D} = 19.4 Hz, CD₂), 41.0 (CH₂COOH), 68.0 (CHOH), 178.0 (COOH) ppm. MS (ESI): *m/z* (%): 176 (M+H⁺, 26), 194 (M+NH₄⁺, 100). HRMS mass calcd.: C₉H₁₆D₂O₃⁻ 175.1309; found: 175.1311. IR (cm⁻¹): ν_{max} 913, 1218 (C-O), 1681 (C=O), 2103 (CD₂), 2174 (CD₂), 2856, 2916, 2952, 3050 (COO-H), 3536 (O-H). Melting point: 61-63 °C. Colorless powder. Yield: 84%.



[4,4-di-²H]-3-Hydroxydodecanoic acid **75c** (95% D). ¹H NMR (400 MHz, CDCl₃): δ = 0.87 (3H, t, *J* = 7.0 Hz, CH₃), 1.21-1.50 (14H, m, (CH₂)₇CH₃), 2.48 (1H, dd, *J* = 16.5 Hz, 8.9 Hz, CHH'COOH), 2.58 (1H, dd, *J* = 16.5 Hz, 3.2 Hz, CHH'COOH), 4.05 (1H, dd, *J* = 8.9 Hz, 3.2 Hz, CHOH) ppm. ¹³C NMR (100 MHz, CDCl₃): δ = 14.1 (CH₃), 22.7, 25.3, 29.3, 29.4, 29.5, 29.6, 31.9 ((CH₂)₇CH₃), 35.7 (quintet, *J*_{C-D} = 19.8 Hz, CD₂), 41.1 (CH₂COOH), 68.0 (CHOH), 178.0 (COOH) ppm. MS (ESI): *m/z* (%): 201 (M-H₂O, 80), 219 (M+H⁺, 6), 241 (M+Na⁺, 100). HRMS mass calcd.: C₁₂H₂₂D₂O₃NH₄⁺ 236.2189; found: 236.2181. IR (cm⁻¹): ν_{max} 914, 1228 (C-O), 1677 (C=O), 2102 (CD₂), 2179 (CD₂), 2848, 2915, 2953, 3063 (COO-H), 3534 (O-H). Melting point: 73-74 °C. Colorless powder. Yield: 89%.



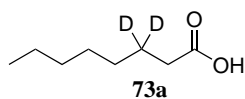
[4,4-di-²H]-3-Hydroxytridecanoic acid **75d** (93% D). ¹H NMR (400 MHz, CDCl₃): δ = 0.88 (3H, t, *J* = 6.8 Hz, CH₃), 1.20-1.48 (16H, m, (CH₂)₈CH₃), 2.47 (1H, dd, *J* = 16.6 Hz, 8.9 Hz, CHH'COOH), 2.58 (1H, dd, *J* = 16.5 Hz, 3.1 Hz, CHH'COOH), 4.02 (1H, dd, *J* = 8.9 Hz, 3.1

Hz, *CHOH*) ppm. ^{13}C NMR (100 MHz, CDCl_3): δ = 14.1 (CH_3), 22.7, 25.2, 29.3, 29.4, 29.56, 29.58, 29.60, 31.9 ($(\text{CH}_2)_8\text{CH}_3$), 35.4-36.2 (m, CD_2), 41.0 (CH_2COOH), 67.9 (*CHOH*), 178.0 (*COOH*) ppm. MS (ESI): m/z (%): 233 ($\text{M}+\text{H}^+$, 7), 250 ($\text{M}+\text{NH}_4^+$, 100). HRMS mass calcd.: $\text{C}_{13}\text{H}_{24}\text{D}_2\text{O}_3\text{NH}_4^+$ 250.2346; found: 250.2340. IR (cm^{-1}): ν_{max} 915, 1219 (C-O), 1681 (C=O), 2100 (CD_2), 2182 (CD_2), 2847, 2914, 2952, 3031 (COO-H), 3534 (O-H). Melting point: 78-80 °C. Colorless powder. Yield: 95%.

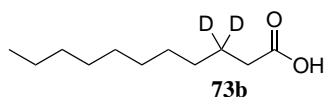
General procedure for the synthesis of deuterated fatty acids **73a-c**

α,α -Dideuterated aldehyde **66b-d** (1 equiv, 10 mmol) was dissolved in 20 mL of a 1:1 methanol: diethyl ether mixture whereafter sodium borohydride (2 equiv, 20 mmol, 0.76 g) was added portionwise. The reaction was stirred for 2 h at room temperature and quenched by the dropwise addition of water. The mixture was acidified by the addition of 2M aq. HCl and the aqueous layer was extracted three times with 20 mL of ethyl acetate. The combined organic phases were washed with 30 mL of brine and dried over MgSO_4 . Removal of the drying agent by filtration and evaporation of the solvent *in vacuo* gave the β,β -dideuterated alcohol (88-96% yield). The obtained crude β,β -dideuterated alcohol (1 equiv, 10 mmol) was dissolved in 30 mL of dry diethyl ether and triethylamine (1.4 equiv, 14 mmol, 2.0 mL) was added. The resulting solution was placed in an ice bath and methanesulfonyl chloride (1.15 equiv, 11.5 mmol, 1.1 mL) was added dropwise. The stirring was continued for 2 h at room temperature, then 25 mL of water was added to the resulting turbid suspension. The phases were separated and the organic phase was washed with 15 mL of saturated aq. NaHCO_3 . Drying over MgSO_4 , filtration and removal of the solvent *in vacuo* gave the desired alkyl methanesulfonate **72a-c** (77-96% yield). To obtain the alkyl nitrile, the mesylate **72a-c** (1 equiv, 10 mmol) was dissolved in dimethyl sulfoxide (30 mL), followed by the addition of potassium cyanide (2.5 equiv, 25 mmol, 1.63 g). Stirring overnight at 120 °C resulted in the formation of a thick precipitate. The reaction mixture was cooled down and partitioned between water (20 mL) and diethyl ether (20 mL). The aqueous layer was extracted three times with diethyl ether (3 x 20 mL) and the combined organic phases were dried over MgSO_4 . Removal of the solvent *in vacuo* yielded the alkyl nitriles (86-95% yield). To a solution of the nitrile (1 equiv, 10 mmol) in 40 mL of methanol was added 4 mL of 10M aq. NaOH (4 equiv, 40 mmol, 1.60 g) and the resulting mixture was stirred at reflux overnight. After cooling down, methanol was removed under reduced pressure and the remaining heterogeneous mixture was heated at reflux for a further 2 h. The suspension was extracted with 20 mL of diethyl ether to remove impurities and unreacted nitrile, followed by acidification with 2M aq. HCl and extraction with diethyl ether (3 x 50 mL). Drying over MgSO_4 and removal of the solvent *in vacuo* yielded the desired deuterium-labelled fatty acids

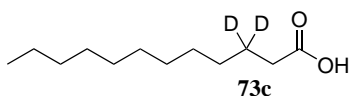
73a–c (58-80% yield).



[3,3-di-²H]-Octanoic acid **73a** (93% D). ¹H NMR (400 MHz, CDCl₃): δ = 0.88 (3H, t, *J* = 6.9 Hz, CH₃), 1.20-1.38 (8H, m, (CH₂)₄CH₃), 2.33 (2H, s, CH₂COOH), 11.56 (1H, br s, COOH) ppm. ¹³C NMR (100 MHz, CDCl₃): δ = 14.1 (CH₃), 22.6, 28.80, 28.84, 31.6 ((CH₂)₄CH₃), 23.5-24.5 (m, CD₂), 34.0 (CH₂COOH), 180.6 (COOH) ppm. IR (cm⁻¹): ν_{max} 934, 1230, 1275 (C-O), 1412, 1705 (C=O), 2857, 2925. Colorless oil. Yield: 58%.



[3,3-di-²H]-Undecanoic acid **73b** (95% D). ¹H NMR (400 MHz, CDCl₃): δ = 0.88 (3H, t, *J* = 6.9 Hz, CH₃), 1.18-1.37 (14H, m, (CH₂)₇CH₃), 2.33 (2H, s, CH₂COOH), 11.31 (1H, br s, COOH) ppm. ¹³C NMR (100 MHz, CDCl₃): δ = 14.1 (CH₃), 22.7, 28.9, 29.2, 29.3, 29.4, 29.6, 31.9 ((CH₂)₇CH₃), 23.5-24.7 (m, CD₂), 33.9 (CH₂COOH), 180.0 (COOH) ppm. IR (cm⁻¹): ν_{max} 927, 1252 (C-O), 1692 (C=O), 2111 (CD₂), 2201 (CD₂), 2850, 2918, 2955, 3019. Colorless oil. Yield: 80%.

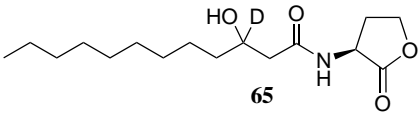


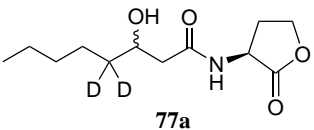
[3,3-di-²H]-Dodecanoic acid **73c** (92% D). ¹H NMR (400 MHz, CDCl₃): δ = 0.88 (3H, t, *J* = 6.6 Hz, CH₃), 1.18-1.37 (16H, m, (CH₂)₈CH₃), 2.32 (2H, s, CH₂COOH), 9.34 (1H, br s, COOH) ppm. ¹³C NMR (100 MHz, CDCl₃): δ = 14.1 (CH₃), 22.7, 28.9, 29.2, 29.3, 29.4, 29.6 (2C), 31.9 ((CH₂)₈CH₃), 23.6-24.8 (m, CD₂), 34.0 (CH₂COOH), 179.9 (COOH) ppm. IR (cm⁻¹): ν_{max} 931, 1275 (C-O), 1429, 1695 (C=O), 2848, 2912. Colorless powder. Melting point: 40-41 °C. Yield: 70%.

General procedure for the synthesis of deuterated AHLs **65**, **77a–d** and **78a–c**

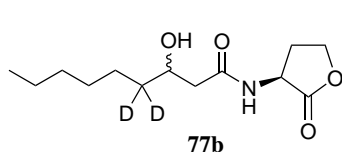
The deuterated analogues of *N*-acyl-L-homoserine lactones **1** and *N*-(3-hydroxyacyl)-L-homoserine lactones **2** were synthesized following the procedure described by Chhabra *et al.*²²⁷ Triethylamine (1 equiv, 2 mmol, 0.28 mL) was added to a stirred solution of L-homoserine lactone hydrobromide **53** (1 equiv, 2 mmol, 0.36 g) in 5 mL of water, followed by the addition of the appropriate deuterated fatty acid (**64**, **73a–c** or **75a–d**, 1 equiv, 2 mmol) and 1-ethyl-3-(3-dimethylaminopropyl)carbodiimide hydrochloride (1 equiv, 2 mmol, 0.38 g). After stirring for 3 h or overnight at room temperature, 15 mL of water was added and the aqueous phase was extracted three times with 20 mL of ethyl acetate. The combined organic phases were washed with 30 mL of saturated aq. NaHCO₃ and 30 mL of brine. Drying over MgSO₄, followed by filtration and evaporation of the solvent *in vacuo* gave the crude product. Purification via column chromatography on silica gel (ethyl acetate:petroleum ether 3:2 to 4:1) yielded the desired

deuterated AHL **65**, **77a-d** and **78a-c** as a colorless powder.

 **65** *N*-(3-Hydroxydodecanoyl-[3-²H])-L-homoserine lactone **65** (89% D). Spectral data were obtained from a 1:1 mixture of diastereomers. ¹H NMR (400 MHz, CDCl₃): δ = 0.88 (3H, t, *J* = 6.9 Hz, CH₃), 1.19-1.57 (16H, m, (CH₂)₈CH₃), 2.13-2.26 (1H, m, OCH₂CHH'), 2.33 (0.5H, d, *J* = 15.4 Hz, CHH'CDOH), 2.35 (0.5H, d, *J* = 15.4 Hz, CHH'CDOH), 2.44 (0.5H, d, *J* = 15.4 Hz, CHH'CDOH), 2.46 (0.5H, d, *J* = 15.4 Hz, CHH'CDOH), 2.81 (1H, dddd, *J* = 12.5 Hz, 8.6 Hz, 5.9 Hz, 1.2 Hz, OCH₂CHH'), 3.13 (1H, br s, OH), 4.0 (0.1H, m, CHOH), 4.29 (1H, ddd, *J* = 11.2 Hz, 9.3 Hz, 6.0 Hz, OCHH'), 4.480 (0.5H, td, *J* = 9.1 Hz, 1.3 Hz, OCHH'), 4.483 (0.5H, td, *J* = 9.1 Hz, 1.4 Hz, OCHH'), 4.56 (0.5H, ddd, *J* = 11.7 Hz, 8.6 Hz, 6.2 Hz, CHN), 4.59 (0.5H, ddd, *J* = 11.8 Hz, 8.7 Hz, 6.3 Hz, CHN), 6.60 (0.5H, d, *J* = 5.8 Hz, NH), 6.65 (0.5H, d, *J* = 5.7 Hz, NH) ppm. ¹³C NMR (100 MHz, CDCl₃): δ = 14.1 (CH₃), 22.7, 25.5, 29.3, 29.5, 29.56, 29.59, 31.9, 36.8, 36.9 ((CH₂)₈CH₃), 29.9 (CH₂CHN), 30.0 (CH₂CHN), 42.5 (CH₂CONH), 42.6 (CH₂CONH), 49.0 (CHN), 49.2 (CHN), 66.1 (CH₂O), 66.2 (CH₂O), 68.2 (t, *J*_{C-D} = 21.6 Hz, CDOH), 68.3 (t, *J*_{C-D} = 21.7 Hz, CDOH), 68.6 (COH_{unlabelled}), 68.7 (COH_{unlabelled}), 173.0 (CONH), 173.1 (CONH), 175.70 (COO), 175.74 (COO) ppm. MS (ESI): *m/z* (%): 301 (M+H⁺, 100). HRMS mass calcd.: C₁₆H₂₉DNO₄H⁺ 301.2232; found: 301.2237. IR (cm⁻¹): ν_{max} 951, 1008, 1178, 1548 (HN-C=O), 1627 (HN-C=O), 1768 (C=O_{lactone}), 2850, 2919, 3315 (N-H or O-H), 3494 (N-H or O-H). Chromatography: EtOAc:petroleum ether 4:1 R_f = 0.16. Melting point: 107-108 °C. Colorless powder. Yield: 65%.

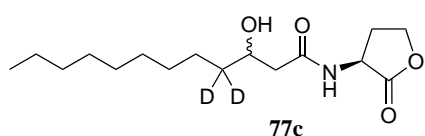
 **77a** *N*-(3-Hydroxyoctanoyl-[4,4-di-²H])-L-homoserine lactone **77a** (86% D). Spectral data were obtained from a 3:2 mixture of diastereomers. ¹H NMR (400 MHz, CDCl₃): δ diastereomer 1 (major): 0.88 (3H, t, *J* = 6.8 Hz, CH₃), 1.19-1.43 (6H, m, (CH₂)₃CH₃), 2.15-2.27 (1H, m, OCH₂CHH'), 2.35 (1H, dd, *J* = 15.6 Hz, 8.9 Hz, CHH'CHOH), 2.43 (1H, dd, *J* = 15.6 Hz, 2.8 Hz, CHH'CHOH), 2.82 (1H, dddd, *J* = 12.8 Hz, 8.4 Hz, 5.9 Hz, 1.1 Hz, OCH₂CHH'), 3.05 (1H, br s, OH), 4.00-4.06 (1H, m, CHOH), 4.29 (1H, ddd, *J* = 11.3 Hz, 9.3 Hz, 6.0 Hz, OCHH'), 4.43-4.50 (1H, m, OCHH'), 4.58 (1H, ddd, *J* = 11.6 Hz, 8.7 Hz, 6.2 Hz, CHN), 6.58 (1H, d, *J* = 5.6 Hz, NH) ppm; diastereomer 2 (minor): 0.88 (3H, t, *J* = 6.8 Hz, CH₃), 1.19-1.43 (6H, m, (CH₂)₃CH₃), 2.15-2.27 (1H, m, OCH₂CHH'), 2.33 (1H, dd, *J* = 15.6 Hz, 8.9 Hz, CHH'CHOH), 2.46 (1H, dd, *J* = 15.6 Hz, 2.8 Hz, CHH'CHOH), 2.82 (1H, dddd, *J* = 12.8 Hz, 8.4 Hz, 5.9 Hz, 1.1 Hz, OCH₂CHH'), 3.05 (1H, br s, OH), 4.00-4.06 (1H, m, CHOH), 4.29 (1H, ddd, *J* = 11.3 Hz, 9.3 Hz, 6.0 Hz, OCHH'), 4.43-4.50 (1H, m, OCHH'), 4.56 (1H, ddd, *J* = 11.5 Hz, 8.7 Hz, 6.1 Hz, CHN), 6.50 (1H, d, *J* = 5.6 Hz, NH) ppm. ¹³C NMR (100 MHz, CDCl₃): δ diastereomer 1 (major): 14.1

(CH₃), 22.4, 25.2, 31.8 ((CH₂)₃CH₃), 29.8 (CH₂CHN), 36.0-36.9 (m, CD₂), 42.7 (CH₂CONH), 49.2 (CHN), 66.20 (CH₂O), 68.6 (COH), 173.1 (CONH), 175.9 (COO) ppm; diastereomer 2 (minor): 14.1 (CH₃), 22.4, 25.2, 31.8 ((CH₂)₃CH₃), 29.7 (CH₂CHN), 36.0-36.9 (m, CD₂), 42.6 (CH₂CONH), 49.0 (CHN), 66.18 (CH₂O), 68.5 (COH), 173.0 (CONH), 175.8 (COO) ppm. MS (ESI): *m/z* (%): 246 (M+H⁺, 100). HRMS mass calcd.: C₁₂H₁₉D₂NO₄H⁺ 246.1669; found: 246.1672. IR (cm⁻¹): ν_{max} 948, 1018, 1177, 1382, 1541 (HN-C=O), 1644 (HN-C=O), 1771 (C=O_{lactone}), 2101 (CD₂), 2179 (CD₂), 2849, 2940, 2957, 3342 (N-H or O-H). Chromatography: EtOAc:petroleum ether 4:1 R_f = 0.15. Melting point: 85-87 °C. Colorless powder. Yield: 48%.



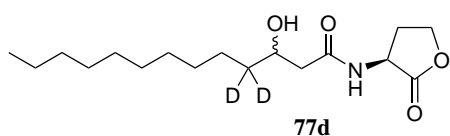
N-(3-Hydroxynonanoyl-[4,4-di-²H])-L-homoserine lactone **77b**

(93% D). Spectral data were obtained from a 3:2 mixture of diastereomers. ¹H NMR (400 MHz, CDCl₃): δ diastereomer 1 (major): 0.88 (3H, t, *J* = 6.8 Hz, CH₃), 1.20-1.45 (8H, m, (CH₂)₄CH₃), 2.13-2.26 (1H, m, OCH₂CHH'), 2.35 (1H, dd, *J* = 15.5 Hz, 8.9 Hz, CHH'CHOH), 2.44 (1H, dd, *J* = 15.5 Hz, 2.8 Hz, CHH'CHOH), 2.82 (1H, dddd, *J* = 12.6 Hz, 8.6 Hz, 5.9 Hz, 1.1 Hz, OCH₂CHH'), 3.10 (1H, br s, OH), 3.99-4.06 (1H, m, CHOH), 4.29 (1H, ddd, *J* = 11.3 Hz, 9.3 Hz, 5.9 Hz, OCHH'), 4.45-4.51 (1H, m, OCHH'), 4.58 (1H, ddd, *J* = 11.6 Hz, 8.7 Hz, 6.2 Hz, CHN), 6.60 (1H, d, *J* = 5.6 Hz, NH) ppm; diastereomer 2 (minor): 0.88 (3H, t, *J* = 6.8 Hz, CH₃), 1.20-1.45 (8H, m, (CH₂)₄CH₃), 2.13-2.26 (1H, m, OCH₂CHH'), 2.33 (1H, dd, *J* = 15.5 Hz, 8.9 Hz, CHH'CHOH), 2.46 (1H, dd, *J* = 15.5 Hz, 2.8 Hz, CHH'CHOH), 2.82 (1H, dddd, *J* = 12.6 Hz, 8.6 Hz, 5.9 Hz, 1.1 Hz, OCH₂CHH'), 3.10 (1H, br s, OH), 3.99-4.06 (1H, m, CHOH), 4.29 (1H, ddd, *J* = 11.3 Hz, 9.3 Hz, 5.9 Hz, OCHH'), 4.45-4.51 (1H, m, OCHH'), 4.56 (1H, ddd, *J* = 11.5 Hz, 8.7 Hz, 6.1 Hz, CHN), 6.55 (1H, d, *J* = 5.6 Hz, NH) ppm. ¹³C NMR (100 MHz, CDCl₃): δ diastereomer 1 (major): 14.1 (CH₃), 22.6, 25.3, 29.1, 31.8 ((CH₂)₄CH₃), 29.8 (CH₂CHN), 35.8-36.7 (m, CD₂), 42.7 (CH₂CONH), 49.1 (CHN), 66.18 (CH₂O), 68.6 (COH), 173.1 (CONH), 175.9 (COO) ppm; diastereomer 2 (minor): 14.1 (CH₃), 22.6, 25.3, 29.1, 31.8 ((CH₂)₄CH₃), 29.7 (CH₂CHN), 35.8-36.7 (m, CD₂), 42.6 (CH₂CONH), 48.9 (CHN), 66.15 (CH₂O), 68.5 (COH), 173.0 (CONH), 175.8 (COO) ppm. MS (ESI): *m/z* (%): 260 (M+H⁺, 100). HRMS mass calcd.: C₁₃H₂₁D₂NO₄H⁺ 260.1831; found: 260.1832. IR (cm⁻¹): ν_{max} 950, 1012, 1174, 1382, 1543 (HN-C=O), 1645 (HN-C=O), 1768 (C=O_{lactone}), 2103 (CD₂), 2184 (CD₂), 2855, 2920, 2956, 3302 (N-H or O-H). Chromatography: EtOAc:petroleum ether 4:1 R_f = 0.18. Melting point: 97-98 °C. Colorless powder. Yield: 58%.



N-(3-Hydroxydodecanoyl)-[4,4-di-²H]-L-homoserine lactone **77c** (95% D). Spectral data were obtained from a 5:4 mixture of diastereomers. ¹H NMR (400 MHz, CDCl₃):

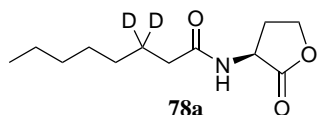
δ diastereomer 1 (major): 0.88 (3H, t, $J = 6.9$ Hz, CH₃), 1.19-1.43 (14H, m, (CH₂)₇CH₃), 2.13-2.26 (1H, m, OCH₂CHH'), 2.35 (1H, dd, $J = 15.4$ Hz, 8.9 Hz, CHH'CHOH), 2.43 (1H, dd, $J = 15.4$ Hz, 2.8 Hz, CHH'CHOH), 2.77-2.86 (1H, m, OCH₂CHH'), 3.11 (1H, br s, OH), 3.98-4.05 (1H, m, CHOH), 4.29 (1H, ddd, $J = 11.2$ Hz, 9.3 Hz, 5.9 Hz, OCHH'), 4.43-4.51 (1H, m, OCHH'), 4.59 (1H, ddd, $J = 11.6$ Hz, 8.8 Hz, 6.1 Hz, CHN), 6.53-6.64 (1H, m, NH) ppm; diastereomer 2 (minor): 0.88 (3H, t, $J = 6.9$ Hz, CH₃), 1.19-1.43 (14H, m, (CH₂)₇CH₃), 2.13-2.26 (1H, m, OCH₂CHH'), 2.33 (1H, dd, $J = 15.3$ Hz, 8.9 Hz, CHH'CHOH), 2.46 (1H, dd, $J = 15.4$ Hz, 2.7 Hz, CHH'CHOH), 2.77-2.86 (1H, m, OCH₂CHH'), 3.11 (1H, br s, OH), 3.98-4.05 (1H, m, CHOH), 4.29 (1H, ddd, $J = 11.2$ Hz, 9.3 Hz, 5.9 Hz, OCHH'), 4.43-4.51 (1H, m, OCHH'), 4.56 (1H, ddd, $J = 11.6$ Hz, 8.7 Hz, 6.1 Hz, CHN), 6.53-6.64 (1H, m, NH) ppm. ¹³C NMR (100 MHz, CDCl₃): δ diastereomer 1 (major): 14.1 (CH₃), 22.7, 25.3, 29.3, 29.5, 29.56, 29.60, 31.9 ((CH₂)₇CH₃), 30.04 (CH₂CHN), 35.8-36.8 (m, CD₂), 42.6 (CH₂CONH), 49.2 (CHN), 66.2 (CH₂O), 68.6 (COH), 173.05 (CONH), 175.67 (COO), 175.75 (COO) ppm; diastereomer 2 (minor): 14.1 (CH₃), 22.7, 25.3, 29.3, 29.5, 29.56, 29.60, 31.9 ((CH₂)₇CH₃), 29.98 (CH₂CHN), 35.8-36.8 (m, CD₂), 42.5 (CH₂CONH), 49.0 (CHN), 66.1 (CH₂O), 68.5 (COH), 173.01 (CONH), 175.67 (COO) ppm. MS (ESI): m/z (%): 302 (M+H⁺, 100). HRMS mass calcd.: C₁₆H₂₇D₂NO₄H⁺ 302.2300; found: 302.2300. IR (cm⁻¹): ν_{max} 952, 1014, 1177, 1382, 1549 (HN-C=O), 1625 (HN-C=O), 1766 (C=O_{lactone}), 2082 (CD₂), 2185 (CD₂), 2851, 2919, 2956, 3326 (N-H or O-H), 3461 (N-H or O-H). Chromatography: EtOAc:petroleum ether 4:1 R_f = 0.15. Melting point: 107-108 °C. Colorless powder. Yield: 63%.



N-(3-Hydroxytridecanoyl)-[4,4-di-²H]-L-homoserine lactone **77d** (93% D). Spectral data were obtained from a 5:4 mixture of diastereomers. ¹H NMR (400 MHz, CDCl₃):

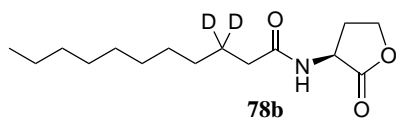
δ diastereomer 1 (major): 0.88 (3H, t, $J = 6.9$ Hz, CH₃), 1.19-1.43 (16H, m, (CH₂)₈CH₃), 2.13-2.25 (1H, m, OCH₂CHH'), 2.35 (1H, dd, $J = 15.4$ Hz, 8.7 Hz, CHH'CHOH), 2.43 (1H, dd, $J = 15.4$ Hz, 2.8 Hz, CHH'CHOH), 2.79-2.87 (1H, m, OCH₂CHH'), 3.04 (1H, br s, OH), 3.98-4.04 (1H, m, CHOH), 4.29 (1H, ddd, $J = 11.2$ Hz, 9.3 Hz, 5.9 Hz, OCHH'), 4.45-4.51 (1H, m, OCHH'), 4.57 (1H, ddd, $J = 11.6$ Hz, 8.6 Hz, 5.7 Hz, CHN), 6.46-6.57 (1H, m, NH) ppm; diastereomer 2 (minor): 0.88 (3H, t, $J = 6.9$ Hz, CH₃), 1.19-1.43 (16H, m, (CH₂)₈CH₃), 2.13-2.25 (1H, m, OCH₂CHH'), 2.33 (1H, dd, $J = 15.5$ Hz, 9.0 Hz, CHH'CHOH), 2.46 (1H, dd, $J = 15.3$ Hz, 2.8 Hz, CHH'CHOH), 2.79-2.87 (1H, m, OCH₂CHH'), 3.04 (1H, br s, OH), 3.98-4.04 (1H,

m, *CHOH*), 4.29 (1H, ddd, $J = 11.2$ Hz, 9.3 Hz, 5.9 Hz, *OCHH'*), 4.45-4.51 (1H, m, *OCHH'*), 4.56 (1H, ddd, $J = 11.6$ Hz, 8.6 Hz, 5.9 Hz, *CHN*), 6.46-6.57 (1H, m, *NH*) ppm. ^{13}C NMR (100 MHz, CDCl_3): δ diastereomer 1 (major): 14.1 (CH_3), 22.7, 25.3, 29.3, 29.5, 29.6 (3C), 31.9 ($(\text{CH}_2)_8\text{CH}_3$), 30.0 (CH_2CHN), 35.7-36.8 (m, CD_2), 42.6 (CH_2CONH), 49.1 (CHN), 66.2 (CH_2O), 68.6 (*COH*), 173.05 (*CONH*), 175.7 (*COO*) ppm; diastereomer 2 (minor): 14.1 (CH_3), 22.7, 25.3, 29.3, 29.5, 29.6 (3C), 31.9 ($(\text{CH}_2)_8\text{CH}_3$), 29.9 (CH_2CHN), 35.7-36.8 (m, CD_2), 42.5 (CH_2CONH), 49.0 (CHN), 66.1 (CH_2O), 68.5 (*COH*), 173.02 (*CONH*), 175.7 (*COO*) ppm. MS (ESI): m/z (%): 316 ($\text{M}+\text{H}^+$, 100). HRMS mass calcd.: $\text{C}_{17}\text{H}_{29}\text{D}_2\text{NO}_4\text{H}^+$ 316.2457; found: 316.2448. IR (cm^{-1}): ν_{max} 948, 1022, 1177, 1382, 1549 (*HN-C=O*), 1641 (*HN-C=O*), 1770 (*C=O_{lactone}*), 2102 (CD_2), 2177 (CD_2), 2849, 2917, 2953, 3312 (N-H or O-H), 3490 (N-H or O-H). Chromatography: EtOAc:petroleum ether 4:1 $R_f = 0.16$. Melting point: 110-112 °C. Colorless powder. Yield: 42%.



N-(Octanoyl-[3,3-di- ^2H])-L-homoserine lactone **78a** (92% D).

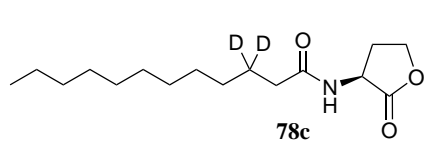
^1H NMR (400 MHz, CDCl_3): $\delta = 0.88$ (3H, t, $J = 6.9$ Hz, CH_3), 1.20-1.36 (8H, m, $(\text{CH}_2)_4\text{CH}_3$), 2.12 (1H, dddd, $J = 12.5$ Hz, 11.5 Hz, 11.5 Hz, 8.8 Hz, *OCH}_2\text{CHH}'*), 2.23 (2H, s, CH_2CONH), 2.88 (1H, dddd, $J = 12.5$ Hz, 8.5 Hz, 5.8 Hz, 1.2 Hz, *OCH}_2\text{CHH}'*), 4.28 (1H, ddd, $J = 11.3$ Hz, 9.3 Hz, 5.8 Hz, *OCHH}'*), 4.47 (1H, td, $J = 9.1$ Hz, 1.0 Hz, *OCHH}'*), 4.54 (1H, ddd, $J = 11.6$ Hz, 8.5 Hz, 5.6 Hz, *CHN*), 5.94 (1H, s, *NH*) ppm. ^{13}C NMR (100 MHz, CDCl_3): $\delta = 14.1$ (CH_3), 22.6, 28.9, 29.0, 31.6 ($(\text{CH}_2)_4\text{CH}_3$), 24.4-25.4 (m, CD_2), 30.6 (CH_2CHN), 36.0 (CH_2CONH), 49.2 (CHN), 66.1 (CH_2O), 173.8 (*CONH*), 175.7 (*COO*) ppm. MS (ESI): m/z (%): 230 ($\text{M}+\text{H}^+$, 100). HRMS mass calcd.: $\text{C}_{12}\text{H}_{19}\text{D}_2\text{NO}_3\text{H}^+$ 230.1725; found: 230.1709. IR (cm^{-1}): ν_{max} 1010, 1170, 1545 (*HN-C=O*), 1643 (*HN-C=O*), 1774 (*C=O_{lactone}*), 2107 (CD_2), 2194 (CD_2), 2852, 2920, 3314 (N-H or O-H). Chromatography: EtOAc:petroleum ether 3:2 $R_f = 0.19$. Melting point: 130-132 °C. Colorless powder. Yield: 55%.



N-(Undecanoyl-[3,3-di- ^2H])-L-homoserine lactone **78b** (95% D).

^1H NMR (400 MHz, CDCl_3): $\delta = 0.88$ (3H, t, $J = 6.9$ Hz, CH_3), 1.21-1.32 (14H, m, $(\text{CH}_2)_7\text{CH}_3$), 2.12 (1H, dddd, $J = 12.5$ Hz, 11.5 Hz, 11.5 Hz, 8.8 Hz, *OCH}_2\text{CHH}'*), 2.23 (2H, s, CH_2CONH), 2.88 (1H, dddd, $J = 12.6$ Hz, 8.5 Hz, 5.8 Hz, 1.1 Hz, *OCH}_2\text{CHH}'*), 4.29 (1H, ddd, $J = 11.3$ Hz, 9.3 Hz, 5.9 Hz, *OCHH}'*), 4.47 (1H, td, $J = 9.1$ Hz, 1.0 Hz, *OCHH}'*), 4.54 (1H, ddd, $J = 11.6$ Hz, 8.5 Hz, 5.6 Hz, *CHN*), 5.96 (1H, d, $J = 5.6$ Hz, *NH*) ppm. ^{13}C NMR (100 MHz, CDCl_3): $\delta = 14.1$ (CH_3), 22.7, 29.0, 29.28, 29.30, 29.5, 29.6, 31.9 ($(\text{CH}_2)_7\text{CH}_3$), 24.7 (quintet, $J_{\text{C-D}} = 19.2$ Hz, CD_2), 30.5 (CH_2CHN), 36.0 (CH_2CONH), 49.2 (CHN), 66.1 (CH_2O), 173.8 (*CONH*), 175.7 (*COO*) ppm.

MS (ESI): m/z (%): 272 ($M+H^+$, 100). HRMS mass calcd.: $C_{15}H_{25}D_2NO_3H^+$ 272.2195; found: 272.2182. IR (cm^{-1}): ν_{max} 1010, 1171, 1547 (HN-C=O), 1643 (HN-C=O), 1779 (C=O_{lactone}), 2113 (CD₂), 2205 (CD₂), 2851, 2919, 3315 (N-H or O-H). Chromatography: EtOAc:petroleum ether 3:2 R_f = 0.21. Melting point: 135-136 °C. Colorless powder. Yield: 69%.

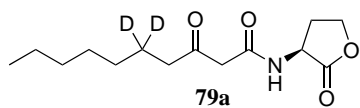


N-(Dodecanoyl-[3,3-di-²H])*L*-homoserine lactone **78c** (92% D). ¹H NMR (400 MHz, CDCl₃): δ = 0.88 (3H, t, J = 6.9 Hz, CH₃), 1.19-1.35 (16H, m, (CH₂)₈CH₃), 2.12 (1H, dddd, J = 12.5 Hz, 11.5 Hz, 11.5 Hz, 8.8 Hz, OCH₂CHH'), 2.23 (2H, s, CH₂CONH), 2.88 (1H, dddd, J = 12.6 Hz, 8.5 Hz, 5.8 Hz, 1.1 Hz, OCH₂CHH'), 4.28 (1H, ddd, J = 11.3 Hz, 9.3 Hz, 5.8 Hz, OCHH'), 4.47 (1H, td, J = 9.1 Hz, 1.0 Hz, OCHH'), 4.53 (1H, ddd, J = 11.6 Hz, 8.5 Hz, 5.6 Hz, CHN), 5.93 (1H, d, J = 4.8 Hz, NH) ppm. ¹³C NMR (100 MHz, CDCl₃): δ = 14.1 (CH₃), 22.7, 29.0, 29.27, 29.32, 29.5, 29.6 (2C), 31.9 ((CH₂)₈CH₃), 24.3-25.4 (m, CD₂), 30.4 (CH₂CHN), 36.0 (CH₂CONH), 49.1 (CHN), 66.1 (CH₂O), 173.8 (CONH), 175.8 (COO) ppm. MS (ESI): m/z (%): 286 ($M+H^+$, 100). HRMS mass calcd.: $C_{16}H_{27}D_2NO_3H^+$ 286.2351; found: 286.2335. IR (cm^{-1}): ν_{max} 1010, 1171, 1546 (HN-C=O), 1643 (HN-C=O), 1775 (C=O_{lactone}), 2110 (CD₂), 2194 (CD₂), 2850, 2918, 3315 (N-H or O-H). Chromatography: EtOAc:petroleum ether 3:2 R_f = 0.23. Melting point: 137-139 °C. Colorless powder. Yield: 52%.

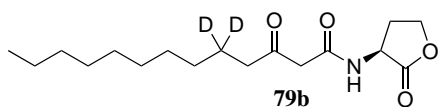
General procedure for the synthesis of deuterated AHLs **79a–c**

To a stirred solution of β,β -dideuterated fatty acid **73a–c** (1 equiv, 2 mmol) in 20 mL of dry dichloromethane, was added 4-(*N,N*-dimethylamino)pyridine (2.1 equiv, 4.2 mmol, 0.51 g), 1-ethyl-3-(3-dimethylaminopropyl)carbodiimide hydrochloride (1.1 equiv, 2.2 mmol, 0.42 g) and Meldrum's acid (1 equiv, 2 mmol, 0.29 g). The resulting clear yellow solution was stirred for 20 h at room temperature. The solvent was removed by rotary evaporation *in vacuo*, the residue was redissolved in ethyl acetate (50 mL) and washed with 30 mL of 2M aq. HCl. Drying over MgSO₄, followed by filtration to remove the drying agent and evaporation of the solvent *in vacuo* yielded acylated Meldrum's acid **76a–c** quantitatively, which was used without further purification. The deuterium-labelled, acylated Meldrum's acid **76a–c** was dissolved in acetonitrile (30 mL), after which triethylamine (1.2 equiv, 2.4 mmol, 0.33 mL) and *L*-homoserine lactone hydrobromide **53** (1 equiv, 2 mmol, 0.36 g) were added. The mixture was stirred at room temperature for 2 h and then heated at reflux overnight. The solvent was removed *in vacuo* and the resulting residue was dissolved in 30 mL of ethyl acetate and 30 mL of water. After separation of both layers, the aqueous phase was extracted two times with 30 mL of ethyl acetate. The combined organic phases were washed with 60 mL of saturated aq. NaHCO₃ and 60 mL of brine. Drying over MgSO₄ and removal of the solvent *in vacuo* yielded crude deuterated AHL

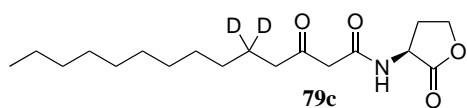
79a–c. Purification via column chromatography on silica gel (ethyl acetate:petroleum ether 3:2 to 4:1) gave the pure product as a colorless powder.



79a (93% D). ^1H NMR (400 MHz, CDCl_3): δ = 0.88 (3H, t, J = 6.8 Hz, CH_3), 1.20-1.32 (8H, m, $(\text{CH}_2)_4\text{CH}_3$), 2.23 (1H, dddd, J = 12.5 Hz, 11.3 Hz, 11.3 Hz, 8.9 Hz, $\text{OCH}_2\text{CHH}'$), 2.51 (2H, s, CH_2CONH), 2.76 (1H, dddd, J = 12.6 Hz, 8.7 Hz, 6.0 Hz, 1.4 Hz, $\text{OCH}_2\text{CHH}'$), 3.47 (2H, s, COCH_2CO), 4.28 (1H, ddd, J = 11.0 Hz, 9.3 Hz, 6.1 Hz, OCHH'), 4.47 (1H, td, J = 9.1 Hz, 1.3 Hz, OCHH'), 4.59 (1H, ddd, J = 11.5 Hz, 8.7 Hz, 6.6 Hz, CHN), 7.66 (1H, d, J = 5.6 Hz, NH) ppm. ^{13}C NMR (100 MHz, CDCl_3): δ = 14.1 (CH_3), 22.6, 28.7, 28.9, 31.6 ($(\text{CH}_2)_4\text{CH}_3$), 22.2-23.4 (m, CD_2), 29.6 (CH_2CHN), 43.6 ($\text{CD}_2\text{CH}_2\text{CO}$), 48.4 (COCH_2CO), 49.0 (CHN), 65.9 (CH_2O), 166.5 (CONH), 175.0 (COO), 206.5 (CH_2COCH_2) ppm. MS (ESI): m/z (%): 272 ($\text{M}+\text{H}^+$, 100), 289 ($\text{M}+\text{NH}_4^+$, 20). HRMS mass calcd.: $\text{C}_{14}\text{H}_{21}\text{D}_2\text{NO}_4\text{H}^+$ 272.1831; found: 272.1833. IR (cm^{-1}): ν_{max} 1010, 1023, 1165, 1356, 1548 ($\text{HN}-\text{C}=\text{O}$), 1646 ($\text{HN}-\text{C}=\text{O}$), 1712 ($\text{C}=\text{O}_{\text{ketone}}$), 1776 ($\text{C}=\text{O}_{\text{lactone}}$), 2112 (CD_2), 2193 (CD_2), 2851, 2918, 2957, 3081 (N-H or O-H), 3284 (N-H or O-H). Chromatography: EtOAc:petroleum ether 3:2 R_f = 0.21. Melting point: 81-82 °C. Colorless powder. Yield: 49%.



79b (95% D). ^1H NMR (400 MHz, CDCl_3): δ = 0.88 (3H, t, J = 6.8 Hz, CH_3), 1.19-1.33 (14H, m, $(\text{CH}_2)_7\text{CH}_3$), 2.24 (1H, dddd, J = 12.5 Hz, 11.3 Hz, 11.3 Hz, 9.0 Hz, $\text{OCH}_2\text{CHH}'$), 2.51 (2H, s, CH_2CONH), 2.76 (1H, dddd, J = 12.5 Hz, 8.7 Hz, 6.1 Hz, 1.4 Hz, $\text{OCH}_2\text{CHH}'$), 3.47 (2H, s, COCH_2CO), 4.28 (1H, ddd, J = 11.0 Hz, 9.3 Hz, 6.1 Hz, OCHH'), 4.48 (1H, td, J = 9.1 Hz, 1.3 Hz, OCHH'), 4.60 (1H, ddd, J = 11.5 Hz, 8.7 Hz, 6.6 Hz, CHN), 7.67 (1H, d, J = 5.7 Hz, NH) ppm. ^{13}C NMR (100 MHz, CDCl_3): δ = 14.1 (CH_3), 22.7, 28.8, 29.3, 29.4, 29.5, 29.6, 31.9 ($(\text{CH}_2)_7\text{CH}_3$), 22.2-23.4 (m, CD_2), 29.7 (CH_2CHN), 43.7 ($\text{CD}_2\text{CH}_2\text{CO}$), 48.2 (COCH_2CO), 49.0 (CHN), 65.9 (CH_2O), 166.4 (CONH), 174.7 (COO), 206.6 (CH_2COCH_2) ppm. MS (ESI): m/z (%): 314 ($\text{M}+\text{H}^+$, 100), 331 ($\text{M}+\text{NH}_4^+$, 21). HRMS mass calcd.: $\text{C}_{17}\text{H}_{27}\text{D}_2\text{NO}_4\text{H}^+$ 314.2295; found: 314.2305. IR (cm^{-1}): ν_{max} 1006, 1016, 1176, 1356, 1544 ($\text{HN}-\text{C}=\text{O}$), 1642 ($\text{HN}-\text{C}=\text{O}$), 1716 ($\text{C}=\text{O}_{\text{ketone}}$), 1776 ($\text{C}=\text{O}_{\text{lactone}}$), 2092 (CD_2), 2164 (CD_2), 2850, 2919, 3071 (N-H or O-H), 3294 (N-H or O-H). Chromatography: EtOAc:petroleum ether 4:1 R_f = 0.37. Melting point: 86-88 °C. Colorless powder. Yield: 66%.

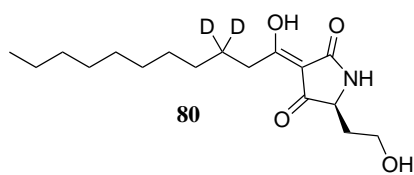


N-(3-Oxotetradecanoyl-[5,5-di-²H])-L-homoserine lactone **79c** (93% D). ¹H NMR (400 MHz, CDCl₃): δ = 0.88 (3H, t, *J* = 6.9 Hz, CH₃), 1.20-1.32 (16H, m, (CH₂)₈CH₃), 2.23 (1H, dddd, *J* = 12.5 Hz, 11.3 Hz, 11.3 Hz, 9.0 Hz, OCH₂CHH'), 2.51 (2H, s, CH₂CONH), 2.76 (1H, dddd, *J* = 12.6 Hz, 8.7 Hz, 6.1 Hz, 1.4 Hz, OCH₂CHH'), 3.47 (2H, s, COCH₂CO), 4.28 (1H, ddd, *J* = 11.1 Hz, 9.3 Hz, 6.1 Hz, OCHH'), 4.48 (1H, td, *J* = 9.1 Hz, 1.3 Hz, OCHH'), 4.59 (1H, ddd, *J* = 11.5 Hz, 8.7 Hz, 6.6 Hz, CHN), 7.66 (1H, d, *J* = 5.4 Hz, NH) ppm.

¹³C NMR (100 MHz, CDCl₃): δ = 14.1 (CH₃), 22.7, 28.8, 29.30, 29.32, 29.4, 29.6, 29.8, 31.9 ((CH₂)₈CH₃), 22.3-23.2 (m, CD₂), 29.6 (CH₂CHN), 43.7 (CD₂CH₂CO), 48.2 (COCH₂CO), 49.0 (CHN), 65.9 (CH₂O), 166.4 (CONH), 174.9 (COO), 206.6 (CH₂COCH₂) ppm. MS (ESI): *m/z* (%): 328 (M+H⁺, 100), 345 (M+NH₄⁺, 19). HRMS mass calcd.: C₁₈H₂₉D₂NO₄H⁺ 328.2457; found: 328.2446. IR (cm⁻¹): ν_{max} 1007, 1016, 1176, 1356, 1544 (HN-C=O), 1641 (HN-C=O), 1716 (C=O_{ketone}), 1775 (C=O_{lactone}), 2101 (CD₂), 2192 (CD₂), 2850, 2918, 2954, 3073 (N-H or O-H), 3294 (N-H or O-H). Chromatography: EtOAc:petroleum ether 3:2 R_f = 0.24. Melting point: 94-95 °C. Colorless powder. Yield: 54%.

Synthesis of tetramic acid **80**

313 mg of *N*-(3-oxotridecanoyl-[5,5-di-²H])-L-homoserine lactone **79b** (1 equiv, 1 mmol) was dissolved in 3 mL of dry methanol under a nitrogen atmosphere. Then 1 equiv of NaOMe in methanol (0.5M, 54 mg in 2 mL) was added and the mixture was stirred at reflux for 3 h. Subsequently, the reaction mixture was poured into 10 mL of water and extracted with 10 mL of diethyl ether. The organic phase was discarded and the aqueous phase was acidified with 2M aq. HCl and extracted three times with 10 mL of diethyl ether. Drying of the combined organic phases over MgSO₄, evaporation of the solvent *in vacuo* and recrystallization from hexane yielded 250 mg of tetramic acid **80** as a colorless powder.



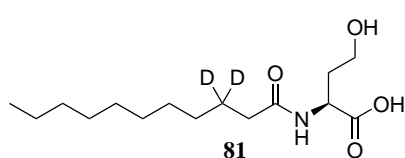
3-(1-Hydroxyundecylidene-[5,5-di-²H])-5-(2-hydroxyethyl)pyrrolidine-2,4-dione **80** (95% D). ¹H NMR (400 MHz, CD₃OD): δ = 0.88 (3H, t, *J* = 6.8 Hz, CH₃), 1.20-1.37 (14H, m, (CH₂)₇CH₃), 1.68-1.79 (1H, m, HOCH₂CHH'), 1.96-2.05 (1H, m, HOCH₂CHH'), 2.80 (2H, s, CH₂CONH), 3.62-3.73 (2H, m, HOCH₂), 3.96 (1H, m, CHN) ppm.

¹³C NMR (100 MHz, CD₃OD): δ = 14.4 (CH₃), 23.7, 30.1, 30.3, 30.4, 30.6, 30.7, 33.1 ((CH₂)₇CH₃), 26.2 (quintet, J_{C-D} = 19.1 Hz, CD₂), 33.9 (CD₂CH₂CO), 35.7 (CH₂CHN), 59.3 (CH₂OH), 60.0-61.5 (m, CHN), 101.5-102.3 (m, COCCO), 175.5-177.1 (m, CONH), 191.0-191.6 (m, CD₂CH₂CHOH), 197.8-198.5 (m, NHCHCO) ppm. MS (ESI): *m/z* (%): 314 (M+H⁺, 100). HRMS mass calcd.: C₁₇H₂₇D₂NO₄H⁺ 314.2295; found: 314.2297.

Melting point: 80-81 °C. Colorless powder. Yield: 80%.

Synthesis of ring-opened AHL **81**

200 mg of *N*-(undecanoyl-[3,3-di-²H])-L-homoserine lactone **78b** (1 equiv, 0.74 mmol) was dissolved in 2 mL of acetonitrile at 0 °C. Then 2 mL of 2M aq. NaOH (5 equiv, 3.7 mmol, 0.15 g) was added and the mixture was stirred overnight at room temperature. The reaction mixture was extracted with 5 mL of ethyl acetate. The organic phase was discarded and the aqueous phase acidified to pH 2 with 2M aq. HCl. Extraction with ethyl acetate (3 x 5 mL), followed by drying over MgSO₄ and evaporation of the combined organic phases *in vacuo* and recrystallization from acetone gave 188 mg of ring-opened AHL **81** as a colorless powder.



N-(Undecanoyl-[3,3-di-²H])-L-homoserine **81** (95% D). ¹H NMR (400 MHz, CD₃OD): δ = 0.91 (3H, t, J = 6.8 Hz, CH₃), 1.23-1.40 (14H, m, (CH₂)₇CH₃), 1.81-1.91 (1H, m, HOCH₂CHH'), 2.05-2.15 (1H, m, HOCH₂CHH'), 2.24 (2H, s, CH₂CONH), 3.57-3.71 (2H, m, HOCH₂), 4.52 (1H, dd, J = 9.3 Hz, 4.6 Hz, CHN) ppm. ¹³C NMR (100 MHz, CD₃OD): δ = 14.4 (CH₃), 23.7, 30.1, 30.43, 30.46, 30.65, 30.71, 33.1 ((CH₂)₇CH₃), 26.0-27.0 (m, CD₂), 35.3 (CH₂CHN), 36.7 (CH₂CONH), 50.9 (CHN), 59.3 (CH₂OH), 175.5 (CONH), 176.5 (COOH) ppm. MS (ESI): m/z (%): 290 (M+H⁺, 100), 312 (M+Na⁺, 38). HRMS mass calcd.: C₁₅H₂₇D₂NO₄H⁺ 290.2295; found: 290.2296. Melting point: 114-115 °C. Colorless powder. Yield: 88%.

5.3 GC-MS conditions for the analysis of deuterated AHLs

GC-MS Analyses were carried out according to the procedure developed by Cataldi *et al.* with minor modifications.²⁴¹ Conditions applied were: inlet pressure 77.1 kPa; He: 23.3 mL/min; injection volume: 1 μ L; injector temperature: 250 °C; transfer line: 300 °C; electron energy: 70 eV. The oven temperature program was: initial temperature and hold for 5 min at 100 °C, then increasing at a ramp of 10 °C per min to 300 °C. The injector was operated in splitless mode (60 s valve time). The carrier gas used was helium with a constant flow of 1 mL/min. AHLs were dissolved in dichloromethane. For the derivatization, 100 μ L of 99:1 BSTFA-TMCS [*N,O*-bis(trimethylsilyl)trifluoroacetamide - trimethylchlorosilane] was added to 100 μ L of dichloromethane containing the AHL and the mixture was allowed to stand for 10 min at room temperature prior to injection in the GC.

5.4 Synthesis of 1,4-oxazepane-2,5-diones

General procedure A: *N*-acylation of a primary amine

Triethylamine (1 equiv) was added to a stirred solution of the amino acid methyl ester hydrochloride (1 equiv) in water (5 mL/mmol methyl ester), followed by the addition of the appropriate carboxylic acid (1 equiv) and 1-ethyl-3-(3-dimethylaminopropyl)carbodiimide hydrochloride (1 equiv). After stirring overnight at room temperature, water (15 mL/mmol methyl ester) was added and the aqueous phase was extracted three times with ethyl acetate. The combined organic phases were washed with saturated aq. NaHCO₃ and brine. Drying over MgSO₄, followed by filtration and evaporation of the solvent *in vacuo* gave the crude product. If necessary, a purification step via column chromatography was included.

General procedure B: *N*-acylation of a secondary amine

The *N*-acylation was executed according to the procedure of Falorni *et al.* with minor adaptations.³³⁰ Briefly, the appropriate fatty acid (1 equiv) was dissolved in ethyl acetate (2 mL/mmol fatty acid) and cooled to 0 °C whereafter *N*-methylmorpholine (1 equiv) was added, followed by the dropwise addition of isobutyl chloroformate (1 equiv). The resulting turbid suspension was stirred for 20 min at 0 °C. The secondary amine (1.05 equiv), dissolved in a minimal amount of ethyl acetate, was added at the same temperature and after 2 h the reaction mixture was allowed to warm to room temperature and stirred overnight. Water was added and the aqueous phase was extracted twice with ethyl acetate. The combined organic phases were washed with a saturated solution of aq. NaHCO₃ and brine, dried (MgSO₄) and the solvent was removed via rotary evaporation to yield the *N*-acylated product.

General procedure C: hydrolysis

5 Equiv of 2M aq. NaOH were added to the methyl ester dissolved in methanol (ratio MeOH:H₂O 3:1). The reaction mixture was left to stir at room temperature for 3 h to overnight, followed by an extraction step with hexane. The aqueous phase was acidified with 2M aq. HCl and extracted three times with ethyl acetate. After washing with brine, followed by drying (MgSO₄) and removal of the drying agent by filtration, the solvent was removed by rotary evaporation to yield the crude hydrolyzed product, which was purified, if applicable, via recrystallization in diethyl ether:hexane.

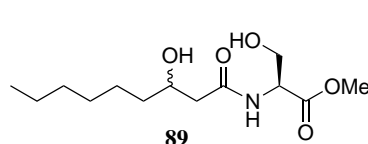
General procedure D: cyclization

The free carboxylic acid was dissolved in dry CH₂Cl₂ to obtain a 20 mM solution whereafter 1.1 equiv of EDC.HCl and 0.2 equiv of DMAP were added. The resulting reaction mixture was stirred overnight at room temperature, after which the solvent was removed *in vacuo* and the

residue redissolved in ethyl acetate:water 1:1. The aqueous phase was extracted twice with ethyl acetate, the organic phases were combined and subsequently washed with a saturated solution of aq. NaHCO₃ and brine. Drying with MgSO₄, filtration and rotary evaporation of the solvent yielded the crude seven-membered ring-containing product, which was purified via column chromatography.

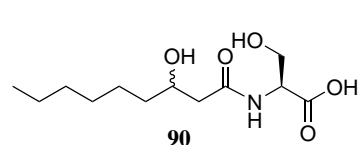
Synthesis of serine derivatives

Compound **89** was synthesized by reacting L-serine methyl ester hydrochloride **88** (1 equiv, 20 mmol, 3.1 g) with β -hydroxynonanoic acid **58d** (1 equiv, 20 mmol, 3.48 g), following general procedure A to yield 2.91 g (10.6 mmol, 53% yield) of compound **89**. Diastereomers (ratio 1:1) could not be separated via flash chromatography (ethyl acetate:petroleum ether 4:1).



Methyl *N*-(3-hydroxynonanoyl)-L-serinate **89**. Spectral data were obtained from a 1:1 mixture of diastereomers. ¹H NMR (400 MHz, CDCl₃): δ = 0.89 (3H, t, J = 6.8 Hz, CH₂CH₃), 1.22-1.62 (10H, m, (CH₂)₅CH₃), 2.35 (0.5H, dd, J = 14.8 Hz, 9.4 Hz, COCHH'CHOH), 2.36 (1H, dd, J = 14.7 Hz, 9.3 Hz, COCHH'CHOH), 2.467 (0.5H, d, J = 14.7 Hz, COCHH'CHOH), 2.474 (0.5H, d, J = 14.7 Hz, COCHH'CHOH), 3.54 (0.5H, br s, CHOH or CH₂OH), 3.80 (3H, s, OCH₃), 3.70-4.10 (4.5H, m, CH₂OH or CHOH, CHOH and CH₂OH), 4.64-4.72 (1H, m, CHNH), 7.02 (0.5H, d, J = 7.7 Hz, NH), 7.08 (0.5H, d, J = 7.7 Hz, NH) ppm. ¹³C NMR (100 MHz, CDCl₃): δ = 14.1 (CH₂CH₃), 22.6, 25.50, 25.53, 31.8, 37.0, 37.1 ((CH₂)₅CH₃), 43.15, 43.21 (COCH₂CHOH), 52.77, 52.84 (OCH₃), 54.7 (CHNH), 62.7 (CH₂OH), 68.8, 69.0 (CHOH), 171.1, 171.3 (CONH), 172.6, 172.9 (COO) ppm. MS (ESI): m/z (%): 276 (M+H⁺, 100). HRMS mass calcd.: C₁₃H₂₅NO₅H⁺ 276.1805; found: 276.1804. IR (cm⁻¹) ν_{max} 1061, 1546 (HN-C=O), 1622, 1652 (HN-C=O), 1722, 1742 (C=O), 2854, 2924, 2952, 3290 (N-H or O-H). Chromatography: EtOAc:petroleum ether 4:1 R_f = 0.24. Melting point: 65-67 °C. Colorless powder. Yield: 53%.

Compound **90** was synthesized by hydrolyzing methyl *N*-(3-hydroxynonanoyl)-L-serinate **89** (1 equiv, 0.36 mmol, 100 mg) according to general procedure C to yield 86 mg (0.33 mmol, 91% yield) of compound **90**. Diastereomers (ratio 1:1) could not be separated.

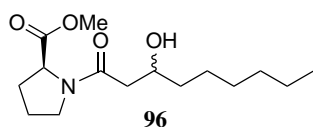


N-(3-Hydroxynonanoyl)-L-serine **90**. Spectral data were obtained from a 1:1 mixture of diastereomers. ¹H NMR (400 MHz, CD₃OD): δ = 0.81 (3H, t, J = 6.8 Hz, CH₃), 1.10-1.45 (10H, m, (CH₂)₅CH₃), 2.25-2.35 (2H, m, COCH₂CHOH), 3.73 (1H, dd, J = 11.2 Hz, 3.9 Hz, CHH'OH), 3.81 (1H, ddd, J = 11.2 Hz, 4.8 Hz, 1.9 Hz, CHH'OH), 3.83-3.92 (1H, m, CHOH), 4.41 (1H,

dd, $J = 7.8$ Hz, 4.0 Hz, CHNH) ppm. ^{13}C NMR (100 MHz, CD_3OD): $\delta = 13.0$ (CH_3), 22.3, 25.21, 25.22, 29.0, 31.6, 36.8 ($(\text{CH}_2)_5\text{CH}_3$), 43.1, 43.2 (COCH_2CHOH), 54.7 (CHNH), 61.48, 61.55 (CH_2OH), 68.3, 68.4 (CHOH), 172.0 (CONH), 172.96, 173.02 (COO) ppm. MS (ESI): m/z (%): 262 ($\text{M}+\text{H}^+$, 100), 284 ($\text{M}+\text{Na}^+$, 40). HRMS mass calcd.: $\text{C}_{12}\text{H}_{23}\text{NO}_5\text{H}^+$ 262.1649; found: 262.1653. IR (cm^{-1}) ν_{max} 1055, 1204, 1414, 1531 (HN-C=O), 1614 (HN-C=O), 1657, 1728 (C=O), 2851, 2920, 3341 (N-H or O-H). Melting point: 112-114 °C. Colorless powder. Yield: 91%.

Synthesis of proline derivatives

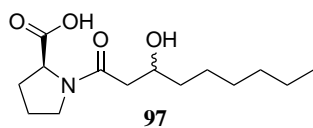
Compound **96** was synthesized by reacting L-proline methyl ester hydrochloride **95** (1 equiv, 10 mmol, 1.66 g) with β -hydroxynonanoic acid **58d** (1 equiv, 10 mmol, 1.74 g), following general procedure A. After purification via flash chromatography (ethyl acetate:petroleum ether 1:1), 1.67 g (6.6 mmol, 66% yield) of compound **96** was obtained. Diastereomers (ratio 1:1) could not be separated via flash chromatography. Both diastereomers existed as a mixture of two rotamers in a 5:1 ratio.



Methyl *N*-(3-hydroxynonanoyl)-L-prolinate **96**. Spectral data were obtained from a 1:1 mixture of diastereomers. ^1H NMR (400 MHz, CDCl_3): $\delta = 0.88$ (3H, t, $J = 6.5$ Hz, CH_2CH_3), 1.21-1.62 (10H, m, $(\text{CH}_2)_5\text{CH}_3$), 1.88-2.26 (4H, m, $(\text{CH}_2)_2\text{CH}_2\text{N}$), 2.26-2.55 (2H, m, COCH_2CHOH), 3.45-3.75 (2H, m, CH_2N), 3.74, 3.75 (2.5H, 2 x s, OCH_3), 3.766, 3.772 (0.5H, 2 x s, OCH_3), 3.95-4.10 (1H, m, CHOH), 4.37 (0.1H, dd, $J = 8.6$ Hz, 2.5 Hz, CHN), 4.41 (0.1H, dd, $J = 8.4$ Hz, 2.6 Hz, CHN), 4.49 (0.4H, dd, $J = 8.6$ Hz, 3.7 Hz, CHN), 4.53 (0.4H, dd, $J = 8.4$ Hz, 3.5 Hz, CHN) ppm. ^{13}C NMR (100 MHz, CDCl_3): $\delta = 14.0$ (CH_2CH_3), 22.5, 29.10, 29.14, 29.2, 29.6, 31.7, 36.4, 36.5 ($(\text{CH}_2)_5\text{CH}_3$), 24.5, 24.6, 25.4, 25.5 ($(\text{CH}_2)_2\text{CH}_2\text{N}$), 40.2, 40.6 (COCH_2CHOH), 40.69, 40.71 (COCH_2CHOH), 46.1, 46.2 (CH_2N), 47.0, 47.1 (CH_2N), 52.18, 52.20 (OCH_3), 52.5, 52.6 (OCH_3), 58.4, 58.5 (CHN), 59.2, 59.4 (CHN), 67.7, 68.0 (CHOH), 68.1, 68.3 (CHOH), 171.7, 171.8 (CON), 171.9, 172.0 (CON), 172.2, 172.3 (COO), 172.6 (COO) ppm. MS (ESI): m/z (%): 286 ($\text{M}+\text{H}^+$, 100). HRMS mass calcd.: $\text{C}_{15}\text{H}_{27}\text{NO}_4\text{H}^+$ 286.2013; found: 286.2012. IR (cm^{-1}) ν_{max} 1038, 1173, 1196, 1300, 1373, 1393, 1435, 1626 (N-C=O), 1744 (C=O), 2859, 2928, 2953, 3438 (O-H). Chromatography: EtOAc:petroleum ether 1:1 $R_f = 0.12$. Colorless oil. Yield: 66%.

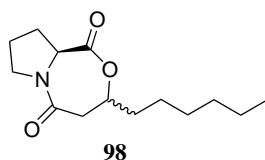
Compound **97** was synthesized by hydrolyzing methyl *N*-(3-hydroxynonanoyl)-L-prolinate **96** (1 equiv, 5 mmol, 1.43 g) according to general procedure C to give 1.21 g (4.45 mmol) of compound **97** in 89% yield. Both diastereomers existed as a mixture of two rotamers in a 5:1

ratio.



N-(3-Hydroxynonanoyl)-L-proline **97**. Spectral data were obtained from a mixture of two diastereomers in a 1:1 ratio. ^1H NMR (400 MHz, CDCl_3): δ = 0.88 (3H, t, J = 6.4 Hz, CH_3), 1.23-1.61 (10H, m, $(\text{CH}_2)_5\text{CH}_3$), 1.88-2.38 (4H, m, $(\text{CH}_2)_2\text{CH}_2\text{N}$), 2.38-2.56 (2H, m, COCH_2CHOH), 3.45-3.76 (2H, m, CH_2N), 4.03-4.11 (1H, m, CHOH), 4.37 (0.1H, dd, J = 6.9 Hz, 4.0 Hz, CHN), 4.46 (0.1H, dd, J = 7.5 Hz, 3.3 Hz, CHN), 4.50-4.58 (0.8H, m, CHN), 7.50 (1H, br s, COOH) ppm. ^{13}C NMR (100 MHz, CDCl_3): δ = 14.1 (CH_3), 21.0, 28.7, 28.8, 29.2, 31.8, 36.1, 36.4, 36.5 ($(\text{CH}_2)_5\text{CH}_3$), 24.5, 24.6, 25.49, 25.51 ($(\text{CH}_2)_2\text{CH}_2\text{N}$), 40.6, 40.7 (COCH_2CHOH), 40.9, 41.1 (COCH_2CHOH), 46.4 (CH_2N), 47.5, 47.6 (CH_2N), 59.02, 58.98 (CHN), 59.4, 59.5 (CHN), 68.0, 68.5 (CHOH), 172.2, 172.4 (CON and COO), 172.7, 172.8 (CON), 174.3 (COO) ppm. MS (ESI): m/z (%): 272 ($\text{M}+\text{H}^+$, 100). HRMS mass calcd.: $\text{C}_{14}\text{H}_{25}\text{NO}_4\text{H}^+$ 272.1856; found: 272.1865. IR (cm^{-1}) ν_{max} 1045, 1173, 1198, 1240, 1373, 1392, 1628 ($\text{N}-\text{C}=\text{O}$), 1703, 1740 ($\text{C}=\text{O}$), 2889, 2930, 2972, 2982, 3448 ($\text{O}-\text{H}$), 3651 ($\text{O}-\text{H}$). Melting point: 51-53 °C. Colorless powder. Yield: 89%.

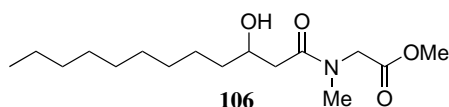
Compound **98** was synthesized by ring closing carboxylic acid **97** (1 equiv, 2 mmol, 0.54 g) according to general procedure D to give 0.43 g of cyclic compound **98** in 84% yield after flash chromatography (ethyl acetate:petroleum ether 1:1). Diastereomers (ratio 1:1) could not be separated via flash chromatography.



(9*aS*)-3-Hexylhexahydro-1*H*,5*H*-pyrrolo[2,1-*c*][1,4]oxazepine-1,5-dione **98**. Spectral data were obtained from a mixture of two diastereomers in a 1:1 ratio. ^1H NMR (400 MHz, CDCl_3): δ = 0.89 (3H, t, J = 6.5 Hz, CH_3), 1.24-1.55 (8H, m, $(\text{CH}_2)_4\text{CH}_3$), 1.56-1.80 (2H, m, $\text{CH}_2(\text{CH}_2)_4\text{CH}_3$), 1.80-2.02 (2H, m, NCH_2CH_2), 2.15-2.24 (1H, m, $\text{NCH}_2\text{CH}_2\text{CHH}'$), 2.55-2.64 (1H, m, $\text{NCH}_2\text{CH}_2\text{CHH}'$), 2.76 (1H, dd, J = 18.5 Hz, 11.5 Hz, $\text{COCHH}'\text{CH}-\text{O}$), 2.86 (1H, dd, J = 18.5 Hz, 2.4 Hz, $\text{COCHH}'\text{CH}-\text{O}$), 3.58-3.69 (2H, m, CH_2N), 4.67 (1H, dd, J = 7.0 Hz, 7.0 Hz, CHN), 4.72-4.82 (1H, m, $\text{CH}-\text{O}$) ppm. ^{13}C NMR (100 MHz, CDCl_3): δ = 14.0 (CH_3), 22.0 (NCH_2CH_2), 22.5, 25.2, 29.6, 31.6 ($(\text{CH}_2)_4\text{CH}_3$), 28.9 ($\text{NCH}_2\text{CH}_2\text{CH}_2$), 35.0 ($\text{CH}_2(\text{CH}_2)_4\text{CH}_3$), 42.4 ($\text{COCH}_2\text{CH}-\text{O}$), 48.3 (CH_2N), 55.7 (CHN), 73.5 ($\text{CH}-\text{O}$), 166.9 (CON), 169.6 (COO) ppm. MS (ESI): m/z (%): 254 ($\text{M}+\text{H}^+$, 100). HRMS mass calcd.: $\text{C}_{14}\text{H}_{23}\text{NO}_3\text{H}^+$ 254.1751; found: 254.1763. IR (cm^{-1}) ν_{max} 1223, 1383, 1438, 1616 ($\text{N}-\text{C}=\text{O}$), 1748 ($\text{C}=\text{O}$), 2859, 2902. Melting point: 87-89 °C. Colorless powder. Yield: 84%.

Synthesis of sarcosine derivatives

Compound **106** was synthesized by reacting sarcosine methyl ester hydrochloride **104** (1 equiv, 10 mmol, 1.40 g) with β -hydroxydodecanoic acid **58g** (1 equiv, 10 mmol, 2.16 g), following general procedure A. After flash chromatography (ethyl acetate:petroleum ether 3:1), 1.87 g (6.2 mmol, 62% yield) of compound **106** was obtained.

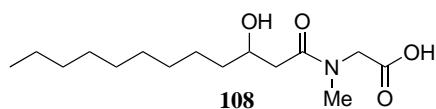


Methyl *N*-(3-hydroxydodecanoyl)sarcosinate **106**. Spec-

tral data were obtained from a mixture of two rotamers in a 4:1 ratio. ^1H NMR (400 MHz, CDCl_3): δ rotamer

1 (major): 0.88 (3H, t, $J = 6.8$ Hz, CH_2CH_3), 1.19-1.61 (16H, m, $(\text{CH}_2)_8\text{CH}_3$), 2.40 (1H, dd, $J = 16.5$ Hz, 9.4 Hz, $\text{COCHH}'\text{CHOH}$), 2.55 (1H, dd, $J = 16.5$ Hz, 2.4 Hz, $\text{COCHH}'\text{CHOH}$), 3.07 (3H, s, NCH_3), 3.75 (3H, s, OCH_3), 3.93 (1H, br d, $J = 2.8$ Hz, CHOH), 3.98-4.07 (1H, m, CHOH), 4.09 (1H, d, $J = 17.3$ Hz, $\text{CHH}'\text{N}$), 4.19 (1H, d, $J = 17.4$ Hz, $\text{CHH}'\text{N}$) ppm; rotamer 2 (minor): 0.88 (3H, t, $J = 6.8$ Hz, CH_2CH_3), 1.19-1.61 (16H, m, $(\text{CH}_2)_8\text{CH}_3$), 2.25 (1H, dd, $J = 16.2$ Hz, 9.2 Hz, $\text{COCHH}'\text{CHOH}$), 2.35-2.41 (1H, m, $\text{COCHH}'\text{CHOH}$), 2.99 (3H, s, NCH_3), 3.79 (3H, s, OCH_3), 3.98-4.07 (2H, m, CHOH and CHOH), 3.99 (1H, d, $J = 18.2$ Hz, $\text{CHH}'\text{N}$), 4.10 (1H, d, $J = 18.2$ Hz, $\text{CHH}'\text{N}$) ppm. ^{13}C NMR (100 MHz, CDCl_3): δ rotamer 1 (major): 14.1 (CH_2CH_3), 22.6, 29.3, 29.5, 29.6, 31.9, 36.4 ($(\text{CH}_2)_8\text{CH}_3$), 36.5 (NCH_3), 39.5 (COCH_2CHOH), 49.1 (CH_2N), 52.2 (OCH_3), 68.7 (CHOH), 169.6 (CON), 173.6 (COO) ppm; rotamer 2 (minor): 14.1 (CH_2CH_3), 22.6, 29.3, 29.5, 29.6, 31.9, 36.4 ($(\text{CH}_2)_8\text{CH}_3$), 34.7 (NCH_3), 39.2 (COCH_2CHOH), 51.3 (CH_2N), 52.5 (OCH_3), 68.7 (CHOH), 169.1 (CON), 173.3 (COO) ppm. MS (ESI): m/z (%): 302 ($\text{M}+\text{H}^+$, 100). HRMS mass calcd.: $\text{C}_{16}\text{H}_{31}\text{NO}_4\text{H}^+$ 302.2326; found: 302.2337. IR (cm^{-1}) ν_{max} 1210, 1418, 1471, 1489, 1634 (N-C=O), 1746 (C=O), 2852, 2922, 2954, 3478 (O-H). Chromatography: EtOAc:petroleum ether 3:1 $R_f = 0.29$. Melting point: 52-54 °C. Colorless powder. Yield: 62%.

Compound **108** was synthesized by hydrolyzing 1.56 g of methyl ester **106** (1 equiv, 5.2 mmol) according to general procedure C to yield 1.33 g (4.6 mmol, 89% yield) of compound **108**.



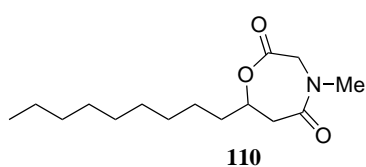
N-(3-Hydroxydodecanoyl)sarcosine **108**. Spectral data

were obtained from a mixture of two rotamers in a 3:1 ratio. ^1H NMR (400 MHz, CDCl_3): δ rotamer 1 (ma-

major): 0.89 (3H, t, $J = 6.8$ Hz, CH_2CH_3), 1.19-1.65 (16H, m, $(\text{CH}_2)_8\text{CH}_3$), 2.49 (1H, dd, $J = 16.3$ Hz, 9.2 Hz, $\text{COCHH}'\text{CHOH}$), 2.57 (1H, dd, $J = 16.2$ Hz, 2.7 Hz, $\text{COCHH}'\text{CHOH}$), 3.10 (3H, s, NCH_3), 3.97-4.21 (3H, m, CHOH and CH_2N), 7.85 (1H, br s, COOH) ppm; rotamer 2 (minor): 0.89 (3H, t, $J = 6.8$ Hz, CH_2CH_3), 1.19-1.65 (16H, m, $(\text{CH}_2)_8\text{CH}_3$), 2.40-

2.50 (2H, m, COCH₂CHOH), 3.01 (3H, s, NCH₃), 3.97-4.21 (3H, m, CHOH and CH₂N), 7.85 (1H, br s, COOH) ppm. ¹³C NMR (100 MHz, CDCl₃): δ rotamer 1 (major): 14.1 (CH₂CH₃), 22.7, 25.6, 25.7, 29.3, 29.5, 29.6, 31.9, 35.9, 36.3 ((CH₂)₈CH₃), 36.8 (NCH₃), 39.6 (COCH₂CHOH), 49.5 (CH₂N), 68.2 (CHOH), 172.2 (CON), 174.1 (COO) ppm; rotamer 2 (minor): 14.1 (CH₂CH₃), 22.7, 25.6, 25.7, 29.3, 29.5, 29.6, 31.9, 35.9, 36.3 ((CH₂)₈CH₃), 35.0 (NCH₃), 39.2 (COCH₂CHOH), 51.3 (CH₂N), 68.7 (CHOH), 171.3 (CON), 173.6 (COO) ppm. MS (ESI): *m/z* (%): 288 (M+H⁺, 100). HRMS mass calcd.: C₁₅H₂₉NO₄H⁺ 288.2169; found: 288.2172. IR (cm⁻¹) *ν*_{max} 1258, 1402, 1418, 1497, 1638 (N-C=O), 1726 (C=O), 2849, 2918, 3353 (O-H). Melting point: 71-73 °C. Colorless powder. Yield: 83%.

Cyclic compound **110** was synthesized by ring closing carboxylic acid **108** (1 equiv, 0.50 mmol, 0.14 g) according to general procedure D. After purification via flash chromatography (ethyl acetate:petroleum ether 2:1), 84 mg (0.31 mmol, 62% yield) of cyclic compound **110** was obtained.

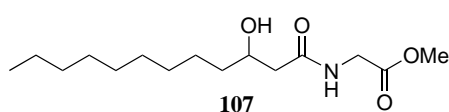
**110**

4-Methyl-7-nonyl-1,4-oxazepane-2,5-dione **110**. ¹H NMR (400 MHz, CDCl₃): δ = 0.88 (3H, t, *J* = 6.8 Hz, CH₂CH₃), 1.20-1.80 (16H, m, (CH₂)₈CH₃), 2.85 (1H, dd, *J* = 17.5 Hz, 9.5 Hz, COCHH'CH-O), 2.91 (1H, dd, *J* = 17.5 Hz, 3.7 Hz,

COCHH'CH-O), 3.08 (3H, s, NCH₃), 3.96 (1H, d, *J* = 15.8 Hz, CHH'N), 4.53 (1H, d, *J* = 15.8 Hz, CHH'N), 4.63-4.71 (1H, m, CH-O) ppm. ¹³C NMR (100 MHz, CDCl₃): δ = 14.3 (CH₂CH₃), 22.8, 25.2, 29.35, 29.42, 29.57, 29.62, 32.0, 35.7 ((CH₂)₈CH₃), 37.2 (NCH₃), 42.3 (COCH₂CH-O), 52.7 (CH₂N), 76.1 (CH-O), 167.8 (CON), 168.9 (COO) ppm. MS (ESI): *m/z* (%): 270 (M+H⁺, 100). HRMS mass calcd.: C₁₅H₂₇NO₃H⁺ 270.2064; found: 270.2058. IR (cm⁻¹) *ν*_{max} 1213, 1339, 1493, 1624 (N-C=O), 1736 (C=O), 2857; 2924. Chromatography: EtOAc:petroleum ether 2:1 R_f = 0.23. Melting point: 81-83 °C. Colorless powder. Yield: 62%.

Synthesis of glycine derivatives

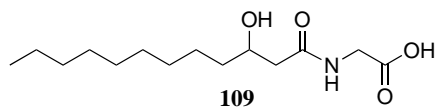
Compound **107** was synthesized by reacting glycine methyl ester hydrochloride **105** (1 equiv, 15 mmol, 1.89 g) with β-hydroxydodecanoic acid **58g** (1 equiv, 15 mmol, 3.24 g), following general procedure A. After purification via flash chromatography (ethyl acetate:petroleum ether 3:1), 2.83 g (9.9 mmol, 66% yield) of compound **107** was obtained.

**107**

Methyl *N*-(3-hydroxydodecanoyl)glycinate **107**. ¹H NMR (400 MHz, CDCl₃): δ = 0.88 (3H, t, *J* = 6.9 Hz, CH₂CH₃), 1.19-1.59 (16H, m, (CH₂)₈CH₃), 2.32 (1H, dd, *J* = 15.1 Hz, 9.1 Hz, COCHH'CHOH), 2.44 (1H, dd, *J* = 15.1 Hz, 2.7 Hz, COCHH'CHOH),

3.34 (1H, br d, $J = 3.6$ Hz, CHOH), 3.77 (3H, s, OCH_3), 3.97-4.05 (1H, m, CHOH), 4.06-4.14 (2H, m, CH_2NH), 6.34 (1H, br s, NH) ppm. ^{13}C NMR (100 MHz, CDCl_3): $\delta = 14.1$ (CH_2CH_3), 22.7, 25.4, 25.5, 29.3, 29.55, 29.59, 31.9, 36.9 ($(\text{CH}_2)_8\text{CH}_3$), 41.1 (CH_2NH), 42.7 (COCH_2CHOH), 52.5 (OCH_3), 68.7 (CHOH), 170.6 (CONH), 172.7 (COO) ppm. MS (ESI): m/z (%): 288 ($\text{M}+\text{H}^+$, 100). HRMS mass calcd.: $\text{C}_{15}\text{H}_{29}\text{NO}_4\text{H}^+$ 288.2169; found: 288.2168. IR (cm^{-1}) ν_{max} 1221, 1379, 1392, 1434, 1442, 1550 (HN-C=O), 1643 (HN-C=O), 1742 (C=O), 2851, 2919, 2956, 3312 (O-H). Chromatography: EtOAc:petroleum ether 3:1 $R_f = 0.27$. Melting point: 77-79 °C. Colorless powder. Yield: 66%.

Compound **109** was synthesized by hydrolyzing methyl ester **107** (1 equiv, 6.1 mmol, 1.75 g) according to general procedure C to yield 1.35 g (4.9 mmol, 81% yield) of compound **109**.

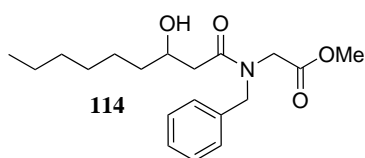


N-(3-Hydroxydodecanoyl)glycine **109**. ^1H NMR (400 MHz, CD_3OD): $\delta = 0.80$ (3H, t, $J = 6.9$ Hz, CH_3), 1.14-1.43 (16H, m, $(\text{CH}_2)_8\text{CH}_3$), 2.25 (1H, dd, $J = 14.3$ Hz,

7.6 Hz, $\text{COCHH}'\text{CHOH}$), 2.30 (1H, dd, $J = 14.3$ Hz, 5.3 Hz, $\text{COCHH}'\text{CHOH}$), 3.78 (1H, d, $J = 17.8$ Hz, $\text{CHH}'\text{NH}$), 3.85 (1H, d, $J = 17.8$ Hz, $\text{CHH}'\text{NH}$), 3.84-3.90 (1H, m, CHOH) ppm. ^{13}C NMR (100 MHz, CD_3OD): $\delta = 13.1$ (CH_3), 22.3, 25.3, 29.1, 29.3, 31.7, 36.7 ($(\text{CH}_2)_8\text{CH}_3$), 40.4 (CH_2NH), 43.2 (COCH_2CHOH), 68.3 (CHOH), 171.7 (CONH), 173.3 (COO) ppm. MS (ESI): m/z (%): 274 ($\text{M}+\text{H}^+$, 100), 296 ($\text{M}+\text{Na}^+$, 28). HRMS mass calcd.: $\text{C}_{14}\text{H}_{27}\text{NO}_4\text{H}^+$ 274.2013; found: 274.2009. IR (cm^{-1}) ν_{max} 1246, 1262, 1421, 1447, 1556 (HN-C=O), 1640 (HN-C=O), 1708 (C=O), 2849, 2922, 3262 (O-H), 3326 (O-H). Melting point: 92-94 °C. Colorless powder. Yield: 94%.

Synthesis of *N*-benzyl-1,4-oxazepane-2,5-dione **116**

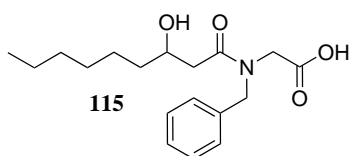
Compound **114** was synthesized by reacting the methyl ester of *N*-benzyl glycine **113** (1 equiv, 3.0 mmol, 0.59 g) with β -hydroxynonanoic acid **58d** (1 equiv, 3.0 mmol, 0.52 g), following general procedure B to yield 0.55 g (1.6 mmol, 55% yield) of ester **114**.



Methyl *N*-benzyl-*N*-(3-hydroxynonanoyl)glycinate **114**. Spectral data were obtained from a mixture of two rotamers in a 7:3 ratio. ^1H NMR (400 MHz, CDCl_3): δ rotamer 1 (major): 0.87 (3H, t, $J = 6.6$ Hz, CH_2CH_3), 1.26-1.61 (10H, m, $(\text{CH}_2)_5\text{CH}_3$), 2.49 (1H, dd, $J = 16.2$ Hz, 9.4 Hz, $\text{COCHH}'\text{CHOH}$), 2.62 (1H, dd, $J = 16.2$ Hz, 2.4 Hz, $\text{COCHH}'\text{CHOH}$), 3.73 (3H, s, OCH_3), 3.85-4.15 (4H, m, CHOH and CHOH and CH_2COO), 4.55-4.77 (2H, m, $\text{C}_6\text{H}_5\text{CH}_2\text{N}$), 7.16-7.41 (5H, m, 5 x CH_{arom}) ppm; rotamer 2 (minor): 0.87 (3H, t, $J = 6.6$ Hz, CH_2CH_3), 1.26-1.61 (10H, m, $(\text{CH}_2)_5\text{CH}_3$), 2.32 (1H, dd, $J = 16.3$ Hz,

9.3 Hz, COCHH'CHOH), 2.45 (1H, dd, $J = 16.3$ Hz, 2.3 Hz, COCHH'CHOH), 3.72 (3H, s, OCH₃), 3.85-4.15 (4H, m, CHOH and CHOH and CH₂COO), 4.55-4.77 (2H, m, C₆H₅CH₂N), 7.16-7.41 (5H, m, 5 x CH_{arom}) ppm. ¹³C NMR (100 MHz, CDCl₃): δ rotamer 1 (major): 14.1 (CH₂CH₃), 22.6, 25.5, 29.3, 31.8, 36.4 ((CH₂)₅CH₃), 39.4 (COCH₂CHOH), 46.9 (NCH₂COO), 52.1 (C₆H₅CH₂N), 52.2 (OCH₃), 68.3 (CHOH), 126.7, 128.4, 129.1 (5 x CH_{arom}) 135.6 (C_{arom}), 169.7 (CON), 174.0 (COO) ppm; rotamer 2 (minor): 14.1 (CH₂CH₃), 22.6, 25.5, 29.3, 31.8, 36.4 ((CH₂)₅CH₃), 39.4 (COCH₂CHOH), 48.2 (NCH₂COO), 49.5 (C₆H₅CH₂N), 52.5 (OCH₃), 68.2 (CHOH), 127.8, 128.0, 128.7 (5 x CH_{arom}) 136.2 (C_{arom}), 169.3 (CON), 173.4 (COO) ppm. MS (ESI): m/z (%): 336 (M+H⁺, 100). HRMS mass calcd.: C₁₉H₂₉NO₄H⁺ 336.2169; found: 336.2176. IR (cm⁻¹) ν_{max} 1001, 1175, 1200, 1368, 1406, 1435, 1452, 1634 (N-C=O), 1709, 1748 (C=O), 2857, 2928, 2953, 3451 (O-H). Yellow oil. Yield: 55%.

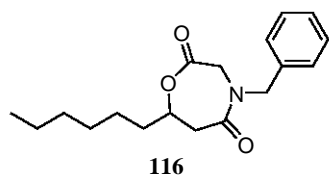
Compound **115** was synthesized by hydrolyzing methyl ester **114** (1 equiv, 1.5 mmol, 0.50 g) according to general procedure C to give 0.41 g (1.3 mmol) of compound **115** in 86% yield.



N-Benzyl-*N*-(3-hydroxynonanoyl)glycine **115**. Spectral data were obtained from a mixture of two rotamers in a 1.9:1 ratio. ¹H NMR (400 MHz, CDCl₃): δ rotamer 1 (major): 0.86-0.91 (3H, m, CH₃), 1.19-1.68 (10H, m, (CH₂)₅CH₃), 2.45-2.65 (2H, m, COCH₂CHOH), 3.90-4.21 (3H, m, CHOH and CH₂COO), 4.58 (1H, d, $J = 16.8$ Hz, C₆H₅CHH'N), 4.78-4.86 (1H, m, C₆H₅CHH'N), 7.10-7.41 (5H, m, 5 x CH_{arom}), 7.60 (1H, br s, COOH) ppm; rotamer 2 (minor): 0.86-0.91 (3H, m, CH₃), 1.19-1.68 (10H, m, (CH₂)₅CH₃), 2.45-2.65 (2H, m, COCH₂CHOH), 3.90-4.21 (3H, m, CHOH and CH₂COO), 4.45-4.55 (1H, m, C₆H₅CHH'N), 4.78-4.86 (1H, m, C₆H₅CHH'N), 7.10-7.41 (5H, m, 5 x CH_{arom}), 7.60 (1H, br s, COOH) ppm. ¹³C NMR (100 MHz, CDCl₃): δ rotamer 1 (major): 14.1 (CH₃), 22.61, 22.64, 25.5, 25.6, 29.2, 31.8, 35.9, 36.3 ((CH₂)₅CH₃), 39.5 (COCH₂CHOH), 47.1 (NCH₂COO), 52.3 (C₆H₅CH₂N), 68.5 (CHOH), 126.8, 128.4, 129.1 (5 x CH_{arom}) 135.2 (C_{arom}), 172.4 (CON), 174.4 (COO) ppm; rotamer 2 (minor): 14.1 (CH₃), 22.61, 22.64, 25.5, 25.6, 29.2, 31.8, 35.9, 36.3 ((CH₂)₅CH₃), 39.5 (COCH₂CHOH), 48.0 (NCH₂COO), 49.6 (C₆H₅CH₂N), 68.7 (CHOH), 127.8, 128.1, 128.8 (5 x CH_{arom}) 136.2 (C_{arom}), 171.5 (CON), 173.6 (COO) ppm. MS (ESI): m/z (%): 322 (M+H⁺, 100). HRMS mass calcd.: C₁₈H₂₇NO₄H⁺ 322.2013; found: 322.2009. IR (cm⁻¹) ν_{max} 1188, 1213, 1420, 1476, 1626 (N-C=O), 1730 (C=O), 2855, 2927, 3310 (O-H). Melting point 91-93 °C. Colorless powder. Yield: 86%.

Cyclic compound **116** was synthesized by ring closing carboxylic acid **115** (1 equiv, 0.86 mmol, 0.28 g) according to general procedure D. After purification via flash chromatography (ethyl

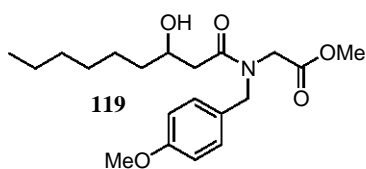
acetate:petroleum ether 4:1), 0.20 g (0.65 mmol, 75% yield) of cyclic compound **116** was obtained.



4-Benzyl-7-hexyl-1,4-oxazepane-2,5-dione **116**. ^1H NMR (400 MHz, CDCl_3): δ = 0.88 (3H, t, J = 6.8 Hz, CH_3), 1.21-1.55 (8H, m, $(\text{CH}_2)_4\text{CH}_3$), 1.58-1.81 (2H, m, $\text{CH}_2(\text{CH}_2)_4$), 2.90-3.02 (2H, m, $\text{COCH}_2\text{CH-O}$), 3.94 (1H, d, J = 15.9 Hz, $\text{CHH}'\text{COO}$), 4.31 (1H, d, J = 15.9 Hz, $\text{CHH}'\text{COO}$), 4.49 (1H, d, J = 14.7 Hz, $\text{C}_6\text{H}_5\text{CHH}'\text{N}$), 4.67 (1H, tt, J = 12.6 Hz, 4.6 Hz, CH-O), 4.89 (1H, d, J = 14.7 Hz, $\text{C}_6\text{H}_5\text{CHH}'\text{N}$), 7.23-7.38 (5H, m, 5 x CH_{arom}) ppm. ^{13}C NMR (100 MHz, CDCl_3): δ = 14.0 (CH_3), 22.5, 25.0, 28.9, 31.6 ($(\text{CH}_2)_4\text{CH}_3$), 35.6 ($\text{CH}_2(\text{CH}_2)_4$), 42.2 ($\text{COCH}_2\text{CH-O}$), 50.2 (CH_2COO), 52.1 ($\text{C}_6\text{H}_5\text{CH}_2\text{N}$), 76.0 (CH-O), 128.1, 128.2, 129.0 (5 x CH_{arom}), 135.9 (C_{arom}), 167.5 (CON), 168.8 (COO) ppm. MS (ESI): m/z (%): 304 ($\text{M}+\text{H}^+$, 100). HRMS mass calcd.: $\text{C}_{18}\text{H}_{25}\text{NO}_3\text{H}^+$ 304.1907; found: 304.1904. IR (cm^{-1}) ν_{max} 1134, 1161, 1233, 1296, 1344, 1423, 1439, 1454, 1638 (N-C=O), 1749 (C=O), 2849, 2920, 2951. Chromatography: EtOAc:petroleum ether 4:1 R_f = 0.33. Melting point 53-55 °C. Colorless powder. Yield: 75%.

Synthesis of *N*-PMB-1,4-oxazepane-2,5-dione **121**

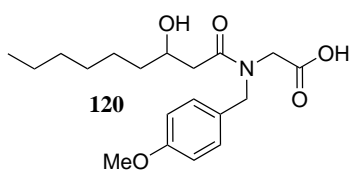
Compound **119** was synthesized by reacting the methyl ester of *N*-PMB glycine **118** (1 equiv, 25 mmol, 5.23 g) with β -hydroxynonanoic acid **58d** (1 equiv, 25 mmol, 4.36 g), following general procedure B to yield 7.1 g (19.5 mmol, 78% yield) of ester **119**.



Methyl *N*-(3-hydroxynonanoyl)-*N*-(4-methoxybenzyl)glycinate **119**. Spectral data were obtained from a mixture of two rotamers in a 2.4:1 ratio. ^1H NMR (400 MHz, CDCl_3): δ rotamer 1 (major): 0.85-0.90 (3H, m, CH_2CH_3), 1.21-1.63 (10H, m, $(\text{CH}_2)_5\text{CH}_3$), 2.50 (1H, dd, J = 16.1 Hz, 9.4 Hz, $\text{COCHH}'\text{CHOH}$), 2.63 (1H, dd, J = 16.2 Hz, 2.3 Hz, $\text{COCHH}'\text{CHOH}$), 3.72 (3H, s, COOCH_3), 3.83 (3H, s, $\text{C}_{arom}\text{OCH}_3$), 3.84-4.03 (2H, m, CH_2COO), 4.01-4.11 (1H, m, CHOH), 4.49-4.69 (2H, m, $\text{C}_6\text{H}_5\text{CH}_2\text{N}$), 6.89 (2H, d, J = 8.6 Hz, 2 x OCCH_{arom}), 7.11 (2H, d, J = 8.6 Hz, 2 x $\text{CH}_2\text{CCH}_{arom}$) ppm; rotamer 2 (minor): 0.85-0.90 (3H, m, CH_2CH_3), 1.21-1.63 (10H, m, $(\text{CH}_2)_5\text{CH}_3$), 2.30 (1H, dd, J = 16.3 Hz, 9.1 Hz, $\text{COCHH}'\text{CHOH}$), 2.43 (1H, dd, J = 16.3 Hz, 2.2 Hz, $\text{COCHH}'\text{CHOH}$), 3.71 (3H, s, COOCH_3), 3.79 (3H, s, $\text{C}_{arom}\text{OCH}_3$), 3.84-4.03 (2H, m, CH_2COO), 4.01-4.11 (1H, m, CHOH), 4.49-4.69 (2H, m, $\text{C}_6\text{H}_5\text{CH}_2\text{N}$), 6.85 (2H, d, J = 8.6 Hz, 2 x OCCH_{arom}), 7.15 (2H, d, J = 8.6 Hz, 2 x $\text{CH}_2\text{CCH}_{arom}$) ppm. ^{13}C NMR (100 MHz, CDCl_3): δ rotamer 1 (major): 14.1 (CH_2CH_3), 22.6, 25.5, 29.2, 29.3, 31.8, 36.4 ($(\text{CH}_2)_5\text{CH}_3$), 39.4 (COCH_2CHOH), 46.6

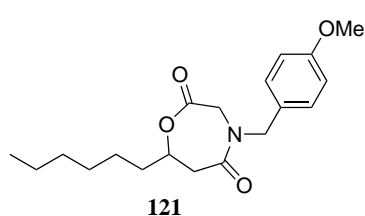
(NCH₂COO), 51.6 (C₆H₅CH₂N), 52.2 (COOCH₃), 55.33 (C_{arom}OCH₃), 68.3 (CHOH), 114.4 (2 x OCCH_{arom}), 128.2 (2 x CH₂CCH_{arom}), 129.9 (CH₂C_{arom}), 159.4 (CH₃OC_{arom}), 169.7 (CON), 173.8 (COO) ppm; rotamer 2 (minor): 14.1 (CH₂CH₃), 22.6, 25.5, 29.2, 29.3, 31.8, 36.4 ((CH₂)₅CH₃), 39.5 (COCH₂CHOH), 47.9 (NCH₂COO), 48.9 (C₆H₅CH₂N), 52.5 (COOCH₃), 55.29 (C_{arom}OCH₃), 68.1 (CHOH), 114.1 (2 x OCCH_{arom}), 127.3 (2 x CH₂CCH_{arom}), 128.6 (CH₂C_{arom}), 159.3 (CH₃OC_{arom}), 169.3 (CON), 173.4 (COO) ppm. MS (ESI): *m/z* (%): 366 (M+H⁺, 100). HRMS mass calcd.: C₂₀H₃₁NO₅H⁺ 366.2275; found: 366.2268. IR (cm⁻¹) ν_{max} 1032, 1173, 1200, 1246, 1422, 1437, 1512, 1612, 1632 (N-C=O), 1748 (C=O), 2857, 2928, 2953, 3478 (O-H). Yellow oil. Yield: 78%.

Methyl ester **119** (1 equiv, 19.2 mmol, 7.0 g) was hydrolyzed following general procedure C to yield 6.4 g (18.2 mmol) of carboxylic acid **120** in 95% yield.



N-(3-Hydroxynonanoyl)-*N*-(4-methoxybenzyl)glycine **120**. Spectral data were obtained from a mixture of two rotamers in a 2.3:1 ratio. ¹H NMR (400 MHz, CDCl₃): δ rotamer 1 (major): 0.87-0.93 (3H, m, CH₂CH₃), 1.24-1.71 (10H, m, (CH₂)₅CH₃), 2.58 (1H, dd, *J* = 16.0 Hz, 9.0 Hz, COCHH'CHOH), 2.65 (1H, dd, *J* = 16.0 Hz, 2.5 Hz, COCHH'CHOH), 3.83 (3H, s, OCH₃), 4.03 (1H, d, *J* = 17.4 Hz, CHH'COO), 4.11 (1H, d, *J* = 17.3 Hz, CHH'COO), 4.01-4.21 (1H, m, CHOH), 4.54 (1H, d, *J* = 16.3 Hz, C₆H₅CHH'N), 4.63 (1H, d, *J* = 16.3 Hz, C₆H₅CHH'N), 6.92 (2H, d, *J* = 8.5 Hz, 2 x OCCH_{arom}), 7.13 (2H, d, *J* = 8.5 Hz, 2 x CH₂CCH_{arom}) ppm; rotamer 2 (minor): 0.87-0.93 (3H, m, CH₂CH₃), 1.24-1.71 (10H, m, (CH₂)₅CH₃), 2.45-2.54 (2H, m, COCH₂CHOH), 3.82 (3H, s, OCH₃), 3.89 (1H, d, *J* = 18.7 Hz, CHH'COO), 3.95 (1H, d, *J* = 18.7 Hz, CHH'COO), 4.01-4.21 (1H, m, CHOH), 4.42 (1H, d, *J* = 14.7 Hz, C₆H₅CHH'N), 4.83 (1H, d, *J* = 14.8 Hz, C₆H₅CHH'N), 6.87 (2H, d, *J* = 8.5 Hz, 2 x OCCH_{arom}), 7.18 (2H, d, *J* = 8.5 Hz, 2 x CH₂CCH_{arom}) ppm. ¹³C NMR (100 MHz, CDCl₃): δ rotamer 1 (major): 14.1 (CH₂CH₃), 22.6, 25.5, 25.6, 29.19, 29.23, 31.8, 35.8, 36.4 ((CH₂)₅CH₃), 39.6 (COCH₂CHOH), 46.9 (NCH₂COO), 51.8 (C₆H₅CH₂N), 55.35 (OCH₃), 68.4 (CHOH), 114.5 (2 x OCCH_{arom}), 127.0 (CH₂C_{arom}), 128.3 (2 x CH₂CCH_{arom}), 159.5 (CH₃OC_{arom}), 172.4 (CON), 174.3 (COO) ppm; rotamer 2 (minor): 14.1 (CH₂CH₃), 22.6, 25.5, 25.6, 29.19, 29.23, 31.8, 35.8, 36.4 ((CH₂)₅CH₃), 39.5 (COCH₂CHOH), 47.6 (NCH₂COO), 48.9 (C₆H₅CH₂N), 55.29 (OCH₃), 68.7 (CHOH), 114.2 (2 x OCCH_{arom}), 128.2 (CH₂C_{arom}), 129.9 (2 x CH₂CCH_{arom}), 159.3 (CH₃OC_{arom}), 171.7 (CON), 173.4 (COO) ppm. MS (ESI): *m/z* (%): 352 (M+H⁺, 100). HRMS mass calcd.: C₁₉H₂₉NO₅H⁺ 352.2118; found: 352.2110. IR (cm⁻¹) ν_{max} 1036, 1175, 1225, 1246, 1398, 1483, 1512, 1620 (N-C=O), 1724 (C=O), 2857, 2920, 3380 (O-H). Melting point: 70-72 °C. Colorless powder. Yield: 95%.

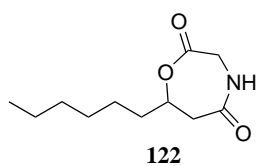
Cyclic compound **121** was synthesized by ring closing carboxylic acid **120** (1 equiv, 17.5 mmol, 6.17 g) according to general procedure D. After purification via flash chromatography (ethyl acetate:petroleum ether 1:1), 2.33 g (7 mmol, 40% yield) of compound **121** was obtained.



7-Hexyl-4-(4-methoxybenzyl)-1,4-oxazepane-2,5-dione **121**. ^1H NMR (400 MHz, CDCl_3): δ = 0.88 (3H, t, J = 6.7 Hz, CH_2CH_3), 1.21-1.55 (8H, m, $(\text{CH}_2)_4\text{CH}_3$), 1.56-1.80 (2H, m, $\text{CH}_2(\text{CH}_2)_4$), 2.88-3.00 (2H, m, $\text{COCH}_2\text{CH-O}$), 3.80 (3H, s, OCH_3), 3.94 (1H, d, J = 15.9 Hz, $\text{CHH}'\text{COO}$), 4.28 (1H, d, J = 15.9 Hz, $\text{CHH}'\text{COO}$), 4.43 (1H, d, J = 14.6 Hz, $\text{C}_6\text{H}_5\text{CHH}'\text{N}$), 4.64 (1H, tt, J = 12.7 Hz, 4.5 Hz, CH-O), 4.81 (1H, d, J = 14.6 Hz, $\text{C}_6\text{H}_5\text{CHH}'\text{N}$), 6.87 (2H, d, J = 8.6 Hz, 2 x $\text{OCCH}_{\text{arom}}$), 7.19 (2H, d, J = 8.6 Hz, 2 x $\text{CH}_2\text{CCH}_{\text{arom}}$) ppm. ^{13}C NMR (100 MHz, CDCl_3): δ = 14.0 (CH_2CH_3), 22.5, 25.0, 28.8, 31.6 ($(\text{CH}_2)_4\text{CH}_3$), 35.6 ($\text{CH}_2(\text{CH}_2)_4$), 42.1 ($\text{COCH}_2\text{CH-O}$), 50.0 (CH_2COO), 51.4 ($\text{C}_6\text{H}_5\text{CH}_2\text{N}$), 55.3 (OCH_3), 76.0 (CH-O), 114.3 (2 x $\text{OCCH}_{\text{arom}}$), 127.9 ($\text{CH}_2\text{C}_{\text{arom}}$), 129.6 (2 x $\text{CH}_2\text{CCH}_{\text{arom}}$), 159.4 ($\text{CH}_3\text{OC}_{\text{arom}}$), 167.6 (CON), 168.7 (COO) ppm. MS (ESI): m/z (%): 334 ($\text{M}+\text{H}^+$, 100). HRMS mass calcd.: $\text{C}_{19}\text{H}_{27}\text{NO}_4\text{H}^+$ 334.2013; found: 334.2001. IR (cm^{-1}) ν_{max} 1032, 1175, 1182, 1204, 1223, 1244, 1306, 1325, 1352, 1512, 1628 (N-C=O), 1730 (C=O), 2855, 2926, 2954. Chromatography: EtOAc:petroleum ether 1:1 R_f = 0.28. Melting point: 54-56 °C. Colorless powder. Yield: 40%.

Removal of the *N*-PMB group of **121**

N-PMB-protected 1,4-oxazepane-2,5-dione **121** (1 equiv, 6.9 mmol, 2.3 g) was dissolved in 250 mL of a 4:1 ethyl acetate-water mixture and cooled to 0 °C. Ceric ammonium nitrate (CAN, 5 equiv, 34.5 mmol, 18.9 g) was added and after 2 h, 150 mL of a saturated solution of aq. NaHCO_3 was added. After a slow phase separation, the aqueous phase was extracted twice with 150 mL of ethyl acetate. The combined organic phases were washed once with brine. Drying with MgSO_4 , filtration and removal of the solvent *in vacuo* yielded the crude seven-membered ring, which was purified immediately via column chromatography (ethyl acetate:petroleum ether 1:1), to yield 200 mg of compound **122** as a colorless powder (14% yield).

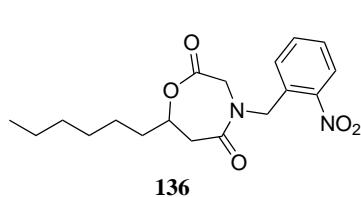


7-Hexyl-1,4-oxazepane-2,5-dione **122**. ^1H NMR (400 MHz, CDCl_3): δ = 0.89 (3H, t, J = 6.5 Hz, CH_3), 1.22-1.61 (8H, m, $(\text{CH}_2)_4\text{CH}_3$), 1.61-1.83 (2H, m, $\text{CH}_2(\text{CH}_2)_4$), 2.83 (2H, d, J = 6.8 Hz, $\text{COCH}_2\text{CH-O}$), 3.85 (1H, dd, J = 15.3 Hz, 7.4 Hz, $\text{CHH}'\text{COO}$), 4.40 (1H, d, J = 15.3 Hz, $\text{CHH}'\text{COO}$), 4.72 (1H, quint., J = 6.5 Hz, CH-O), 6.18 (1H, d, J = 7.6 Hz, NH) ppm. ^{13}C NMR (100 MHz, CDCl_3): δ = 14.0 (CH_3), 22.5, 25.1, 28.8, 31.6 ($(\text{CH}_2)_4\text{CH}_3$),

35.1 ($\text{CH}_2(\text{CH}_2)_4$), 41.7 ($\text{COCH}_2\text{CH-O}$), 44.5 (CH_2COO), 74.7 (CH-O), 167.9 (CONH), 170.5 (COO) ppm. MS (ESI): m/z (%): 214 ($\text{M}+\text{H}^+$, 100). HRMS mass calcd.: $\text{C}_{11}\text{H}_{19}\text{NO}_3\text{H}^+$ 214.1438; found: 214.1438. IR (cm^{-1}) ν_{max} 1090, 1113, 1348, 1422, 1447, 1489, 1551 (HN-C=O), 1638 (HN-C=O), 1707, 1738 (C=O), 2849, 2924, 2953, 3256 (N-H). Chromatography: EtOAc:petroleum ether 1:1 R_f = 0.15. Melting point: 62-64 °C. Colorless powder. Yield: 14%.

Synthesis of *N*-(2-nitrobenzyl)-1,4-oxazepane-2,5-dione **136**

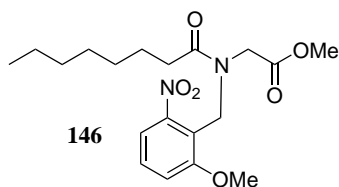
To a stirred suspension of glycine methyl ester hydrochloride **105** (1 equiv, 20 mmol, 2.51 g) in dry methanol (30 mL) under a nitrogen atmosphere and at 0 °C, was added triethylamine (1 equiv, 20 mmol, 2.8 mL) followed by 2-nitrobenzaldehyde **132** (1.1 equiv, 22 mmol, 3.32 g). The bulb was entirely covered with aluminium foil and the reaction mixture was stirred for 2 h at room temperature and then cooled down to 0 °C. Sodium borohydride (2 equiv, 20 mmol, 1.51 g) was portionwise added. The ice bath was removed and after 1 h the reaction was quenched by the addition of H_2O (50 mL). Extraction with diethyl ether (3 x 50 mL), washing with brine (50 mL), drying (MgSO_4) and evaporation of the solvent *in vacuo* gave methyl (2-nitrobenzyl)glycinate **133** (3.14 g, 70% crude yield) as a yellow oil. To avoid premature photolysis, compound **133** was immediately *N*-acylated, hydrolyzed and cyclized according to general procedures B, C and D. The resulting 1,4-oxazepane-2,5-dione **136** with a photolabile *N*-protecting group was purified via column chromatography (ethyl acetate:petroleum ether 1:1) to yield 7-hexyl-4-(2-nitrobenzyl)-1,4-oxazepane-2,5-dione **136** as a yellow powder in 40% total yield.



7-Hexyl-4-(2-nitrobenzyl)-1,4-oxazepane-2,5-dione **136**. ^1H NMR (400 MHz, CDCl_3): δ = 0.89 (3H, t, J = 6.8 Hz, CH_3), 1.22-1.56 (8H, m, $(\text{CH}_2)_4\text{CH}_3$), 1.59-1.83 (2H, m, $\text{CH}_2(\text{CH}_2)_4$), 2.93-3.06 (2H, m, $\text{COCH}_2\text{CH-O}$), 3.95 (1H, d, J = 15.8 Hz, $\text{CHH}'\text{COO}$), 4.44 (1H, d, J = 15.7 Hz, $\text{CHH}'\text{COO}$), 4.66-4.72 (1H, m, CH-O), 4.72 (1H, d, J = 15.2 Hz, $\text{C}_6\text{H}_5\text{CHH}'\text{N}$), 4.86 (1H, d, J = 15.2 Hz, $\text{C}_6\text{H}_5\text{CHH}'\text{N}$), 7.53-7.63 (2H, m, 2 x CH_{arom}), 8.11-8.20 (2H, m, 2 x CH_{arom}) ppm. ^{13}C NMR (100 MHz, CDCl_3): δ = 14.0 (CH_3), 22.5, 25.0, 28.8, 31.5 ($(\text{CH}_2)_4\text{CH}_3$), 35.6 ($\text{CH}_2(\text{CH}_2)_4$), 42.1 ($\text{COCH}_2\text{CH-O}$), 50.6 (CH_2COO), 51.7 ($\text{C}_6\text{H}_5\text{CH}_2\text{N}$), 76.0 (CH-O), 122.8, 123.2, 130.1, 134.0 (4 x CH_{arom}), 138.2 ($\text{CH}_2\text{C}_{\text{arom}}$), 148.6 ($\text{O}_2\text{NC}_{\text{arom}}$), 167.1 (CON), 168.9 (COO) ppm. MS (ESI): m/z (%): 349 ($\text{M}+\text{H}^+$, 100). IR (cm^{-1}) ν_{max} 1108, 1215, 1246, 1402 (NO_2), 1473, 1512, 1584 (NO_2), 1614 (N-C=O), 1725 (C=O), 2867, 2915. Chromatography: EtOAc:petroleum ether 1:1 R_f = 0.19. Melting point: 48-50 °C. Yellow powder. Yield: 40%.

Synthesis of PPG-protected test substrate 146

To a stirred suspension of glycine methyl ester hydrochloride **105** (1 equiv, 2.5 mmol, 0.32 g) in methanol:DMF 1:1 (20 mL) at room temperature, was added 0.5 g 2-methoxy-6-nitrobenzaldehyde **142** (1.1 equiv, 2.8 mmol), followed by the addition of triethylamine (2 equiv, 5 mmol, 0.7 mL). The bulb was entirely covered with aluminium foil and the reaction mixture was stirred for 1 h at room temperature. The bulb was placed in an ice bath and sodium borohydride (2 equiv, 5 mmol, 0.19 g) was added portionwise. The ice bath was removed and after stirring overnight, the reaction was quenched by the addition of H₂O (20 mL). Extraction with diethyl ether (3 x 20 mL), washing with brine (2 x 20 mL), drying over MgSO₄ and removal of the solvent *in vacuo* gave methyl (2-methoxy-6-nitrobenzyl)glycinate **145** (0.41 g, 58% crude yield) as a orange oil. 0.4 g Of methyl (2-methoxy-6-nitrobenzyl)glycinate **145** (1 equiv, 1.6 mmol) was dissolved in 10 mL THF:H₂O 1:1 in an aluminium foil-covered bulb, followed by the addition of potassium carbonate (2 equiv, 3.2 mmol, 0.44 g) and the dropwise addition of octanoyl chloride **54e** (1 equiv, 1.6 mmol, 0.27 mL). After vigorous stirring for 2 h at room temperature, the reaction mixture was extracted with ethyl acetate (3 x 15 mL). The combined organic phases were washed (1 x 30 mL of a saturated aq. NaHCO₃-solution, 1 x 30 mL brine) and dried (MgSO₄), followed by evaporation of the solvent *in vacuo* to yield crude **146**. This compound **146** was purified via column chromatography (ethyl acetate:petroleum ether 2:1) to give 285 mg (30% total yield) of *N*-PPG protected ester **146** as an orange oil.



Methyl *N*-(2-methoxy-6-nitrobenzyl)-*N*-octanoylglycinate **146**. Spectral data were obtained from a mixture of two rotamers in a 1.7:1 ratio. ¹H NMR (400 MHz, CDCl₃): δ rotamer 1 (major): 0.81-0.88 (3H, m, CH₂CH₃), 1.16-1.39 (8H, m, (CH₂)₄CH₃), 1.61-1.70 (2H, m, CH₂(CH₂)₄CH₃), 2.56 (2H, t, *J* = 7.6 Hz, CH₂CON), 3.62 (3H, s, COOCH₃), 3.87 (3H, s, C_{arom}OCH₃), 3.89 (2H, s, NCH₂COO), 4.77-4.80 (2H, m, CH₂C_{arom}), 7.05-7.46 (3H, m, 3 x CH_{arom}) ppm; rotamer 2 (minor): 0.81-0.88 (3H, m, CH₂CH₃), 1.16-1.39 (8H, m, (CH₂)₄CH₃), 1.47-1.61 (2H, m, CH₂(CH₂)₄CH₃), 2.12 (2H, t, *J* = 7.6 Hz, CH₂CON), 3.69 (3H, s, COOCH₃), 3.84 (3H, s, C_{arom}OCH₃), 4.05 (2H, s, NCH₂COO), 4.77-4.80 (2H, m, CH₂C_{arom}), 7.05-7.46 (3H, m, 3 x CH_{arom}) ppm. ¹³C NMR (100 MHz, CDCl₃): δ rotamer 1 (major): 14.04 (CH₂CH₃), 22.6, 29.1, 29.4, 31.7 ((CH₂)₄CH₃), 25.1 (CH₂(CH₂)₄CH₃), 32.8 (CH₂CON), 42.0 (CH₂C_{arom}), 45.6 (NCH₂COO), 51.8 (COOCH₃), 56.3 (C_{arom}OCH₃), 114.8, 116.1, 129.4 (3 x CH_{arom}), 118.0 (CH₂C_{arom}), 151.4 (C_{arom}NO₂), 158.9 (C_{arom}OCH₃), 169.8 (CON), 174.4 (COO) ppm; rotamer 2 (minor): 14.02 (CH₂CH₃), 22.5, 29.0, 29.2, 31.6 ((CH₂)₄CH₃), 24.9 (CH₂(CH₂)₄CH₃), 33.1 (CH₂CON), 40.9 (CH₂C_{arom}),

49.7 (NCH₂COO), 52.3 (COOCH₃), 56.2 (C_{arom}OCH₃), 114.1, 115.8, 129.2 (3 x CH_{arom}), 119.4 (CH₂C_{arom}), 150.7 (C_{arom}NO₂), 158.5 (C_{arom}OCH₃), 169.9 (CON), 173.6 (COO) ppm. MS (ESI): *m/z* (%): 381 (M+H⁺, 100). IR (cm⁻¹) ν_{max} 1058, 1175, 1195, 1204, 1223, 1244, 1311, 1333, 1343 (NO₂), 1542 (NO₂), 1648 (N-C=O), 1720 (C=O), 2844, 2931. Chromatography: EtOAc:petroleum ether 2:1 R_f = 0.26. Orange oil. Yield: 30%.

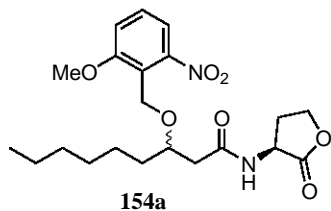
Synthesis of PPG-protected HO-AHL 154a

To a solution of 404 mg of ethyl 3-hydroxynonanoate **55d** (1 equiv, 2 mmol) in 10 mL of anhydrous THF were added triethylamine (2.2 equiv, 4.4 mmol, 0.613 mL) and chlorotrimethylsilane (2 equiv, 4 mmol, 0.51 mL). After stirring for 17 h at room temperature, 20 mL of diethyl ether was added and the reaction mixture was cooled to 0 °C. Then 1 mL of a saturated aq. NaHCO₃-solution was added, followed by 25 mL of cold water. After phase separation, the aqueous phase was washed twice with diethyl ether (2 x 20 mL). The combined organic phases were dried over MgSO₄, the drying agent was removed by filtration and after removal of the solvent *in vacuo*, crude trimethyl silyl ether **151a** was obtained.

To an ice-cold solution of this silyl ether **151a** in anhydrous CH₂Cl₂ (20 mL) in an aluminium foil-covered bulb was added 2-methoxy-6-nitrobenzaldehyde **142** (1 equiv, 2 mmol, 362 mg) and trimethylsilyl triflate (0.1 equiv, 0.2 mmol, 40 μ L). The resulting reaction mixture was stirred at 0 °C for 1 h, followed by the addition of 0.32 mL of triethylsilane (1 equiv, 2 mmol). The reaction mixture was allowed to warm to room temperature and stirred overnight. Then 60 mL of diethyl ether was added, followed by washing of the organic phase with a saturated aq. NaHCO₃-solution (40 mL) and brine (40 mL). Drying and evaporation of the solvent yielded crude ethyl 3-((2-methoxy-6-nitrobenzyl)oxy)nonanoate **152a** as an orange oil. This crude ester **152a** was hydrolyzed with 5 equiv of NaOH (10 mmol, 5 mL of a 2M aq. solution) in 15 mL of THF:MeOH 2:1. The reaction mixture was left to stir at room temperature overnight, followed by an extraction step with hexane. The aqueous phase was acidified with 2M aq. HCl and extracted three times with ethyl acetate. After washing with brine, followed by drying (MgSO₄) and removal of the drying agent by filtration, the solvent was removed by rotary evaporation to yield the crude hydrolyzed product **153a**.

The crude PPG-protected fatty acid **153a** (1 equiv, 2 mmol) was brought into an aluminium foil-covered bulb with 5 mL of H₂O, followed by the addition of 0.31 mL of Et₃N (1 equiv, 2 mmol), 430 mg of EDC.HCl (1 equiv, 2 mmol) and 408 mL of lactone **53** (1 equiv, 2 mmol). The turbid reaction mixture was stirred overnight at room temperature. Then 10 mL of water and 10 mL of ethyl acetate were added. After phase separation, the aqueous phase was extracted twice with 10 mL of ethyl acetate. The combined organic phases were washed with a saturated

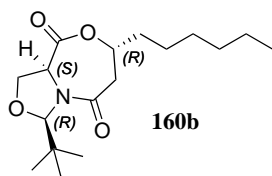
aq. NaHCO_3 -solution (20 mL) and brine (20 mL) to yield the crude PPG-protected AHL **154a**. Purification via column chromatography (ethyl acetate:petroleum ether 1:1) gave 204 mg of pure **154a** in 24% total yield.



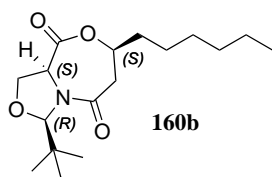
N-(3-((2-methoxy-6-nitrobenzyl)oxy)nonanoyl)-L-homoserine lactone **154a**. Spectral data were obtained from a 1:1 mixture of diastereomers. ^1H NMR (400 MHz, CDCl_3): δ = 0.90 (3H, t, J = 6.5 Hz, CH_2CH_3), 1.23-1.42 (8H, m, $(\text{CH}_2)_4\text{CH}_3$), 1.51-1.75 (2H, m, $\text{CH}_2(\text{CH}_2)_4$), 2.16-2.30 (1H, m, $\text{OCH}_2\text{CHH}'$), 2.45 (1H, dd, J = 15.3 Hz, 6.8 Hz, $\text{CHH}'\text{CONH}$), 2.69 (1H, dd, J = 15.3 Hz, 3.3 Hz, $\text{CHH}'\text{CONH}$), 2.68-2.77 (1H, m, $\text{OCH}_2\text{CHH}'$), 3.76-3.84 (1H, m, $\text{CH-OCH}_2\text{C}_{arom}$), 3.95 (3H, s, OCH_3), 4.26 (1H, ddd, J = 10.7 Hz, 9.4 Hz, 6.1 Hz, $\text{OCHH}'\text{CH}_2$), 4.42-4.51 (1H, m, $\text{OCHH}'\text{CH}_2$), 4.60-4.74 (1H, m, CHN), 4.78-4.86 (2H, m, $\text{OCH}_2\text{C}_{arom}$), 6.98 (1H, d, J = 7.1 Hz, NH), 7.17 (1H, d, J = 7.8 Hz, CH_{arom}), 7.39-7.48 (2H, m, 2 x CH_{arom}) ppm. ^{13}C NMR (100 MHz, CDCl_3): δ = 14.1 (CH_2CH_3), 22.6, 25.1, 29.3, 31.7 ($(\text{CH}_2)_4\text{CH}_3$), 33.8 ($\text{CH}_2(\text{CH}_2)_4$), 41.4 (CH_2CONH), 49.2 (NCH), 56.3 (OCH_3), 66.0 ($\text{CH}_2\text{CH}_2\text{O}$), 70.3 ($\text{OCH}_2\text{C}_{arom}$), 77.1 (CH-OCH_2), 114.7, 116.1, 129.7 (CH_{arom}), 119.8 ($\text{CH}_2\text{C}_{arom}$), 152.3 ($\text{C}_{arom}\text{NO}_2$), 158.5 ($\text{C}_{arom}\text{OCH}_3$), 171.6 (CON), 175.2 (COO) ppm. MS (ESI): m/z (%): 423 ($\text{M}+\text{H}^+$, 100). IR (cm^{-1}) ν_{max} 941, 1038, 1050, 1377, 1390 (NO_2), 1548 (NO_2), 1589 (HN-C=O), 1648 (HN-C=O), 1771 ($\text{C=O}_{lactone}$), 2832, 2933, 2987, 3212 (N-H). Chromatography: EtOAc:petroleum ether 1:1 R_f = 0.1. Melting point: 62-64 °C. Yellow powder. Yield: 24%.

Synthesis of 2-*t*butyloxazolidine protected oxazepane-2,5-dione **160b**

*t*Bu-Oxazolidine **157b** (1.05 equiv, 4.0 mmol, 0.75 g) was *N*-acylated according to general procedure B. The *N*-acylated 2-*t*Bu-oxazolidine **158b** was immediately subjected to a hydrolysis and cyclization reaction according to general procedures C and D. The crude oxazepane-2,5-dione **160b**, present as a 1:1 mixture of diastereomers, was purified via column chromatography (Reveleris X2 automated flash chromatography instrument: gradient increase over 5 column volumes (CV) from 100% hexane to 90% hexane 10% ethyl acetate, hold 5 CV, gradient increase over 10 CV to 50% hexane - 50% ethyl acetate, hold 2 CV, then 2 CV 100% ethyl acetate) followed by recrystallization in diethyl ether:hexane to successfully separate both diastereomers and to give 0.28 g (0.91 mmol, 24% yield) of (*RRS*)-**160b**, 0.33 g (1.1 mmol, 28% yield) of (*RSS*)-**160b** and 0.13 g (0.42 mmol, 11% yield) of a mixture of (*RRS*)/(*RSS*)-**160b**



(*3R,7R,9aS*)-3-(*t*Butyl)-7-hexyltetrahydro-3*H,5H,9H*-oxazolo[4,3-*c*]-[1,4]oxazepine-5,9-dione (*RRS*)-**160b** (*trans*-diastereomer). ¹H NMR (400 MHz, CDCl₃): δ = 0.89 (3H, t, *J* = 6.8 Hz, CH₂CH₃), 0.95 (9H, s, C(CH₃)₃), 1.19-1.55 (8H, m, (CH₂)₄CH₃), 1.63-1.84 (2H, m, CH₂(CH₂)₄CH₃), 2.72 (1H, d, *J* = 16.6 Hz, COCHH'CH-O), 3.14 (1H, dd, *J* = 16.5 Hz, 11.2 Hz, COCHH'CH-O), 4.44 (1H, dd, *J* = 9.1 Hz, 9.1 Hz, CHH'-O), 4.52 (1H, dd, *J* = 9.3 Hz, 8.3 Hz, CHH'-O), 4.68-4.79 (2H, m, CH₂CH-O and CH₂CHN), 5.36 (1H, s, NCH-O) ppm. ¹³C NMR (100 MHz, CDCl₃): δ = 14.0 (CH₂CH₃), 22.5, 24.5, 28.9, 31.6 ((CH₂)₄CH₃), 25.9 (C(CH₃)₃), 37.2 (CH₂(CH₂)₄CH₃), 38.7 (C(CH₃)₃), 42.6 (COCH₂CH-O), 59.4 (OOCCHN), 69.2 (CH₂-O), 79.7 (CH₂CH-O), 96.2 (NCH-O), 166.3 (CON), 171.7 (COO) ppm. MS (ESI): *m/z* (%): 312 (M+H⁺, 100). HRMS mass calcd.: C₁₇H₂₉NO₄⁻ 310.2024; found: 310.2016. IR (cm⁻¹) ν_{max} 1119, 1179, 1215, 1231, 1362, 1369, 1381, 1680 (N-C=O), 1703, 1711 (C=O), 2870, 2930, 2970, 2980. Chromatography: EtOAc:petroleum ether 3:1 R_f = 0.29. Melting point: 94-96 °C. Colorless powder. Yield: 24%.



(*3R,7S,9aS*)-3-(*t*Butyl)-7-hexyltetrahydro-3*H,5H,9H*-oxazolo[4,3-*c*]-[1,4]oxazepine-5,9-dione (*RSS*)-**160b** (*cis*-diastereomer). ¹H NMR (400 MHz, CDCl₃): δ = 0.89 (3H, t, *J* = 6.8 Hz, CH₂CH₃), 0.95 (9H, s, C(CH₃)₃), 1.21-1.58 (8H, m, (CH₂)₄CH₃), 1.61-1.89 (2H, m, CH₂(CH₂)₄CH₃), 2.85 (1H, dd, *J* = 17.7 Hz, 9.8 Hz, COCHH'CH-O), 2.97 (1H, dd, *J* = 17.6 Hz, 2.6 Hz, COCHH'CH-O), 4.36 (1H, dd, *J* = 9.2 Hz, 8.0 Hz, CHH'-O), 4.62 (1H, dd, *J* = 9.2 Hz, 9.2 Hz, CHH'-O), 4.71-4.83 (2H, m, CH₂CH-O and CH₂CHN), 5.44 (1H, s, NCH-O) ppm. ¹³C NMR (100 MHz, CDCl₃): δ = 14.0 (CH₂CH₃), 22.5, 24.5, 28.8, 31.5 ((CH₂)₄CH₃), 26.4 (C(CH₃)₃), 35.5 (CH₂(CH₂)₄CH₃), 38.9 (C(CH₃)₃), 42.5 (COCH₂CH-O), 55.1 (OOCCHN), 68.6 (CH₂-O), 75.2 (CH₂CH-O), 97.0 (NCH-O), 167.6 (CON), 168.5 (COO) ppm. MS (ESI): *m/z* (%): 312 (M+H⁺, 100). HRMS mass calcd.: C₁₇H₂₉NO₄⁻ 310.2024; found: 310.2028. IR (cm⁻¹) ν_{max} 1076, 1125, 1175, 1211, 1233, 1354, 1364, 1375, 1396, 1649 (N-C=O), 1738 (C=O), 2889, 2924, 2970, 2982. Chromatography: EtOAc:petroleum ether 3:1 R_f = 0.28. Melting point: 96-98 °C. Colorless needle-like crystals. Yield: 28%.

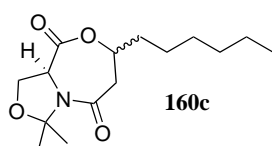
The absolute configuration of (*RSS*)-**160b** was determined as C4 (*S*), C6 (*R*) and C1 (*S*) and confirmed by a refined Flack parameter of -0.03(12). Additionally, the C₆H₁₃ alkyl chain showed positional disorder, which could be modeled in two parts with final occupancy factors of 0.502 and 0.498, respectively.

Crystal data for compound (RSS)-160b. C₁₇H₂₉NO₄, M = 311.41, orthorhombic, space group

$P2_12_12_1$ (No. 19), $a = 5.65117(9)$ Å, $b = 11.07138(12)$ Å, $c = 29.0073(4)$ Å, $V = 1814.88(4)$ Å³, $Z = 4$, $T = 293(2)$ K, $\rho_{calc} = 1.140$ g cm⁻³, $\mu(\text{Cu-K}\alpha) = 0.647$ mm⁻¹, $F(000) = 680$, 62469 reflections measured, 3718 unique ($R_{int} = 0.0826$) which were used in all calculations. The final $R1$ was 0.0531 ($I > 2\sigma(I)$) and $wR2$ was 0.1624 (all data). The asymmetric unit contains two crystallographic independent molecules.

Synthesis of 2,2-dimethyloxazolidine protected oxazepane-2,5-dione **160c**

To methyl *N*-(3-hydroxynonanoyl)-*L*-serinate **89** (1 equiv, 2 mmol, 0.55 mg), dissolved in dry toluene (20 mL) under a nitrogen atmosphere, were sequentially added 2,2-dimethoxypropane (DMP) (5 equiv, 10 mmol, 1.2 mL) and *p*-toluenesulfonic acid monohydrate (0.1 equiv, 0.2 mmol, 40 mg). The mixture was heated at reflux in a Dean-Stark apparatus for 3 h to remove water. After cooling to ambient temperature, water (20 mL) was added. The aqueous phase was extracted twice with ethyl acetate (2 x 20 mL), the organic phases were combined and washed with brine (20 mL), dried (MgSO₄), filtered and the solvent was removed *in vacuo*. The crude oxazolidine **158c** was hydrolyzed and cyclized according to the general procedures C and D to yield compound **160c** (0.10 g, 0.36 mmol) in 18% total yield after column chromatography (Reveleris X2 automated flash chromatography instrument: 5 column volumes (CV) 100% hexane, gradient increase over 15 CV to 50% hexane - 50% ethyl acetate, hold 2 CV, then 2 CV 100% ethyl acetate). Diastereomers (ratio 1.3:1) could not be separated via flash chromatography.

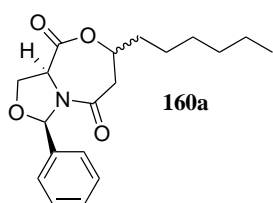


(9a*S*)-7-Hexyl-3,3-dimethyltetrahydro-3*H*,5*H*,9*H*-oxazolo[4,3-*c*][1,4]-oxazepine-5,9-dione **160c**. Spectral data were obtained from a 1.3:1 mixture of diastereomers. ¹H NMR (400 MHz, CDCl₃): δ diastereomer 1 (major): 0.91 (3H, t, $J = 6.8$ Hz, CH₂CH₃), 1.25-1.82 (10H, m, (CH₂)₅CH₃), 1.61, 1.64, (2 x 3H, 2 x s, C(CH₃)₂), 2.63 (1H, dd, $J = 15.1$ Hz, 2.2 Hz, COCHH'CH-O), 3.06 (1H, dd, $J = 15.1$ Hz, 11.7 Hz, COCHH'CH-O), 4.23-4.33 (1H, m, CHH'-O), 4.59-4.67 (1H, m, CHH'-O), 4.70-4.81 (2H, m, CH-O and CHN) ppm; diastereomer 2 (minor): 0.91 (3H, t, $J = 6.8$ Hz, CH₂CH₃), 1.25-1.82 (10H, m, (CH₂)₅CH₃), 1.62, 1.69 (2 x 3H, 2 x s, C(CH₃)₂), 2.80 (1H, dd, $J = 18.5$ Hz, 10.8 Hz, COCHH'CH-O), 2.88 (1H, dd, $J = 18.5$ Hz, 2.8 Hz, COCHH'CH-O), 4.23-4.33 (1H, m, CHH'-O), 4.51 (1H, dd, $J = 9.6$ Hz, 7.6 Hz, CHH'-O), 4.59-4.67 (1H, m, CHN), 4.70-4.81 (1H, m, CH-O) ppm. ¹³C NMR (100 MHz, CDCl₃): δ diastereomer 1 (major): 14.0 (CH₂CH₃), 22.5, 24.5, 28.8, 28.9, 31.6, 34.8, 37.5 ((CH₂)₅CH₃), 23.5, 24.9 (C(CH₃)₂), 25.1 (C(CH₃)₂), 43.1 (COCH₂CH-O), 59.7 (CHN), 65.8 (CH₂-O), 79.8 (CH-O), 96.6 (O-C-N), 164.8 (CON), 167.9 (COO) ppm; diastereomer 2 (minor): 14.0 (CH₂CH₃), 22.5, 24.5, 28.8, 28.9, 31.6, 34.8, 37.5 ((CH₂)₅CH₃), 23.8, 25.3

(C(CH₃)₂), 25.1 (C(CH₃)₂), 43.4 (COCH₂CH-O), 54.6 (CHN), 65.7 (CH₂-O), 73.8 (CH-O), 98.3 (O-C-N), 166.9 (CON), 167.1 (COO) ppm. MS (ESI): *m/z* (%): 284 (M+H⁺, 100). HRMS mass calcd.: C₁₅H₂₅NO₄H⁺ 284.1856; found: 284.1856. IR (cm⁻¹) ν_{max} 1072, 1085, 1155, 1209, 1233, 1252, 1335, 1381, 1418, 1632 (N-C=O), 1667, 1703, 1742 (C=O), 2889, 2916, 2932, 2972, 2982. Chromatography: EtOAc:petroleum ether 3:1 R_f = 0.21. Melting point: 88-90 °C. Colorless needle-like crystals. Yield: 18%.

Synthesis of 2-phenyloxazolidine protected oxazepane-2,5-dione **160a**

To a stirred solution of L-serine methyl ester hydrochloride **88** (1 equiv, 20 mmol, 3.1 g) in 60 mL of anhydrous CH₂Cl₂ and 15 mL Et₃N at room temperature was added 4.8 g of anhydrous MgSO₄ (2 equiv, 40 mmol), followed by freshly distilled benzaldehyde **112** (1.1 equiv, 22 mmol, 2.24 mL) under a nitrogen atmosphere. The reaction mixture was stirred at room temperature overnight, filtered and the filtrate was concentrated under reduced pressure. The resulting 2-phenyloxazolidine **157a** was *N*-acylated analogously to the *t*Bu-derivative **157b**, followed by hydrolysis and cyclization (procedures C and D) to give the 1,4-oxazepane-2,5-dione **160a**, as a 1:1-mixture of diastereomers in 53% overall yield (3.5 g, 10.6 mmol). Diastereomers (ratio 1:1) could not be separated via flash chromatography (ethyl acetate:petroleum ether 3:1).

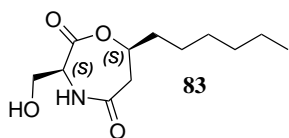


(3*R*,9*aS*)-7-Hexyl-3-phenyltetrahydro-3*H*,5*H*,9*H*-oxazolo[4,3-*c*][1,4]-oxazepine-5,9-dione **160a**. Spectral data were obtained from a 1:1 mixture of diastereomers. ¹H NMR (400 MHz, CDCl₃): δ diastereomer 1: 0.88-0.95 (3H, m, CH₃), 1.28-1.90 (10H, m, (CH₂)₅CH₃), 2.75 (1H, d, *J* = 15.8 Hz, COCHH'CH-O), 3.17 (1H, dd, *J* = 15.8 Hz, 11.2 Hz, COCHH'CH-O), 4.35-4.44 (1H, m, CHH'-O), 4.47-4.54 (1H, m, CHH'-O), 4.75-4.83 (1H, m, CH₂CH-O), 4.85-4.97 (1H, m, CH₂CHN), 6.50 (1H, s, NCH-O), 7.27-7.42 (5H, m, 5 x CH_{arom}) ppm; diastereomer 2: 0.88-0.95 (3H, m, CH₂CH₃), 1.28-1.90 (10H, m, (CH₂)₅CH₃), 2.91 (2H, d, *J* = 6.8 Hz, COCH₂CH-O), 4.35-4.44 (1H, m, CHH'-O), 4.47-4.54 (1H, m, CHH'-O), 4.75-4.83 (1H, m, CH₂CH-O), 4.85-4.97 (1H, m, CH₂CHN), 6.52 (1H, s, NCH-O), 7.27-7.42 (5H, m, 5 x CH_{arom}) ppm. ¹³C NMR (100 MHz, CDCl₃): δ diastereomer 1: 14.0 (CH₃), 22.5, 24.5, 28.9, 31.57, 35.1 ((CH₂)₅CH₃), 41.9 (COCH₂CH-O), 59.0 (CH₂CHN), 68.1 (CH₂-O), 79.9 (CH₂CH-O), 89.9 (O-CHN), 126.1, 128.7, 129.2 (5 x CH_{arom}), 137.2 (C_{arom}), 165.4 (CON), 169.3 (COO) ppm; diastereomer 2: 14.0 (CH₃), 22.5, 24.5, 28.8, 31.58, 37.4 ((CH₂)₅CH₃), 42.1 (COCH₂CH-O), 54.2 (CH₂CHN), 67.1 (CH₂-O), 74.2 (CH₂CH-O), 91.7 (O-CHN), 126.3, 126.8, 129.1 (5 x CH_{arom}) 137.0 (C_{arom}), 166.0 (CON), 167.5 (COO) ppm. MS (ESI): *m/z* (%): 332 (M+H⁺, 100). HRMS mass calcd.: C₁₉H₂₅NO₄H⁺ 332.1856; found: 332.1868. IR (cm⁻¹) ν_{max} 1061, 1117, 1221, 1389, 1425, 1655 (N-C=O), 1676, 1703, 1724

(C=O), 2857, 2926, 2953. Chromatography: EtOAc:petroleum ether 3:1 R_f = 0.14. Melting point: 96-98 °C. Colorless powder. Yield: 53%.

Debenzylation of 2-phenyloxazolidine **160a**

500 mg (1 equiv, 1.5 mmol) of 2-phenyloxazolidine **160a** (d.r. 1:1) was dissolved in 30 mL of ethyl acetate whereafter 250 mg of Pd(OH)₂/C (20 wt% loading) was added and the reaction mixture was stirred under a H₂ atmosphere at room temperature for 6 h. Subsequently, the reaction mixture was filtered through celite and the solvent removed *in vacuo*. The crude mixture was purified via column chromatography (ethyl acetate: petroleum ether 1:1 to 100% ethyl acetate) to yield 82 mg (0.32 mmol, 22% yield) of deprotected compound **83**, alongside with 334 mg (1 mmol) of recovered 2-phenyloxazolidine **160a** (d.r. 1:3).



(3*S*,7*S*)-7-Hexyl-3-(hydroxymethyl)-1,4-oxazepane-2,5-dione (*SS*)-**83**. ¹H NMR (400 MHz, CDCl₃): δ = 0.89 (3H, t, J = 6.7 Hz, CH₃), 1.23-1.57 (8H, m, (CH₂)₄CH₃), 1.58-1.83 (2H, m, CH₂(CH₂)₄CH₃), 2.60-2.66 (1H, m, CH₂OH), 2.79 (1H, dd, J = 18.7 Hz, 3.0 Hz, COCHH'CH-O), 2.87 (1H, dd, J = 18.6 Hz, 11.3 Hz, COCHH'CH-O), 3.89 (1H, ddd, J = 12.3 Hz, 8.3 Hz, 4.3 Hz, CHH'OH), 4.06 (1H, ddd, J = 12.0 Hz, 5.0 Hz, 5.0 Hz, CHH'OH), 4.46-4.51 (1H, m, CHN), 4.73-4.81 (1H, m, CH-O), 6.45 (1H, br s, NH) ppm. ¹³C NMR (100 MHz, CDCl₃): δ = 14.0 (CH₃), 22.5, 25.1, 28.8, 31.5 ((CH₂)₄CH₃), 34.9 (CH₂(CH₂)₄CH₃), 41.7 (COCH₂CH-O), 52.8 (CHN), 61.1 (CH₂OH), 73.7 (CH-O), 169.5 (CONH), 171.6 (COO) ppm. MS (ESI): m/z (%): 244 (M+H⁺, 100). HRMS mass calcd.: C₁₂H₂₁NO₄H⁺ 244.1543; found: 244.1543. IR (cm⁻¹) ν_{max} 1013, 1028, 1072, 1084, 1134, 1186, 1231, 1329, 1391, 1429, 1624 (HN-C=O), 1742 (C=O), 2853, 2916, 2953, 3098 (O-H or N-H), 3206 (O-H or N-H). Chromatography: EtOAc:petroleum ether 1:1 R_f = 0.08. Melting point: 81-83 °C. Colorless powder. Yield: 22%.

5.5 Biotesting

Microorganisms, media and culture conditions

The fluorescent *Pseudomonas* CMR12a used in this study was previously isolated from the red cocoyam rhizosphere in Cameroon.³⁴⁷ The studied *Pseudomonas* strains were routinely maintained on Luria-Bertani (LB) medium at 28 °C. The different mutant strains were constructed by Dr. Nam Phuong Kieu.

Table 5.1: Microorganisms used in this study. Abbreviations used: PHZ = phenazine, CLP1 = sessilin, CLP2 = orfamide.

Strain	Relevant characteristics	Reference
<i>Pseudomonas</i>		
CMR12a	PHZ ⁺ , CLP1 ⁺ , CLP2 ⁺ , wild type (Cameroon)	Perneel <i>et al.</i> (2007) ³⁴⁷
ΔphzRΔcmrR	PHZ ⁻ , CLP1 ⁺ , CLP2 ⁺ , mutant with deletions of the <i>phzR</i> and the <i>cmrR</i> genes	This study
ΔphzIΔcmrI	PHZ ⁻ , CLP1 ⁺ , CLP2 ⁺ , mutant with deletions of the <i>phzI</i> and the <i>cmrI</i> genes	De Maeyer <i>et al.</i> (2011) ³⁶¹
ΔphzIΔcmrIR	PHZ ⁻ , CLP1 ⁺ , CLP2 ⁺ , mutant with deletions of the <i>phzI</i> , the <i>cmrI</i> and the <i>cmrR</i> genes	This study
ΔphzIRΔcmrI	PHZ ⁻ , CLP1 ⁺ , CLP2 ⁺ , mutant with deletions of the <i>phzI</i> , the <i>phzR</i> and the <i>cmrI</i> genes	This study
ΔcmrIR	PHZ ⁺ , CLP1 ⁺ , CLP2 ⁺ , mutant with deletion of the Cmr operon	This study
ΔphzIR	PHZ ⁻ , CLP1 ⁺ , CLP2 ⁺ , mutant with deletion of the phenazine biosynthesis operon	D'Aes <i>et al.</i> (2011) ²⁰¹
ΔphzIRΔcmrIR	PHZ ⁻ , CLP1 ⁺ , CLP2 ⁺ , mutant with deletion of the Phz and the Cmr operon	This study
NodT2	PHZ ⁺ , CLP1 ⁺ , CLP2 ⁺ , mutant with deletion of the <i>nodT</i> gene	This study
ΔphzI	PHZ ⁻ , CLP1 ⁺ , CLP2 ⁺ , mutant with deletion of the <i>phzI</i> gene	De Maeyer <i>et al.</i> (2011) ³⁶¹
ΔCLP1	PHZ ⁺⁺ , CLP1 ⁻ , CLP2 ⁺ , mutant with insertion in CLP1 biosynthesis genes, Gm ^R	D'Aes <i>et al.</i> (2011) ²⁰¹

Plant growth assay

Lettuce (cv. Cobham green) seeds or *A. thaliana* Col-0 seeds were surface sterilized with 1% bleach for 45 seconds. After six washes with sterile distilled water, the seeds were germinated on MS medium (Murashige and Skoog medium including vitamins, Duchefa Biochemie, Haarlem, the Netherlands) containing 0.8% plant agar (Duchefa Biochemie, Haarlem, the Netherlands). The plates were covered with aluminium foil and the plants were grown for 3 d in a growth chamber at 16 °C, with a 16 h light cycle and 80% relative humidity.

The compounds to be tested were dissolved in ethanol to obtain a 100 mM stock solution. These solutions were sterilized by filtration through a Whatman 0.2 μm filter and added to cooled MS agar medium containing vitamins to obtain the desired 10 μM concentration (25 μL of the

stock solution to 250 mL of medium). Three-day-old seedlings were transferred to the agar plates containing the compound to be tested. At least three plates were used per treatment. The control plates contained the same amount of sterile ethanol. Plants were grown for 14 d in a growth chamber at 16 °C, with a 16 h light cycle and 80% relative humidity. The primary root length was measured using a ruler.

Fungal growth inhibition assay

The effect of the compounds C10 **1g** and TA12 **11a** on fungal growth was evaluated with the fungi *B. cinerea* and *R. solani*. The compounds were added, dissolved in ethanol (100 mM stock solution) and sterilized by filtration through a Whatman 0.2 μm filter, to the cooled liquid Difco Potato Dextrose agar medium (250 mL) to reach a concentration of 50 μM . The same (125 μL) amount of sterile ethanol was added to the medium (250 mL) for the control plates. An agar cube (diameter = 5 mm), taken from an actively growing fungal colony, was placed in the center of the plates. After 2 d stored in the dark, the growth was assessed by measuring the radius of the area covered by the fungal mycelium.

Analysis of phenazine production

A 10 mM stock solution of each AHL was prepared in ethanol and sterilized by filtration through a Whatman 0.2 μm filter. 50 μL of the applicable stock solution was added to 50 mL of LB medium to obtain a final concentration of 10 μM of a certain AHL. For the control samples, an identical amount of sterile ethanol was added. The media were inoculated with the different strains and incubated overnight on a shaker at 28 °C. The phenazine production was quantified spectrophotometrically via measurement at $\lambda = 369 \text{ nm}$ and $\epsilon = 11393 \text{ M}^{-1} \text{ cm}^{-1}$ on the supernatants of the cultures with pure LB medium as a blank. An estimation of the extinction coefficient was derived before from a standard curve for unsubstituted phenazine (Sigma-Aldrich), dissolved in water at different concentrations.³⁵¹ To compare different samples, a correction for OD_{620} was made.

Swarming assay

Swarming assays were performed with soft LB agar (0.6% agar) plates. A bacterial colony was transferred from an agar plate to an Eppendorf tube filled with 1 mL of sterile water. The suspension was vortexed, then centrifuged for 10 min at 10000 g and the supernatant was discarded to avoid interference of the metabolites produced on agar plates. The bacterial pellet was resuspended in 1 mL of sterile water and the optical density (OD) was measured at 620 nm. A dilution to 10^5 CFU/mL was made and a 5 μL drop was placed in the center of a soft LB agar plate. To study the effect of different AHLs, agar plates containing 10 μM of AHL were

prepared via the addition of 500 μL of a sterile 10 mM AHL solution in ethanol to 500 mL of cooled (50 °C) molten medium. The same volume of sterile ethanol was added to the medium used to prepare the control plates. The plates were placed without cover in a laminar flow for 5 min to allow evaporation of the drop. Three replicates per condition were included. The plates were incubated at 28 °C for 41 h whereafter photos were taken.

HPLC analysis of CLP production

Samples were analyzed at Gembloux Agro-Bio Tech by reverse-phase LC-ESI-MS (HPLC Waters Alliance 2695/diode array detector, coupled with Waters SQD mass spectrometer) on an X-terra MS C18 column (100 x 4.6 mm, 3.5 μm , Waters) and eluted with a gradient of acetonitrile in water acidified with 0.1% formic acid as described before.²⁰¹

Analysis of CLP production on agar plates

All cells were scraped off from the agar plate and diluted into 6 mL of water:acetonitrile 1:1. The resulting suspension was sonicated (Sonoplus, Bandelin Electronic, Berlin) for 1 min, centrifuged for 5 min at 10000 g and the supernatant analyzed on HPLC to determine the amount of CLP.

Quantification of CLP production

LB medium was freshly prepared and autoclaved. A bacterial colony was transferred from an agar plate to an Eppendorf tube filled with 1 mL of sterile water. The suspension was vortexed, then centrifuged for 10 min at 10000 g and the supernatant was discarded. The bacterial pellet was resuspended in 1 mL of sterile water and the optical density (OD) was measured at 620 nm. From this tube, the required amount was added to the LB medium to obtain a final bacterial concentration of 10^5 CFU/mL. This inoculated medium was transferred to a 6-well plate (2.5 mL/well). Three replicates were included for each condition tested. To test the effect of HO8 **2e**, a 10 mM stock solution was prepared in ethanol and sterilized by filtration through a Whatman 0.2 μm filter. 50 μL of the applicable stock solution was added to 50 mL of LB medium to obtain a final concentration of 10 μM of a certain AHL. The same volume of sterile ethanol was added to the medium used to prepare the control. After the incubation at 28 °C for 17, 24, 41, 48 h or 130 h, 3 x 100 μL of medium out of each well was transferred to a 96-well plate to measure the OD at 620 nm. The remaining suspension was brought into a sterile Eppendorf and centrifuged for 10 min at 10000 g. The supernatant was filtered through a Whatman 0.2 μm filter and stored in an LC vial to determine the extracellular amount of CLP. The cell pellet was resuspended in 1 mL of sterile water and centrifuged once more for 10 min at 10000 g. The supernatant was removed and the cell pellet resuspended in water:acetonitrile 1:1. This mixture

was ultra-sonicated (Sonoplus, Bandelin Electronic, Berlin) for 1 min, centrifuged for 5 min at 10000 g and the supernatant analyzed on HPLC to determine the intracellular amount of CLP.

Data analysis

Statistical analysis of data was performed using the software package SPSS 24.0 for Windows (SPSSinc, Illinois, USA). After controlling the conditions of normality and homogeneity of variances, Tukey's test ($\alpha = 0.05$) was performed.

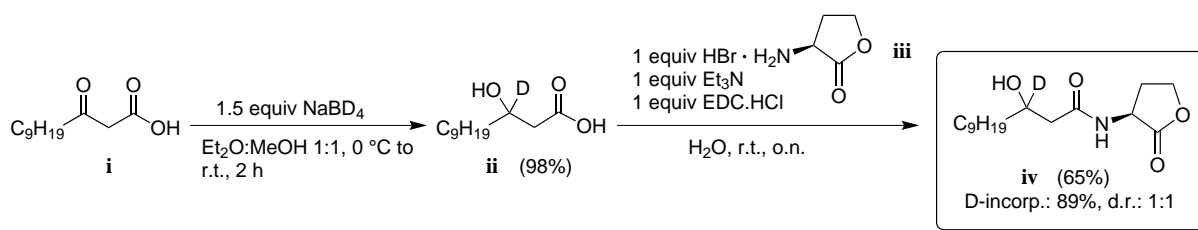
Chapter 6

Summary

Nowadays it is generally accepted that microorganisms can communicate with each other and regulate their gene expression in a cell density-dependent manner. Because this type of gene regulation is linked with the population density or quorum, the term ‘quorum sensing’ is used to describe this phenomenon. Gram-negative bacteria rely on *N*-acylated-L-homoserine lactones (AHLs) for this type of communication. As quorum sensing plays a pivotal role in both pathogenic and symbiotic bacteria-host interactions, a thorough understanding of this type of communication will grant mankind many advantages, for example the ability to interfere with bacterial infections.

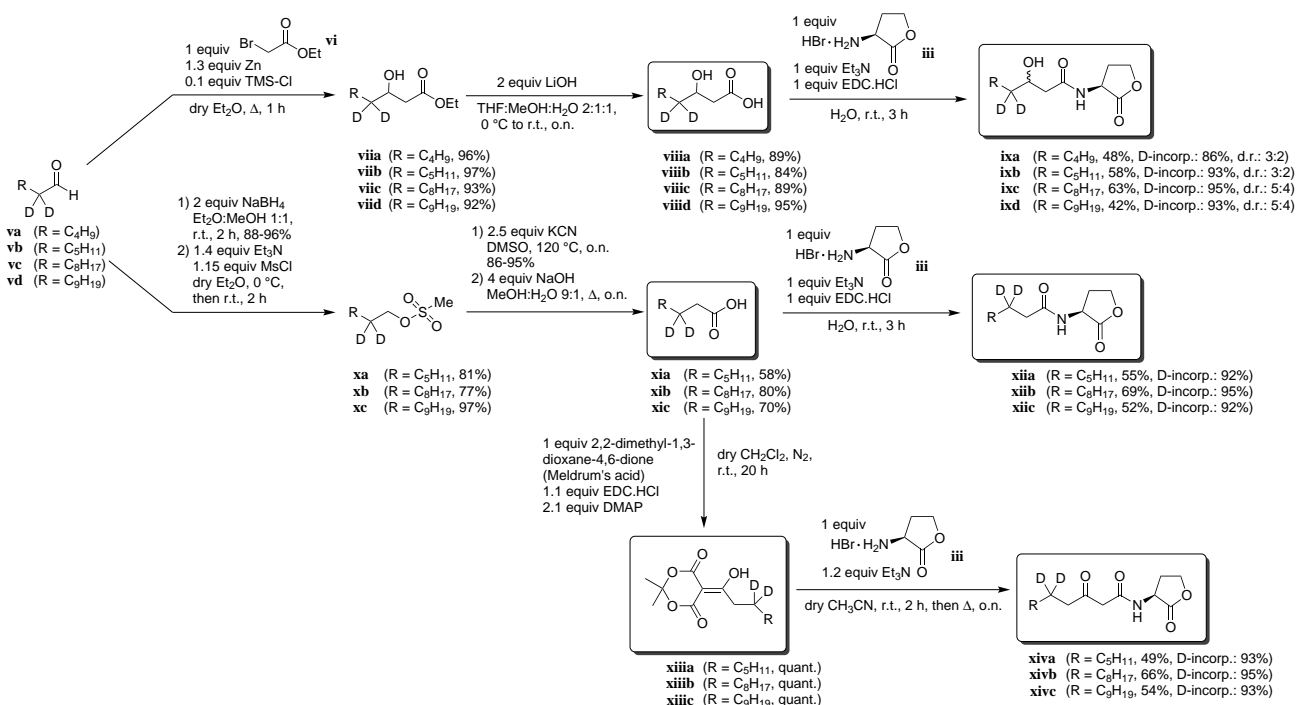
In light of the evergrowing human population, an increasing amount of pressure is put on the agriculture to produce a sufficient amount of food. To combat several plagues, most farmers rely on synthetic plant protection agents. Confronted with resistance and substantial side effects on the environment, alternatives need to be sought. One possibility is via the application of biocontrol agents. Often, these microorganisms rely on secondary metabolites to combat the malicious organism. Cyclic lipopeptides (CLPs) are examples of such secondary metabolites with antifungal or antimicrobial properties. Although the production of some CLPs is quorum sensing-regulated, this is not a general rule. Often, the exact regulation is poorly understood. Therefore, another advantage of a profound understanding of quorum sensing could be the ability to fine-tune the secondary metabolite production of biocontrol agents.

In a first part of this research, isotope-labelled AHLs were synthesized. To be able to study the metabolization of the fatty acid tail of AHLs, the isotope-label was included in the acyl chain of the AHL. In a first approach, β -oxododecanoic acid **i** was reduced with sodium borodeuteride to yield monodeuterated β -hydroxydodecanoic acid **ii**. This labelled fatty acid **ii** was coupled to L-homoserine lactone hydrobromide **iii** to yield *N*-(3-hydroxydodecanoyl-[3-²H])-L-homoserine lactone **iv** (Scheme 6.1).



Scheme 6.1. Synthesis of *N*-(3-hydroxydodecanoyl-[3-²H])-L-homoserine lactone **iv**.

As only the AHLs bearing the hydroxy moiety can be accessed via this route, an alternative approach was sought to synthesize AHLs belonging to all the different classes, starting from one easily available deuterated building block. Aliphatic aldehydes were therefore deuterated at the α -position via a DMAP-catalyzed H/D-exchange reaction. These labelled aldehydes **v** were transformed to the corresponding dideuterated β -hydroxy fatty acids **viii** via a Reformatsky reaction with ethyl bromoacetate **vi**, followed by alkaline hydrolysis (Scheme 6.2). Alternatively, the deuterated aldehydes **v** were further elaborated to unfunctionalized [3,3-di-²H]-fatty acids **xi** via a chain extension to shift the deuterium label from the acidic α -position to the β -position. EDC-mediated coupling of these fatty acids **xi** with Meldrum's acid yielded the third deuterated precursor **xiii**. Reaction of the deuterated precursors **viii**, **xi** and **xiii** with L-homoserine lactone hydrobromide **iii** yielded deuterated AHLs **ix**, **xii** and **xiv** (Scheme 6.2).

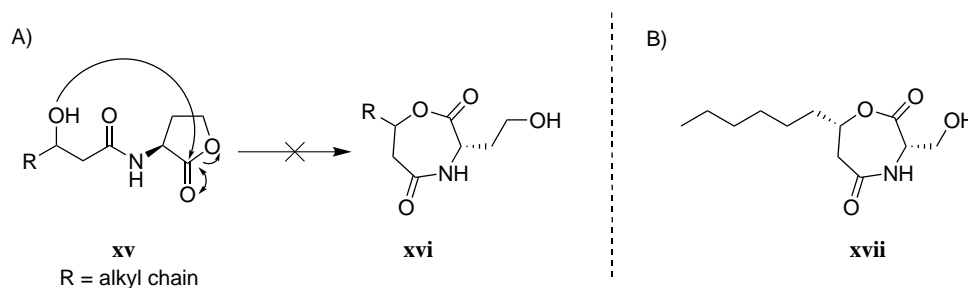


Scheme 6.2. Transformation of α,α -dideuterated aldehydes **v** into deuterated AHLs **ix**, **xii** and **xiv**.

The NMR spectra and MS fragmentation patterns of the labelled analogues **iv**, **ix**, **xii** and **xiv** were studied extensively. To be able to compare the spectral data with the unlabelled analogues, a broad library of natural *N*-acyl-, *N*-(3-hydroxyacyl)- and *N*-(3-oxoacyl)-L-homoserine lac-

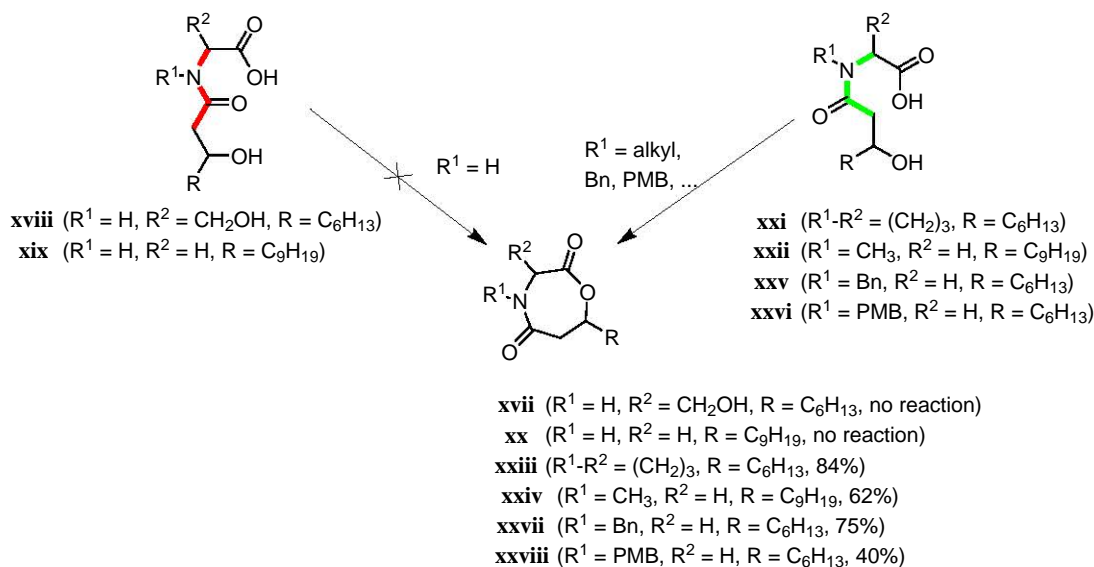
tones was synthesized.

In a second part of this research, a hypothetical rearrangement of *N*-(3-hydroxyacyl)-L-homoserine lactones **xv** toward 1,4-oxazepane-2,5-diones **xvi** was studied (Scheme 6.3). This rearrangement was not yet reported in literature, but the natural product serratin (**xvii**) fits in this type of rearrangement product quite well. Serratin (**xvii**) had been isolated from a bacterial culture of *Serratia marcescens*.



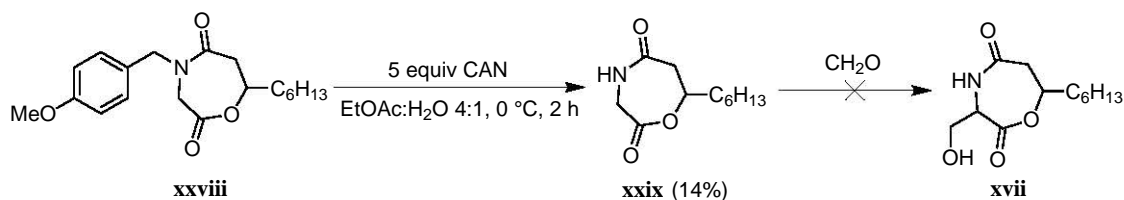
Scheme 6.3. A) Possible rearrangement of *N*-(3-hydroxyacyl)-L-homoserine lactones **xv** toward seven-membered ring **xvi**. B) Structure of the bacterial metabolite serratin (**xvii**).

Several reaction conditions were evaluated but the proposed rearrangement of *N*-(3-hydroxyacyl)-L-homoserine lactones **xv** was never observed. *N*-(3-Hydroxynonanoyl)-L-serine **xviii** and *N*-(3-hydroxydodecanoyl)glycine **xix** failed to cyclize to the desired seven-membered ring structures **xvii** and **xx** as well (Scheme 6.4). However, when repeating this reaction with *N*-(3-hydroxynonanoyl)-L-proline **xxi** and *N*-(3-hydroxydodecanoyl)sarcosine **xxii**, 1,4-oxazepane-2,5-diones **xxiii** and **xxiv** were obtained in good yields (Scheme 6.4). This difference in reactivity can be explained by the preference of a secondary amide for the *trans*-conformation. The introduction of a third substituent at nitrogen, as is the case for proline and sarcosine derivatives **xxi** and **xxii**, gives rise to an elevated amount of *cis*-amide structures which are required for the cyclization to occur. The presence of *cis*- and *trans*-rotamers was confirmed via 2D-NOESY and ^1H and ^{13}C NMR analysis. It was therefore decided that a spontaneous rearrangement of a *N*-(3-hydroxyacyl) amino acid derivative could not be the origin of serratin-like structures.



Scheme 6.4. Cyclization of *N*-(3-hydroxyacyl)amino acid derivatives **xviii**, **xix**, **xxi**, **xxii**, **xxv** and **xxvi** to 1,4-oxazepane-2,5-diones **xvii**, **xx**, **xxiii**, **xxiv**, **xxvii** and **xxviii**.

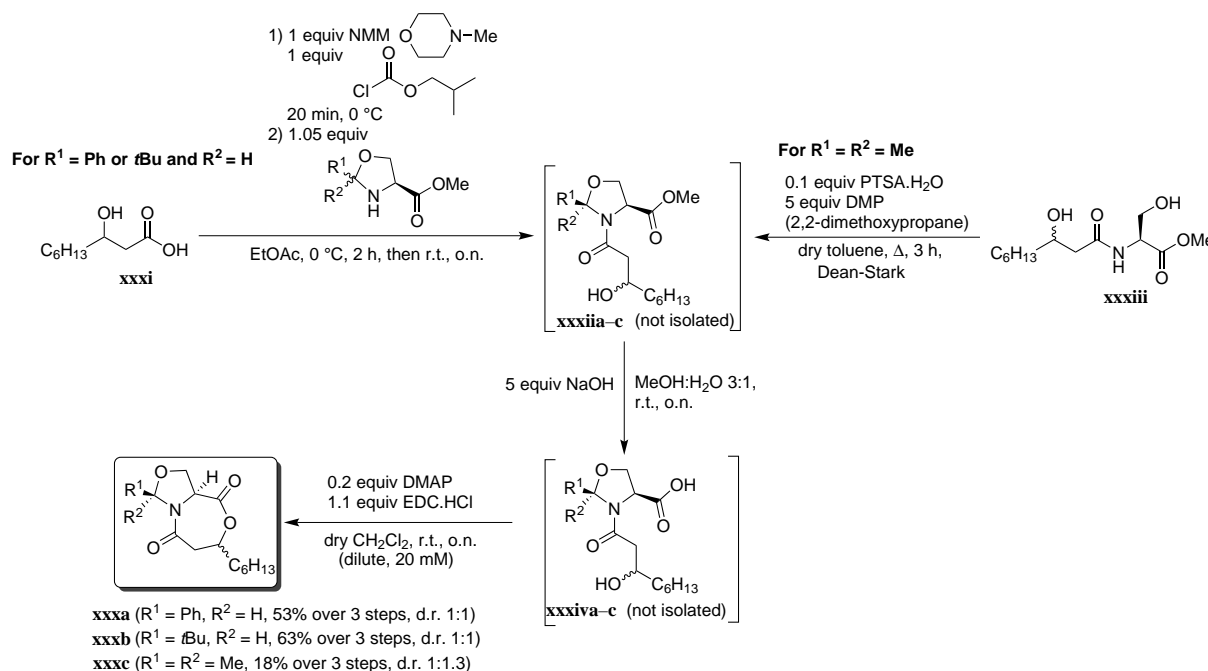
From these results it was clear that seven-membered rings, especially those containing two lactams or one lactam and one lactone bond are extremely difficult to synthesize by cyclization, and that it is necessary to introduce a third substituent at the amide nitrogen to force the linear precursor in the correct conformation for cyclization to proceed. However, to obtain the natural product serratin (**xvii**), this *N*-substituent should be a removable one. The intrinsic lability of the lactone moiety excludes many common protecting groups used for the synthesis of seven-membered lactams as the reaction conditions needed for their removal will open the lactone bond. Several reaction conditions were evaluated to remove the *N*-benzyl group from **xxvii** but none was able to deliver the deprotected compound **xxix**. When ceric ammonium nitrate (CAN) was used to remove the *N*-PMB group from **xxviii**, deprotected 1,4-oxazepane-2,5-dione **xxix** was obtained (Scheme 6.5). Attempts to introduce a hydroxymethyl substituent on compound **xxix** via reaction with (para)formaldehyde were unsuccessful.



Scheme 6.5. CAN-mediated *N*-deprotection of **xxviii** to **xxix**.

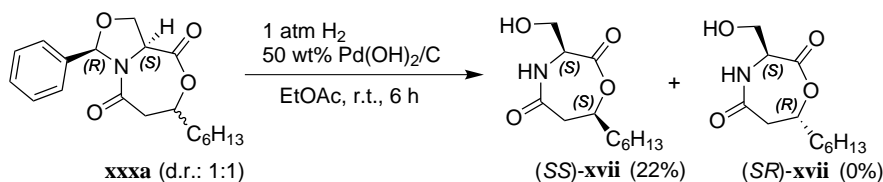
Subsequently, the application of serine-derived oxazolidines (so-called pseudo-prolines) was evaluated as an alternative. Bicyclic compounds **xxx** containing a 2-phenyloxazolidine (**xxxa**), 2-*t*Bu-oxazolidine (**xxxb**), and a 2,2-dimethyloxazolidine (**xxxc**) were successfully synthesized (Scheme 6.6). Although several reaction conditions were evaluated to deprotect the oxazolidine

moiety from **xxxa–c**, none was able to deliver serratin (**xvii**).



Scheme 6.6. Synthesis of oxazolidine-containing bicyclic structures **xxxa–c**.

However, the 2-phenyloxazolidine moiety was successfully removed from **xxxa** via palladium-catalyzed hydrogenolysis (Scheme 6.7). Remarkably, only the (*RSS*)-diastereomer of **xxxa** was deprotected to yield serratin (**xvii**).



Scheme 6.7. Hydrogenolytic removal of the 2-phenyloxazolidine moiety of **xxxa**.

When comparing the spectral data of this synthesized analogue (*SS*)-**xvii** with those reported for the isolated serratin, some discrepancies were found. Careful examination of literature data led to the conclusion that the actual structure of serratin (**xvii**) is a symmetrical serratamide analogue **xxxv** (Figure 6.1).

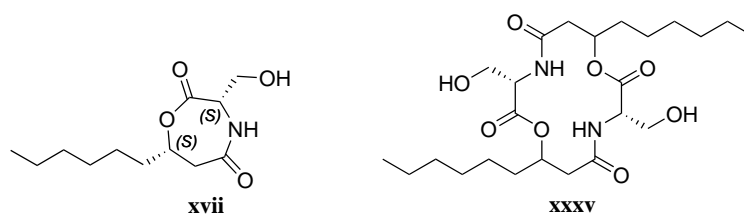


Figure 6.1. Reported structure of serratin (**xvii**) and proposed actual structure **xxxv** of this natural product.

In a third part of this PhD thesis, the biological activity of some AHLs was studied. As the assays evaluating the effect of the synthesized AHLs on plant growth showed a lot of variation, this effect was not studied in depth.

Subsequently, the influence of some AHLs on the cyclic lipopeptide (CLP)-production of the promising biocontrol strain *Pseudomonas* CMR12a was studied extensively. This strain produces two types of CLPs, sessilin and orfamide, and possesses two QS systems, PhzI/PhzR and CmrI/CmrR, but their involvement in the CLP-production was not clear. At first it was studied whether the fatty acid chain of the AHLs was recycled into the produced CLPs of this strain. After feeding experiments with isotope-labelled AHL **ixa**, it was concluded that no such recycling took place. Via swarming assays with different QS mutant strains, it was concluded that the PhzI/PhzR system was crucial to halt the swarming behavior (Figure 6.2) and that the AHL *N*-(3-hydroxyoctanoyl)-L-homoserine lactone (HO8) played a crucial role.

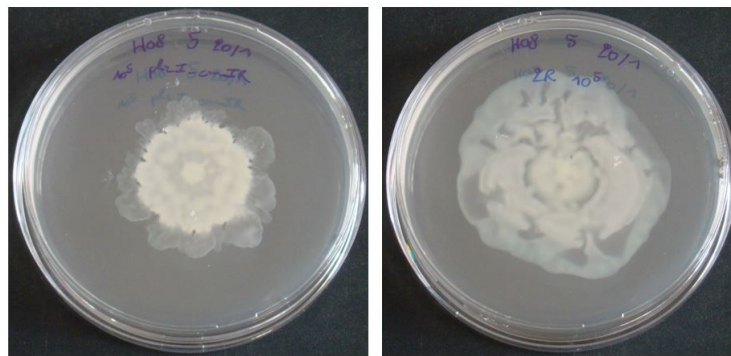


Figure 6.2. Left: typical swarming phenotype observed with an active Phz-operon. Right: typical swarming phenotype observed with an inactive Phz-operon.

To further study the effect of HO8 on the CLP-production, a switch to liquid culture was made to allow quantification of the CLP-production. As orfamide stimulates swarming and sessilin opposes swarming, it was expected that sessilin production was stimulated via HO8 through the Phz-operon. However, analysis of the CLP-production of different QS-mutants did not reveal a difference in sessilin production. On the other hand, the orfamide production was clearly reduced in mutants lacking an active Phz-operon. The orfamide production could be restored to wild type levels after complementation with HO8 to a *phzI*-mutant (unable to produce HO8 but able to respond to exogenous added HO8). It was observed that mutants with a high sessilin to orfamide ratio displayed a stronger swarming phenotype than those with a higher amount of orfamide. So it was hypothesized that the interaction between sessilin and orfamide determines the swarming phenotype. This was confirmed by combining a strain (Δ CLP1) with a high orfamide production and a clear swarming behavior and a strain (Δ PhzIR) with a high sessilin production and a clear swarming behavior as well. Combination of these two swarming strains

resulted in a sessile phenotype (Figure 6.3). It was therefore hypothesized that both orfamide and sessilin can stimulate swarming, but when they are both present in a high amount, they can impede each other and inhibit swarming.

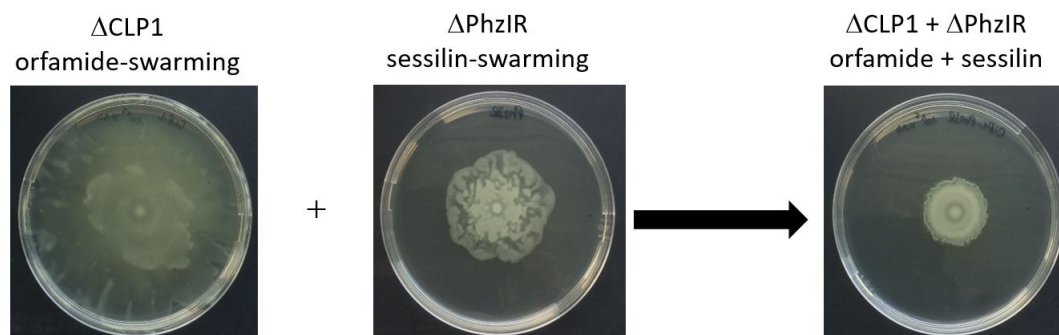


Figure 6.3. Observed swarming phenotype of mutant strains Δ CLP1, Δ PhzIR and a co-culture of both strains.

In this PhD thesis isotope-labelled AHLs were synthesized which can be used as a tool to study the metabolism of AHLs. Secondly, the possible rearrangement of *N*-(3-hydroxyacyl)-L-homoserine lactones was investigated and proven to be very unlikely. This investigation resulted in the successful development of a synthetic entry toward 1,4-oxazepane-2,5-diones, which are extremely difficult to synthesize due to the presence of a lactam with a preference for the *trans*-conformation and a labile lactone moiety in one ring structure. By applying the disclosed methodology on the synthesis of the natural product serratin, the incorrect structural assignment of this compound was identified. Thirdly, the profound effect of a QS signal molecule, HO8, on the swarming behavior of *Pseudomonas* species CMR12a, was demonstrated. This influence goes presumably via an elegant fine-tuning of the ratio of the two produced CLPs, orfamide and sessilin via the control of orfamide production.

Chapter 7

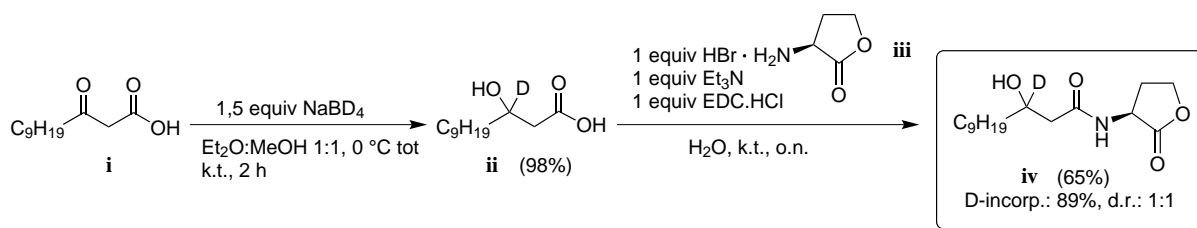
Samenvatting

Tegenwoordig wordt algemeen aanvaard dat micro-organismen met elkaar kunnen communiceren en hun genexpressie op een populatieafhankelijke manier kunnen coördineren. Aangezien dit type van genregulatie gekoppeld is aan de populatiedensiteit of quorum, wordt de term ‘quorum sensing’ gebruikt om dit fenomeen te beschrijven. Gram-negatieve bacteriën gebruiken *N*-geacyleerde-L-homoserine lactonen (AHLs) voor dit type communicatie. Aangezien quorum sensing een cruciale rol speelt in bacterie-gastheerinteracties van zowel pathogene als symbiotische bacteriën, zal een diepgaand inzicht in dit soort communicatie de mensheid vele voordelen bieden, zoals de mogelijkheid om bacteriële infecties te verstoren.

Door de immer groeiende menselijke bevolking wordt steeds meer druk uitgeoefend op de landbouw om voldoende voedsel te produceren. Om verschillende plagen te bestrijden, vertrouwen de meeste boeren op synthetische plantenbeschermingsmiddelen. Door toenemende resistentie en bepaalde bijwerkingen op het milieu, moeten er echter alternatieven gezocht worden. Een mogelijk alternatief is het gebruik van micro-organismen als biologische bestrijdingsmiddelen. Vaak zijn deze micro-organismen afhankelijk van hun secundaire metabolieten om het ziekteverwekkende organisme te bestrijden. Cyclische lipopeptiden (CLPs) zijn een voorbeeld van dergelijke secundaire metabolieten met antifungale en antimicrobiële eigenschappen. Hoewel de productie van enkele CLPs quorum sensing gereguleerd is, is dit niet altijd het geval. Bovendien is het onderliggende controlemechanisme achter de biosynthese van CLPs onvoldoende in kaart gebracht. Daarom is een ander voordeel van een diepgaand inzicht in quorum sensing de mogelijkheid om de productie van secundaire metabolieten van deze micro-organismen beter te begrijpen en te sturen.

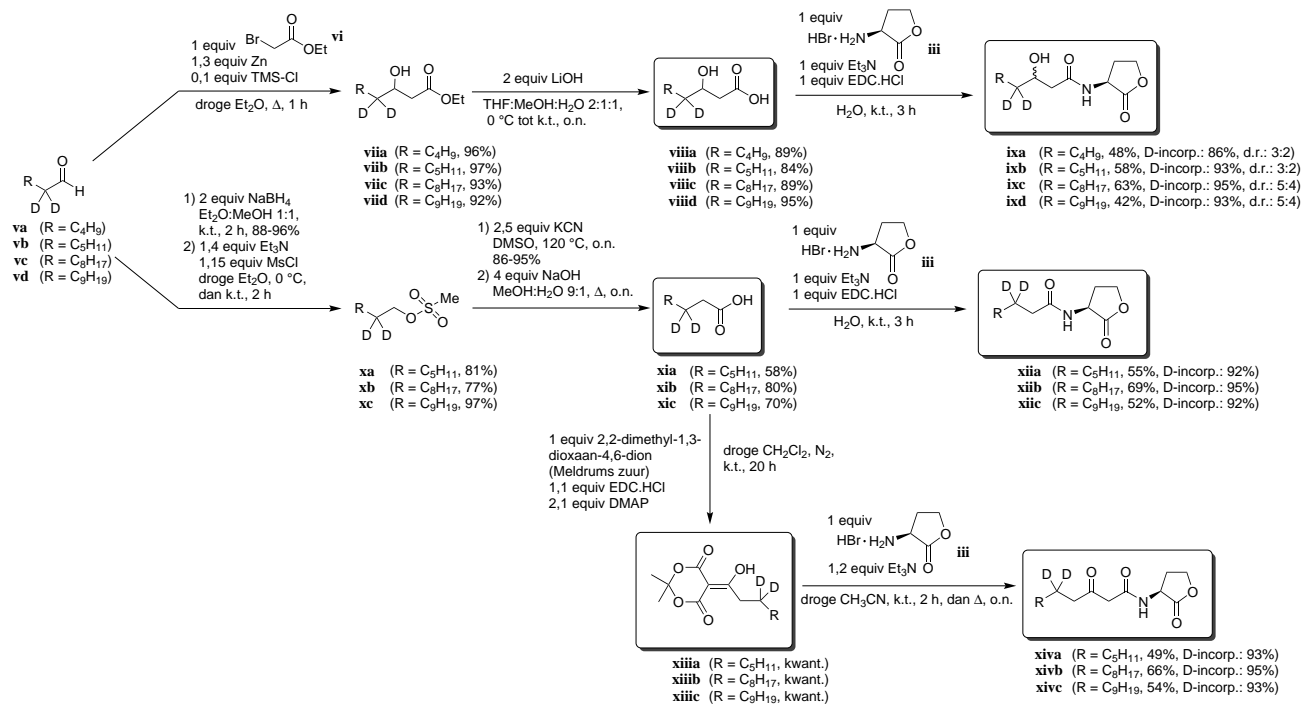
In een eerste onderdeel van dit onderzoek werden isotoopgelabelde AHLs gesynthetiseerd. Om de metabolisatie van de vetzuurstaart van AHLs te kunnen bestuderen, werd het isotooplabel in de acylketen van het AHL geplaatst. In een eerste benadering werd β -oxododecaanzuur **i** gereduceerd met natriumboordeuteride om aldus monogedeutereerd β -hydroxydodecaanzuur **ii** te bekomen. Dit gelabelde vetzuur **ii** werd gekoppeld met L-homoserine lacton waterstofbromide **iii**, waardoor *N*-(3-hydroxydodecanoyl-[3-²H])-L-homoserine lacton **iv** bekomen werd

(Schema 7.1).



Schema 7.1. Synthese van *N*-(3-hydroxydodecanoyl-[3-²H])-L-homoserine lacton **iv**.

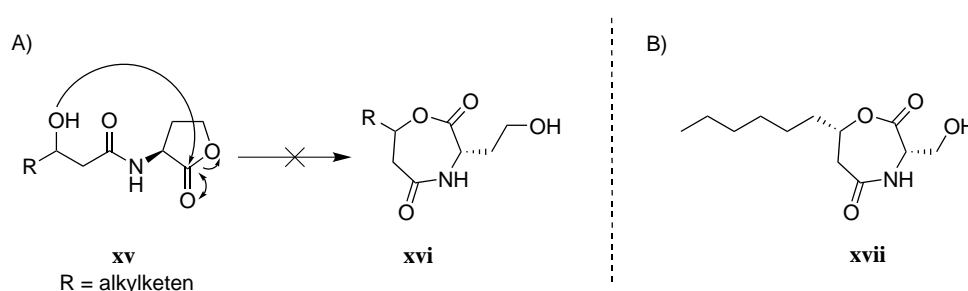
Aangezien alleen de AHLs met een hydroxygroep toegankelijk zijn via deze route, werd er een alternatieve aanpak gezocht om AHLs behorende tot alle verschillende klassen te synthetiseren, vertrekkende vanuit een gemakkelijk beschikbare gedeutereerde bouwsteen. Daarom werden alifatische aldehyden gedeutereerd op de α -plaats via een DMAP-gekatalyzeerde H/D-uitwisselingsreactie. Deze gelabelde aldehyden **v** werden omgezet in de overeenkomstige di-gedeutereerde β -hydroxyvetzuren **viii** via een Reformatskyreactie met ethylbroomacetaat **vi**, gevolgd door een alkalische hydrolyse (Schema 7.2). Anderzijds werden de gedeutereerde aldehyden **v** verder omgezet tot niet-gefunctionaliseerde [3,3-di-²H]-vetzuren **xi** via een ketenverlenging met als doel het deuteriumlabel van de relatief zure α -plaats te verplaatsen naar de β -plaats. Koppeling van deze vetzuren **xi** met Meldrums zuur door middel van EDC leverde de derde gedeutereerde precursor **xiii**. Reactie van deze gedeutereerde precursoren **viii**, **xi** en **xiii** met L-homoserine lacton waterstofbromide **iii** gaf gedeutereerde AHLs **ix**, **xii** en **xiv** (Schema 7.2).



Schema 7.2. Omzetting van α,α -digeutereerde aldehyden **v** tot gedeutereerde AHLs **ix**, **xii** en **xiv**.

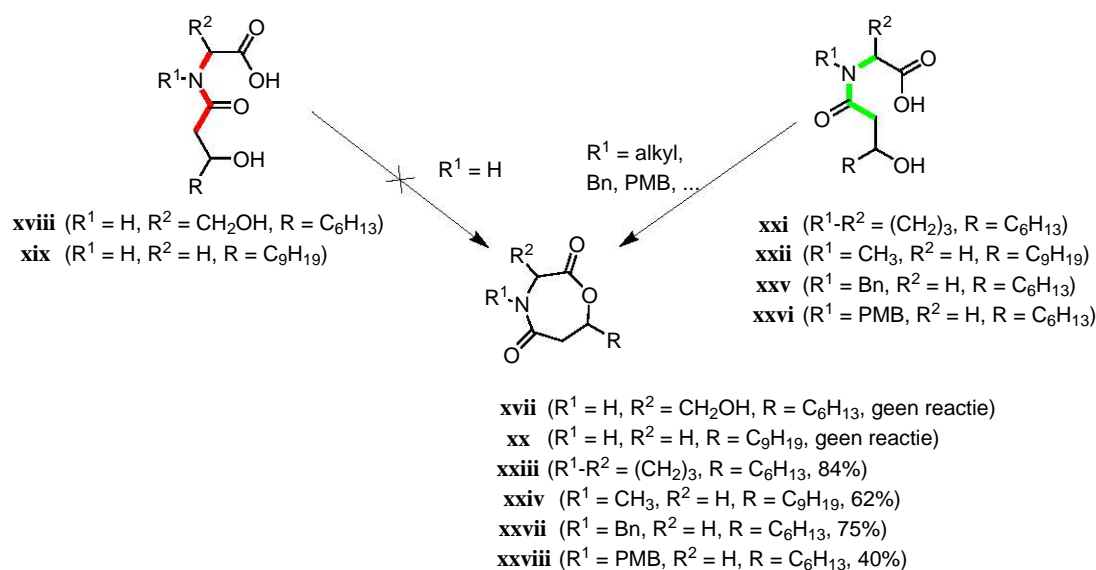
De NMR spectra en het MS fragmentatiepatroon van de gelabelde analogen **iv**, **ix**, **xii** en **xiv** werden uitvoerig bestudeerd. Om de spectrale gegevens te vergelijken met de niet-gelabelde analogen, werd een ruime bibliotheek van natuurlijke *N*-acyl-, *N*-(3-hydroxyacyl)- en *N*-(3-oxoacyl)-L-homoserine lactonen gesynthetiseerd.

In een tweede deel van dit onderzoek werd de mogelijke omlegging van *N*-(3-hydroxyacyl)-L-homoserine lactonen **xv** tot 1,4-oxazepaan-2,5-dionen **xvi** (Schema 7.3) bestudeerd. Deze omlegging werd nog niet in de literatuur beschreven, maar het natuurproduct serratine (**xvii**) past vrij goed in dit type omleggingsproduct. Serratine (**xvii**) werd reeds uit een bacteriële cultuur van *Serratia marcescens* geïsoleerd.



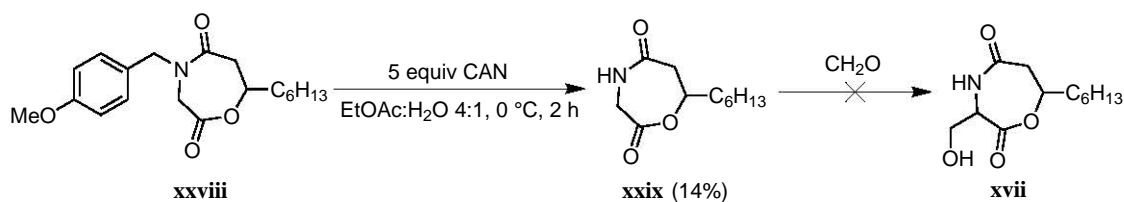
Schema 7.3. A) De mogelijke omlegging van *N*-(3-hydroxyacyl)-L-homoserine lactonen **xv** tot de zevenring **xvi**. B) Structuur van het natuurproduct serratine (**xvii**).

Verscheidene reactieomstandigheden werden geëvalueerd, maar de vooropgestelde omlegging van *N*-(3-hydroxyacyl)-L-homoserine lactonen **xv** werd nooit vastgesteld. *N*-(3-Hydroxynonanoyl)-L-serine **xviii** en *N*-(3-hydroxydodecanoyl)glycine **xix** faalden eveneens in de cyclisatie tot de gewenste zevenringstructuren **xvii** en **xx** (Schema 7.4). Echter, wanneer deze reactie werd herhaald met *N*-(3-hydroxynonanoyl)-L-proline **xxi** en *N*-(3-hydroxydodecanoyl)sarcosine **xxii**, werden 1,4-oxazepaan-2,5-dionen **xxiii** en **xxiv** verkregen in een goed rendement (Schema 7.4). Dit verschil in reactiviteit kan verklaard worden door de voorkeur van een secundair amide voor de *trans*-conformatie. De invoering van een derde substituent op stikstof, zoals het geval is voor proline- en sarcosinederivaten **xxi** en **xxii**, leidt tot een verhoogd aandeel *cis*-amide-structuren die vereist zijn voor de cyclisatie. De aanwezigheid van *cis*- en *trans*-rotameren werd bevestigd via 2D-NOESY en ^1H en ^{13}C NMR analyse.



Schema 7.4. Ringsluiting van *N*-(3-hydroxyacyl)aminozuurderivaten **xviii**, **xix**, **xxi**, **xxii**, **xxv** en **xxvi** tot 1,4-oxazepaan-2,5-dionen **xvii**, **xx**, **xxiii**, **xxiv**, **xxvii** en **xxviii**.

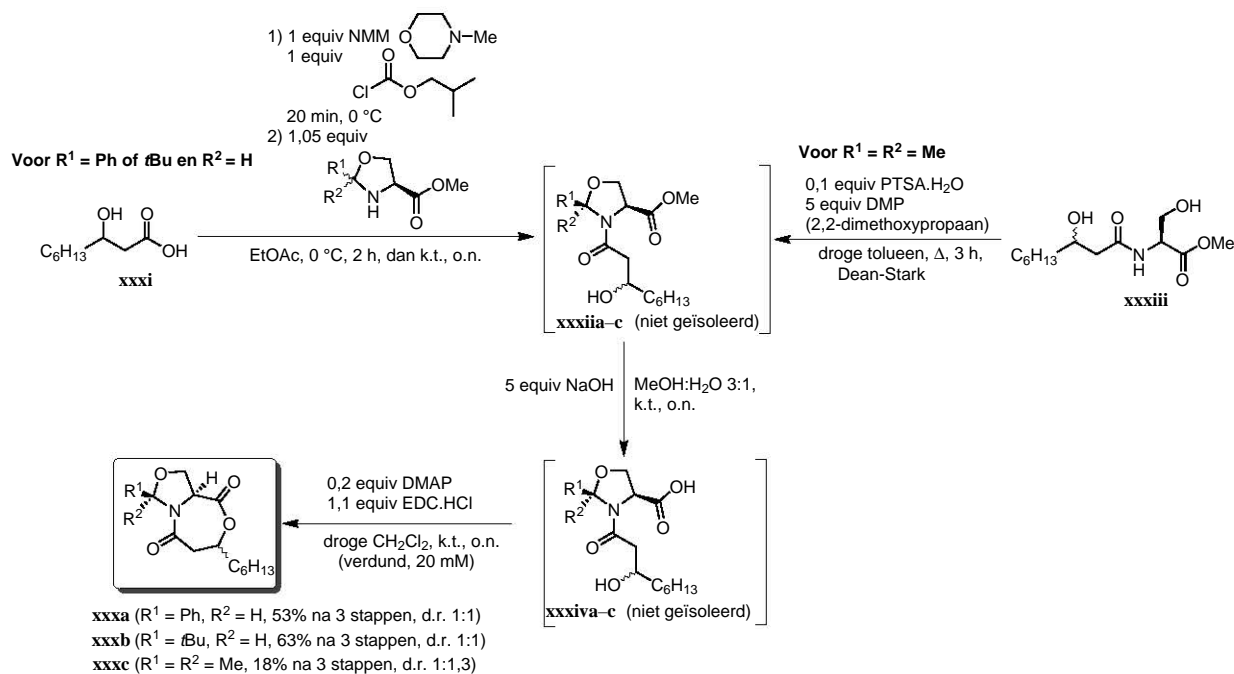
Uit deze resultaten bleek dat zevenringen, in het bijzonder deze die twee lactamen of één lactam en één lacton bevatten, extreem moeilijk te synthetiseren zijn door middel van cyclisatie en het noodzakelijk is om een substituent te introduceren op het stikstofatoom van de lactambinding om de lineaire precursor in de correcte conformatie te dwingen zodat cyclisatie kan plaatsvinden. Om het natuurproduct serratine (**xvii**) te verkrijgen, moet deze *N*-substituent echter verwijderd kunnen worden. De intrinsieke labiliteit van het lacton sluit veel beschermende groepen uit die vaak gebruikt worden voor de synthese van zevenringbevattende lactamen, aangezien de omstandigheden die nodig zijn voor de verwijdering ervan de lactonbinding zullen openen. Verschillende reactieomstandigheden werden getest om de *N*-benzylgroep van **xxvii** te verwijderen, maar geen methode slaagde erin de ontschermdde verbinding **xxix** te leveren. Wanneer ceriumammoniumnitraat (CAN) werd gebruikt om de *N*-PMB groep van **xxviii** te verwijderen, werd het ontschermdde 1,4-oxazepaan-2,5-dion **xxix** verkregen (Schema 7.5). Pogingen om een hydroxymethylgroep op verbinding **xxix** in te voeren via reactie met (para)formaldehyde waren niet succesvol.



Schema 7.5. *N*-Ontscherming van **xxviii** tot **xxix** met CAN.

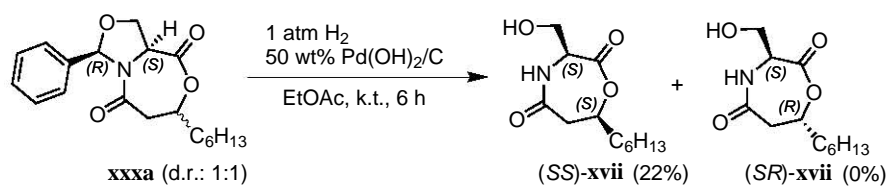
Vervolgens werd het gebruik van serine-afgeleide oxazolidinen (zogenaamde pseudoprolines) als een mogelijke oplossing geëvalueerd. Bicyclische verbindingen die een 2-fenylloxazolidine

(**xxxa**), een 2-*t*Bu-oxazolidine (**xxxb**) of een 2,2-dimethyloxazolidine (**xxxc**) bevatten werden succesvol gesynthetiseerd (Schema 7.6). Hoewel verscheidene reactieomstandigheden werden getest om de oxazolidine-eenheid van **xxxa–c** te verwijderen, kon serratine (**xvii**) niet verkregen worden.



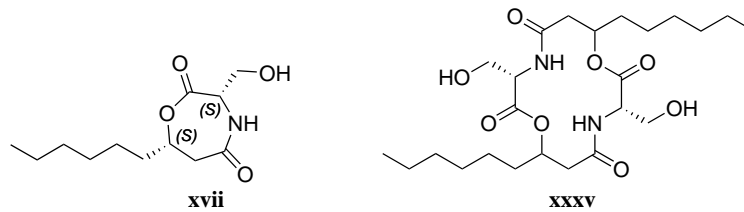
Schema 7.6. Synthese van oxazolidinebevattende bicyclische structuren **xxxa–c**.

Echter, de 2-fenyloxazolidinegroep werd succesvol verwijderd door middel van palladium-gekatalyzeerde hydrogenolyse (Schema 7.7). Opmerkelijk genoeg werd alleen het (*RSS*)-diastereomeer van **xxxa** ontschermd tot serratine (**xvii**).



Schema 7.7. Verwijdering van de 2-fenyloxazolidinegroep van **xxxa** via hydrogenolyse.

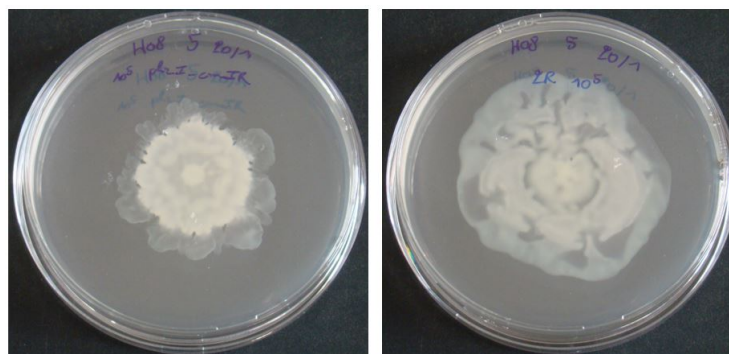
Bij het vergelijken van de spectrale data van de gesynthetiseerde verbinding (*SS*)-**xvii** met de gerapporteerde data voor het geïsoleerde serratine, werden er een aantal discrepanties opgemerkt. Zorgvuldige vergelijking met literatuurgegevens leidde tot de conclusie dat de werkelijke structuur van serratine (**xvii**) een symmetrisch serratamolide analog **xxxv** is (Figuur 7.1).



Figuur 7.1. Gerapporteerde structuur van serratine (xvii) en voorgestelde werkelijke structuur xxxv van dit natuurproduct.

In een derde deel van dit doctoraat werd de biologische activiteit van sommige AHLs bestudeerd. Aangezien de experimenten die het effect van de gesynthetiseerde AHLs op plantengroei moesten testen, veel variatie vertoonden, werd dit effect niet verder in detail bestudeerd.

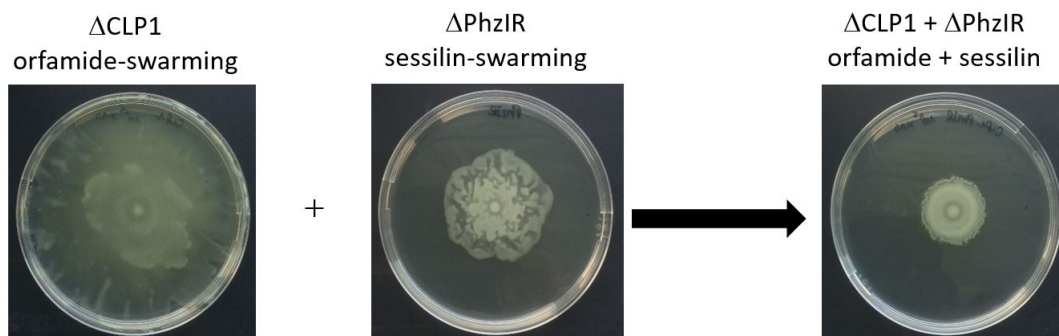
De invloed van sommige AHLs op de cyclische lipopeptiden (CLP)-productie van de veelbelovende biocontrolestam *Pseudomonas* CMR12a werd daarentegen uitgebreid bestudeerd. Deze stam produceert twee soorten CLPs, sessiline en orfamide, en beschikt over twee QS-systemen, PhzI/PhzR en CmrI/CmrR. De rol van deze QS systemen in de CLP-productie was echter nog niet duidelijk. Aanvankelijk werd onderzocht of de vetzuurketen van de AHLs herbruikt werd voor de biosynthese van de CLPs. Na het uitvoeren van een experiment met het isotoopgelabelde AHL **ixa** werd geconcludeerd dat er geen dergelijke recyclage plaatsvond. Via swarming assays met verschillende QS mutantstammen werd geconcludeerd dat het PhzI/PhzR systeem van cruciaal belang is om het swarmgedrag van deze stam tegen te gaan (Figuur 7.2) en dat het AHL *N*-(3-hydroxyoctanoyl)-L-homoserine lacton (HO8) hierbij een cruciale rol speelt.



Figuur 7.2. Links: het typische swarmingfenotype dat vastgesteld wordt wanneer er een actief Phz-operon aanwezig is. Rechts: het typische swarmingfenotype dat vastgesteld wordt wanneer er geen actief Phz-operon aanwezig is.

Om het effect van HO8 op de CLP-productie verder te bestuderen werd er overgeschakeld naar vloeibare bacteriële culturen om aldus de kwantificatie van de CLP-productie mogelijk te maken. Aangezien orfamide swarming stimuleert en sessiline geassocieerd is met het inhiberen van swarming, werd verwacht dat HO8 de productie van sessiline zou stimuleren via

het Phz-operon. Bij analyse van de sessilineproductie werden er echter geen verschillen tussen de verschillende QS-mutanten waargenomen. De productie van orfamide was echter duidelijk gedaald in mutanten zonder een actief Phz-operon. De productie van orfamide kon hersteld worden tot het wildtype-niveau na complementatie met HO8 aan een *phzI*-mutant (niet in staat om HO8 te produceren maar wel in staat te reageren op exogeen toegevoegd HO8). Er werd vastgesteld dat mutanten met een hoge sessiline ten opzichte van orfamide ratio een sterker swarmingfenotype vertoonden dan mutanten met een hoger orfamidegehalte. Hierdoor werd verondersteld dat de interactie tussen sessiline en orfamide het uiteindelijke swarmingfenotype bepaalt. Deze hypothese werd bevestigd door een stam (ΔCLP1) met een hoge orfamideproductie en een duidelijk swarminggedrag te combineren met een andere stam (ΔPhzIR) met een hoge sessilineproductie en eveneens een duidelijk swarminggedrag. Combinatie van deze twee swarmende stammen resulteerde in een sessiel fenotype (Figuur 7.3). Derhalve werd de hypothese vooropgesteld dat zowel orfamide als sessiline swarmen kunnen stimuleren, maar als ze beide in een hoge concentratie aanwezig zijn, ze elkaar belemmeren en swarmen verhinderd wordt.



Figuur 7.3. Het geobserveerde swarmingfenotype van mutantstammen ΔCLP1 , ΔPhzIR en een co-cultuur van beide stammen.

In dit doctoraatsonderzoek werden isotoopgelabelde AHLs gesynthetiseerd die gebruikt kunnen worden om de metabolisering van AHLs te bestuderen. Ten tweede werd de mogelijke omlegging van *N*-(3-hydroxyacyl)-L-homoserine lactonen onderzocht maar deze bleek zeer onwaarschijnlijk. Dit onderzoek resulteerde in de succesvolle ontwikkeling van een methode voor de synthese van 1,4-oxazepaan-2,5-dionen, die uiterst moeilijk te synthetiseren zijn door de aanwezigheid van een lactam met een voorkeur voor de *trans*-conformatie en een labiel lacton in één ringstructuur. Door de ontwikkelde methodologie toe te passen op de synthese van het natuurproduct serratine, werd de foutieve structurele toewijzing van deze verbinding geïdentificeerd. Daarnaast werd de invloed van een QS-siginaalmolecule, HO8, op het swarminggedrag van *Pseudomonas* CMR12a aangetoond. Deze verbinding oefent vermoedelijk zijn effect uit

door een elegante controle van de verhouding van de twee geproduceerde CLPs, orfamide en sessiline, via de controle van de orfamideproductie.

Chapter 8

Appendix

Table 8.1: Influence of AHLs or AHL degradation products on plants. NM: not mentioned.

AHL	Stereochemistry	Concentration	Plant	Effect	Assay
HL 19 ⁸⁰	NM	10 nM	Bean	Increase (+ 20-30%) of stomatal conductance and transpiration.	Plants were grown in sterile pots for 14 d, then 10 nM of the compound in a nutrient solution was applied to roots. The effect on the leaves was measured 42 h after application.
HL 19 ⁵⁵	L	1 nM - 100 μ M	<i>A. thaliana</i> , <i>M. truncatula</i>	Biphasic growth response: increased root growth at concentrations <1 μ M, reduced root growth at concentrations > 50 μ M.	72 h After germination, plants were transferred to 0.5MS agar medium containing the compound. Root length was measured after 10-14 d.
HSe 25 ⁸⁰	NM	10 nM	Bean	Increase (+ 20-30%) of stomatal conductance and transpiration.	Plants were grown in sterile pots for 14 d, then 10 nM of the compound in a nutrient solution was applied to roots. The effect on the leaves was measured 42 h after application.
HSe 25 ⁵⁵	L	1 nM - 100 μ M	<i>A. thaliana</i> , <i>M. truncatula</i>	Biphasic growth response: increased root growth at concentrations <1 μ M, reduced root growth at concentrations > 50 μ M.	72 h After germination, plants were transferred to 0.5MS agar medium containing the compound. Root length was measured after 10-14 d.
HSe 25 ⁵⁵	D	1 nM - 100 μ M	<i>A. thaliana</i> , <i>M. truncatula</i>	No effect.	72 h After germination, plants were transferred to 0.5MS agar medium containing the compound. Root length was measured after 10-14 d.
C4 1a ⁸³	NM	1 - 10 μ M	Tomato	Enhanced expression of specific genes involved in defense and other functions, accumulation of salicylic acid in roots and leaves.	Four-week-old plants grown in sterile quartz sand, application of the AHL solution on the sand and effect measured after 5-24 h.

Continued on next page

Table 8.1 – Continued from previous page

AHL	Stereochemistry	Concentration	Plant	Effect	Assay
C4 1a ⁶⁸	D/L	10 μ M	<i>A. thaliana</i>	Root growth promoted (1.2-fold increase). No increased resistance against pathogens.	Floating hydroponic system with 11 d old seedlings in 0.5MS medium, AHLs added to the liquid medium. Measurement of the roots 14 d after the treatment.
C4 1a ⁷¹	NM	10 μ M	<i>A. thaliana</i>	Root elongation.	Seedlings first grown until two leaves and roots reached 2 cm in length and then transferred to 0.5MS agar medium containing the AHL. Roots were measured after 7 d.
C4 1a ⁵⁴	NM	12 - 192 μ M	<i>A. thaliana</i>	No effect on root growth or root hair development.	Seedlings germinated and grown on 0.2MS medium containing the AHL, primary root length measured 10 d after germination.
C6 1c ⁶⁶	NM	2 nM	<i>M. truncatula</i>	Exudation of QS mimics.	Application of agar blocks containing the AHL for 48 h on top of the roots of six-day-old seedlings or via spraying of the AHL solution.
C6 1c ⁶⁹	NM	6 μ M	<i>A. thaliana</i>	Promotion of shoot and root biomass accumulation and increased root length.	Plants grown for 10 d, then transferred to 0.5MS medium containing the AHL. Plants measured after 4 d.
C6 1c ⁸³	NM	10 μ M	Tomato	Enhanced expression of specific genes involved in defense and other functions, accumulation of salicylic acid in roots and leaves.	Four-week-old plants grown in sterile quartz sand, application of the AHL solution on the sand and effect measured after 5-24 h.
C6 1c ⁶⁸	D/L	10 μ M	<i>A. thaliana</i>	Root growth promoted (1.2-fold increase). No increased resistance against pathogens.	Floating hydroponic system with 11 d old seedlings in 0.5MS medium, AHL added to the liquid medium. Measurement of the roots 14 d after the treatment.
C6 1c ⁷¹	NM	10 μ M	<i>A. thaliana</i>	Root elongation.	Seedlings first grown until two leaves and roots reached 2 cm in length and then transferred to 0.5MS agar medium containing the AHL. Roots were measured after 7 d.
C6 1c ⁷⁰	NM	3-12 μ M	<i>A. thaliana</i>	Promotion of shoot and root biomass accumulation and increased root length.	Plants grown for 5 d, then transferred to 0.5MS medium containing the AHL. Plants measured after 11 d.
C6 1c ⁷⁹	D/L	1 - 10 - 100 μ M	Barley	No effect on plant morphology, increased K ⁺ uptake, NO-accumulation.	Two-day-old seedlings were transferred to full strength MS agar medium containing the AHL, plants analyzed after 10 d.
C6 1c ⁵⁵	L	1 nM - 100 μ M	<i>A. thaliana</i> , <i>M. truncatula</i>	Biphasic growth response: increased root growth at concentrations <1 μ M, reduced root growth at concentrations > 50 μ M.	72 h After germination, plants were transferred to 0.5MS agar medium containing the AHL. Root length was measured after 10-14 d.

Continued on next page

Table 8.1 – Continued from previous page

AHL	Stereochemistry	Concentration	Plant	Effect	Assay
C6 1c ⁵⁴	NM	12 - 192 μ M	<i>A. thaliana</i>	No effect on root growth or root hair development.	Seedlings germinated and grown on 0.2MS medium containing the AHL, primary root length measured 10 d after germination.
oxo6 3c ⁸⁰	NM	10 nM	Bean	No effect on stomatal conductance and transpiration.	Plants were grown in sterile pots for 14 d, then 10 nM of the compound in a nutrient solution was applied to roots. The effect on the leaves was measured 42 h after application.
oxo6 3c ⁷¹	NM	10 nM - 100 μ M	<i>A. thaliana</i>	A dose-dependent positive effect on root elongation was observed but a concentration of 100 μ M resulted in a root length reduction.	Seedlings first grown until two leaves and roots reached 2 cm in length and then transferred to 0.5MS agar medium containing the AHL. Roots were measured after 7 d.
oxo6 3c ^{72,73}	D/L	1 μ M	<i>A. thaliana</i>	Increased primary root length, accumulation of the calmodulin protein.	Seedlings first grown until two leaves and roots reached 2 cm in length and then transferred to 0.5MS agar medium containing the AHL. Roots were measured after 7 d.
oxo6 3c ⁵⁵	L	1 nM - 100 μ M	<i>A. thaliana</i> , <i>M. truncatula</i>	Biphasic growth response: increased root growth at concentrations <1 μ M, reduced root growth at concentrations > 50 μ M.	72 h After germination, plants were transferred to 0.5MS agar medium containing the AHL. Root length was measured after 10-14 d.
C8 1e ⁷¹	NM	10 μ M	<i>A. thaliana</i>	Root elongation.	Seedlings first grown until two leaves and roots reached 2 cm in length and then transferred to 0.5MS agar medium containing the AHL. Roots were measured after 7 d.
C8 1e ⁵⁴	NM	12-192 μ M	<i>A. thaliana</i>	Dose-dependent inhibitory effect on primary root growth. No effect on root hair development.	Seedlings germinated and grown on 0.2MS medium containing the AHL, primary root length measured 10 d after germination.
C8 1e ⁷⁹	D/L	1-10-100 μ M	Barley	Increase in leaf and root dry weights and stimulation of lateral root formation, slight root elongation, increased K^+ uptake, NO-accumulation.	Two-day-old seedlings were transferred to full strength MS agar medium containing the AHL, analyzed after 10 d.
C8 1e ⁵⁵	L	1 nM - 100 μ M	<i>A. thaliana</i> , <i>M. truncatula</i>	Biphasic growth response: increased root growth at concentrations <1 μ M, reduced root growth at concentrations > 50 μ M.	72 h After germination, plants were transferred to 0.5MS agar medium containing the AHL. Root length was measured after 10-14 d.
oxo8 3e ⁷¹	NM	10 nM - 100 μ M	<i>A. thaliana</i>	A dose-dependent positive effect on root elongation was observed but a concentration of 100 μ M resulted in a root length reduction.	Seedlings first grown until two leaves and roots reached 2 cm in length and then transferred to 0.5MS agar medium containing the AHL. Roots were measured after 7 d.

Continued on next page

Table 8.1 – Continued from previous page

AHL	Stereochemistry	Concentration	Plant	Effect	Assay
oxo8 3e ⁸¹	L	2.1 μ M	Sugar cane	Increase of root dry mass (133%) and root length (69%). Increase of bud length (21%) and dry weight (43%). Elongation of root cells.	Sugar cane culms were submerged in a solution containing the AHL and grown for 8 d. Every other day, the culms were irrigated with the AHL solution.
oxo8 3e ⁸¹	D	2.1 μ M	Sugar cane	Increase of root dry mass (21%) and root length (12%). Decrease of bud length (-28%) and dry weight (-40%). Elongation of root cells.	Sugar cane culms were submerged in a solution containing the AHL and grown for 8 d. Every other day, the culms were irrigated with the AHL solution.
oxo8 3e ⁵⁵	L	1 nM - 100 μ M	<i>A. thaliana</i> , <i>M. truncatula</i>	Biphasic growth response: increased root growth at concentrations <1 μ M, reduced root growth at concentrations > 50 μ M.	72 h After germination, plants were transferred to 0.5MS agar medium containing the AHL. Root length was measured after 10-14 d.
C10 1g ⁵⁴	NM	12 - 192 μ M	<i>A. thaliana</i>	Dose-dependent inhibitory effect on primary root growth, shift in root architecture toward a more branched system, more lateral root primordia, root hair development.	Seedlings germinated and grown on 0.2MS medium containing the AHL, primary root length measured 10 d after germination.
C10 1g ⁷⁸	NM	10-100 nM	Mung bean	No effect on adventitious root formation.	Seedling in liquid culture 0.25MS medium containing the AHL, effect measured after 7 d.
C10 1g ⁶⁸	D/L	10 μ M	<i>A. thaliana</i>	Decreased root growth.	Floating hydroponic system with 11 d old seedlings in 0.5MS medium, AHL added to the liquid medium. Measurement of the roots 14 d after the treatment.
C10 1g ⁷¹	NM	10 μ M	<i>A. thaliana</i>	No effect.	Seedlings first grown until two leaves and roots reached 2 cm in length and then transferred to 0.5MS agar medium containing the AHL. Roots were measured after 7 d.
C10 1g ⁷²	D/L	50 μ M	<i>A. thaliana</i>	Inhibition primary root growth, promotion of lateral root growth and root hair formation.	Seeds were grown for 3 d, seedlings with a similar root length were transferred to 0.5MS agar plates containing the AHL. Measurement after 7 d.
C10 1g ⁷⁷	NM	10 - 50 μ M	<i>A. thaliana</i>	Concentrations > 10 μ M: decrease of root length, increase of number of lateral roots.	Seedlings germinated and grown on 0.2MS medium containing the AHL, roots measured 14 d after germination.
C10 1g ⁵⁵	L	1 nM - 100 μ M	<i>A. thaliana</i> , <i>M. truncatula</i>	Biphasic growth response: increased root growth at concentrations <1 μ M, reduced root growth at concentrations > 50 μ M.	72 h After germination, plants were transferred to 0.5MS agar medium containing the AHL. Root length was measured after 10-14 d.

Continued on next page

Table 8.1 – Continued from previous page

AHL	Stereochemistry	Concentration	Plant	Effect	Assay
oxo10 3g ⁷⁸	NM	10-100 nM	Mung bean	Induces auxin-dependent adventitious root formation.	Seedling in liquid culture 0.25MS medium containing the AHL, effect measured after 7 d.
oxo10 3g ⁵⁵	L	1 nM - 100 μ M	<i>A. thaliana</i> , <i>M. truncatula</i>	Biphasic growth response: increased root growth at concentrations <1 μ M, reduced root growth at concentrations > 50 μ M.	72 h After germination, plants were transferred to 0.5MS agar medium containing the AHL. Root length was measured after 10-14 d.
C12 1i ⁷¹	NM	10 μ M	<i>A. thaliana</i>	Root length reduction.	Seedlings first grown until two leaves and roots reached 2 cm in length and then transferred to 0.5MS agar medium containing the AHL. Roots were measured after 7 d.
C12 1i ⁷²	D/L	50 μ M	<i>A. thaliana</i>	Inhibition primary root growth, promotion of lateral root growth and root hair formation.	Seeds were grown for 3 d, seedlings with a similar root length were transferred to 0.5MS agar plates containing the AHL. Measurement after 7 d.
C12 1i ⁵⁴	NM	12 - 192 μ M	<i>A. thaliana</i>	Dose-dependent inhibitory effect on primary root growth, shift in root architecture toward a more branched system, more lateral root primordia, root hair development.	Seedlings germinated and grown on 0.2MS medium containing the AHL, primary root length measured 10 d after germination.
C12 1i ⁷⁹	D/L	1 - 10 - 100 μ M	Barley	Increase in leaf and root dry weights and stimulation of lateral root formation, increased K ⁺ uptake.	Two-day-old seedlings were transferred to full strength MS agar medium containing the AHL, analyzed after 10 d.
C12 1i ⁵⁵	L	1 nM 100 μ M	<i>A. thaliana</i> , <i>M. truncatula</i>	Biphasic growth response: increased root growth at concentrations <1 μ M, reduced root growth at concentrations > 50 μ M.	72 h After germination, plants were transferred to 0.5MS agar medium containing the AHL. Root length was measured after 10-14 d.
oxo12 3i ⁶⁶	NM	2 nM - 2 μ M	<i>M. truncatula</i>	Accumulation different proteins, exudation QS mimics.	Application of agar blocks containing the AHL for 24-48 h on top of the roots of three-day-old seedlings or via spraying of the AHL solution.
oxo12 3i ^{69,70}	NM	6 μ M	<i>A. thaliana</i>	Increased resistance against a pathogen but to a lesser extent than oxo14.	Five-week-old plants in a hydroponic system were pretreated with AHLs for 3 d, then exposed to the pathogen. Effect monitored after 4 d.
oxo12 3i ⁵⁵	L	1 nM - 100 μ M	<i>A. thaliana</i> , <i>M. truncatula</i>	Biphasic growth response: increased root growth at concentrations <1 μ M, reduced root growth at concentrations > 50 μ M.	72 h After germination, plants were transferred to 0.5MS agar medium containing the AHL. Root length was measured after 10-14 d.

Continued on next page

Table 8.1 – Continued from previous page

AHL	Stereochemistry	Concentration	Plant	Effect	Assay
oxo12 3i ⁵⁵	D	1 nM - 100 μ M	<i>A. thaliana</i> , <i>M. truncatula</i>	No effect.	72 h After germination, plants were transferred to 0.5MS agar medium containing the AHL. Root length was measured after 10-14 d.
ring-opened					
oxo12 55	L	1 nM - 100 μ M	<i>A. thaliana</i> , <i>M. truncatula</i>	Biphasic growth response: increased root growth at concentrations <1 μ M, reduced root growth at concentrations > 50 μ M.	72 h After germination, plants were transferred to 0.5MS agar medium containing the AHL. Root length was measured after 10-14 d.
HO12 2i ⁵⁵	L	1 nM - 100 μ M	<i>A. thaliana</i> , <i>M. truncatula</i>	Biphasic growth response: increased root growth at concentrations <1 μ M, reduced root growth at concentrations > 50 μ M.	72 h After germination, plants were transferred to 0.5MS agar medium containing the AHL. Root length was measured after 10-14 d.
C14 1k ⁷¹	NM	10 μ M	<i>A. thaliana</i>	Root length reduction.	Seedlings first grown until two leaves and roots reached 2 cm in length and then transferred to 0.5MS agar medium containing the AHL. Roots were measured after 7 d.
C14 1k ⁵⁴	NM	12-192 μ M	<i>A. thaliana</i>	Dose-dependent inhibitory effect on primary root growth, no effect on root hair formation.	Seedlings germinated and grown on 0.2MS medium containing the AHL, primary root length measured 10 d after germination.
oxo14 3k ⁶⁷	L	1 μ M	<i>M. truncatula</i>	An increase in nodule numbers, but no effect on root length or lateral root number was observed.	Seedlings were transferred to Fähræus medium agar plates containing the AHL. After 3 d they were inoculated with <i>Sinorhizobium meliloti</i> , then grown for 21 d.
oxo14 3k ⁶⁷	L	1 μ M	Alfalfa, white clover	No effect on nodule number or root length.	Seedlings were transferred to FM agar plates containing the AHL. After 3 d they were inoculated with <i>Sinorhizobium meliloti</i> , then grown for 21 d.
oxo14 3k ^{69,70,82}	NM	6 μ M	<i>A. thaliana</i>	Increased resistance against pathogens. No effect on root or shoot growth.	Five-week-old plants in a hydroponic system were pretreated with AHLs for 3 d, then exposed to the pathogen. Effect monitored after 4 d. For the effect on growth: plants grown for 10 d, then transferred to MS medium containing the AHL. Plants measured after 4 d.
oxo14 3k ⁶⁹	NM	6 μ M	Barley	Increased resistance against a fungal pathogen.	Seedlings were grown for 5 d on solid medium, then pretreated with AHLs for 3 d in a hydroponic system, then exposed to the pathogen. Effect monitored after 5 d.

Continued on next page

Table 8.1 – Continued from previous page

AHL	Stereochemistry	Concentration	Plant	Effect	Assay
oxo14 3k ⁵⁵	L	1 nM - 100 μ M	<i>A. thaliana</i> , <i>M. truncatula</i>	Biphasic growth response: increased root growth at concentrations <1 μ M, reduced root growth at concentrations > 50 μ M.	72 h After germination, plants were transferred to 0.5MS agar medium containing the AHL. Root length was measured after 10-14 d.
HO14 2k ^{69,70}	NM	6 μ M	<i>A. thaliana</i>	Increased resistance against pathogens but to a lesser extent than oxo14 3k .	Five-week-old plants in a hydroponic system were pretreated with AHLs for 3 d, then exposed to the pathogen. Effect monitored after 4 d.
oxo16 3m ⁵⁵	L	1 nM - 100 μ M	<i>A. thaliana</i> , <i>M. truncatula</i>	Biphasic growth response: increased root growth at concentrations <1 μ M, reduced root growth at concentrations > 50 μ M.	72 h After germination, plants were transferred to 0.5MS agar medium containing the AHL. Root length was measured after 10-14 d.
oxo16:1 3l ⁶⁶	L	1 - 10 nM	<i>M. truncatula</i>	Accumulation different proteins.	Application of agar blocks containing the AHL for 24-48 h on top of the roots of three-day-old seedlings or via spraying of the AHL solution.

References

1. K. H. Nealson, T. Platt, J. W. Hastings, *J. Bacteriol.* **1970**, *104*, 313–322.
2. C. Fuqua, E. P. Greenberg, *Nat. Rev. Mol. Cell Biol.* **2002**, *3*, 685–695.
3. M. B. Miller, B. L. Bassler, *Annu. Rev. Microbiol.* **2001**, *55*, 165–199.
4. A. L. Schaefer, E. P. Greenberg, C. M. Oliver, Y. Oda, J. J. Huang, G. Bittan-Banin, C. M. Peres, S. Schmidt, K. Juhaszova, J. R. Sufrin, C. S. Harwood, *Nature* **2008**, *454*, 595–596.
5. C. Grandclément, M. Tannières, S. Moréra, Y. Dessaux, D. D. Faure, *FEMS Microbiol. Rev.* **2016**, *40*, 86–116.
6. R. J. Redfield, *Trends Microbiol.* **2002**, *10*, 365–370.
7. A. W. Decho, R. L. Frey, J. L. Ferry, *Chem. Rev.* **2011**, *111*, 86–99.
8. B. A. Hense, C. Kuttler, J. Müller, M. Rothballer, A. Hartmann, J.-U. Kreft, *Nat. Rev. Microbiol.* **2007**, *5*, 230–239.
9. G. F. Kaufmann, R. Sartorio, S. H. Lee, C. J. Rogers, M. M. Meijler, J. A. Moss, B. Clapham, A. P. Brogan, T. J. Dickerson, K. D. Janda, *Proc. Natl. Acad. Sci. U.S.A.* **2005**, *102*, 309–314.
10. T. Defoirdt, N. Boon, P. Bossier, W. Verstraete, *Aquaculture* **2004**, *240*, 69–88.
11. J. P. Gerdt, H. E. Blackwell, *ACS Chem. Biol.* **2014**, *9*, 2291–2299.
12. A. M. Stevens, Y. Queneau, L. Soulere, S. von Bodman, A. Doutheau, *Chem. Rev.* **2011**, *111*, 4–27.
13. W. R. J. D. Galloway, J. T. Hodgkinson, S. D. Bowden, M. Welch, D. R. Spring, *Chem. Rev.* **2011**, *111*, 28–67.
14. A. Fleming, *Br. J. Exp. Pathol.* **1929**, *10*, 226–236.
15. K. Lewis, *Nature* **2012**, *485*, 439–440.
16. M. A. Fischbach, C. T. Walsh, *Science* **2009**, *325*, 1089–1093.
17. S. A. Sieber, M. A. Marahiel, *Chem. Rev.* **2005**, *105*, 715–738.
18. H. Gross, J. E. Loper, *Nat. Prod. Rep.* **2009**, *26*, 1408–1446.
19. O. Nybroe, J. Sørensen in *Production of cyclic lipopeptides by fluorescent pseudomonads*, Springer, **2004**, pp. 147–172.
20. J. M. Raaijmakers, I. de Bruijn, O. Nybroe, M. Ongena, *FEMS Microbiol. Rev.* **2010**, *34*, 1037–1062.
21. X. Cui, R. Harling, P. Mutch, D. Darling, *Eur. J. Plant Path.* **2005**, *111*, 297–308.

22. J.-F. Dubern, B. J. Lugtenberg, G. V. Bloemberg, *J. Bacteriol.* **2006**, *188*, 2898–2906.
23. J.-F. Dubern, E. R. Coppoolse, W. J. Stiekema, G. V. Bloemberg, *Microbiology* **2008**, *154*, 2070–2083.
24. G. Licciardello, I. Bertani, L. Steindler, P. Bella, V. Venturi, V. Catara, *Mol. Plant-Microbe Interact.* **2009**, *22*, 1514–1522.
25. G. Licciardello, C. P. Strano, I. Bertani, P. Bella, A. Fiore, V. Fogliano, V. Venturi, V. Catara, *J. Biotechnol.* **2012**, *159*, 274–282.
26. D. L. Val, J. E. Cronan, *J. Bacteriol.* **1998**, *80*, 2644–2651.
27. T. T. Hoang, S. A. Sullivan, J. K. Cusick, H. P. Schweizer, *Microbiology* **2002**, *148*, 3849–3856.
28. J. K. Lithgow, A. Wilkinson, A. Hardman, B. Rodelas, F. Wisniewski-Dye, P. Williams, J. A. Downie, *Mol. Microbiol.* **2000**, *37*, 81–97.
29. A. M. Pomini, G. P. Manfio, W. L. Araújo, A. J. Marsaioli, *J. Agric. Food Chem.* **2005**, *53*, 6262–6265.
30. M. R. Parsek, D. L. Val, B. L. Hanzelka, J. E. Cronan, E. P. Greenberg, *Proc. Natl. Acad. Sci. U.S.A.* **1999**, *96*, 4360–365.
31. W. T. Watson, T. D. Minogue, D. L. Val, S. B. von Bodman, M. E. A. Churchill, *Mol. Cell* **2002**, *9*, 685–694.
32. W. Nasser, S. Reverchon, *Anal. Bioanal. Chem.* **2007**, *387*, 381–390.
33. J. P. Pearson, C. Van Delden, B. H. Iglewski, *J. Bacteriol.* **1999**, *181*, 1203–1210.
34. T. S. Charlton, R. de Nys, A. Netting, N. Kumar, M. Hentzer, M. Givskov, S. Kjelleberg, *Environ. Microbiol.* **2000**, *2*, 530–541.
35. T. R. I. Cataldi, G. Bianco, S. Abate, *J. Mass Spectrom.* **2008**, *43*, 82–96.
36. E. A. Yates, B. Philipp, C. Buckley, S. Atkinson, S. R. Chhabra, R. E. Sockett, M. Goldner, Y. Dessaux, M. Camara, H. Smith, P. Williams, *Infect. Immun.* **2002**, *70*, 5635–5646.
37. L. Delalande, D. Faure, A. Raffoux, S. Uroz, C. D'Angelo-Picard, M. Elasri, A. Carlier, R. Berruyer, A. Petit, P. Williams, Y. Dessaux, *FEMS Microbiol. Ecol.* **2005**, *52*, 13–20.
38. M. Frommberger, N. Hertkorn, M. Englmann, S. Jakoby, A. Hartmann, A. Kettrup, P. Schmitt-Kopplin, *Electrophoresis* **2005**, *26*, 1523–1532.
39. J. J. Michels, E. J. Allain, S. A. Borchardt, P. Hu, W. F. McCoy, *J. Chrom. A* **2000**, *898*, 153–165.
40. S. A. Borchardt, E. J. Allain, J. J. Michels, G. W. Stearns, R. F. Kelly, W. F. McCoy, *Appl. Environ. Microbiol.* **2001**, *67*, 3174–3179.
41. C. A. Lowery, J. Park, C. Gloeckner, M. M. Meijler, R. S. Mueller, H. I. Boshoff, R. L. Ulrich, C. E. Barry III, D. H. Bartlett, V. V. Kravchenko *et al.*, *J. Am. Chem. Soc.* **2009**,

- 131, 14473–14479.
42. A. K. Struss, A. Nunes, J. Waalen, C. A. Lowery, P. Pullanikat, J. R. Denery, D. J. Conrad, G. F. Kaufmann, K. D. Janda, *Anal. Chem.* **2013**, *85*, 3355–3362.
 43. S. Uroz, Y. Dessaux, P. Oger, *ChemBioChem* **2009**, *10*, 205–216.
 44. Y.-H. Dong, J.-L. Xu, X.-Z. Li, L.-H. Zhang, *Proc. Natl. Acad. Sci.* **2000**, *97*, 3526–3531.
 45. Y.-H. Dong, L.-H. Wang, J.-L. Xu, H.-B. Zhang, X.-F. Zhang, L.-H. Zhang, *Nature* **2001**, *411*, 813–817.
 46. A. Carlier, R. Chevrot, Y. Dessaux, D. Faure, *Mol. Plant-Microbe Interact.* **2004**, *17*, 951–957.
 47. A. Holm, E. Vikström, *Front. Plant Sci.* **2014**, *5*, 309–314.
 48. S. Uroz, J. Heinonsalo, *FEMS Microbiol. Ecol.* **2008**, *65*, 271–278.
 49. C.-S. Wong, C.-L. Koh, C.-K. Sam, J. W. Chen, Y. M. Chong, W.-F. Yin, K.-G. Chan, *Sensors* **2013**, *13*, 12943–12957.
 50. J. R. Leadbetter, E. P. Greenberg, *J. Bacteriol.* **2000**, *182*, 6921–6926.
 51. Y. H. Lin, J. L. Xu, J. Y. Hu, L. H. Wang, S. L. Ong, J. R. Leadbetter, L. H. Zhang, *Mol. Microbiol.* **2003**, *47*, 849–860.
 52. J. J. Huang, J.-I. Han, L.-H. Zhang, J. R. Leadbetter, *Appl. Environ. Microbiol.* **2003**, *69*, 5941–5949.
 53. J. J. Huang, A. Petersen, M. Whiteley, J. R. Leadbetter, *Appl. Environ. Microbiol.* **2006**, *72*, 1190–1197.
 54. R. Ortíz-Castro, M. Martínez-Trujillo, J. López-Bucio, *Plant Cell Environ.* **2008**, *31*, 1497–1509.
 55. A. G. Palmer, A. C. Senechal, A. Mukherjee, J.-M. Ané, H. E. Blackwell, *ACS Chem. Biol.* **2014**, *9*, 1834–1845.
 56. A. Butler, M. Sandy, *Nature* **2009**, *460*, 848–854.
 57. M. Syrpas, E. Ruysbergh, L. Blommaert, B. Vanelslander, K. Sabbe, W. Vyverman, N. De Kimpe, S. Mangelinckx, *Mar. Drugs* **2014**, *12*, 352–367.
 58. M. Sandy, J. N. Carter-Franklin, J. D. Martin, A. Butler, *Chem. Commun.* **2011**, *47*, 12086–12088.
 59. J. W. van Schijndel, E. G. Vollenbroek, R. Wever, *Biochim. Biophys. Acta* **1993**, *1161*, 249–256.
 60. S. Uroz, S. R. Chhabra, M. Camara, P. Williams, P. Oger, Y. Dessaux, *Microbiology* **2005**, *151*, 3313–3322.
 61. P. K. Chowdhary, N. Keshavan, H. Q. Nguyen, J. A. Peterson, J. E. González, D. C. Haines, *Biochemistry* **2007**, *46*, 14429–14437.

62. M. Elasri, S. Delorme, P. Lemanceau, G. Stewart, B. Laue, E. Glickmann, P. M. Oger, Y. Dessaux, *Appl. Environ. Microbiol.* **2001**, *67*, 1198–1209.
63. M. Sanchez-Contreras, W. D. Bauer, M. Gao, J. B. Robinson, J. A. Downie, *Philos. Trans. R. Soc. Lond. B Biol. Sci.* **2007**, *362*, 1149–1163.
64. W. D. Bauer, U. Mathesius, *Curr. Opin. Plant Biol.* **2004**, *7*, 429–433.
65. M. Teplitski, U. Mathesius, K. P. Rumbaugh, *Chem. Rev.* **2011**, *111*, 100–116.
66. U. Mathesius, S. Mulders, M. Gao, M. Teplitski, G. Caetano-Anollés, B. G. Rolfe, W. D. Bauer, *Proc. Natl. Acad. Sci. U.S.A.* **2003**, *100*, 1444–1449.
67. D. F. Veliz-Vallejos, G. E. van Noorden, M. Yuan, U. Mathesius, *Front. Plant Sci.* **2014**, *5*, 551–564.
68. U. von Rad, I. Klein, P. I. Dobrev, J. Kottova, E. Zazimalova, A. Fekete, A. Hartmann, P. Schmitt-Kopplin, J. Durner, *Planta* **2008**, *229*, 73–85.
69. A. Schikora, S. T. Schenk, E. Stein, A. Molitor, A. Zuccaro, K.-H. Kogel, *Plant Physiol.* **2011**, *157*, 1407–1418.
70. S. T. Schenk, E. Stein, K.-H. Kogel, A. Schikora, *Plant Signal. Behav.* **2012**, *7*, 178–181.
71. F. Liu, Z. Bian, Z. Jia, Q. Zhao, S. Song, *Mol. Plant Microbe Interact.* **2012**, *25*, 677–683.
72. Q. Zhao, C. Zhang, Z. Jia, Y. Huang, H. Li, S. Song, *Front. Plant Sci.* **2015**, *5*, 807–820.
73. Q. Zhao, M. Li, Z. Jia, F. Liu, H. Ma, Y. Huang, S. Song, *Mol. Plant Microbe Interact.* **2016**, *29*, 774–785.
74. S. Song, Z. Jia, J. Xu, Z. Zhang, Z. Bian, *Biochem. Biophys. Res. Comm.* **2011**, *414*, 355–360.
75. J. López-Bucio, G. Acevedo-Hernández, E. Ramírez-Chávez, J. Molina-Torres, L. Herrera-Estrella, *Curr. Opin. Plant Biol.* **2006**, *9*, 523–529.
76. S.-C. Kim, K. D. Chapman, E. B. Blancaflor, *Plant Sci.* **2010**, *178*, 411–419.
77. A. Morquecho-Contreras, A. Méndez-Bravo, R. Pelagio-Flores, J. Raya-González, R. Ortíz-Castro, J. López-Bucio, *Plant Physiol.* **2010**, *152*, 1659–1673.
78. X. Bai, C. D. Todd, R. Desikan, Y. Yang, X. Hu, *Plant Physiol.* **2012**, *158*, 725–736.
79. S. Rankl, B. Gunsé, T. Sieper, C. Schmid, C. Poschenrieder, P. Schröder, *Plant Sci.* **2016**, *253*, 130–140.
80. C. M. Joseph, D. A. Phillips, *Plant Physiol. Biochem.* **2003**, *41*, 189–192.
81. V. G. Olher, N. P. Ferreira, A. G. Souza, L. U. Chiavelli, A. F. Teixeira, W. D. Santos, S. M. Santin, O. Ferrarese Filho, C. C. Silva, A. M. Pomini, *J. Nat. Prod.* **2016**, *79*, 1316–1321.
82. S. T. Schenk, C. Hernández-Reyes, B. Samans, E. Stein, C. Neumann, M. Schikora, M. Reichelt, A. Mithöfer, A. Becker, K.-H. Kogel, A. Schikora, *Plant Cell* **2014**, *26*, 2708–2723.

83. R. Schuhegger, A. Ihring, S. Gantner, G. Bahnweg, C. Knappe, G. Vogg, P. Hutzler, M. Schmid, F. Van Breusegem, L. Eberl, A. Hartmann, C. Langebartels, *Plant Cell Environ.* **2006**, *29*, 909–918.
84. S. T. Schenk, A. Schikora, *Front. Plant Sci.* **2015**, *5*, 784–790.
85. A. Schikora, S. T. Schenk, A. Hartmann, *Plant Mol. Biol.* **2016**, *90*, 605–612.
86. J. F. González, V. Venturi, *Trends Plant Sci.* **2013**, *18*, 167–174.
87. R. P. Singh, R. S. Baghel, C. Reddy, B. Jha, *Front. Plant Sci.* **2015**, *6*, 117–130.
88. F. Weinberger, J. Beltran, J. A. Correa, U. Lion, G. Pohnert, N. Kumar, P. Steinberg, B. Kloareg, P. Potin, *J. Phycol.* **2007**, *43*, 235–241.
89. I. Joint, K. Tait, M. E. Callow, J. A. Callow, D. Milton, P. Williams, M. Cámara, *Science* **2002**, *298*, 1207–1207.
90. M. Givskov, R. de Nys, M. Manefield, L. Gram, R. Maximilien, L. Eberl, S. Molin, P. D. Steinberg, S. Kjelleberg, *J. Bacteriol.* **1996**, *178*, 6618–6622.
91. M. Manefield, T. B. Rasmussen, M. Henzter, J. B. Andersen, P. Steinberg, S. Kjelleberg, M. Givskov, *Microbiology* **2002**, *148*, 1119–1127.
92. T. H. Jakobsen, S. K. Bragason, R. K. Phipps, L. D. Christensen, M. van Gennip, M. Alhede, M. Skindersø, T. O. Larsen, N. Høiby, T. Bjarnsholt, M. Givskov, *Appl. Environ. Microbiol.* **2012**, 2410–2421.
93. T. Persson, T. H. Hansen, T. B. Rasmussen, M. E. Skindersø, M. Givskov, J. Nielsen, *Org. Biomol. Chem.* **2005**, *3*, 253–262.
94. C. Niu, S. Afre, E. Gilbert, *Lett. Appl. Microbiol.* **2006**, *43*, 489–494.
95. B. Girenavar, M. L. Cepeda, K. A. Soni, A. Vikram, P. Jesudhasan, G. K. Jayaprakasha, S. D. Pillai, B. S. Patil, *Int. J. Food Microbiol.* **2008**, *125*, 204–208.
96. O. M. Vandeputte, M. Kiendrebeogo, S. Rajaonson, B. Diallo, A. Mol, M. El Jaziri, M. Baucher, *Appl. Environ. Microbiol.* **2010**, *76*, 243–253.
97. L. Y. Tan, W.-F. Yin, K.-G. Chan, *Sensors* **2013**, *13*, 3975–3985.
98. E. Mahmoudi, S. Tarzaban, P. Khodaygan, *J. Plant Path.* **2014**, *96*, 295–301.
99. G. Degrassi, G. Devescovi, R. Solis, L. Steindler, V. Venturi, *FEMS Microbiol. Lett.* **2007**, *269*, 213–220.
100. M. Teplitski, J. B. Robinson, W. D. Bauer, *Mol. Plant Microbe Interact.* **2000**, *13*, 637–648.
101. M. Gao, M. Teplitski, J. B. Robinson, W. D. Bauer, *Mol. Plant Microbe Interact.* **2003**, *16*, 827–834.
102. H. K. Patel, Z. R. Suárez-Moreno, G. Degrassi, S. Subramoni, J. F. González, V. Venturi, *Front. Plant Sci.* **2013**, *4*, 447–412.

103. C. Götz, A. Fekete, I. Gebefuegi, S. T. Forczek, K. Fuksová, X. Li, M. Englmann, M. Gryndler, A. Hartmann, M. Matucha, P. Schmitt-Kopplin, P. Schröder, *Anal. Bioanal. Chem.* **2007**, *389*, 1447–1457.
104. C. Götz-Rösch, T. Sieper, A. Fekete, P. Schmitt-Kopplin, A. Hartmann, P. Schröder, *Front. Plant Sci.* **2015**, *6*, 205–228.
105. T. Sieper, S. Forczek, M. Matucha, P. Krämer, A. Hartmann, P. Schröder, *New Phytol.* **2014**, *201*, 545–555.
106. M. Morikawa, Y. Hirata, T. Imanaka, *Biochim. Biophys. Acta* **2000**, *1488*, 211–218.
107. S. Dufour, M. Deleu, K. Nott, B. Wathelet, P. Thonart, M. Paquot, *Biochim. Biophys. Acta* **2005**, *1726*, 87–95.
108. S. Caboche, M. Pupin, V. Leclère, A. Fontaine, P. Jacques, G. Kucherov, *Nucleic Acids Res.* **2008**, *36*, D326–D331.
109. T. H. Nielsen, J. Sørensen, *Appl. Environ. Microbiol.* **2003**, *69*, 861–868.
110. H. Hashizume, Y. Nishimura in *Cyclic Lipopeptide Antibiotics, Vol. 35* (Ed.: A. ur Rahman), Elsevier, **2008**, pp. 693–751.
111. A. Ballio, F. Bossa, D. Giorgio, A. Nola, C. Manetti, M. Paci, A. Scaloni, A. L. Segre, *FEBS J.* **1995**, *234*, 747–758.
112. W. Li, H. Rokni-Zadeh, M. De Vleeschouwer, M. G. Ghequire, D. Sinnaeve, G.-L. Xie, J. Rozenski, A. Madder, J. C. Martins, R. De Mot, *PloS one* **2013**, *8*, e62946.
113. J. M. Raaijmakers, I. de Bruijn, M. J. D. de Kock, *Mol. Plant Microbe Interact.* **2006**, *19*, 699–710.
114. H. Rokni-Zadeh, W. Li, A. Sanchez-Rodriguez, D. Sinnaeve, J. Rozenski, J. C. Martins, R. De Mot, *Appl. Environ. Microbiol.* **2012**, *78*, 4826–4834.
115. C. L. Bender, F. Alarcón-Chaidez, D. C. Gross, *Microbiol. Mol. Biol. Rev.* **1999**, *63*, 266–292.
116. N. Roongsawang, K. Washio, M. Morikawa, *Int. J. Mol. Sci.* **2011**, *12*, 141–172.
117. H. Gross, V. O. Stockwell, M. D. Henkels, B. Nowak-Thompson, J. E. Loper, W. H. Gerwick, *Chem. Biol.* **2007**, *14*, 53–63.
118. I. Vallet-Gely, A. Novikov, L. Augusto, P. Liehl, G. Bolbach, M. Péchy-Tarr, P. Cosson, C. Keel, M. Caroff, B. Lemaitre, *Appl. Environ. Microbiol.* **2010**, *76*, 910–921.
119. C. Molina-Santiago, Z. Udaondo, A. Daddaoua, A. Roca, J. Martín, I. Pérez-Victoria, F. Reyes, J.-L. Ramos, *Microb. Biotechnol.* **2015**, *8*, 716–725.
120. S. Baré, V. M. Coiro, A. Scaloni, A. Di Nola, M. Paci, A. L. Segre, A. Ballio, *FEBS J.* **1999**, *266*, 484–492.
121. M. Ongena, P. Jacques, *Trends Microbiol.* **2008**, *16*, 115–125.

-
122. K. Arima, A. Kakinuma, G. Tamura, *Biochem. Biophys. Res. Commun.* **1968**, *31*, 488–494.
123. F. Peypoux, M. J. Bonmatin, J. Wallach, *Appl. Microbiol. Biotechnol.* **1999**, *51*, 553–563.
124. G. Pirri, A. Giuliani, S. F. Nicoletto, L. Pizzuto, A. C. Rinaldi, *Cent. Eur. J. Biol.* **2009**, *4*, 258–273.
125. V. Miao, M.-F. Coeffet-LeGal, P. Brian, R. Brost, J. Penn, A. Whiting, S. Martin, R. Ford, I. Parr, M. Bouchard, *Microbiology* **2005**, *151*, 1507–1523.
126. P. W. Lindum, U. Anthoni, C. Christophersen, L. Eberl, S. Molin, M. Givskov, *J. Bacteriol.* **1998**, *180*, 6384–6388.
127. R. Finking, M. A. Marahiel, *Annu. Rev. Microbiol.* **2004**, *58*, 453–488.
128. N. Roongsawang, S. P. Lim, K. Washio, K. Takano, S. Kanaya, M. Morikawa, *FEMS Microbiol. Lett.* **2006**, *252*, 143–151.
129. T. Stachelhaus, H. D. Mootz, M. A. Marahiel, *Chem. Biol.* **1999**, *6*, 493–505.
130. G. L. Challis, J. Ravel, C. A. Townsend, *Chem. Biol.* **2000**, *7*, 211–224.
131. I. de Bruijn, M. J. de Kock, M. Yang, P. de Waard, T. A. van Beek, J. M. Raaijmakers, *Mol. Microbiol.* **2007**, *63*, 417–428.
132. H. Jenke-Kodama, E. Dittmann, *Nat. Prod. Rep.* **2009**, *26*, 874–883.
133. K. Eppelmann, T. Stachelhaus, M. A. Marahiel, *Biochemistry* **2002**, *41*, 9718–9726.
134. J. Gerard, R. Lloyd, T. Barsby, P. Haden, M. T. Kelly, R. J. Andersen, *J. Nat. Prod.* **1997**, *60*, 223–229.
135. D. Konz, S. Doekel, M. A. Marahiel, *J. Bacteriol.* **1999**, *181*, 133–140.
136. I. de Bruijn, M. de Kock, P. de Waard, T. van Beek, J. Raaijmakers, *J. Bacteriol.* **2008**, *190*, 2777–2789.
137. R. H. Lambalot, A. M. Gehring, R. S. Flugel, P. Zuber, M. LaCelle, M. A. Marahiel, R. Reid, C. Khosla, C. T. Walsh, *Chem. Biol.* **1996**, *3*, 923–936.
138. M. A. Fischbach, C. T. Walsh, *Chem. Rev.* **2006**, *106*, 3468–3496.
139. P. J. Belshaw, C. T. Walsh, T. Stachelhaus, *Science* **1999**, *284*, 486–489.
140. T. Stachelhaus, C. T. Walsh, *Biochemistry* **2000**, *39*, 5775–5787.
141. S. A. Sieber, M. A. Marahiel, *J. Bacteriol.* **2003**, *185*, 7036–7043.
142. R. M. Kohli, J. W. Trauger, D. Schwarzer, M. A. Marahiel, C. T. Walsh, *Biochemistry* **2001**, *40*, 7099–7108.
143. J. Grünwald, S. A. Sieber, M. A. Marahiel, *Biochemistry* **2004**, *43*, 2915–2925.
144. M. A. Marahiel, L. O. Essen in *Nonribosomal Peptide Synthetases: Mechanistic and Structural Aspects of Essential Domains*, Vol. 458, Academic Press, **2009**, pp. 337–351.
145. K. Hoffmann, E. Schneider-Scherzer, H. Kleinkauf, R. Zocher, *J. Biol. Chem.* **1994**, *269*,
-

- 12710–12714.
146. C. J. Balibar, F. H. Vaillancourt, C. T. Walsh, *Chem. Biol.* **2005**, *12*, 1189–1200.
147. A. M. Gehring, I. Mori, R. D. Perry, C. T. Walsh, *Biochemistry* **1998**, *37*, 11637–11650.
148. L. Rouhiainen, L. Paulin, S. Suomalainen, H. Hyytiäinen, W. Buikema, R. Haselkorn, K. Sivonen, *Mol. Microbiol.* **2000**, *37*, 156–167.
149. F. I. Kraas, V. Helmetag, M. Wittmann, M. Strieker, M. A. Marahiel, *Chem. Biol.* **2010**, *17*, 872–880.
150. F. I. Kraas, T. W. Giessen, M. A. Marahiel, *FEBS Lett.* **2012**, *586*, 283–288.
151. D. B. Hansen, S. B. Bumpus, Z. D. Aron, N. L. Kelleher, C. T. Walsh, *J. Am. Chem. Soc.* **2007**, *129*, 6366–6367.
152. C. T. Walsh, R. V. O'Brien, C. Khosla, *Angew. Chem. Int. Ed.* **2013**, *52*, 7098–7124.
153. T. Kitten, T. G. Kinscherf, J. L. McEvoy, D. K. Willis, *Mol. Microbiol.* **1998**, *28*, 917–929.
154. B. Koch, T. H. Nielsen, D. Sørensen, J. B. Andersen, C. Christophersen, S. Molin, M. Givskov, J. Sørensen, O. Nybroe, *Appl. Environ. Microbiol.* **2002**, *68*, 4509–4516.
155. J. B. Andersen, B. Koch, T. H. Nielsen, D. Sørensen, M. Hansen, O. Nybroe, C. Christophersen, J. Sørensen, S. Molin, M. Givskov, *Microbiology* **2003**, *149*, 37–46.
156. J.-F. Dubern, E. L. Lagendijk, B. J. Lugtenberg, G. V. Bloemberg, *J. Bacteriol.* **2005**, *187*, 5967–5976.
157. N. Wang, S.-E. Lu, A. R. Records, D. C. Gross, *J. Bacteriol.* **2006**, *188*, 3290–3298.
158. J. D'Aes, K. De Maeyer, E. Pauwelyn, M. Höfte, *Environ. Microbiol. Rep.* **2010**, *2*, 359–372.
159. C. Berry, W. G. D. Fernando, P. C. Loewen, T. R. de Kievit, *Biol. Control* **2010**, *55*, 211–218.
160. K. Lapouge, M. Schubert, F. H. Allain, D. Haas, *Mol. Microbiol.* **2008**, *67*, 241–253.
161. T. G. Kinscherf, D. K. Willis, *J. Bacteriol.* **1999**, *181*, 4133–4136.
162. I. de Bruijn, J. Raaijmakers, *Appl. Environ. Microbiol.* **2009**, *75*, 4753–4761.
163. S.-E. Lu, N. Wang, J. Wang, Z. J. Chen, D. C. Gross, *Mol. Plant-Microbe Interact.* **2005**, *18*, 324–333.
164. K. Washio, S. P. Lim, N. Roongsawang, M. Morikawa, *Biosci. Biotech. Biochem.* **2010**, *74*, 992–999.
165. I. de Bruijn, J. Raaijmakers, *J. Bacteriol.* **2009**, *191*, 1910–1923.
166. L. Eberl, M. K. Winson, C. Sternberg, G. S. Stewart, G. Christiansen, S. R. Chhabra, B. Bycroft, P. Williams, S. Molin, M. Givskov, *Mol. Microbiol.* **1996**, *20*, 127–136.
167. R. Van Houdt, M. Givskov, C. W. Michiels, *FEMS Microbiol. Rev.* **2007**, *31*, 407–424.
168. E. R. Sullivan, *Curr. Opin. Biotechnol.* **1998**, *9*, 263–269.

-
169. D. Vollenbroich, M. Özel, J. Vater, R. M. Kamp, G. Pauli, *Biologicals* **1997**, *25*, 289–297.
170. K. Reder-Christ, Y. Schmidt, M. Dörr, H.-G. Sahl, M. Josten, J. M. Raaijmakers, H. Gross, G. Bendas, *Biochim. Biophys. Acta* **2012**, *1818*, 566–573.
171. C. Carrillo, J. A. Teruel, F. J. Aranda, A. Ortiz, *Biochim. Biophys. Acta* **2003**, *1611*, 91–97.
172. E. Pradel, Y. Zhang, N. Pujol, T. Matsuyama, C. I. Bargmann, J. J. Ewbank, *Proc. Natl. Acad. Sci. U.S.A.* **2007**, *104*, 2295–2300.
173. M. Mazzola, I. de Bruijn, M. F. Cohen, J. M. Raaijmakers, *Appl. Environ. Microbiol.* **2009**, *75*, 6804–6811.
174. J. R. Mireles, A. Toguchi, R. M. Harshey, *J. Bacteriol.* **2001**, *183*, 5848–5854.
175. I. Kuiper, E. L. Lagendijk, R. Pickford, J. P. Derrick, G. E. Lamers, J. E. Thomas-Oates, B. J. Lugtenberg, G. V. Bloemberg, *Mol. Microbiol.* **2004**, *51*, 97–113.
176. T. R. Neu, *Microbiol. Rev.* **1996**, *60*, 151–166.
177. Y. Zhang, R. M. Miller, *Appl. Environ. Microbiol.* **1994**, *60*, 2101–2106.
178. R. Bar-Ness, N. Avrahamy, T. Matsuyama, M. Rosenberg, *J. Bacteriol.* **1988**, *170*, 4361–4364.
179. F. Ahimou, P. Jacques, M. Deleu, *Enzyme Microb. Technol.* **2000**, *27*, 749–754.
180. I. Grangemard, J. Wallach, R. Maget-Dana, F. Peypoux, *Appl. Biochem. Biotech.* **2001**, *90*, 199–210.
181. C. N. Mulligan, *Curr. Opin. Colloid Interface Sci.* **2009**, *14*, 372–378.
182. S. M. Mandal, A. E. Barbosa, O. L. Franco, *Biotechnol. Adv.* **2013**, *31*, 338–345.
183. D. Cooper, C. Macdonald, S. Duff, N. Kosaric, *Appl. Environ. Microbiol.* **1981**, *42*, 408–412.
184. T. Yoneda, E. Masatsuji, T. Tsuzuki, K. Furuya, M. Takama, Y. Miyota, S. Ito in *Surfactant for use in external preparations for skin*, Patent WO 1999062482 A1, **1999**.
185. T. Yoneda in *Cosmetic composition comprising a lipopeptide*, Patent WO2005020950 A1, **2004**.
186. M. Kanlayavattanakul, N. Lourith, *Int. J. Cosmet. Sci.* **2010**, *32*, 1–8.
187. Kaneka in *Kaneka surfactin - Biosurfactant made by fermentation technology of KANEKA*, **2005**, pp. 1–2.
188. L.-M. Whang, P.-W. G. Liu, C.-C. Ma, S.-S. Cheng, *J. Hazard. Mater.* **2008**, *151*, 155–163.
189. N. Awasthi, A. Kumar, R. Makkar, S. Cameotra, *J. Environ. Sci. Health. B* **1999**, *34*, 793–803.
190. N. Olivera, M. Commendatore, A. Moran, J. Esteves, *J. Ind. Microbiol. Biotechnol.* **2000**, *25*, 70–73.
-

191. C. N. Mulligan, *Environ. Pollut.* **2005**, *133*, 183–198.
192. R. Makkar, S. S. Cameotra, *J. Ind. Microbiol. Biotechnol.* **1997**, *18*, 37–42.
193. N. Youssef, D. Simpson, K. Duncan, M. McInerney, M. Folmsbee, T. Fincher, R. Knapp, *Appl. Environ. Microbiol.* **2007**, *73*, 1239–1247.
194. C. N. Mulligan, R. N. Yong, B. F. Gibbs, S. James, H. Bennett, *Environ. Sci. Technol.* **1999**, *33*, 3812–3820.
195. I. M. Banat, R. S. Makkar, S. S. Cameotra, *Appl. Microbiol. Biotechnol.* **2000**, *53*, 495–508.
196. C. Vilhena, A. Bettencourt, *Mini Rev. Med. Chem.* **2012**, *12*, 202–209.
197. T. Schneider, A. Müller, H. Miess, H. Gross, *Int. J. Med. Microbiol.* **2014**, *304*, 37–43.
198. Y.-Z. Zhang, X. Sun, D. J. Zeckner, R. K. Sachs, W. L. Current, J. Gidda, M. Rodriguez, S.-H. Chen, *Bioorg. Med. Chem. Lett.* **2001**, *11*, 903–907.
199. M. Kracht, H. Rokos, M. Özel, M. Kowall, G. Pauli, J. Vater, *J. Antibiot.* **1999**, *52*, 613–619.
200. F. E. Olorunleke, N. Kieu Phuong, M. Höfte in *Bacteria-plant interactions: advanced research and future trends*, Caister Academic Press, **2015**, pp. 167–198.
201. J. D’Aes, K. H. H. Gia, K. De Maeyer, J. Pannecoque, I. Forrez, M. Ongena, L. E. P. Dietrich, L. S. Thomashow, D. V. Mavrodi, M. Höfte, *Phytopathology* **2011**, *101*, 996–1004.
202. F. E. Olorunleke, G. K. H. Hua, N. P. Kieu, Z. W. Ma, M. Höfte, *Environ. Microbiol. Rep.* **2015**, *7*, 774–781.
203. Z. Ma, N. Geudens, N. P. Kieu, D. Sinnaeve, M. Ongena, J. C. Martins, M. Höfte, *Front. Microbiol.* **2016**, *7*, 382–397.
204. P. D. Shaw, G. Ping, S. L. Daly, C. Cha, J. E. Cronan, K. L. Rinehart, S. K. Farrand, *Proc. Natl. Acad. Sci. U. S. A.* **1997**, *94*, 6036–6041.
205. K. H. McClean, M. K. Winson, L. Fish, A. Taylor, S. R. Chhabra, M. Camara, M. Daykin, J. H. Lamb, S. Swift, B. W. Bycroft, G. Stewart, P. Williams, *Microbiology* **1997**, *143*, 3703–3711.
206. J. B. Andersen, A. Heydorn, M. Hentzer, L. Eberl, O. Geisenberger, B. B. Christensen, S. Molin, M. Givskov, *Appl. Environ. Microbiol.* **2001**, *67*, 575–585.
207. L. Steindler, V. Venturi, *FEMS Microbiol. Lett.* **2007**, *266*, 1–9.
208. M. T. G. Holden, S. R. Chhabra, R. de Nys, P. Stead, N. J. Bainton, P. J. Hill, M. Manefield, N. Kumar, M. Labatte, D. England, S. Rice, M. Givskov, G. P. C. Salmond, G. Stewart, B. W. Bycroft, S. A. Kjelleberg, P. Williams, *Mol. Microbiol.* **1999**, *33*, 1254–1266.
209. X. J. Li, A. Fekete, M. Englmann, C. Götz, M. Rothballer, M. Frommberger, K. Bud-

- drus, J. Fekete, C. P. Cai, P. Schröder, A. Hartmann, G. N. Chen, P. Schmitt-Kopplin, *J. Chromatogr. A* **2006**, *1134*, 186–193.
210. C. A. Ortori, S. Atkinson, S. R. Chhabra, M. Camara, P. Williams, D. A. Barrett, *Anal. Bioanal. Chem.* **2007**, *387*, 497–511.
211. T. A. Gould, J. Herman, J. Krank, R. C. Murphy, M. E. A. Churchill, *J. Bacteriol.* **2006**, *188*, 773–783.
212. K. Kai, A. Tani, H. Hayashi, *Bioorg. Med. Chem.* **2010**, *18*, 3776–3782.
213. A. L. May, M. E. Eisenhauer, K. S. Coulston, S. R. Campagna, *Anal. Chem.* **2012**, *84*, 1243–1252.
214. D. Jakubczyk, C. Barth, A. Kubas, F. Anastassacos, P. Koelsch, K. Fink, U. Schepers, G. Brenner-Weiss, S. Bräse, *Anal. Bioanal. Chem.* **2012**, *403*, 473–482.
215. D. Jakubczyk, C. Merle, G. Brenner-Weiss, B. Luy, S. Bräse, *Eur. J. Org. Chem.* **2013**, *2013*, 5323–5330.
216. D. Jakubczyk, G. Brenner-Weiss, S. Bräse, *Eur. J. Org. Chem.* **2014**, *2014*, 592–597.
217. C. A. Ortori, J. F. Dubern, S. R. Chhabra, M. Camara, K. Hardie, P. Williams, D. A. Barrett, *Anal. Bioanal. Chem.* **2011**, *399*, 839–850.
218. K. G. Heumann, *Fresenius' Z. Anal. Chem.* **1986**, *325*, 661–666.
219. A. E. Mutlib, *Chem. Res. Toxicol.* **2008**, *21*, 1672–1689.
220. T. Goromaru, H. Matsuura, T. Furuta, S. Baba, *Chem. Pharm. Bull.* **1984**, *32*, 3179–3186.
221. T. Goromaru, H. Matsuura, T. Furuta, S. Baba, N. Yoshimura, T. Miyawaki, T. Sameshima, *Drug Metabol. Dispos.* **1982**, *10*, 542–546.
222. A. R. Branfman, M. F. McComish, R. J. Bruni, M. M. Callahan, R. Robertson, D. W. Yesair, *Drug Metabol. Dispos.* **1983**, *11*, 206–210.
223. J. T. Hodgkinson, W. R. Galloway, M. Casoli, H. Keane, X. Su, G. P. Salmond, M. Welch, D. R. Spring, *Tetrahedron Lett.* **2011**, *52*, 3291–3294.
224. J. K. Gawroński, *Tetrahedron Lett.* **1984**, *25*, 2605–2608.
225. J. G. Cao, Z. Y. Wei, E. A. Meighen, *Biochem. J.* **1995**, *312*, 439–444.
226. S. P. Chavan, K. Shivasankar, R. Sivappa, *J. Chem. Res.* **2004**, *2004*, 406–407.
227. S. R. Chhabra, P. Stead, N. J. Bainton, G. P. C. Salmond, G. Stewart, P. Williams, B. W. Bycroft, *J. Antibiot.* **1993**, *46*, 441–454.
228. P. Moya, Á. Cantín, M.-A. Castillo, J. Primo, M. A. Miranda, E. Primo-Yúfera, *J. Org. Chem.* **1998**, *63*, 8530–8535.
229. H. M. Keizer, J. J. Gonzalez, M. Segura, P. Prados, R. P. Sijbesma, E. W. Meijer, J. de Mendoza, *Chem.-Eur. J.* **2005**, *11*, 4602–4608.
230. Y. Sekiyama, Y. Fujimoto, K. Hasumi, A. Endo, *J. Org. Chem.* **2001**, *66*, 5649–5654.

231. X. Ariza, G. Asins, J. Garcia, F. G. Hegardt, K. Makowski, D. Serra, J. Velasco, *J. Labelled Comp. Radiopharm.* **2010**, *53*, 556–558.
232. A. Giuffrida, D. Piomelli, *FEBS Lett.* **1998**, *422*, 373–376.
233. L. Siekmann, H. Breuer, *J. Clin. Chem. Clin. Biochem.* **1982**, *20*, 883–892.
234. H. Mudhar, A. Witty, *Tetrahedron Lett.* **2010**, *51*, 4972–4974.
235. S. O. Nwaukwa, P. M. Keehn, *Tetrahedron Lett.* **1982**, *23*, 3135–3138.
236. Y. X. Qiao, J. Hu, H. A. Li, L. Hua, Y. Hu, B. Feng, Z. S. Hou, *J. Electrochem. Soc.* **2010**, *157*, 124–129.
237. J. Poldy, R. Peakall, R. A. Barrow, *Tetrahedron Lett.* **2008**, *49*, 2446–2449.
238. S. R. Chhabra, C. Harty, D. S. W. Hooi, M. Daykin, P. Williams, G. Telford, D. I. Pritchard, B. W. Bycroft, *J. Med. Chem.* **2003**, *46*, 97–104.
239. A. P. Tulloch, *Can. J. Chem.* **1977**, *55*, 1135–1142.
240. C. Barth, D. Jakubczyk, A. Kubas, F. Anastassacos, G. Brenner-Weiss, K. Fink, U. Schepers, S. Bräse, P. Koelsch, *Langmuir* **2012**, *28*, 8456–8462.
241. T. R. I. Cataldi, G. Bianco, M. Frommberger, P. Schmitt-Kopplin, *Rapid Commun. Mass Spectrom.* **2004**, *18*, 1341–1344.
242. T. R. I. Cataldi, G. Blanco, L. Palazzo, V. Quaranta, *Anal. Biochem.* **2007**, *361*, 226–235.
243. A. W. Decho, P. T. Visscher, J. Ferry, T. Kawaguchi, L. J. He, K. M. Przekop, R. S. Norman, R. P. Reid, *Environ. Microbiol.* **2009**, *11*, 409–420.
244. T. R. I. Cataldi, G. Bianco, S. Abate, *J. Mass Spectrom.* **2009**, *44*, 182–192.
245. J. G. Cao, E. A. Meighen, *J. Biol. Chem.* **1989**, *264*, 21670–21676.
246. A. Eberhard, *J. Bacteriol.* **1972**, *109*, 1101–1105.
247. M. Luna, S. García, O. García, Á. Trigos, *Nat. Prod. Res.* **2013**, *27*, 49–53.
248. D. Dwivedi, R. Jansen, G. Molinari, M. Nimtz, B. N. Johri, V. Wray, *J. Nat. Prod.* **2008**, *71*, 637–641.
249. H. H. Wasserman, J. J. Keggi, J. E. McKeon, *J. Am. Chem. Soc.* **1962**, *84*, 2978–2982.
250. V. Soto-Cerrato, B. Montaner, M. Martinell, M. Vilaseca, E. Giralt, R. Pérez-Tomás, *Biochem. Pharmacol.* **2005**, *71*, 32–41.
251. N. J. Cartwright, *Biochem. J.* **1955**, *60*, 238–242.
252. N. J. Cartwright, *Biochem. J.* **1957**, *67*, 663–669.
253. M. Ovadis, X. G. Liu, S. Gavriel, Z. Ismailov, I. Chet, L. Chernin, *J. Bact.* **2004**, *186*, 4986–4993.
254. C. Galli, G. Illuminati, L. Mandolini, *J. Am. Chem. Soc.* **1973**, *95*, 8374–8379.
255. C. Galli, G. Illuminati, L. Mandolini, P. Tamborra, *J. Am. Chem. Soc.* **1977**, *99*, 2591–2597.

256. L. Mandolini, *J. Am. Chem. Soc.* **1978**, *100*, 550–554.
257. G. Illuminati, L. Mandolini, *Acc. Chem. Res.* **1981**, *14*, 95–102.
258. F. Aiello, A. Brizzi, A. Garofalo, F. Grande, G. Ragno, R. Dayam, N. Neamati, *Bioorg. Med. Chem.* **2004**, *12*, 4459–4466.
259. T. Matsuyama, T. Tanikawa, Y. Nakagawa in *Serrawettins and Other Surfactants Produced by Serratia* (Ed.: G. Soberón-Chávez), Springer Berlin Heidelberg, Berlin, Heidelberg, **2011**, pp. 93–120.
260. H. Li, T. Tanikawa, Y. Sato, Y. Nakagawa, T. Matsuyama, *Microbiol. Immunol.* **2005**, *49*, 303–310.
261. O. El Mahdi, J.-P. Lavergne, J. Martinez, P. Viallefont, E. M. Essassi, C. Riche, *Eur. J. Org. Chem.* **2000**, *1*, 251–255.
262. O. David, W. J. N. Meester, H. Bieräugel, H. E. Schoemaker, H. Hiemstra, J. H. van Maarseveen, *Angew. Chem. Int. Ed.* **2003**, *42*, 4373–4375.
263. K. Ha, J.-C. M. Monbaliu, B. C. Williams, G. G. Pillai, C. E. Ocampo, M. Zeller, C. V. Stevens, A. R. Katritzky, *Org. Biomol. Chem.* **2012**, *10*, 8055–8058.
264. H. Bieräugel, H. E. Schoemaker, H. Hiemstra, J. H. van Maarseveen, *Org. Biomol. Chem.* **2003**, *1*, 1830–1832.
265. J. P. A. Rutters, Y. Verdonk, R. de Vries, S. Ingemann, H. Hiemstra, V. Levacher, J. H. van Maarseveen, *Chem. Comm.* **2012**, *48*, 8084–8086.
266. M. V. D’Auria, V. Sepe, R. D’Orsi, F. Bellotta, C. Debitus, A. Zampella, *Tetrahedron* **2007**, *63*, 131–140.
267. F. E. Koehn, O. J. McConnell, R. E. Longley, S. H. Sennett, J. K. Reed, *J. Med. Chem.* **1994**, *37*, 3181–3186.
268. P. Fu, M. Jamison, S. La, J. B. MacMillan, *Org. Lett.* **2014**, *16*, 5656–5659.
269. C. G. Pitt, Y. Bao, J. Thompson, M. C. Wani, H. Rosenkrantz, J. Metterville, *J. Med. Chem.* **1986**, *29*, 1231–1237.
270. L. R. Dick, A. A. Cruikshank, A. T. Destree, L. Grenier, T. A. McCormack, F. D. Melandri, S. L. Nunes, V. J. Palombella, L. A. Parent, L. Plamondon, R. L. Stein, *J. Biol. Chem.* **1997**, *272*, 182–188.
271. W. E. Stewart, T. H. Siddall, *Chem. Rev.* **1970**, *70*, 517–551.
272. C. Dugave, L. Demange, *Chem. Rev.* **2003**, *103*, 2475–2532.
273. A. Nefzi, J. M. Ostresh, R. A. Houghten, *Tetrahedron Lett.* **1997**, *38*, 4943–4946.
274. V. Krchňák, A. S. Weichsel, *Tetrahedron Lett.* **1997**, *38*, 7299–7302.
275. C. W. Becker, B. T. Dembofsky, J. E. Hall, R. T. Jacobs, D. E. Pivonka, C. J. Ohnmacht, *Synthesis* **2005**, 2549–2561.

276. A. Jabs, M. S. Weiss, R. Hilgenfeld, *J. Mol. Biol.* **1999**, *286*, 291–304.
277. C. H. Hassall, T. G. Martin, J. A. Schofield, *Tetrahedron Lett.* **1964**, *5*, 3741–3743.
278. C. M. Deber, F. A. Bovey, J. P. Carver, E. R. Blout, *J. Am. Chem. Soc.* **1970**, *92*, 6191–6198.
279. W. J. Wedemeyer, E. Welker, H. A. Scheraga, *Biochemistry* **2002**, *41*, 14637–14644.
280. G. Ma, H. Nguyen, D. Romo, *Org. Lett.* **2007**, *9*, 2143–2146.
281. H. Nguyen, G. Ma, T. Gladysheva, T. Fremgen, D. Romo, *J. Org. Chem.* **2011**, *76*, 2–12.
282. M. Groll, R. Huber, B. C. M. Potts, *J. Am. Chem. Soc.* **2006**, *128*, 5136–5141.
283. E. Oshimura, Y. Yamashita, K. Sakamoto, *J. Oleo Sci.* **2007**, *56*, 115–121.
284. H. Takahashi, Y. Nakayama, H. Hori, K. Kihara, H. Okabayashi, M. Okuyama, *J. Colloid Interface Sci.* **1976**, *54*, 102–107.
285. K. Yahagi, K. Tsujii, *J. Colloid Interface Sci.* **1987**, *117*, 415–424.
286. G. Cerichelli, L. Luchetti, G. Mancini, *Langmuir* **1997**, *13*, 4767–4769.
287. F. Segat-Dioury, O. Lingibé, B. Graffe, M.-C. Sacquet, G. Lhomme, *Tetrahedron* **2000**, *56*, 233–248.
288. B. Kitir, M. Baldry, H. Ingmer, C. A. Olsen, *Tetrahedron* **2014**, *70*, 7721–7732.
289. P. Jeschke, J. Benet-Buchholz, A. Harder, W. Etzel, M. Schindler, W. Gau, H.-C. Weiss, *Bioorg. Med. Chem. Lett.* **2006**, *16*, 4410–4415.
290. S. Richard Baker, A. F. Parsons, M. Wilson, *Tetrahedron Lett.* **1998**, *39*, 331–332.
291. L. P. Kuang, J. Zhou, S. Chen, K. Ding, *Synthesis* **2007**, 3129–3134.
292. R. M. Williams, R. W. Armstrong, J. S. Dung, *J. Am. Chem. Soc.* **1984**, *106*, 5748–5750.
293. A. Ollivier, M. Goubert, A. Tursun, I. Canet, M.-E. Sinibaldi, *Arkivoc* **2010**, 108–126.
294. S. Hanessian, S. Marcotte, R. Machaalani, G. B. Huang, *Org. Lett.* **2003**, *5*, 4277–4280.
295. J. J. Fleming, M. D. McReynolds, J. Du Bois, *J. Am. Chem. Soc.* **2007**, *129*, 9964–9975.
296. J. Yoshimura, M. Yamaura, T. Suzuki, H. Hashimoto, *Chem. Lett.* **1983**, 1001–1002.
297. J. R. Porter, J. F. Traverse, A. H. Hoveyda, M. L. Snapper, *J. Am. Chem. Soc.* **2001**, *123*, 10409–10410.
298. T. Meiresonne, G. Verniest, N. De Kimpe, S. Mangelinckx, *J. Org. Chem.* **2015**, *80*, 5111–5124.
299. A. Imramovský, J. Vinšová, J. M. Ferriz, M. Pour, M. Doležal, *Tetrahedron Lett.* **2006**, *47*, 5007–5011.
300. A. P. Pelliccioli, J. Wirz, *Photochem. Photobiol. Sci.* **2002**, *1*, 441–458.
301. J. E. T. Corrie, T. Furuta, R. Givens, A. L. Yousef, M. Goeldner in *Photoremovable Protecting Groups Used for the Caging of Biomolecules*, Wiley-VCH Verlag GmbH & Co. KGaA, **2005**, pp. 1–94.

-
302. P. Klán, T. Šolomek, C. G. Bochet, A. Blanc, R. Givens, M. Rubina, V. Popik, A. Kostikov, J. Wirz, *Chem. Rev.* **2013**, *113*, 119–191.
303. W. D. Meutermans, S. W. Golding, G. T. Bourne, L. P. Miranda, M. J. Dooley, P. F. Alewood, M. L. Smythe, *J. Am. Chem. Soc.* **1999**, *121*, 9790–9796.
304. W. D. F. Meutermans, G. T. Bourne, S. W. Golding, D. A. Horton, M. R. Campitelli, D. Craik, M. Scanlon, M. L. Smythe, *Org. Lett.* **2003**, *5*, 2711–2714.
305. C. P. Holmes, *J. Org. Chem.* **1997**, *62*, 2370–2380.
306. A. R. Katritzky, Y.-J. Xu, A. V. Vakulenko, A. L. Wilcox, K. R. Bley, *J. Org. Chem.* **2003**, *68*, 9100–9104.
307. Y. Tatsu, T. Nishigaki, A. Darszon, N. Yumoto, *FEBS Lett.* **2002**, *525*, 20–24.
308. E. C. B. Johnson, S. B. H. Kent, *Chem. Comm.* **2006**, 1557–1559.
309. L. P. Miranda, W. D. F. Meutermans, M. L. Smythe, P. F. Alewood, *J. Org. Chem.* **2000**, *65*, 5460–5468.
310. B. Shen, D. Löffler, K.-P. Zeller, M. Übele, G. Reischl, H.-J. Machulla, *J. Fluor. Chem.* **2007**, *128*, 1461–1468.
311. D. A. Horton, G. T. Bourne, J. Coughlan, S. M. Kaiser, C. M. Jacobs, A. Jones, A. Rühmann, J. Y. Turner, M. L. Smythe, *Org. Biomol. Chem.* **2008**, *6*, 1386–1395.
312. J. P. Van der Berg, W. A. Velema, W. Szymanski, A. J. M. Driessen, B. L. Feringa, *Chem. Sci.* **2015**, *6*, 3593–3598.
313. S. Hatakeyama, H. Mori, K. Kitano, H. Yamada, M. Nishizawa, *Tetrahedron Lett.* **1994**, *35*, 4367–4370.
314. O. R. Martin, W. Zhou, X. Wu, S. Front-Deschamps, S. Moutel, K. Schindl, P. Jeandet, C. Zbaeren, J. A. Bauer, *J. Med. Chem.* **2006**, *49*, 6000–6014.
315. T. Tsunoda, M. Suzuki, R. Noyori, *Tetrahedron Lett.* **1980**, *21*, 1357–1358.
316. T. Tsunoda, M. Suzuki, R. Noyoro, *Tetrahedron Lett.* **1979**, *20*, 4679–4680.
317. P. Neveu, I. Aujard, C. Benbrahim, T. Le Saux, J.-F. Allemand, S. Vríz, D. Bensimon, L. Jullien, *Angew. Chem. Int. Ed.* **2008**, *47*, 3744–3746.
318. M. Ogata, H. Matsumoto, S. Kida, S. Shimizu, K. Tawara, Y. Kawamura, *J. Med. Chem.* **1987**, *30*, 1497–1502.
319. S. A. Miller, S. L. Griffiths, D. Seebach, *Helv. Chim. Acta* **1993**, *76*, 563–595.
320. A. Becerril, J. L. León-Romo, J. Aviña, E. Castellanos, E. Juaristi, *Arkivoc* **2002**, *12*, 4–14.
321. S. Wolfe, G. Militello, C. Ferrari, S. K. Hasan, S. L. Lee, *Tetrahedron Lett.* **1979**, *20*, 3913–3916.
322. T. Haack, M. Mutter, *Tetrahedron Lett.* **1992**, *33*, 1589–1592.
323. D. Skropeta, K. A. Jolliffe, P. Turner, *J. Org. Chem.* **2004**, *69*, 8804–8809.
-

324. T. Wöhr, M. Mutter, *Tetrahedron Lett.* **1995**, *36*, 3847–3848.
325. T. Wöhr, F. Wahl, A. Nefzi, B. Rohwedder, T. Sato, X. Sun, M. Mutter, *J. Am. Chem. Soc.* **1996**, *118*, 9218–9227.
326. P. Dumy, M. Keller, D. E. Ryan, B. Rohwedder, T. Wöhr, M. Mutter, *J. Am. Chem. Soc.* **1997**, *119*, 918–925.
327. M. Keller, C. Sager, P. Dumy, M. Schutkowski, G. S. Fischer, M. Mutter, *J. Am. Chem. Soc.* **1998**, *120*, 2714–2720.
328. J. K. Clegg, J. R. Cochrane, N. Sayyadi, D. Skropeta, P. Turner, K. A. Jolliffe, *Austr. J. Chem.* **2009**, *62*, 711–719.
329. D. Seebach, J. D. Aebi, *Tetrahedron Lett.* **1984**, *25*, 2545–2548.
330. M. Falorni, S. Conti, G. Giacomelli, S. Cossu, F. Soccolini, *Tetrahedron: Asymmetry* **1995**, *6*, 287–294.
331. D. Seebach, B. Amatsch, R. Amstutz, A. K. Beck, M. Doler, M. Egli, R. Fitzi, M. Gautschi, B. Herradoön, P. C. Hidber, J. J. Irwin, R. Locher, M. Maestro, T. Maetzke, A. Mourino, E. Pfammatter, D. A. Plattner, C. Schickli, W. B. Schweizer, P. Seiler, G. Stucky, W. Petter, J. Escalante, E. Juaristi, D. Quintana, C. Miravittles, E. Molins, *Helv. Chim. Acta* **1992**, *75*, 913–934.
332. F. Fülöp, K. Pihlaja, *Tetrahedron* **1993**, *49*, 6701–6706.
333. M. D. Andrews, A. G. Brewster, K. M. Crapnell, A. J. Ibbett, T. Jones, M. G. Moloney, K. Prout, D. Watkin, *J. Chem. Soc. Perkin Trans. 1* **1998**, 223–235.
334. S. S. Jew, S. Terashima, K. Koga, *Tetrahedron* **1979**, *35*, 2345–2352.
335. B. J. van Lierop, W. R. Jackson, A. J. Robinson, *Tetrahedron* **2010**, *66*, 5357–5366.
336. M. Serra, S. M. Tambini, M. Di Giacomo, E. G. Peviani, L. Belvisi, L. Colombo, *Eur. J. Org. Chem.* **2015**, *2015*, 7557–7570.
337. A. Yang, *Studies of reductive lithiation methods for the preparation of organolithium compounds and applications of the palladium catalyzed zinc-ene cyclization*, PhD Thesis, University of Pittsburgh, **2007**.
338. X. Cong, F. Hu, K.-G. Liu, Q.-J. Liao, Z.-J. Yao, *J. Org. Chem.* **2005**, *70*, 4514–4516.
339. J. Sélambarom, S. Monge, F. Carré, J. P. Roque, A. A. Pavia, *Tetrahedron* **2002**, *58*, 9559–9566.
340. J. S. Panek, C. E. Masse, *J. Org. Chem.* **1998**, *63*, 2382–2384.
341. J. Chun, L. He, H.-S. Byun, R. Bittman, *J. Org. Chem.* **2000**, *65*, 7634–7640.
342. E. J. Corey, G. A. Reichard, *J. Am. Chem. Soc.* **1992**, *114*, 10677–10678.
343. C. H. Hassall, Moschidi.Mc, W. A. Thomas, *J. Chem. Soc. B* **1971**, 1757–1761.
344. E. V. Komleva, V. V. Fedorova, N. I. Petukhova, V. V. Zorin, *Bash. Khim. Z.* **2010**, *17*,

- 68–71.
345. D. Fravel, *Annu. Rev. Phytopathol.* **2005**, *43*, 337–359.
346. H.-L. Wei, L.-Q. Zhang, *Antonie Leeuwenhoek* **2006**, *89*, 267–280.
347. M. Perneel, J. Heyrman, A. Adiobo, K. De Maeyer, J. M. Raaijmakers, P. De Vos, M. Höfte, *J. Appl. Microbiol.* **2007**, *103*, 1007–1020.
348. P. G. Owusu-Darko, A. Paterson, E. L. Omenyo, *J. Agric. Chem. Environ.* **2014**, *3*, 22–29.
349. R. P. Pacumbaba, J. G. Wutoh, S. A. Eyango, J. T. Tambong, L. M. Nyochembeng, *J. Phytopathol.* **1992**, *135*, 265–273.
350. J. D’Aes, N. P. Kieu, V. Leclere, C. Tokarski, F. E. Olorunleke, K. De Maeyer, P. Jacques, M. Höfte, M. Ongena, *Environ. Microbiol.* **2014**, *16*, 2282–2300.
351. K. De Maeyer, *The versatile role of quorum sensing and phenazines in the biocontrol strain Pseudomonas sp. CMR12a*, PhD Thesis, Ghent University, **2012**.
352. J. D’Aes, *Biological activity and regulation of cyclic lipopeptides and phenazines produced by biocontrol strain Pseudomonas CMR12a*, PhD Thesis, Ghent University, **2012**.
353. Y.-L. Huang, S. Dobretsov, J.-S. Ki, L.-H. Yang, P.-Y. Qian, *Microb. Ecol.* **2007**, *54*, 384–392.
354. M. Syrpas, *Occurrence and synthesis of bacterial metabolites in the marine environment and study of their chemical interactions with diatoms*, PhD Thesis, Ghent University, **2015**.
355. E. C. Marfori, S. Kajiyama, E. Fukusaki, A. Kobayashi, *Phytochemistry* **2003**, *62*, 715–721.
356. F. Vinale, M. Nigro, K. Sivasithamparam, G. Flematti, E. L. Ghisalberti, M. Ruocco, R. Varlese, R. Marra, S. Lanzuise, A. Eid, S. L. Woo, M. Lorito, *FEMS Microbiol. Lett.* **2013**, *347*, 123–129.
357. F. Vinale, G. Manganiello, M. Nigro, P. Mazzei, A. Piccolo, A. Pascale, M. Ruocco, R. Marra, N. Lombardi, S. Lanzuise, R. Varlese, P. Cavallo, M. Lorito, S. L. Woo, *Molecules* **2014**, *19*, 9760–9772.
358. F. Vinale, G. Flematti, K. Sivasithamparam, M. Lorito, R. Marra, B. W. Skelton, E. L. Ghisalberti, *J. Nat. Prod.* **2009**, *72*, 2032–2035.
359. X. Mo, Q. Li, J. Ju, *RSC Adv.* **2014**, *4*, 50566–50593.
360. D. A. Hogan, Å. Vik, R. Kolter, *Mol. Microbiol.* **2004**, *54*, 1212–1223.
361. K. De Maeyer, J. D’Aes, G. K. H. Hua, M. Perneel, L. Vanhaecke, H. Noppe, M. Höfte, *Microbiol.* **2011**, *157*, 459–472.
362. F. E. Olorunleke, N. P. Kieu, E. De Waele, M. Timmerman, M. Ongena, M. Höfte, *MicrobiologyOpen* **2017**, *6*, 499–511.

363. C. L. Berry, M. Nandi, J. Manuel, A. K. C. Brassinga, W. G. D. Fernando, P. C. Loewen, T. R. de Kievit, *Biol. Control* **2014**, *69*, 82–89.
364. E. Ruysbergh, C. V. Stevens, N. De Kimpe, S. Mangelinckx, *RSC Adv.* **2016**, *6*, 73717–73730.
365. G. W. Huisman, O. de Leeuw, G. Eggink, B. Witholt, *Appl. Environ. Microbiol.* **1989**, *55*, 1949–1954.
366. L. S. Pierson III, D. W. Wood, E. A. Pierson, S. T. Chancey, *Eur. J. Plant Path.* **1998**, *104*, 1–9.
367. M. Katsara, T. Tselios, S. Deraos, G. Deraos, M.-T. Matsoukas, E. Lazoura, J. Matsoukas, V. Apostolopoulos, *Curr. Med. Chem.* **2006**, *13*, 2221–2232.
368. Y. Peng, H. Sun, Z. Nikolovska-Coleska, S. Qiu, C.-Y. Yang, J. Lu, Q. Cai, H. Yi, S. Kang, D. Yang, S. Wang, *J. Med. Chem.* **2008**, *51*, 8158–8162.
369. F. Aiello, A. Brizzi, O. De Grazia, A. Garofalo, F. Grande, M. S. Sinicropi, R. Dayam, N. Neamati, *Eur. J. Med. Chem.* **2006**, *41*, 914–917.
370. A. Yajima, *Biosci. Biotechnol. Biochem.* **2011**, *75*, 1418–1429.
371. B. Hasdemir, H. Ç. Onar, A. Yusufoglu, *Tetrahedron: Asymmetry* **2012**, *23*, 1100–1105.
372. M. De Vleeschouwer, D. Sinnaeve, J. Van den Begin, T. Coenye, J. C. Martins, A. Maddar, *Chem. Eur. J.* **2014**, *20*, 7766–7775.
373. D. Ogunniyi, *Bioresour. Technol.* **2006**, *97*, 1086–1091.
374. H. Mutlu, M. A. Meier, *Eur. J. Lipid Sci. Technol.* **2010**, *112*, 10–30.
375. G. Y. Ishmuratov, Y. V. Legostaeva, L. Garifullina, L. Botsman, R. Muslukhov, G. Tolstikov, *Russ. J. Org. Chem.* **2014**, *50*, 1075–1081.
376. Z. Pai, A. Tolstikov, P. Berdnikova, G. Kustova, T. Khlebnikova, N. Selivanova, A. Shangina, V. Kostrovskii, *Russ. Chem. Bull.* **2005**, *54*, 1847–1854.
377. T. B. Khlebnikova, Z. P. Pai, L. A. Fedoseeva, Y. V. Mattsat, *React. Kinet. Catal. Lett.* **2009**, *98*, 9–17.
378. *Rigaku Oxford Diffraction CrysAlis PRO*, Rigaku Oxford Diffraction, Yarnton, England, **2015**.
379. O. V. Dolomanov, L. J. Bourhis, R. J. Gildea, J. A. Howard, H. Puschmann, *J. Appl. Crystallogr.* **2009**, *42*, 339–341.
380. G. Sheldrick, *Acta Crystallogr. Sect. A* **2008**, *64*, 112–122.
381. G. M. Sheldrick, *Acta Crystallogr. Sect. C* **2015**, *71*, 3–8.

Curriculum Vitae

Personalia

Ewout Ruysbergh

Born: Ghent, 21 November 1989

Guido Gezellestraat 11

9810 Eke

Belgium

ewoutruysbergh@hotmail.com

Education

2010 - 2012 Master of Bioscience Engineering - Chemistry and Bioprocess Technology

Ghent University - greatest distinction

Master thesis:

“Screening en biomimetische synthese van quorum sensing-beïnvloedende metabolieten van de microalg Nitzschia”

Promoters: Prof. Dr. ir. N. De Kimpe & Prof. Dr. ir. S. Mangelinckx

2007 - 2010 Bachelor of Bioscience Engineering: Chemistry and Food technology

Ghent University - great distinction

2001 - 2007 Latin-Sciences

Don Boscollege, Zwijnaarde

Experience

2016 - ... Process Engineer at Oleon, Ertvelde

2012 - 2016 Doctoral researcher

“Reactivity of N-(3-hydroxyacyl)amino acids and influence of their corresponding homoserine lactones on cyclic lipopeptide production”

Promoters: Prof. Dr. ir. S. Mangelinckx, Prof. Dr. ir. N. De Kimpe & Prof. Dr. ir. C. Stevens

Publications in international journals with peer review (A1)

Ruysbergh, E., Van Hecke, K., Stevens, C. V., De Kimpe, N., Mangelinckx, S. Synthesis of 1,4-Oxazepane-2,5-diones via Cyclization of Rotationally Restricted Amino Acid Precursors and Structural Reassignment of Serratin. *J. Org. Chem.*, **2017**, 82, 6210-6222.

Ruysbergh, E., Stevens, C. V., De Kimpe, N., Mangelinckx, S. Synthesis and analysis of stable isotope-labelled *N*-acyl homoserine lactones. *RSC Adv.* **2016**, 6, 73717-73730.

Bossou, A. D., Ahoussi, E., **Ruysbergh, E.**, Adams, A., Smagghe, G., De Kimpe, N., Avlessia, F., Sohounhloouea, D. C. K., Mangelinckx, S. Characterization of volatile compounds from three *Cymbopogon* species and *Eucalyptus citriodora* from Benin and their insecticidal activities against *Tribolium castaneum*. *Ind. Crops Prod.* **2015**, 76, 306-317.

Syrpas, M., **Ruysbergh, E.**, Blommaert, L., Vanelslander, B., Sabbe, K., Vyverman, W., De Kimpe, N., Mangelinckx, S. Haloperoxidase Mediated Quorum Quenching by *Nitzschia cf pelucida*: Study of the Metabolization of *N*-Acyl Homoserine Lactones by a Benthic Diatom. *Mar. Drugs.* **2014**, 12, 352-367.

Syrpas, M., **Ruysbergh, E.**, Stevens, C., De Kimpe, N., Mangelinckx, S. Synthesis and biological evaluation of novel *N*- α -haloacylated homoserine lactones as quorum sensing modulators. *Beilstein J. Org. Chem.* **2014**, 10, 2539-2549.

Conferences and seminars

Green Chemistry for the 21st Century Chemical Industries, The Educational Workshop. Antwerp, Belgium, 2015.

Syrpas, M., **Ruysbergh, E.**, Blommaert, L., Vanelslander, B., Sabbe, K., Vyverman, W., Stevens, C., De Kimpe, N., Mangelinckx, S. Synthesis and biological evaluation of naturally and non-naturally occurring halogenated analogues of *N*-acylated homoserine lactones as quorum sensing modulators (oral presentation), 20th National symposium of applied biological sciences, Louvain-la-Neuve, Belgium, January 2015

Ruysbergh, E., De Kimpe, N., Stevens, C.V., Mangelinckx S. Synthesis of stable isotope labelled *N*-acyl homoserine lactones (poster presentation), 18th Sigma Aldrich Organic Synthesis Meeting, Blankenberge, Belgium, December 2014.

Syrpas, M., **Ruysbergh, E.**, De Kimpe, N., Mangelinckx, S. Synthesis and biological evaluation of *N*-(2-halo-3-ketoacyl) and *N*-(2,2-dihalo-3-ketoacyl) homoserine lactones (poster pre-

sentation), 17th Sigma Aldrich Organic Synthesis Meeting, Blankenberge, Belgium, December 2013.

Syrpas, M., **Ruysbergh, E.**, Mangelinckx, S., De Kimpe, N. Synthesis and biological evaluation of *N*-alpha-haloacylated homoserine lactones, Abstracts of Papers of the American Chemical Society, Volume: 245 Meeting Abstract: 226-ORGN, 245th National spring meeting of the American Chemical Society (ACS), New Orleans, Louisiana New Orleans, LA, USA, April 2013.

Ruysbergh, E., Syrpas, M., Mangelinckx, S., De Kimpe, N. Synthesis and biological evaluation of *N*-(α -haloacyl)-homoserine lactones (poster presentation), 16th Sigma Aldrich Organic Synthesis Meeting, Spa, Belgium, December 2012.